Precision moulding of polymer micro components

Optimization, Simulation, Tooling, Quality Control and Multi-Material Application

Tosello, Guido

Publication date:
2008

Document Version
Publisher's PDF, also known as Version of record

Precision Moulding of Polymer Micro Components

Optimization, Simulation, Tooling, Quality Control and Multi-Material Application

PhD Thesis

$$(EIv'')''=q-\rho A\ddot{v}$$

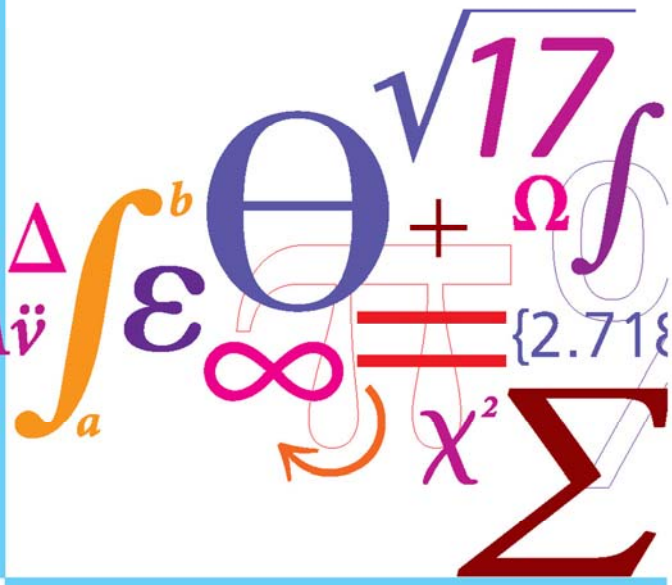

Guido Tosello
February 2008

DTU Mechanical Engineering
Department of Mechanical Engineering

Preface

This thesis has been prepared as one of requirements of the Ph.D. degree at the Technical University of Denmark (DTU), Department of Mechanical Engineering.

The work has been carried out from March 2005 to December 2007 at the Department of Manufacturing Engineering and Management and at the Department of Mechanical Engineering from January to February 2008 at the Technical University of Denmark (DTU) under the supervision of Prof. Hans Nørgaard Hansen, Dr. Peter Torben Tang and Associate professor Erik M. Kjær. From March to April 2007 and in November 2007, 10 weeks were spent at University of Freiburg (Germany), Institute of Microsystems Technology (IMTEK), Department for Process Technology under the supervision of Dr. Andreas Schoth.

I would like to thank all my supervisors for their inspiration and contribution to my work. In particular, I would like to express my gratitude to Prof. Hans Nørgaard Hansen for his inspiration, great collaboration, highly valuable contribution to my work and for giving me the opportunity to carry out the Ph.D. programme at DTU.

I want to thank Dr. Peter T. Tang for his advices and the collaboration in connection with the tooling and electroplating research activity during the project.

Dr. Andreas Schoth is thanked for the great hospitality at IMTEK and his contribution to my work, especially in connection with process control and simulation.

The work was funded by the Technical University of Denmark. Financial support by the Danish Innovation Consortium “PolyMetal” (Selective Metallization of Polymers, project number 61568) and the European Network of Excellence 4M (Multi-Material Micro Manufacturing: Technology and Applications, project number FP6-500274-1) is gratefully acknowledged.

Lyngby, February 2008

Guido Tosello

Abstract (English)

The present research work contains a study concerning polymer micro components manufacturing by means of the micro injection moulding (μIM) process. The overall process chain was considered and investigated during the project, including part design and simulation, tooling, process analysis, part optimization, quality control, and multi-material solutions.

A series of experimental investigations were carried out on the influence of the main μIM process factors on the polymer melt flow within micro cavities. These investigations were conducted on a conventional injection moulding machine adapted to the production of micro polymer components, as well as on a micro injection moulding machine. A new approach based on coordinate optical measurement of flow markers was developed during the project for the characterization of the melt flow. In-line pressure measurements were also performed to characterize the process in terms of injection time depending on the process factors. The process quality in terms of repeatability was assessed over a broad range of the process factors. The results show that the main influencing factor on the micro injection process is the injection speed.

Defects of injection moulded parts as weld lines were investigated on polymer micro parts. Design of experiments and atomic force microscopy were employed to characterize depth and width of weld lines depending on μIM process factors. Experiments showed that the temperature of the mould, the injection speed and the weld lines position with respect to gate location were the most important parameters on the weld lines of the micro injection moulded part. Optimization following the analysis leaded to a decrease of weld lines depth and width of at least 35%.

A round robin among European partners of the Network of Excellence 4M (Multi-Material Micro Manufacturing) was performed in order to assess the performance of newly developed hybrid technologies for micro tooling. A new manufacturing route was established including µEDM of silicon, selective etching and electroforming. The tool produced using the new process chain showed significant advancements in terms of miniaturization, accuracy, high aspect ratio, multi-scale integration and surface finishing characteristics. The tool was tested on an injection moulding machine for the production of polymer micro fluidics systems.

New methods for the validation of commercially available injection moulding simulation software were developed and implemented during the project. Software predictions in terms of injection time, injection pressure and flow pattern of micro injection moulded parts were improved by using advanced optimization strategies. The importance of material characterization at micro scale, of machine's dynamic behaviour implementation and of micro geometry modelling was shown in a quantitative study.

Insert moulding and hot embossing processes were investigated for the manufacturing of multi-material miniaturized components. A mould was developed and validated for the production of hybrid polymer/metal miniaturized parts by over moulding. Micro metal inserts with thickness down to 20 µm were moulded in a polymer matrix. The influence of metal surface treatment, insert thicknesses, different material combinations and different processes on the bonding strength between polymer matrix and metal part was determined.

Resume (Dansk)

Dette Ph.D. projekt indeholder studier vedrørende fremstilling af mikrokomponenter i polymerer ved hjælp af mikrosprøjtestøbning. Den overordnede proceskæde har været undersøgt i projektet inklusiv komponent design og simulering, værktøjsteknologier, procesanalyse og -optimering, kvalitetskontrol og multi-materiale løsninger.

En række eksperimentelle undersøgelser er blevet gennemført for at kortlægge væsentlige procesparametres indflydelse på polymersmeltens flow i værktøjskaviteter med mikrogeometrier. Disse forsøg blev gennemført på konventionelle sprøjtestøbemaskiner (tilpasset til produktion af mikrokomponenter) samt på dedikerede mikrosprøjtestøbemaskiner. En ny tilgang til karakterisering af smeltens flow baseret på optisk koordinatmåling af såkaldte flow markers er blevet udviklet i projektet. In-line trykmålinger i værktøjskaviteten blev gennemført for at karakterisere processen. Proceskvaliteten blev beskrevet gennem repeterbarheden over en bred række procesparametre. Resultaterne viste, at den vigtigste procesparameter i denne sammenhæng var indsprøjtningshastigheden.

Defekter ved mikrosprøjtestøbte emner blev undersøgt gennem en analyse af såkaldte weld lines (svejselinier). Statistisk forsøgsplanlægning og AFM blev anvendt til at undersøge dybde og bredde af weld lines som funktion af procesparametre. Resultaterne viste at værktøjstemperatur, indløbshastighed samt indløbets fysiske placering var de væsentligste influensparametre. En efterfølgende optimering resulterede i en reduktion dybde og bredde af weld lines på op til 35%.

En round robin blandt europæiske partnere i det europæiske 4M Network of Excellence (Multi-Material Micro Manufacture) blev gennemført for at karakterisere en nyudviklet såkaldt hybrid værktøjsteknologi. Denne hybride proceskæde

inkluderede mikrognistbearbejdning af Si, selektiv ætsning og elektrodeponering. Det producerede værktøj viste signifikante fordele i forhold til traditionelle fremstillingsmetoder baseret på miniaturisering, nøjagtighed, aspekt forhold (aspect ratio), multi-skala integration på samme komponent samt overfladekvalitet. Værktøjet blev anvendt til at sprøjtestøbe et mikrofluid system.

Nye metoder til validering af kommerciel software til simulering af mikrosprøjtestøbning er blevet udviklet og testet i projektet. Softwareforudsigelser vedrørende sprøjtestøbetid, indsprøjtningstryk og flow af smelten er blevet forbedret via optimerede simuleringsstrategier. Vigtigheden af valide materialedata, implementering af sprøjtestøbemaskinens dynamiske forhold samt den geometriske modellering af komponenterne er blevet demonstreret i et kvantitativt studie.

Insert moulding og hot embossing processer blev undersøgt i forbindelse med etablering af multi-materiale mikrokomponenter. En fleksibel sprøjtestøbeform til insert moulding blev fremstillet og anvendt til eksperimentelle undersøgelser af polymer/metal komponenter. Mikro metal komponenter ned til 20 µm tykkelse blev indstøbt i en polymermatrix. Indflydelsen af metallets overfladeruhed, tykkelse og forskellige procesparametre på adhesionsstyrken mellem plast og metaldel blev undersøgt.

Acknowledgements

A number of experts have been involved in the research during the three years of the Ph.D. project. I want express them my gratitude for their contribution, expertise and commitment to the project.

First of all, I would like to thank Dr. Tech. Prof. Leonardo De Chiffre at Department of Mechanical Engineering at the Technical University of Denmark who first gave me the opportunity to work at DTU and for his encouragement on pursuing the Ph.D. programme. The staffs at the Department of Mechanical Engineering, at the Centre for Geometrical Metrology (CGM) and at Danish Polymer Centre DTU are also thanked for their support and involvement in the project. Especially I thank Mr. René Sobiecki for the collaboration in connection with a large number of time-consuming measurements at CGM-DTU. Moreover, I thank Dr. Giuliano Bissacco for his contribution in connection with micro tooling and micro machining activities during the project and Associate professor Arnaud De Grave for sharing his expertise on design and process chains issues.

Dr. Alberto Gava, Dr. Francesco Marinello, Dr. Giovanni Lucchetta and Dr. Marco Salvador at the Department of Innovation in Mechanics and Management (DIMEG) at the University of Padova (Italy) are thanked for their collaboration and valuable contribution in connection with simulation and weld lines investigation.

Mr. Martin Bondo Jørgensen, R&D director of the Micro-Mechanical Systems department at Sonion Roskilde A/S is thanked for his support and collaboration in connection with the PolyMetal project. All the engineers and technicians at Sonion's Micro-Mechanical Systems and Plast Center are thanked for their help and collaboration during the tooling and moulding activity at the company facility. In particular, I want to thank Mr. Claus Münnecke, production manager at Sonion's Plast Center for sharing his knowledge and for fruitful discussions.

The Polymer Processing Technology Division of the NoE 4M (Multi-Material Micro Manufacturing) is acknowledged for very fruitful meetings, great collaboration and

discussions during these last 3 years of work together. In particular I would like to thank Dr. Andreas Schoth (Head of Division, University of Freiburg, Institute of Microsystems Technology (IMTEK), Germany), Dr. Bertrand Fillon (French Atomic Energy Commission (CEA), Laboratory of Innovation for New Energy Technologies and Nanomaterials (LITEN), France), Mr. Sabino Azcarate (Tekniker Technological Centre, Spain), Prof. Lars Mattsson (School of Industrial Technology and Management (KTH), Department of Production Engineering, Sweden), Dr. Chris Griffiths (Cardiff University, Manufacturing Engineering Center (MEC), United Kingdom), Dr. Pieter Jan Bolt (TNO Science & Industry, The Nederlands).

Dr. Mathias Heckele (Forschungszentrum Karlsruhe (FZK), Institute for Microstructure Technology (IMT), Germany) is thanked for initiating and involving me in the MINAFLOT 4M cross divisional project (Micro-NAno-Fluidics with LOTus effect, i.e. Micro- and nano- structured surfaces for the liquid and gas management in microstructured flowfields), for the great hospitality during my visits at FZK, and for sharing his extensive and deep knowledge in the field of micro-nano manufacturing, hot embossing, LIGA tooling, etc.

Dr. Emanuele M. Barini (Politecnico of Turin, Department of Production Systems and Business Economics (DISPEA), Italy) is thanked for his collaboration and fruitful discussion in connection with statistics and design of experiments.

M.Sc. Reinhold Jurischka and M.Sc. Tim Hösel (both at University of Freiburg, Institute of Microsystems Technology (IMTEK), Germany) are acknowledged for their help in connection with the micro injection moulding experiments at IMTEK.

Last, but not the least, I want to thank the M.Sc. project students I supervised during my Ph.D. for their commitment to the project, their results and their friendship: M.Sc. Paolo Motta, M.Sc. Matteo Guarise, M.Sc. Mauro Dal Molin. Their thesis works represented an important contribution to the project:

- Motta P. (2006) Validation of numerical simulation in micro injection moulding (μIM), M.Sc. Thesis, IPL-DTU, pp.1-202.
- Guarise M. (2007) Filling of micro injection moulded parts: an experimental investigation, M.Sc. Thesis, IPL-DTU, pp.1-176.
- Dal Molin M. (2007) Validation and optimization of FEM simulation of micro injection moulded parts, M.Sc. Thesis, IPL-DTU, pp.1-236.

Table of contents

1 Background and objectives

1.1 Introduction

Micro system technology is one of the key technologies of the new millennium. In the last years the application of micro products has been constantly increasing. The utilisation of micro systems covers very large and differentiated fields of applications. Some examples include informatics components (reading caps for hard disk, ink jet printers nozzles, etc.), medical and biomedical devices (pacemaker, sensors, micro fluidic systems for analysis of bio-fluids, etc.), high technology products (palm sized high definition displays, mobile phones, etc.), motion sensors for the automotive industry, micro components for implant devices such as hearing aid systems (micro connectors, micro switches, etc.) [Alting, 2003].

The essential condition for market success of micro systems is the cost-effective production of micro structures in large scale. In recent years plastic moulding techniques such as injection moulding, which is a suitable process for medium and large scale fabrication, have been adapted for the necessities of micro components fabrication. Injection moulding is a process technology that has been well established in the production of polymer parts in the macro-dimensional range for decades. Therefore, vast know-how and machine technology is available to be made use of in micro injection moulding as well.

Moreover, fabrication costs of moulded micro parts are hardly affected by the complexity of the design. Once a mould insert has been made, several thousands parts can be moulded with little effort. The cost of raw material is in most cases negligibly low, because only small material quantities are required for micro components. Therefore, parts fabricated by micro injection moulding, even from high-end materials, are suitable for applications requiring low-cost and disposable

components [Heckele, 2004]. The result is that plastic products manufactured by micro injection moulding have successful enter the market.

When downscaling systems, products, and their components, the limits of conventional manufacturing techniques are reached. This initiated the improvement of conventional techniques and further development of new ones, as in the case of the micro injection moulding process. Lateral dimensions in the micrometer range, structural details in the sub-micrometer dimensional level and high aspect ratio (aspect ratio = depth/width) of 10 and above are achieved. There is a variety of applications already known for micro moulding of thermoplastic polymers and many more are expected to come up in the future.

Research is required with respect to further development of each step of the micro manufacturing process chain (design, tooling, process, quality control, etc.) for the optimal mass production of polymer-based devices and components in the micro dimensional range.

1.2 Micro injection moulding scenario

Injection moulding is one of the most versatile and important operations for mass production of complex plastic parts. The injection-moulded parts typically have good dimensional tolerance and require almost no finishing and assembly operations. In addition to thermoplastics and thermosets, the process is also being extended to such materials as fibres, ceramics, and powered materials, with polymer as binders. Among all the polymer-processing methods, injection moulding accounts for 32% by weight of all the polymeric material processed [Turng, 2001]. Innovations of conventional injection moulding process have been continuously developed to further extend the applicability, capability, flexibility, productivity, and profitability of this versatile mass-production process.

In particular, micro injection moulding (μIM) is an innovative technology for the replication on medium-large scale of micro components. Micro injection moulding introduces additional design freedom, new application areas, unique geometrical features, and sustainable economical benefits, as well as material properties and part quality that cannot be accomplished by the conventional injection moulding process.

Micro injection moulding (or μIM, also called micro moulding) is referred to the production of parts that have:

- Weight in the range of milligrams, overall dimension, functional features, and tolerance requirements that are expressed in terms of micrometers, as well as miniaturized gate and runner system [see Figure 1, left].
- Overall dimensions in the macro range, weight in the order of grams, and areas with micro features. Such micro structures have dimension, functional features, and tolerance requirements that are expressed in terms of micrometers down to nanometres [see Figure 1, right].

On the base of these definitions, micro moulding can be also regarded as a type of moulding technology recently defined as “Precision Injection Moulding” [Whiteside, 2006].

Among the various micro manufacturing processes, micro injection moulding possesses the advantage of having a wealth of experience available in conventional plastics technology, standardized process sequence, high level of automation and short cycle time.

Due to the miniature characteristics of the moulded parts, however, a special moulding machine and auxiliary equipment are required to perform tasks such as shot volume control, process parameters control, injection, ejection, plastification, inspection, handling, packaging of moulded parts, etc. Furthermore, micro machining technologies are needed to produce the micro cavity.

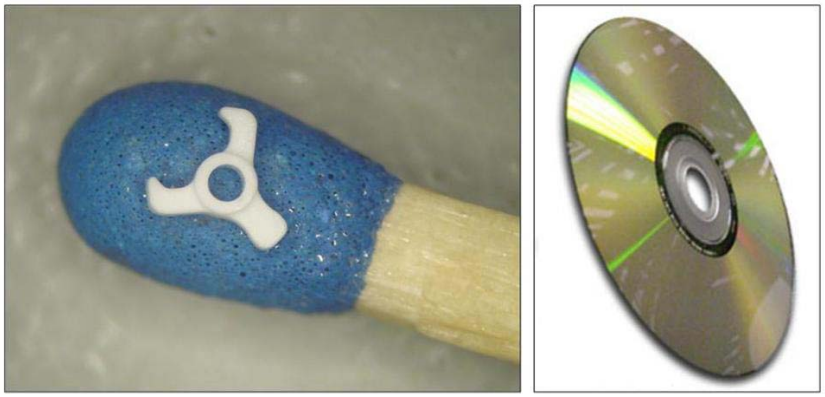

Figure 1 – Example of micro moulded part (micro mechanical actuator, on the left [Ganz, 2005]) and a macro part with micro structured region (DVD disc, on the right).

1.3 Challenges in µIM technology

Micro injection moulding (µIM) requires special attention to the machine equipment, processing and tooling. Characteristics and technical challenges of the µIM process are presented in this section with respect to moulding machine, process, tool, process simulation, multi-material application, assembly, quality control. The following list of challenges is the result of an extensive literature survey on micro injection moulding technology [Tosello, 2005(1)] carried out by the author as starting point of the Ph.D. project, and it provided the motivation for this thesis work.

- Injection moulding machine.
    - Micro injection moulding applications require machines equipped with special metering and injection ram (pistons, plunger) and screws designs to accurately meter the shot volume and to eliminate problems associated with material degradation.
    - With diminishing part volume and shot size, conventional injection moulding machines are no longer an economically and technically viable solution. However, conventional precise and high-speed injection moulding machines can be employed also for µIM. Large and precise runner and sprue are used to have a shot size large enough to reliably control the process and the switch-over point.
    - Control of mould-wall temperature (sometimes near or above the glass transition temperature of the polymer, at the expense of the cycle time) is important to avoid premature solidification of ultra thin sections. In particular the so-called Variotherm process has been developed which employs two fluid circuits at different temperatures to heat up and cool down the mould at filling and cooling stages respectively. Alternatively, the induction heating technique and electric cartridge heaters have been used to generate a peak mould temperature prior to injection [Rogalla, 1997] [Spennemann, 1999].
    - Machine requirements include shut-off nozzle to avoid drooling from the nozzle due to high melt temperature, precise alignment and gentle mould movement to avoid deformation of delicate parts, and local clean room enclosure to avoid contamination of moulded parts.

- Process.
  - In micro injection moulding, under opportune process conditions, filling of the smallest details can take place. However, process optimization for reliable micro and sub-micro scale replication is still a challenge [Monkkonen, 2002]. A limitation exists regarding the achievable aspect ratio of columns, grooves, and walls. These limits depend on the geometry, the polymer type, and the process parameters. Process optimization is therefore of outstanding importance.
  - Given the size and the weight of the micro injection moulded parts, ejection is performed by suction pads, electrostatic charging, blowing out, or direct handling of the sprue still connected to the actual moulded part. New demoulding principles need to be established in order to do not damage tiny micro moulded structures [Michaeli, 2004] [Michaeli, 2006].
- Material characterization.
  - Rheological properties of polymers are determined using conventional capillary rheometers which have limited performance in terms of speed and pressure attained during the tests. Those test conditions are not able to describe completely the polymer behaviour during μIM [Chien, 2005].
  - AFM (atomic force microscopy) and nano-indentation are giving indication on mechanical properties of the micro moulded parts [Whiteside, 2003]. Micro tensile tests have been also investigated to provide mechanical characterization of thermoplastics suitable for micro system moulding [Haberstroh, 2002].
- Tool.
  - Traditional methods of tooling, such as various machining processes (e.g. milling) and electrical discharge machining (EDM) have already reached their limitations with decreasing dimensions of mould inserts and cavities. Micro machining technologies are employed for the manufacturing of the micro cavities [Fleischer, 2005]: micro cutting (i.e. micro milling), ultra precision machining, laser machining, micro EDM,

etc. Existing technologies in the field of microelectronics, such as the LIGA technique, have been employed to fabricate mould inserts and cavities for micro injection moulding. LIGA is an acronym derived from the German words for deep X-ray lithography, electroforming (electroplating), and injection moulding replication [Heckele, 2004].

- Mould air evacuation is needed if micro features' thickness is down to 5 μm, the same order as the dimension of vent for air escape.
- Overall size of sample or batch of micro structures that can be moulded in one step is limited by the shrinkage of the polymer which is a function of the overall size of the parts. The farther a delicate micro structure with high aspect ratio is placed from the centre of shrinkage, the more difficult does demoulding become. Proper tool and part design are needed in order to overcome/compensate shrinkage issues, therefore further development may open the way to larger samples and even lower costs for multiple components produced in one batch.

- Multi-material μIM and integrated solutions.
  - Providing different and new functionalities integrated into the same micro part is a new challenge in micro injection moulding. Two-component, even multi-component micro injection moulding, insert moulding of metal micro inserts in a polymer part in the micro dimensional range, metallization of micro moulded parts are variations of the micro injection moulding process which allow producing a micro product with various electrical properties [Hansen, 2007].
  - Packaging, handling and assembly are always issues in micro engineering of micro parts. Therefore, development of processes to be applied after moulding, such as bonding, and for establishing reliable interconnections to the macroscopic world are needed.
- Simulation.
  - In order to achieve industrial applications within short development times, simulation of the micro injection moulding process is a valuable tool to be employed. Especially dedicated software for polymer micro

replication is not available yet and available packages show limitations in terms of prediction accuracy.

- Quality control.
    - The characterization of μIM moulded parts brings challenges in terms of measurements because of the integrated multi-scale dimensional range of the features to be controlled: macro and micro scale devices, micro scaled features, details in the sub-μm range. Furthermore, three-dimensional measuring capabilities are required, along with sub-μm or even nanometre accuracy.
    - The mass production capability of μIM calls for in-line process control instrumentation. Optical measuring techniques are the most suitable for the quality control of micro moulded parts. However, limitations in terms of accuracy, speed, capability of measuring three-dimensional geometries at micro scale exist. High accuracy quality control of both dimensions and surfaces is still performed off-line.

1.4 Problem identification

Micro injection moulding is facing a number of technological challenges for the reliable mass micro fabrication of polymer-based micro product.

During the present project, based on the challenges listed in the previous section, a selection of issues has been chosen and investigated to further develop the micro injection moulding technology. Micro injection moulding was considered as the process integrating the whole process chain for the fabrication of polymer based micro components. Therefore, the aim of this project has been to increase the knowledge on the micro injection moulding technology, with particular focus on the following process chain elements:

- Process control, analysis, and optimization.
- Part defects control and optimization.
- Micro tooling technology.
- Process simulation.
- In-process assembly (micro insert moulding).

1.5 Structure of the work

The structure of this thesis reflects the problem definition presented in the previous section. The identified five main topics are treated in the following chapters of the thesis and are here below briefly introduced.

- Process analysis and optimization (Chapter 3) – In this chapter the micro injection moulding process has been analyzed considering the moulding of micro parts using both conventional moulding equipment and micro injection moulding machines. The influence of the most important process parameters have been evaluated applying the design of experiment (DOE) techniques to optimize micro part and micro features filling, process repeatability, cavity injection pressure and time.
- Part defects control and optimization (Chapter 4) – The research work focussed on defects of micro injection moulded parts such as weld lines. DOE techniques were integrated with atomic force microscopy and other measuring technologies to characterize micro weld lines at sub-µm level and to find the relationship with important process parameters.
- Tooling technology (Chapter 5) – In this chapter the concept of hybrid tooling is introduced to overcome current limitation of micro machining processes for further miniaturization of micro tool features. A new hybrid tooling process chain developed during the project is presented and the newly obtained results are compared with state-of-the-art micro tooling technologies in a benchmark study.
- Process simulation (Chapter 6) – Implementation strategies of micro injection moulding simulations are presented and validated. Simulation results in terms of flow front position, cavity injection pressure, and cavity injection time are evaluated by comparison with experimental results. A new rheological database suitable for micro moulding simulation is proposed and validated by a comparison with experiments.
- Micro insert moulding (Chapter 7) – The bonding strength of metal micro inserts in a polymer matrix is investigated. Different polymers, metals, insert thicknesses, insert surface treatment are studied. A flexible moulding tool has

been developed for the insert moulding of hybrid metal-polymer miniaturized components and is presented in this chapter.

Furthermore, an introductory chapter (Chapter 2) giving the background information about the micro injection moulding process, the main components of the moulding machines and the moulding steps is placed after the present chapter and before the above mentioned chapters dealing with the research work.

1.6 Manufacturing metrology framework

Metrology has been a fundamental investigation tool throughout the whole research project. Firstly, metrology provided the necessary inputs during the analysis of all the manufacturing processes investigated, and secondly it supplied the decisional quantitative elements for the optimization and validation phases of both experimental and simulative activities.

- Dimensional metrology has been extensively used for the determination of the position of flow markers on the surface of micro injection moulded components (using optical coordinate metrology and optical microscopy), for the measurement of width and depth of micro weld lines (using atomic force microscopy), to evaluate the performance of simulation in terms of dimensional accuracy in the prediction of flow front position (using digital image measurements) etc.
- Surface metrology has been extensively used to benchmark the performance of different direct and hybrid micro tooling technologies in terms of surface finishing (using mechanical profilometry and white light interferometry), to evaluate the replication capability of the injection moulding process (using atomic force microscopy), to characterize metal insert surfaces in order to establish a relation with bonding strength of hybrid metal-polymer miniaturized components (using three-dimensional laser focus profilometry), etc.
- Process metrology was also of great importance in connection with in-process cavity pressure measurement during µIM (using a piezoelectric pressure sensor), bonding strength of micro insert moulded parts (using a pull test machine).

1.7 References

[Alting, 2003] Alting L., Kimura F., Hansen H.N., Bissacco G. (2003) Micro engineering, Annals of the CIRP, Vol.52/2, pp.1-23.

[Chien, 2005] Chien R.D., Jong W.R., Chen S.C. (2005) Study on the rheological behaviour of polymer melt flowing through micro-channels considering the wall-slip effect, Journal of Micromechanics and Microengineering, Vol.15, Issue 8, pp.1389-1396.

[Fleischer, 2005] Fleischer J., Kotschenreuther J. (2005) Manufacturing of micro moulds by conventional and energy assisted processes, Proceedings of the 1st International Conference on Multi-Material Micro Manufacture (4M), Karlsruhe (Germany), 29th June-1st July 2005, pp.9-17.

[Ganz, 2005] Ganz M. (2005) Micro Injection Moulding and Compression Moulding, Workshop at the 1st International Conference on Multi-Material Micro Manufacture (4M): Polymer Technology toward Nano, future technology for Europe, Karslruhe (Germany), 29th June-1st July 2005.

[Haberstroh, 2002] Haberstroh E., Brandt M. (2002) Determination of Mechanical Properties of Thermoplastics Suitable for Micro Systems, Macromolecular Material Engineering, Vol.287, pp.881-888.

[Hansen, 2007] Hansen H.N., Tang P.T., Islam A., Tosello G. (2007) Process chains for manufacturing of miniaturised moulded interconnect devices (MID), 7th International Conference of the European Society for Precision Engineering and Nanotechnology (Euspen), Bremen (Germany), 20-24 May 2007, pp.176-179.

[Heckele, 2004] Heckele M., Schomburg W.K. (2004) Review on micro molding of thermoplastic polymers. J. of Micromechanics and Microengineering, Vol.14, Issue 3, pp.R1-R14.

[Michaeli, 2004] Michaeli W., Gartner R. (2004) Injection molding of micro-structured surfaces, Society of Plastic Engineers (SPE) -

Proceedings of the 62nd Annual Technical Conference ANTEC, Chicago (IL, USA), 16th-20th May 2004, Vol.1, pp.752-756.

[Michaeli, 2006] Michaeli W., Gartner, R. (2006) New demolding concepts for the injection molding of microstructures, Journal of Polymer Engineering, Vol.26, Issue.2, pp.161-177.

[Monkkonen, 2002] Monkkonen K., Hietala J., Paakkonen P., Paakkonen E.J., Kaikuranta T., Pakkanen T.T., Jaaskelainen T. (2002) Replication of Sub-Micron Features Using Amorphous Thermoplastics, Polymer Engineering and Science, Vol.42, Issue 7, pp.1600-1608.

[Rogalla, 1997] Rogalla A., Michaeli W. (1997) Analysis of injection molded microstructures, Society of Plastic Engineers (SPE) - Proceedings of the 55th Annual Technical Conference ANTEC, Toronto (Ontario, Canada), 27th April-2nd May 1997, Vol.1, pp.364-368.

[Spennemann, 1999] Spennemann A., Michaeli W. (1999) Process analysis and machine technology for the injection moulding of microstructures, Society of Plastic Engineers (SPE) - Proceedings of the 57th Annual Technical Conference ANTEC, New York (NY, USA), 2nd-6th May 1999, Vol.1, pp.768-772.

[Tosello, 2005(1)] Tosello, G. (2005) Micro injection moulding (μIM): manufacturing technology for mass-microfabrication, Technical University of Denmark (DTU), Internal report, pp.128.

[Turng, 2001] Turng L.-S. (2001) Special and emerging injection molding processes, Journal of Injection Molding Technology, Vol.5, Issue 3, pp.160-179.

[Whiteside, 2003] Whiteside B.R., Martyn M.T., Coates P.D., Greenway G., Allen P., Hornsby P. (2003) Micromoulding: Process

characteristics and product properties, Society of Plastic Engineers (SPE) – Proceedings of the 61st Annual Technical Conference ANTEC, Nashville (TN, USA), 4th-8th May 2003, Vol.1, pp.592-596.

[Whiteside, 2006] Whiteside B.R., Martyn M.T., Coates P.D. (2006) Introduction to Micromolding – in Precision Injection Moulding, ed. Greener J. and Wimberger-Friedl R., Hanser (Munich, Germany), pp.239-264.

2 Micro injection moulding technology

The development of the micro injection technology encountered a first phase between 1985 and 1995 [Piotter, 2001]. During that period the injection moulding technology for macro parts with micro structured details started and no appropriate machines were available. Only modified commercial units, hydraulically driven and with a clamping force of usually 25 up to 50 tons, could be applied for the subtle way of replicating micro structured mould insert with high aspect ratios by injection moulding. Then a second stage occurred from 1995 to 2000 when, with the collaboration between mechanical engineering companies and research institutes, special micro injection units or even completely new machines for the manufacturing of real micro parts were developed. The task was to reduce the minimal amount of injected resin, which is necessary to guarantee a stable process (i.e. improve the process repeatability) and increase replication capabilities of very small features (down to 20 µm).

After this intense developing stage a number of machines equipped with special features for micro injection have been produced by leading manufacturers. Minimum shot weight down to 25mg are now obtained, micro features can be replicated in a short cycle time, three-dimensional micro product are produced and can be now successfully enter the market.

2.1 Micro moulding with conventional injection moulding machine

Fabrication of micro moulded part comes to be a challenge when conventional injection moulding machines (see Figure 2) are used for the replication very small part. If such machines are adapted to the direct production of micro product, i.e. parts with a part weight down to a milligram (mg), they produce precise but big sprues to achieve the minimum necessary shot weight to perform properly the process. Very

often over 90% of the polymer is wasted and this waste can be an important cost factor (considering e.g. plastic material for medical applications, it is not unusual to have costs up to €70 for 1 kg of special material, e.g. PEEK). Moreover, the big sprue increases cooling time and, along with that, cycle time [Michaeli, 2002].

In conventional injection moulding, an injection cycle is composed of the main phases described in the following (see Figure 3).

1. Plastification – During the plastification phase, the screw is rotating to build up the melt polymer necessary for the injection phase. The pressure pushes the screw backwards. When sufficient polymer has built up (i.e. shot volume is plastificated) rotation stops.
2. Injection, filling and packing phase - When the mould is closed, the screw is pushed (injection). The melt polymer fills the sprue, the runners and the mould cavity (filling). The screw begins rotating again to build up more polymer (packing).
3. Cooling and ejection - After polymer is solidified (cooling), the mould opens and ejector pins remove the moulded part (ejection).

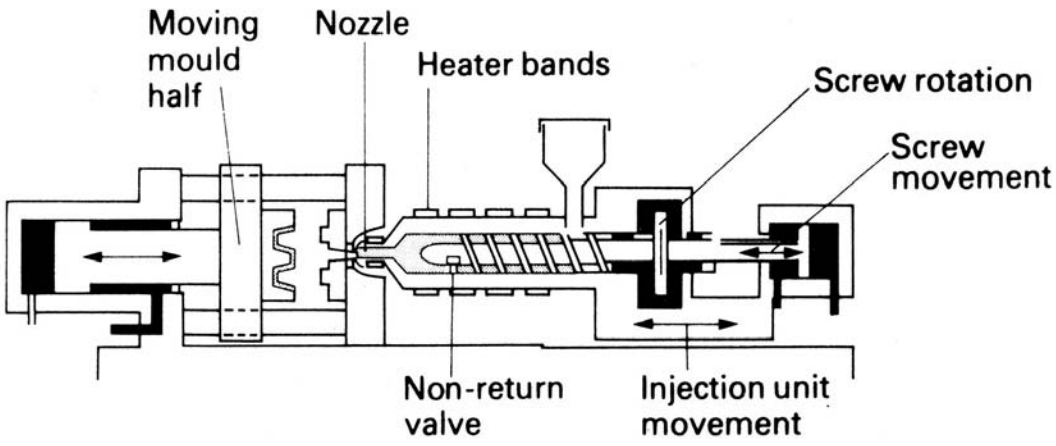

Figure 2 – Schematic view of a hydraulic injection moulding machine with its main components [Mills, 2005].

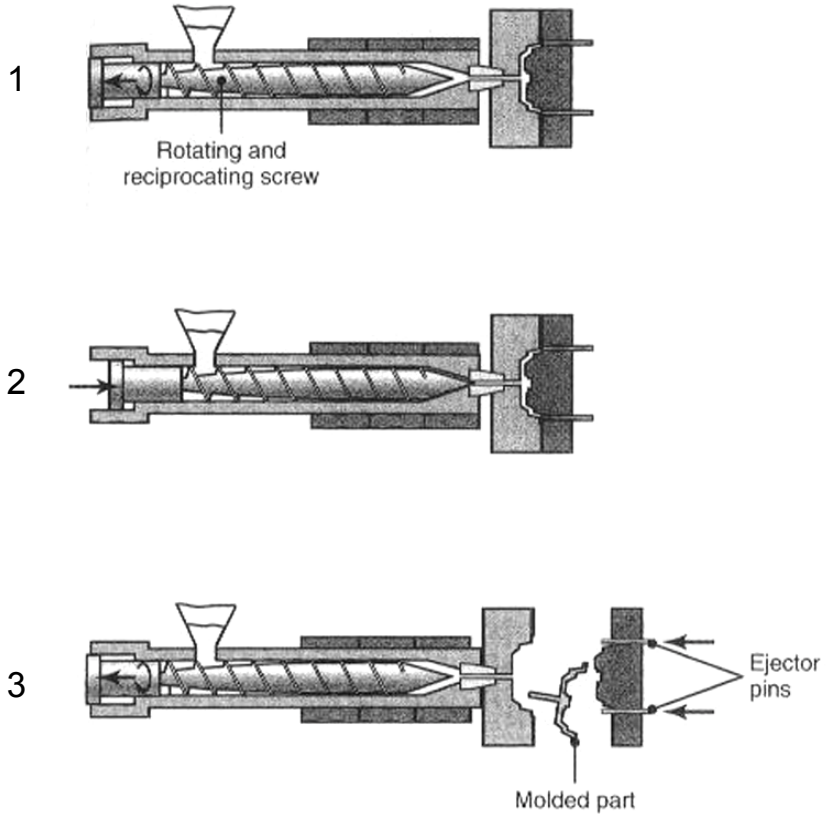

Figure 3 – Phases of the injection moulding process.

A problem which occurs with the small shot weight typical of micro parts is related to the size of pellets used in standard injection moulding. Conventional injection moulding machines utilizes screws with diameters down to 14 mm. Thus the depth of the screw channels should have at least the dimensions of a single grain. Hence, when the screw moves just 1 mm, about 185 mg of plastic are injected. Even one single pellet of poly(methyl methacrylate) (PMMA) weights 24 mg. This exceeds the part weight of e.g. gears for watch industry of 0.8 mg. Again, to produce such gears relatively huge runner systems are used to compensate for this issue.

It is clear these data represent a limit for a correct processing of injection moulded micro part: the minimum shot weight for a stable production lies in the range of some tenth of grams. When producing parts at the lower limit of the machine capacity problems dwelling time of the material will appear with risk of polymer degradation [Michaeli, 2000].

A screw for melting and injecting polymers combines four functions in one single unit:

- Plastification and homogenisation;
- Metering;
- Locking;
- Injection.

A conventional reciprocating screw used in macro machines presents the following problems when it is employed on moulding micro parts:

- It is difficult to control the melt metering accuracy as a result of the screw structure and the limitation to reduce screw size.
- Because of the channel configuration there is a melt back-flow when high injection pressure is applied to fill small and micro cavities.

For further downscaling the injection moulding process, these issues has to be solved by dividing the four functions of the screw at least in two different units:

- A screw for plasticizing and homogenising;
- A piston for metering and injection.

Figure 4 – Comparison of runner systems to mould micro part with conventional injection moulding machines (right) and with micro injection moulding machine (left) [Ganz, 2005].

2.2 Micro injection moulding machine

In order to control metering accuracy and homogeneity of the very small quantities of melt in the micro injection moulding process, new micro moulding machines using an injection system comprising a screw extruder and a plunger injection unit have been developed.

The main difference between the new micro moulding machine design and the conventional macro injection machines with a conventional reciprocating screw injection systems is that by separating melt plastification and melt injection, a small injection plunger a few millimetres in diameter can be used for melt injection to control metering accuracy. At the same time, a screw having sufficient channel depth to properly handle standard plastic pellets and yet provide required screw strength can be employed in micro moulding machines.

The typical solution provided by a micro injection moulding machine consists on the splitting of the four functions of the reciprocating screw (plastification, metering, locking, injecting) into different components (see Figure 5).

The plastification takes place in a dedicated functional part of the machine, which is separated from the injection unit:

- The very small amount of plastics needed is plasticized either by a plasticizing small screw (diameter of 14 mm, see Figure 6) or in an electrically heated cylinder, and then fed into the injection cylinder by a plunger (diameter of 5 mm).
- A second plunger with a diameter of just 5 down to 2 mm depending on the machine configuration injects the molten material into the cavity. It is driven by an electric motor and a precise linear drive. Typically, the shot weight can be varied between 5 and 300 mg.

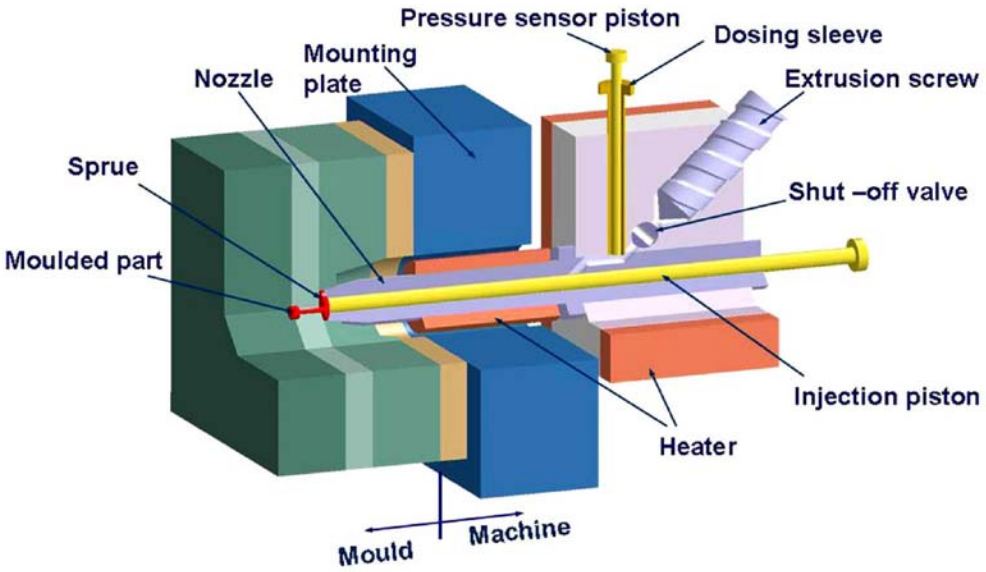

Figure 5 – Injection unit of a micro injection moulding machine [Ganz, 2005].

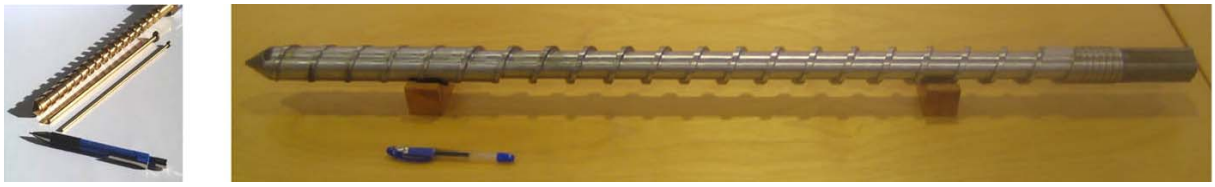

Figure 6 – Comparison of dimension between screw and injection plungers for µIM (left) and a screw for conventional injection moulding (right).

The micro injection moulding process steps are the following (see Figure 7):

1. Plastic pellets are plasticized by the fixed extruder screw and fed into the metering chamber.
2. The shut-off valve closes in order to avoid back-flow from the metering chamber.
3. After the set volume has been achieved, the plunger in the dosage barrel delivers the shot volume to the injection barrel.
4. The injection plunger then pushes the melt into the mould.
5. Once the plunger injection movement is completed, a holding pressure may be applied to the melt. This is achieved by a slight forward movement (maximum 1 mm) of the injection plunger.

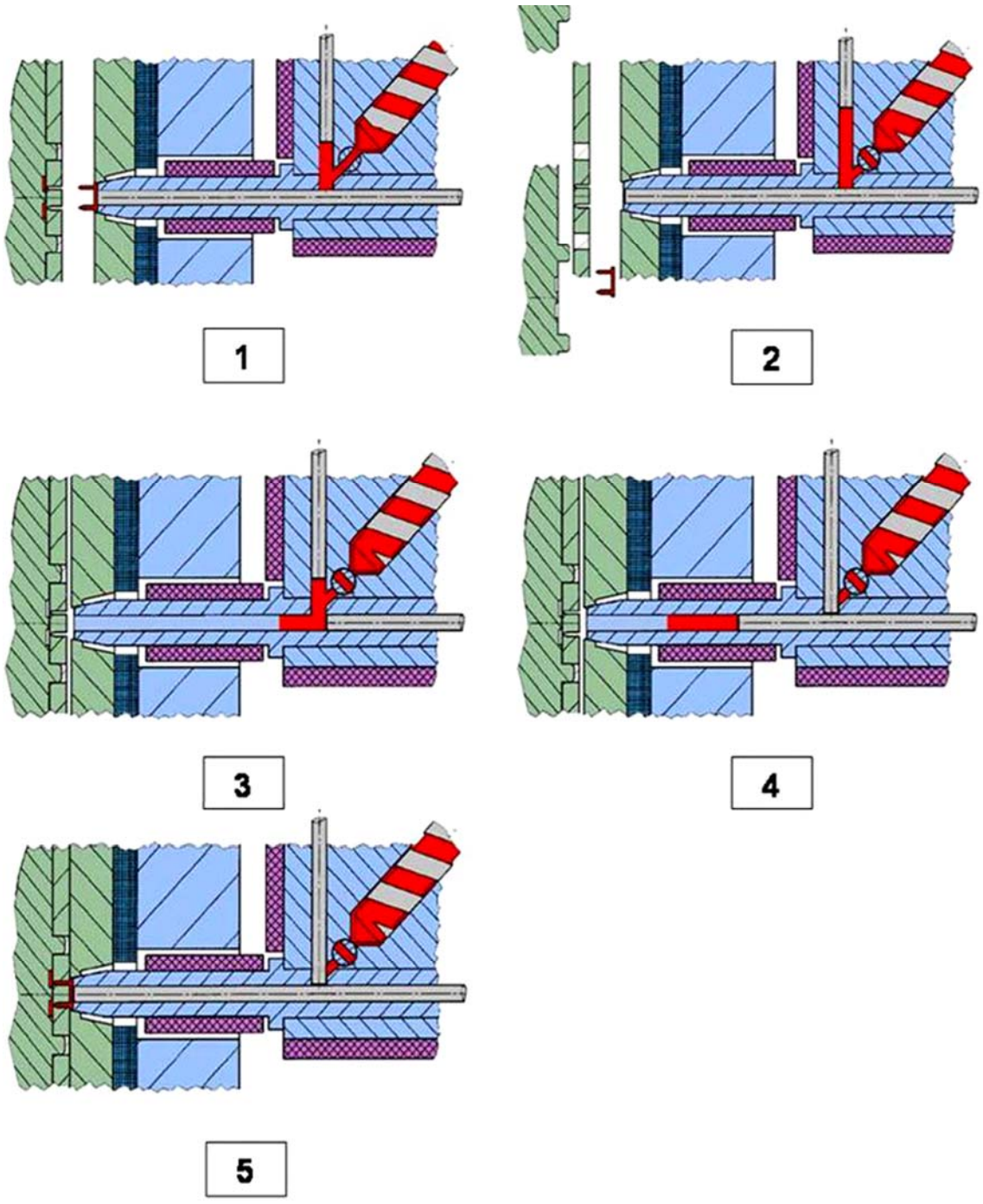

Figure 7 – Micro injection moulding steps [Ganz, 2005].

2.3 Conclusion

In this chapter the background information regarding the production of polymer micro components by conventional injection moulding and micro injection moulding are given. The main steps for the two processes and the main characteristics of the two related machines components were presented.

2.4 References

[Ganz, 2005] Ganz M. (2005) Micro Injection Moulding and Compression Moulding, Workshop at the 1st International Conference on Multi-Material Micro Manufacture (4M): Polymer Technology toward Nano, future technology for Europe, Karslruhe (Germany), 29th June-1st July 2005.

[Michaeli, 2000] Michaeli W., Spennemann A. (2000) Micro injection moulding - Improving the efficiency of a classical processing technology, Proceedings of International Conference on Microtechnologies: MICRO.tec 2000, Hannover (Germany), 25th-27th September 2000, Vol.2, pp.593-596.

[Michaeli, 2002] Michaeli W., Spennemann A., Gärtner R. (2002) New plastification concepts for micro injection moulding, Proceedings of the Conference of Micro System Technologies, Vol.8, pp.55-57.

[Mills, 1993] Mills N.J. (2005) Plastics – Microstructure and engineering applications, Arnold, 3rd edition.

[Piotter, 2001] Piotter V., Bauer W., Benzler T., Emde A. (2001) Injection molding of components for microsystems, Microsystem Technologies, Vol.7, Issue 3, pp.99-102.

3 Process control, analysis, and optimization

Micro injection moulding is a process which enables the mass production of polymer micro products. In order to produce high quality injection moulded micro parts, a crucial aspect to be fully understood and optimized is the filling of the cavity by the molten polymer. As a result, the relationships between filling performance and the different process parameter settings have to be established.

Characterization of the filling phase during micro injection moulding is a challenging task, mainly due to the dimensions of the cavity (typically in the sub-millimetre range, and even down to a few micrometres) and the filling time of the cavity (in the order of few tens of milliseconds).

Different approaches have been recently applied in order to accurately describe the filling of the micro cavity depending on the process parameter settings. For example, methods for the analysis of filling performance are: short shots method, flow-melt visualization method, flow length test.

During the Ph.D. project, two investigations on process filling analysis were carried out. Firstly, moulding of polymer micro component using a conventional injection machine was performed to analyse the filling of a micro cavity. Due to the limitations of conventional moulding in terms of process miniaturization, a new method based on the study of flow markers has been developed. A review of existing filling performance tests, the flow markers method fundamentals, experimental implementation and results are discussed in section 3.1 of this chapter.

Secondly, a large investigation on process filling control using a micro injection moulding machine was carried out. High speed and ultra-high speed moulding was performed over a broad range of mould and melt temperatures to characterize process performance of micro moulding. In-process cavity pressure control and flow markers investigation were combined in an integrated study. Experimental micro

injection moulding, cavity pressure and filling time analysis are discussed in section 3.2.

3.1 Micro cavity filling analysis using weld lines as flow markers

During this project a new method, based on the measurement of the weld lines path on the surface of a micro part, was proposed and investigated. The profile of weld lines is affected by the processing conditions and it works as flow marker of the melt-flow development during the filling of the cavity.

This section is structured as follows. Section 3.1.1 presents the state-of-the-art filling performance methods applied to micro injection moulding. In section 3.1.2 the method based on the use of weld lines as flow marker is introduced. In sections 3.1.3 and 3.1.4 the experiments and the results from the application of the new method are presented. In sections 3.1.5 and 3.1.6 the filling analysis results are presented and discussed respectively.

3.1.1 Filling performance tests

Different approaches can be employed for the analysis of the filling stage of the micro injection moulding process. In the following sub-sections a review of results obtained during recent research works is reported. In particular, three methodologies can be applied in order to characterize filling performances:

- Short-shots, where partial filling is obtain by means of partly-filled mouldings of increasing volume.
- Flow visualization, used to show the progress of the melt front in the cavity during the injection phase.
- Length flow test, used to evaluate the filling capacity of the moulding system in terms of achievable flow length and aspect ratio.

3.1.1.1 Short shots method

In conventional injection moulding (i.e. in the macro-dimensional range), a common approach to study the development of the melt flow inside the cavity is the short shot

analysis. It consists on the injection of a fraction of the molten polymer volume necessary to completely fill the cavity (see Figure 8).

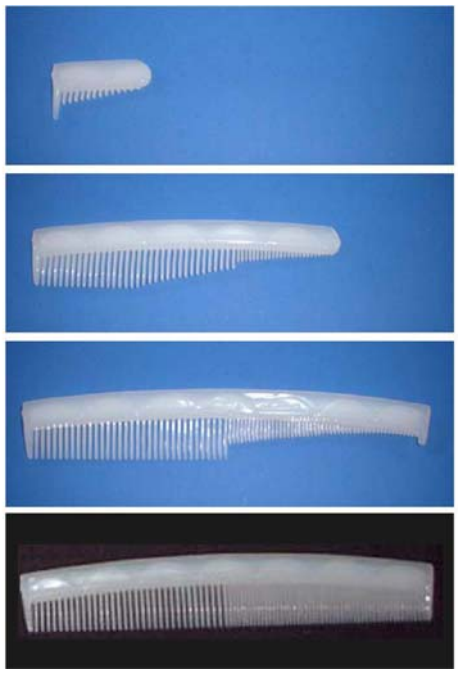

Figure 8 – Short shots of a polypropylene injection moulded comb at different stages of the filling: near beginning of filling, middle of filling, near end of filling and complete part (from top to bottom). Comb dimensions: length = 174 mm, height = 31 mm, thickness = 6 mm. Comb features sections are 1.3x1.8 mm^2 and 1.0x1.8 mm^2 [Jaworski, 2003].

The application of the short shots method to micro injection moulded parts has been shown to be possible when using a micro injection moulding machine provided with an injection plunger [Whiteside, 2005]. One of the main conditions for the applicability of such method is that the resolution of the machine (i.e. the smallest shot volume that can be injected in a controlled manner) has to be smaller than a fraction of the part which is significant to give information about intermediate stages of the filling. This condition can be fulfilled by injection moulding machines having an injection unit with a plunger (see section 2.2). On the other hand, small injection moulding machines with the conventional plastification unit with reciprocating screw cannot provide controlled short shots in the order of fraction of 1 mm^3 (typical volume of

polymer micro parts and/or micro features). Furthermore, in conventional machines, the acceleration of the screw may not be high enough to provide the required injection speed in the very short time needed to produce micro short shots. As a result, despite the fact that it is actually possible to injection mould micro parts with conventional injection moulding machines (especially if electrically driven and capable of high injection speed), with such machines it is not possible to produce reliable micro short shots. Process condition repeatability in terms of actual speed and injection pressure at the very beginning of the screw movement is lower than when it has reached a steady state injection movement. Moreover the produced incomplete micro parts present free surfaces with a deformation due to stress relaxation and thermal contraction. This causes an approximation on the dimensional accuracy on the determination of the actual flow front during the filling, especially if the target is accuracy in the micrometer range. On the other hand, the short shots method has been proven to be a feasible method for a good qualitative representation of the evolution of the filling stage when performing micro injection moulding (see Fig. 2).

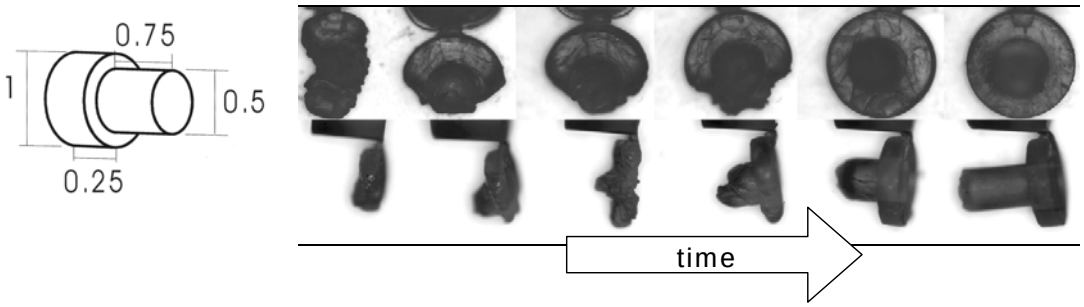

Figure 9 – Series of micro short shots (part volume 0.34 mm^3) [Whiteside, 2005].

3.1.1.2 Flow visualization tests

Flow visualization can also be used to describe the advancement of the flow front into the cavity during the filling stage. It consists of the use of a high speed camera capable of actually recording at high frame rates (in the order of 10^3-10^4 frames per second) the flow advancement inside the micro cavity. In order to achieve such results, the mould has to be provided with a lateral opening (camera access to the

mould) and one side of the cavity made of glass [Yang, 2002] [Han, 2006]. By subsequent image processing of the recorded film of the cavity filling, it is possible to perform a time-dependent analysis of the displacement of the melt-flow front (see Fig. 3).

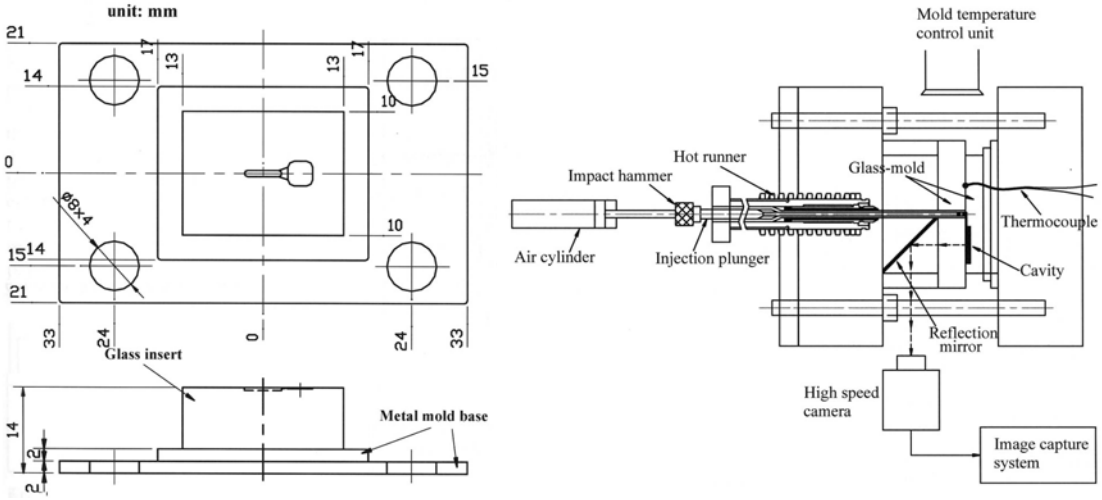

Figure 10 – Schematic diagrams of the glass mould cavity (left) and of the set-up for flow visualization (right) [Yang, 2002].

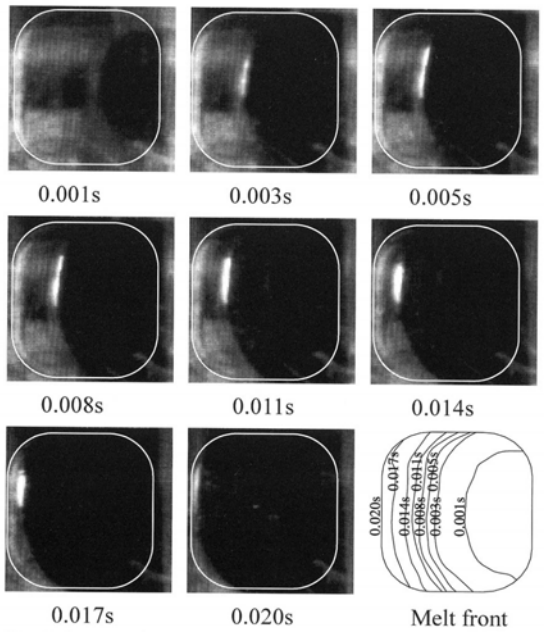

Figure 11 – Images showing the melt fronts during filling of 4x4x0.2 mm^3 shell-shaped cavity [Yang, 2002].

The flow visualization method offers a higher resolution than the short shots method. Furthermore, it can be applied not only to micro injection moulding machines but also to conventional reciprocating screw machines (mainly because the high resolution is provided by the high speed camera). On the other hand, the mould itself is of difficult realization due to the presence of a perfectly aligned optical glass and an optical mirror conveying the image from the cavity, through the glass and on to the external camera. As a consequence, the method appears to be of difficult implementation in an industrial environment.

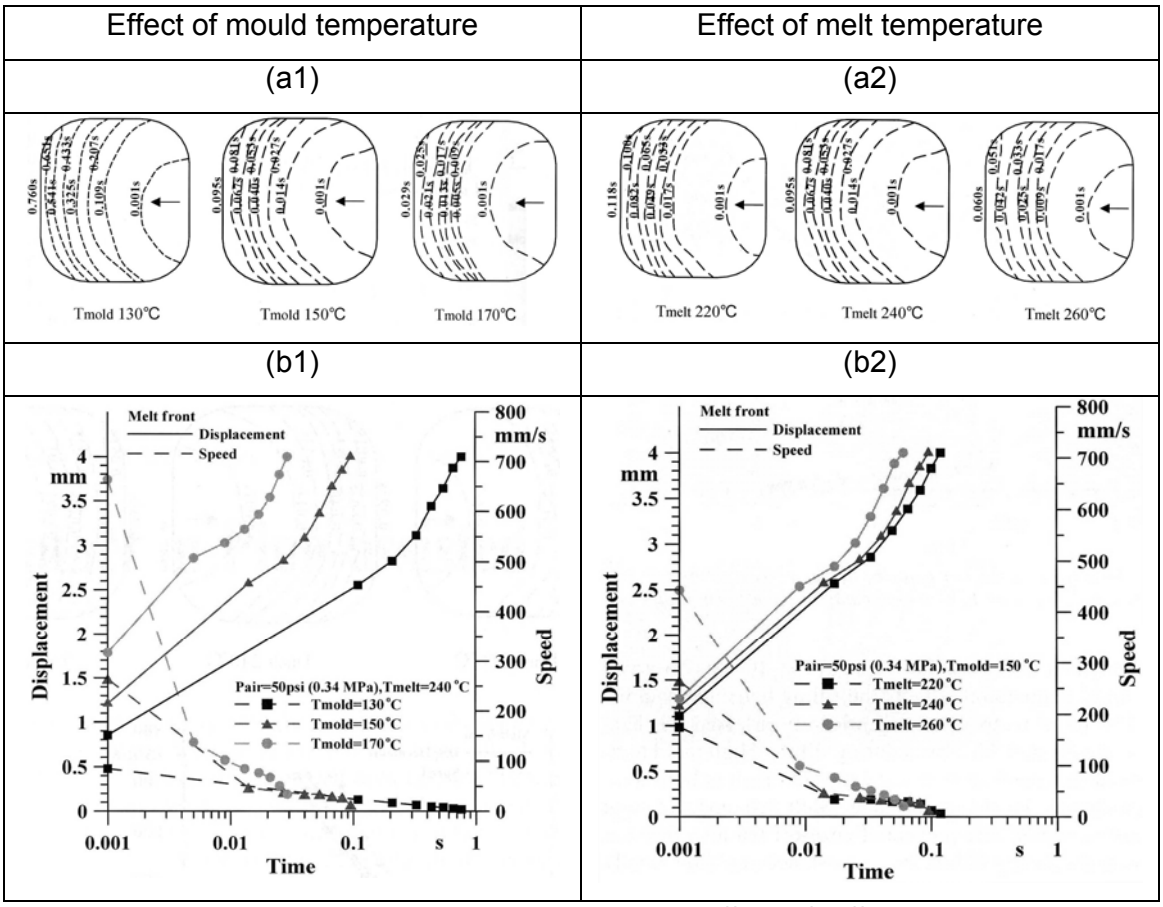

Figure 12 – Filling analysis during micro injection: effect of different mould and melt temperatures on the advancements of the melt fronts (details (a1) and (a2)) and on the injection cavity speed and time (details (b1) and (b2)) [Yang, 2002].

3.1.1.3 Length flow tests

Length flow tests are used to evaluate the filling capacity of the moulding system in terms of flow length in the cavity and aspect ratio. Usually a test cavity having constant cross section and a dominant dimension parallel to the flow front advancing direction is used for the purpose; typically, aspect ratios above 10 are desired [Sha, 2007]. A downscaled version of such approach, commonly employed on conventional injection moulding, has been proposed for the investigation of filling behaviour and processability during micro injection moulding of semi-crystalline polymers (polypropylene and polyoxymethylene) as well as amorphous polymer (acrylonitrile-butadiene-styrene). Investigations were first carried out by moulding under different process factors affecting the replication capabilities and the filling performance of the process. Then, the achieved flow lengths in miniaturized channels, defined as the actual length reached by the melt during the moulding, are determined and compared in order to establish the relation between flow lengths and process parameter settings.

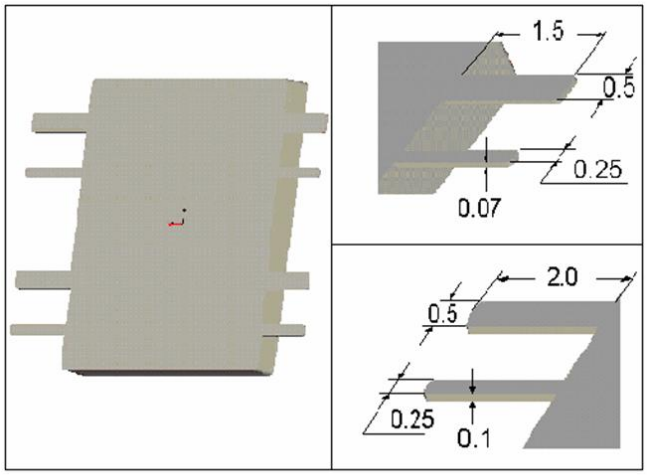

Figure 13 – Part design for a process analysis based on a flow length test [Sha, 2005].

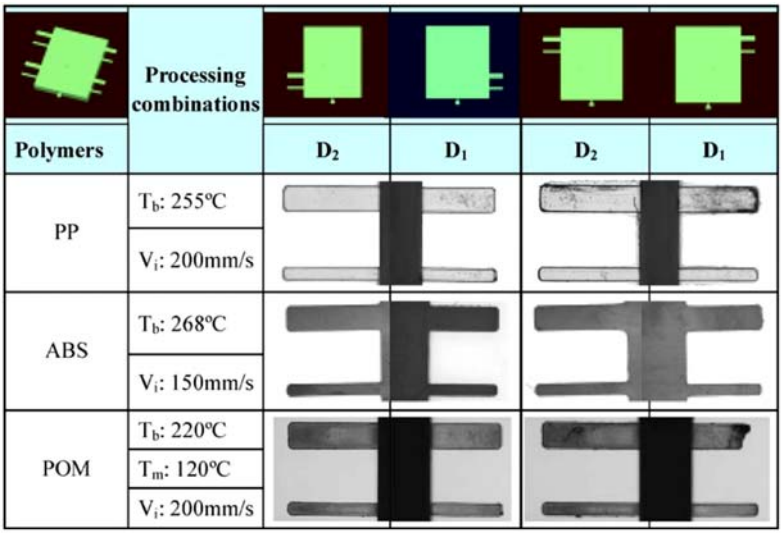

Figure 14 – Flow length evaluation of micro injection moulded features for different polymers (PP, ABS and POM) and different thicknesses (D1 = 100 µm , D2 = 70 µm) [Sha, 2007].

3.1.2 Filling analysis in µIM using weld lines as flow markers

In injection moulding, during the filling of cavities, when two or more flow fronts meet, an imperfection observable as a line is created. This defect of injection moulded parts is referred to as a weld line. Weld lines are influenced by material composition, mould design and process conditions [Wu, 2005]. Particularly related to mould design, the basic situations that conduce to the weld lines formation are the presence of [Fellahi, 1995]:

- Inserts in the cavity.
- Two or more gates for the part filling.
- The presence of regions of varying depths.
- Features in the mould (e.g. pins all through the thickness of the cavity).

Weld lines are visible on the surface of the part (their depth was measured with the atomic force microscope and found to be in the range between 500 nm to 1500 nm [Tosello, 2007(1)]) and they are a clear trace of the development of the flow melt during the filling of the cavity (see Figure 16). In the following, the analysis of the filling stage in micro injection moulding using the weld lines as flow markers is presented [Tosello, 2007(2)] [Tosello, 2007(3)].

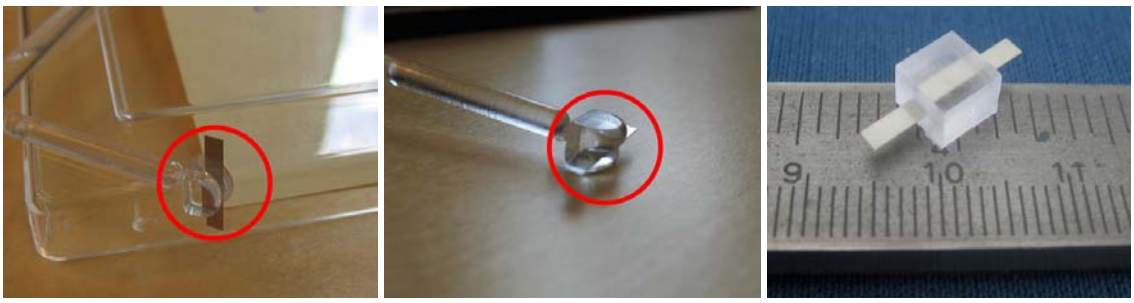

(a) (b) (c)

Figure 15 – Weld lines formation due to the presence of an insert in the cavity during insert moulding (a)(b) and complete insert moulded part (c) (see section 7.2.3 for manufacturing description).

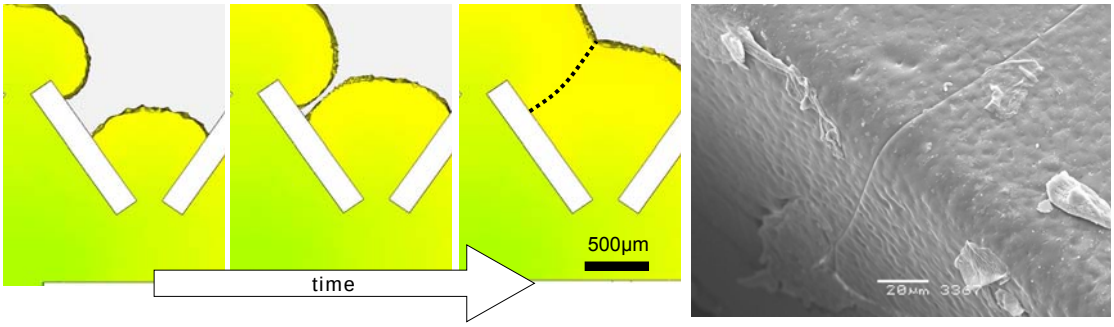

Figure 16 – Simulation of the formation of a weld line due to the presence of a micro feature (width = 200 µm) in the cavity (left). Scanning electron microscope images of the actual weld line shown in the simulation (polymer = polystyrene) (right).

3.1.3 Experimental

In this paragraph the experimental implementation and investigation for the analysis of the filling of micro injection moulded parts are presented. In particular, section 3.1.3.1 describes the design and the manufacturing of the micro cavity, sections 3.1.3.2 and 3.1.3.3 present the design of the experiments technique and its implementation on the injection moulding process respectively. Sections 3.1.3.4 and 3.1.3.5 deal with the dimensional measurement of the weld lines path and the measuring uncertainty estimation respectively.

3.1.3.1 Micro cavity design and manufacture

A micro-cavity has been manufactured by µEDM (Electro Discharge Machining) with a special design specifically developed to exalt the formation of weld lines (see Figure 17). The main objective of the micro part design was to create an effective response variable related to the weld line formation. The micro EDM process allowed for the machining of accurate features in the micro dimensional range: channels as wide as 150 µm, 200 µm, 300 µm, 450 µm and 600 µm were obtained. The thickness of the part was 250 µm. The plateau placed in the middle of the cavity had a thickness of 150 µm. Average surface roughness (Ra) was measured and resulted in a value of 0.15 µm.

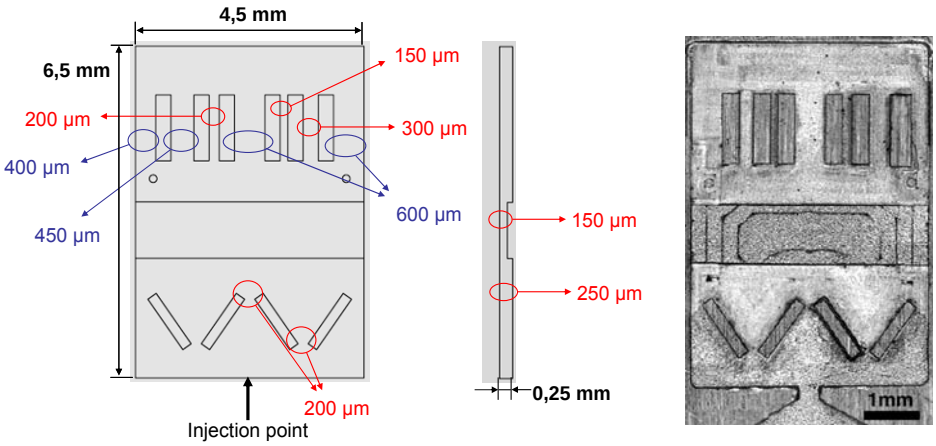

Figure 17 – Micro part design (right) and micro cavity machined by µEDM (left).

3.1.3.2 Design of experiments

The design of experiment (DOE) procedure is used to systematically investigate process or product variables that influence the quality of products. It is possible to identify the process conditions and product components that influence product quality and costs, which in turn enhance the product manufacturability, quality, reliability and productivity [Park, 2004]. Factorial design is frequently used in experiments involving several factors where it is necessary to study single factors effect and joint effect of the factors on a response (i.e. main effect and interactions).

Although the DOE technique is not suitable to explore a wide region in the factor space completely, the method can indicate major trends and so determine a promising direction for further experimentation [Zhao, 2003].

Within the application of DOE, two different approaches can be distinguished [Montgomery, 2001]:

- Full factorial design, widely used in experiments involving several factors where it is necessary to study the joint effect of the factors on a response.
- Fractional factorial design, which are employed to reduce the experimental effort on large DOEs. If it can reasonably assumed that high-order interactions are negligible, information on the main effects and low-order interactions may be obtained by running only a fraction of the complete factorial experiment. These fractional factorial designs are among the most widely used types of designs for product and process design, for process improvement and in screening experiments. In a manufacturing environment such as injection moulding, with processes based on physical phenomena (i.e. thermo-mechanical process), third-order interactions and above can be considered as negligible [Del Vecchio, 1997].

To investigate the influence of process parameters on the weld lines formation in a micro cavity, a series of statistically designed experiments have been carried out.

Experimental planned investigations are widely used as a method to investigate process phenomena in injection moulding and they contemplate the methodical variation of processing conditions to obtain the characterization of the weld lines.

A full factorial design of experiment was implemented in order to consider all kinds of main effects and interactions. In particular the two-level full-factorial design method was used in the DOE studies.

The DOE procedure consisted of the following three steps:

- Planning: definition of the input/output variables and development of the experimental plan.
- Screening: individuation of the parameters which mostly affect the position of weld lines.
- Measuring uncertainty implementation: identification and estimation of sources of uncertainty and analysis of DOE results.

In order to analyze the results of the experimental designs, analysis of variance (ANOVA) was utilized. The ANOVA is used to investigate the relationship between a response variable and one or more independent variables. It can be determined if the difference between the average of the levels is greater than what could reasonably be expected from the variation that occurs within the level.

3.1.3.3 Experimental micro injection moulding

Four different process parameters were varied in order to determine their influence on the micro injection moulding process:

- Melt temperature (Tmelt);
- Mould temperature (Tmould);
- Injection speed (InjVel);
- Packing pressure (Ppack).

A four-factor two-level full factorial design has been carried out performing 2^4=16 moulding experiments (each factor being varied between two levels) (see Table 1 and Table 2). In this way the influence of main effects as well as interactions were evaluated.

Five replications (i.e. five injection moulded parts, see Figure 18) were produced for each of the sixteen moulding experiments. Parts were selected from the production batch after a stable process was obtained. The employed machine for the injection moulding experiments was a conventional injection moulding machine (Ferromatik Milacron K60, see machine characteristics in Table 3) with a reciprocating screw of 32 mm of diameter and a clamping force of 500 kN.

Factors' levels were established with the aim of keeping a realistic industry relevant perspective. In particular:

- Mould temperature was controlled using temperature sensors placed in the mould and set according to specifications given by the material supplier.
- Melt temperature was implemented as barrel temperature. Upper and lower levels were set taking into account recommended values published by the material supplier.

- The minimum level of injection speed was set to assure the complete filling of the cavity, whereas the maximum level was set taking into account the machine's capability and set to 70% of the maximum injection speed limit.
- Packing pressure was set as 8.5% and 85% of the maximum hydraulic pressure (120 bar, corresponding to 180 MPa at injection location).

Polystyrene (BASF PS143E) was employed as polymer material. Polystyrene is a relevant polymer in micro injection moulding for its very high flowability, good biocompatibility, and high transparency.

Process parameters	Low level	High level
Melt temperature	240 °C	270 °C
Mould temperature	45 °C	70 °C
Injection speed	200 mm/s	350 mm/s
Packing pressure (hydraulic)	10 bar	100 bar

Table 1 – Process parameter settings.

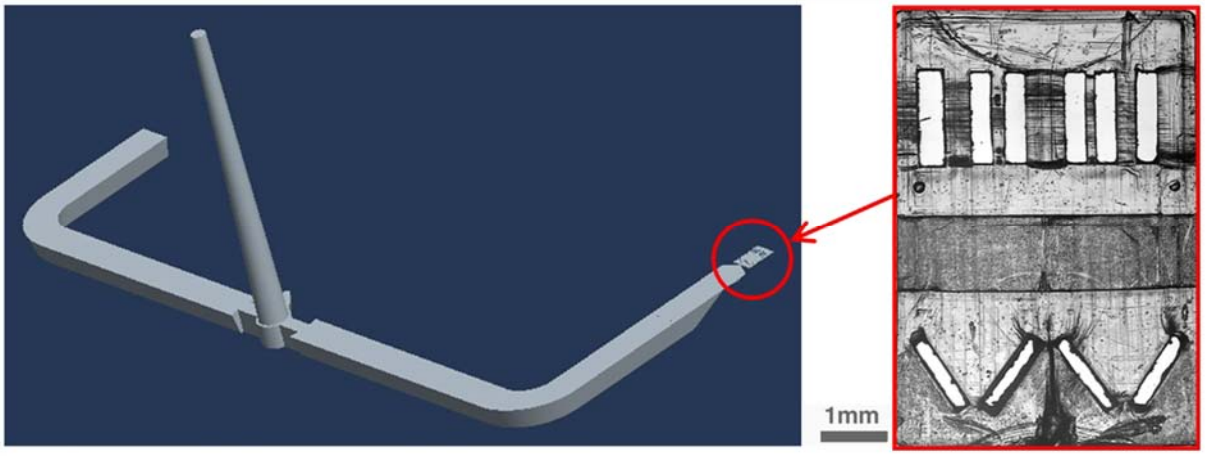

Figure 18 – Sprue, runners and part (left); detailed view of the injection moulded part (right).

Run Order	Tmelt	Tmould	Ppack	Vinj
1	1	1	1	1
2	1	1	-1	1
3	1	1	1	-1
4	1	1	-1	-1
5	-1	-1	1	1
6	1	-1	-1	1
7	1	-1	1	-1
8	-1	-1	-1	-1
9	1	-1	1	1
10	-1	-1	-1	1
11	-1	-1	1	-1
12	1	-1	-1	-1
13	-1	1	1	1
14	-1	1	-1	1
15	-1	1	1	-1
16	-1	1	-1	-1

Table 2 – Four-factor two-level full factorial design of experiments employed in the investigation.

Machine characteristic	Unit	Value
Clamping force	[kN]	500
Injection screw diameter	[mm]	32
Length of screw	[L/D]	15
Number of revolutions (screw)	[min^{-1}]	450
Maximum torque	[Nm]	190
Maximum injection velocity	[mm/s]	500
Maximum pressure (hydraulics)	[MPa]	15
Maximum pressure (plastic)	[MPa]	250
Stroke length for injection screw	[mm]	70
Ejector force	[kN]	33,1
Cylinder capacity	[cm^3]	2,694
Heating zones	[Quantity]	4

Table 3 – Ferromatik Milacron K60 injection moulding machine characteristics.

3.1.3.4 Weld lines path measurements

The characterization of the weld lines was carried out by means of two-dimensional measurements for the geometrical determination of their shape on the surface of the micro injection moulded components. Position and orientation of the weld lines have been investigated by means of an optical CMM (coordinate measuring machine) (see Figure 19, left).

To describe the shape of the weld lines, an accurate and repeatable measuring procedure of the weld lines path on the surface sample was required. This was obtained by using both a repeatable alignment strategy of the workpiece in the measuring workspace of the machine (see Figure 19, right), and successively by defining a repeatable local alignment systems integral with the considered micro features (see Figure 20, left).

Optical measurements of points located on the weld line paths were executed by collecting X coordinates measured at pre-determined values of Y coordinates (see Figure 20, right). Hence, it has been possible to attribute numerical values to position (X and Y coordinates) of the weld lines and then relate the measurements to the level of the process parameters in a subsequent analysis step.

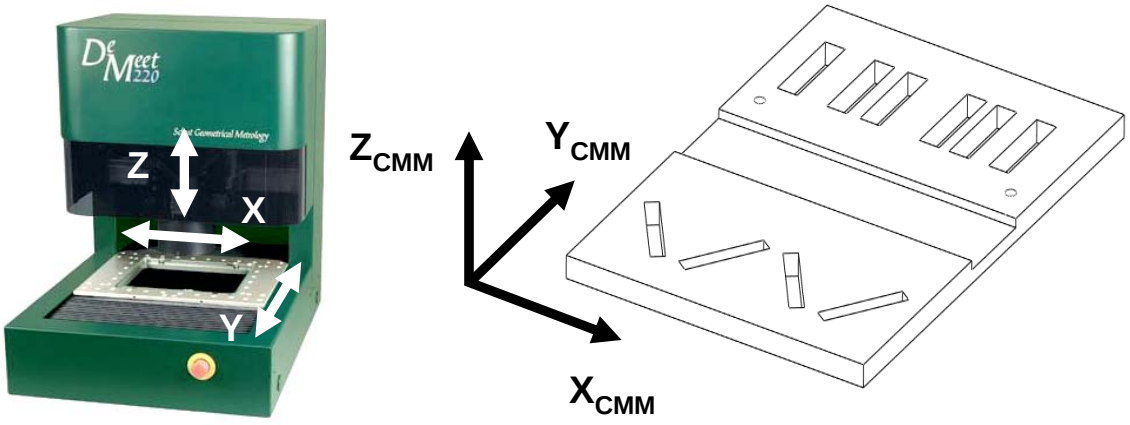

Figure 19 – Optical coordinate measuring machine (CMM) (left) and micro injection moulded part aligned to the coordinate reference system of the machine (right).

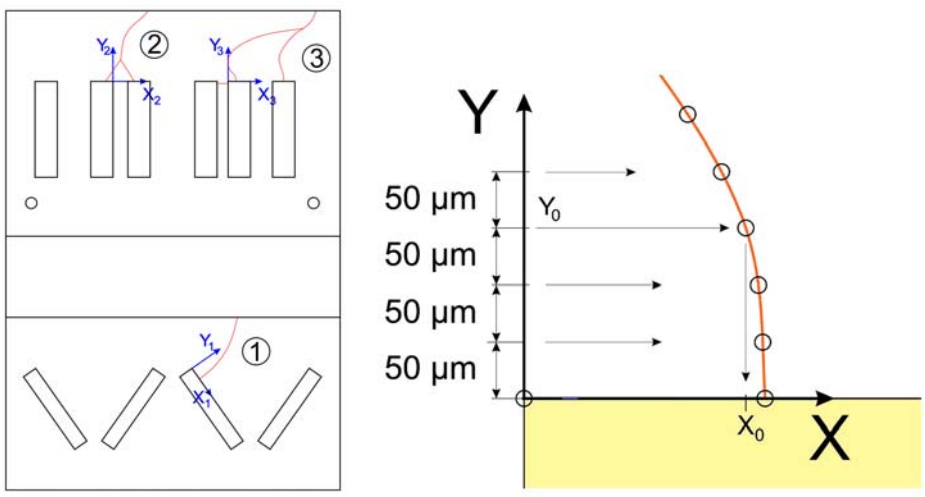

Figure 20 – Micro features coordinate reference system (left) and measuring strategy to determine the coordinate of the points (right).

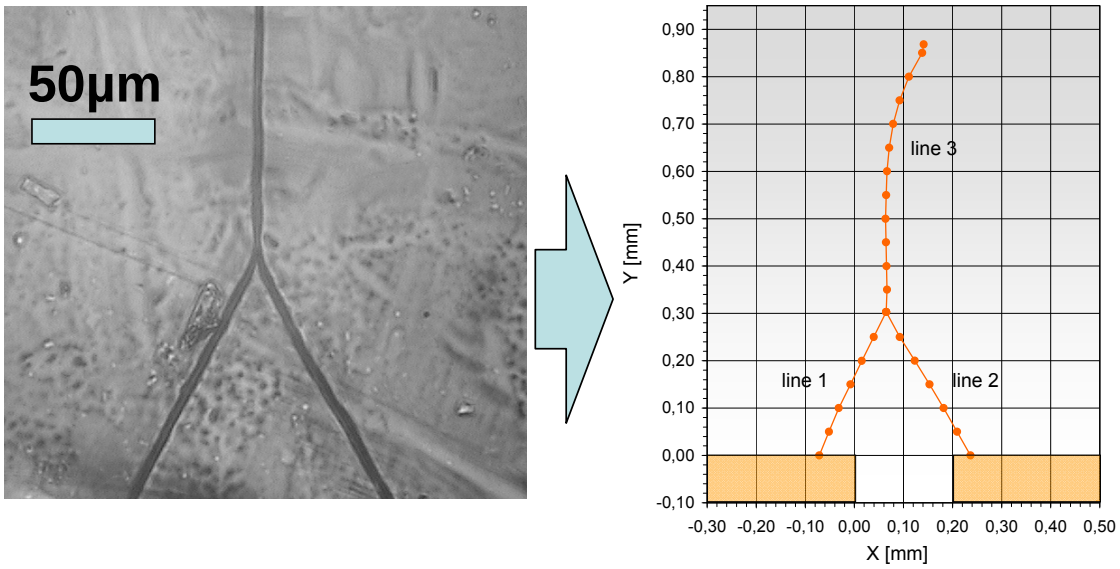

Figure 21 – Visualization of weld lines on the surface of the micro moulded parts (left) and measuring result (right).

3.1.3.5 Measuring uncertainty

An uncertainty assessment has been carried out in order to verify the quality of the measurements. The uncertainty of measurement (U) is a parameter, associated with the result of a measurement, which characterises the dispersion of the values that

could reasonably be attributed to the measurand [ISO, 1993]. Depending on the considered output for the analysis, the uncertainty of the measurements can create a spread of the measurements which can partially/totally hide the effect of the experimental factor on the response. It was therefore important to assess the uncertainty of the measuring equipment and of the procedure.

To calculate the uncertainty of a measurement, the identification of sources of uncertainty is needed. The uncertainty of a measuring process will be the combination of the standard uncertainty to each of the error contributors. The standard uncertainty represents the estimated standard deviation of a measure (dispersion of several measures of the same quantity around a mean value), due to the influence of an uncertainty source. The estimation of uncertainty from each source has to be carried out.

The standard uncertainty can be assessed by Type A evaluation and Type B evaluation [ISO, 1999].

The Type A evaluation of standard uncertainty can be applied when several independent observations have been made for one of the input quantities under the same conditions of measurement. Type A standard uncertainty is the estimated standard deviation u, the positive square root of the variance s of the sample.

- Sample variance
  - $s^2 = \frac{\sum_{1}^{n} (y_i - \bar{y})^2}{n-1}$
  - Where:
    - n is the number of measurements
    - $\bar{y}$ is the average of the n measurements
      - $\bar{y} = \frac{\sum_{1}^{n} y_i}{n}$
- Sample standard deviation
  - $s = \sqrt{\frac{\sum_{1}^{n} (y_i - \bar{y})^2}{n-1}}$

- Standard uncertainty for type A evaluation
    - u = s

The Type B evaluation of standard uncertainty is the evaluation of the uncertainty associated with an estimate x(i) of an input quantity X(i) by means of other than the statistical analysis of a series of observations. The standard uncertainty u(x(i)) is evaluated by scientific judgment based on all available information on the possible variability of X(i). Values belonging to this category may be derived from previous measurement data, experience with or general knowledge of the behaviour and properties of relevant materials and instruments, manufacturer's specifications, data provided in calibration and certificates, etc. Type B standard uncertainty is obtained from an assumed probability density function (rectangular, triangular, U-shaped, step, etc.) based on the degree of belief that an event will occur [ISO, 1999] (see Table 4).
To calculate the uncertainty of a measurement, the identification of sources of uncertainty is needed. Uncertainties in a measuring process are in most cases a mix of known and unknown errors from a number of uncertainty sources contributors. Uncertainty contributors in measurement can be classified as follow [ISO, 1995]:

- Workpiece.
- Equipment:
    - Measurement equipment.
    - Measurement set up.
    - Software and calculations.
- Procedure:
    - Measuring procedure.
    - Metrologist.
    - Definitions of characteristics.
- Environment.
- Reference element.

Type	Graphical representation	Equivalent standard deviation	Use
Normal	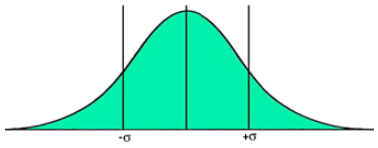	s=σ	When type A evaluations can be shown to follow this distribution
Triangular	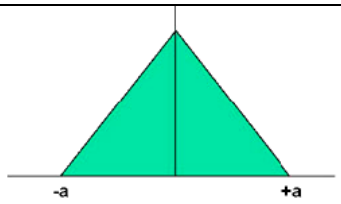	$s = \frac{a}{\sqrt{6}} \approx 0{,}4a$	When “hard limits” can be estimated easier than σ (i.e.: noise, vibrations, etc.)
Rectangular	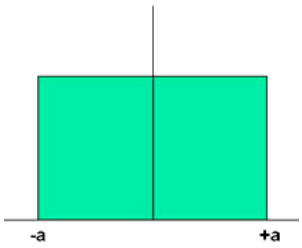	$s = \frac{a}{\sqrt{3}} \approx 0{,}6a$	When only the variation limits are known (i.e.: calibrations certificates, manufacturer’s specifications, etc.)
U-shaped	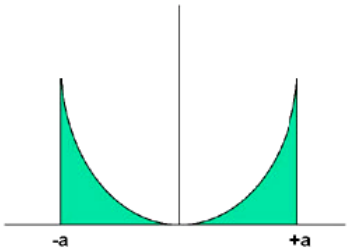	$s = \frac{a}{\sqrt{2}} \approx 0{,}7a$	For cyclic influences (i.e.: temperature variations, etc.)
Step	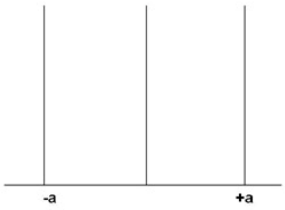	$s = \frac{a}{2\sqrt{3}} \approx 0{,}3a$	When resolution is limited (i.e.: digital readout, Vernier callipers, scale read by operator, etc.)

Table 4 – Probability density function used for type B standard uncertainty evaluation [EA, 1999].

In the specific case presented in this research, different measuring uncertainty sources have been taken into account following the indications given by the standardization body and applied to the employed measuring procedure:

- Repeatability of the measuring process.
- CMM calibration.
- Uncertainty due to temperature variations.
- Resolution of the CMM.
- Repeatability of the injection moulding process.

The uncertainty assessment of the measurements executed with the optical CMM was performed. The considered contributors and the related standard uncertainties in the measurements of the micro moulded part were the following:

- Repeatability of the measurement of both X and Y coordinates [u(rep)] - Repeatability is the closeness of the agreement between the results of successive measurements of the same measurand carried out under the same measuring conditions. In order to assess the repeatability of the measuring process, every weld line of a chosen workpiece was measured 5 times and the whole procedure has been repeated. For every point the standard deviation was calculated. A standard uncertainty due to the repeatability was evaluated for each measuring point; an indicative average value is given:
    - u(rep,X) = 2.8 µm
    - u(rep,Y) = 0.3 µm
- Measuring machine calibration [u(CMM)] – The optical CMM was calibrated using a calibrated glass ruler with parallel lines having a pitch of 100 µm. The calibration range was up to 1000 µm, the same range as the largest length measured on the micro part.
    - u(CMM) = 0.85 µm (both X and Y)
- Temperature [u(temp)] - Influences from temperature, which may be caused by absolute temperature values as well as time and spatial temperature gradients, result in linear expansion, bending, etc. of the measurement setup and the object being measured. For the evaluation of the uncertainty contribution due to the temperature, the following factors have been taken into

account: temperature variations of the measuring room, expansion coefficient of the material α (for polystyrene, $\alpha = 80 \cdot 10^{-6}$ °C^{-1}) and a maximum measured length (conservative assumption) of 1 mm.

- u(temp) = 0.15 µm

- Repeatability of the injection moulding process [U(proc)] – Measurements on 5 different specimens produced within the same batch under the same processing conditions were performed. The standard deviations of the measurements were calculated. For every point the standard deviation is calculated and implemented in a spreadsheet for a punctual uncertainty calculation. Average values were as follows:
  - u(proc,X) = 5.5 µm
  - u(proc,Y) = 2.6 µm

Once all the uncertainty sources have been analysed and the standard uncertainty evaluated for each source, the combined standard uncertainty was calculated. For uncorrelated input quantities (which is the assumption in the case here reported), the combined standard uncertainty $u_c(y)$ is calculated as follows [ISO, 1995].

- Combined standard uncertainty
  - $u_c(y) = \sqrt{\sum_1^n \left(\frac{\partial f}{\partial x_i} \right)^2 u^2(x_i)}$
  - Where:
    - n is the number of uncertainty contributors.
    - f is the model function of the measurement.
    - u(xi) is the standard uncertainty of the i-th uncertainty contributors.

Finally, the expanded uncertainty U was obtained by multiplying the combined standard uncertainty $u_c(y)$ by the coverage factor k. The coverage factor was chosen on the basis of the desired level of confidence. The standard coverage factor k = 2 was used providing a level of confidence of approximately 95%.

Average values of expanded uncertainty for both X and Y coordinates are as follows:

- U(X) = 12 µm
- U(Y) = 6 µm

3.1.4 Analysis of results

The experimental results in terms of weld lines position depending on the process conditions and on the cavity geometry were analyzed. Different analyses were performed and various parameters investigated: one factor at-the-time process analysis (section 3.1.4.1), the effect of micro channel widths on the flow (3.1.4.2), statistical analysis to characterize the polymer flow behaviour through micro features (3.1.4.3) and to fill polymer micro components (3.1.4.4).

3.1.4.1 One factor at-the-time process analysis

In order to isolate the effect of one single factor on the response, a one factor at-the-time analysis was carried out. This simple and immediate analysis was performed as follows. Firstly, a reference process parameter set-up was chosen (e.g. the process set-up combination number 8 indicated in Table 2). Secondly, only one factor at once is considered on a different level than the one considered on the reference process parameter set-up. Finally, the response of the reference set-up is compared with the result of the set-up with the varied factor. Therefore, the resulting number of comparisons is equal to the number of factors (see Table 5).

DOE set-up	Tmelt	Tmould	Ppack	InjVel
8 (reference)	-1	-1	-1	-1
10	-1	-1	-1	1
11	-1	-1	1	-1
12	1	-1	-1	-1
16	-1	1	-1	-1

Table 5 – One factor at-the-time analysis.

The different paths of weld lines obtained with the different settings of process parameters are chosen as response and are shown below [Tosello, 2007(2)]. A variation of mould temperature and of injection speed produces modification of the path of the weld lines. Such position variations are clearly distinguished and larger than the calculated measurement uncertainty. On the other hand, variation of packing pressure and of melt temperature does not produce a significant change.

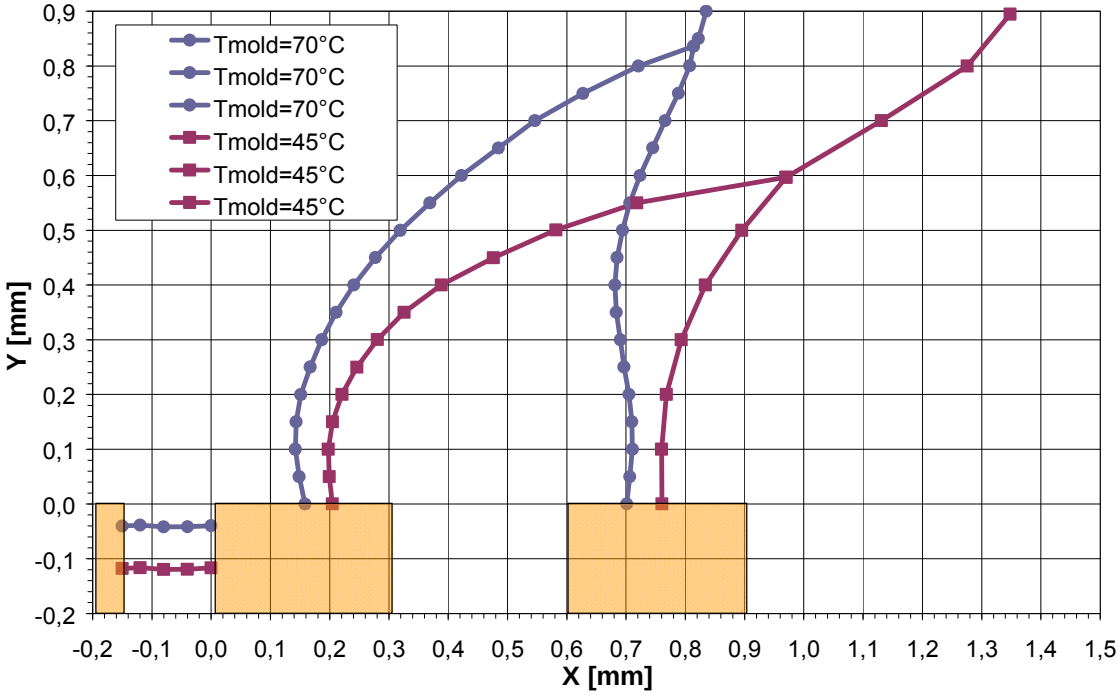

Figure 22 – Effect of the mould temperature variation.

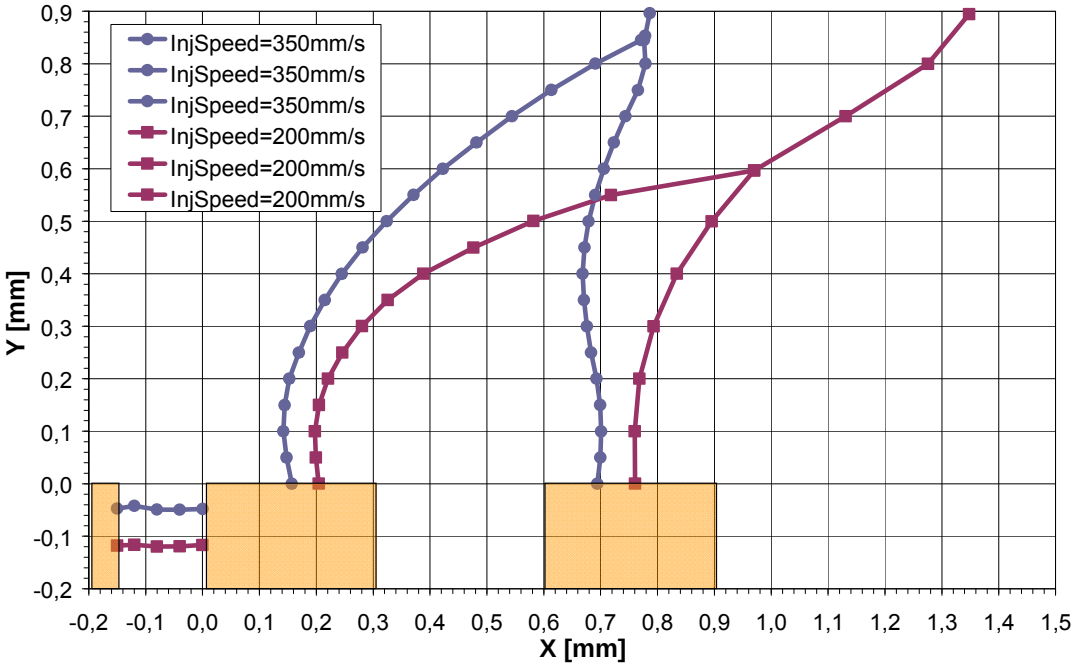

Figure 23 – Effect of the injection speed variation.

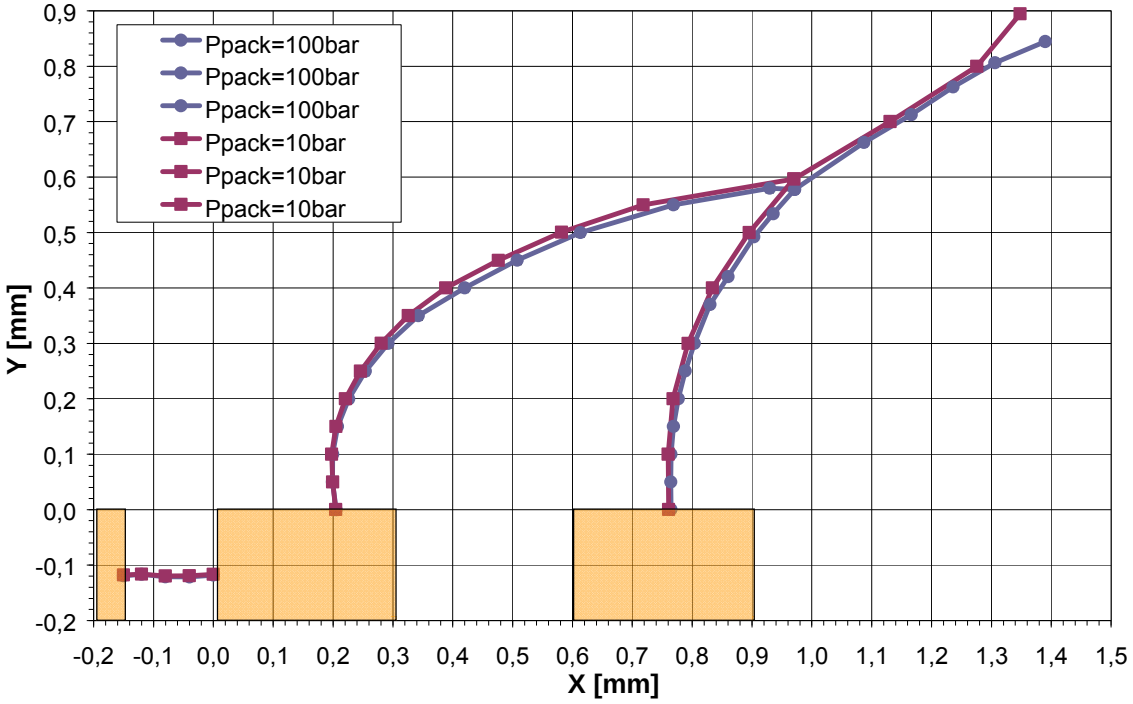

Figure 24 – Effect of the packing pressure variation.

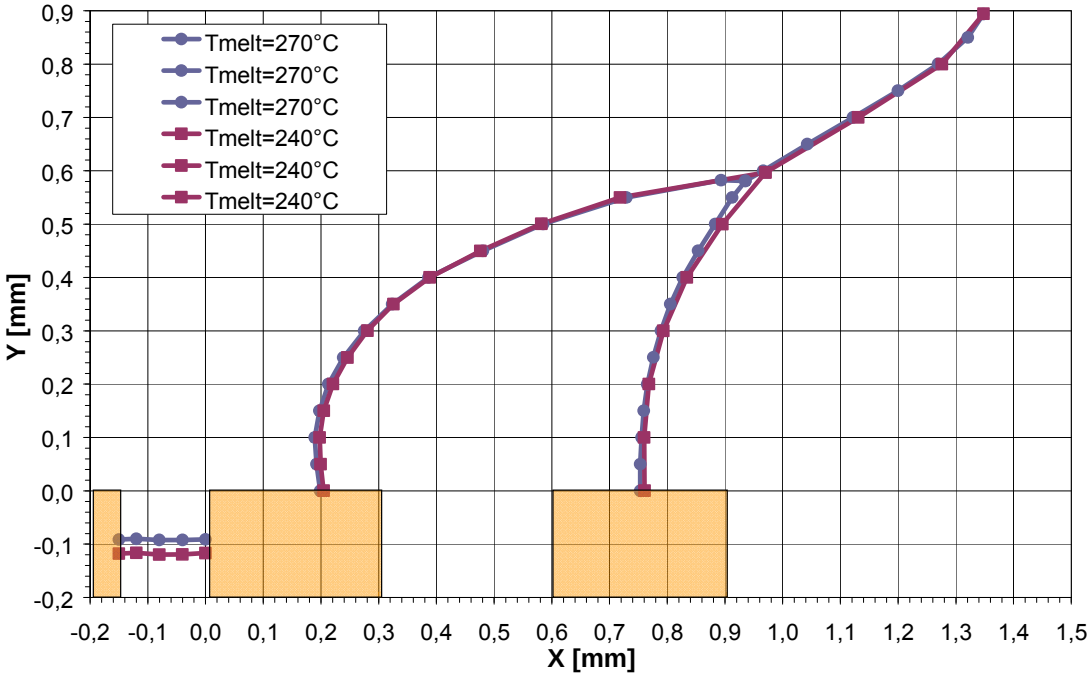

Figure 25 – Effect of the melt temperature variation.

3.1.4.2 Effect of the micro channel width on the flow

The shape of weld lines (i.e. the development of the flow front during the filling of the micro cavity) was found to be influenced by the geometry of the features in the cavity, in particular by their width. In the final part of the cavity, in fact, micro channels of different width were created. By measuring the weld lines path, which represented the flow front path position at the end of filling, it was possible to relate the width of channels and the distance covered by the melt flow towards the end of the cavity (defined as depth of filling) for a given configuration of the process parameters.

The requirement for this analysis is that the flow front after the plateau and at the beginning of the features at the end of the cavity should be as flat as possible (i.e. speed direction parallel to Y direction of the geometry). A typical fountain flow profile would hide the effect of geometry on the side of the cavity, making easier to flow only through central features. In the first half of the cavity (i.e. near the gate) different flow paths are generated having different depth of filling (see Figure 26). To straighten the flow path, a thin plateau was designed and manufactured and it had the effect to create a uniform flow front before entering the second half of the cavity (see Figure 27).

The depth of filling (i.e. the ease of the melt flow to fill micro structures) could be then analysed as function of the width of features. It increases with the width of the structures to be filled. The meeting points of weld lines out of channels 200 µm and 300 µm wide, as well as the horizontal weld line in the channel 150 µm, show such behaviour (see Table 6).

The flow marker method showed also the potential to be used for the validation of software simulation in terms of flow front prediction during the filling of micro cavities (see Figure 28).

Comparison between experimental and simulated weld lines can serve as term of reference to evaluate the accuracy of the simulation results (see chapter 6).

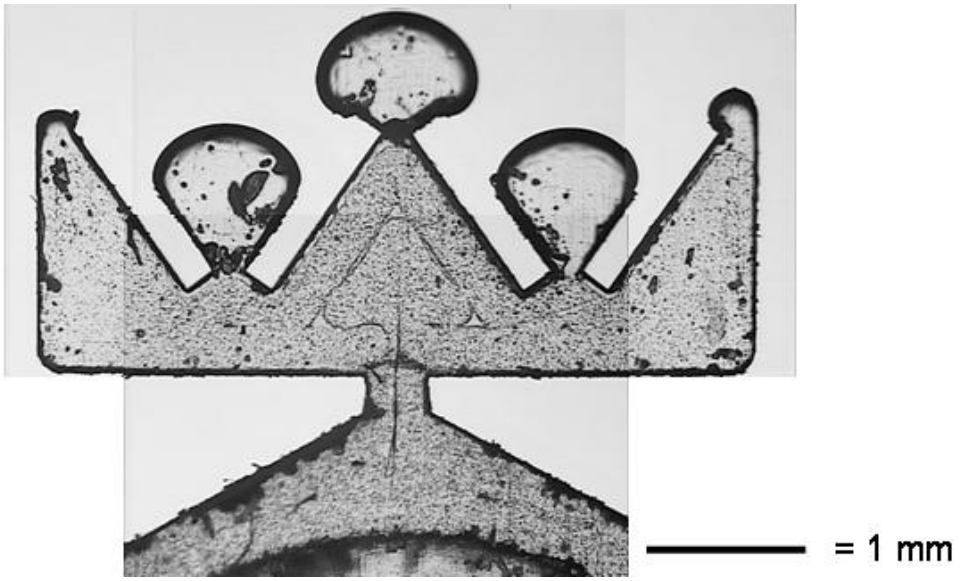

Figure 26 – Experimental short shot showing the flow front shape at the beginning of the cavity filling.

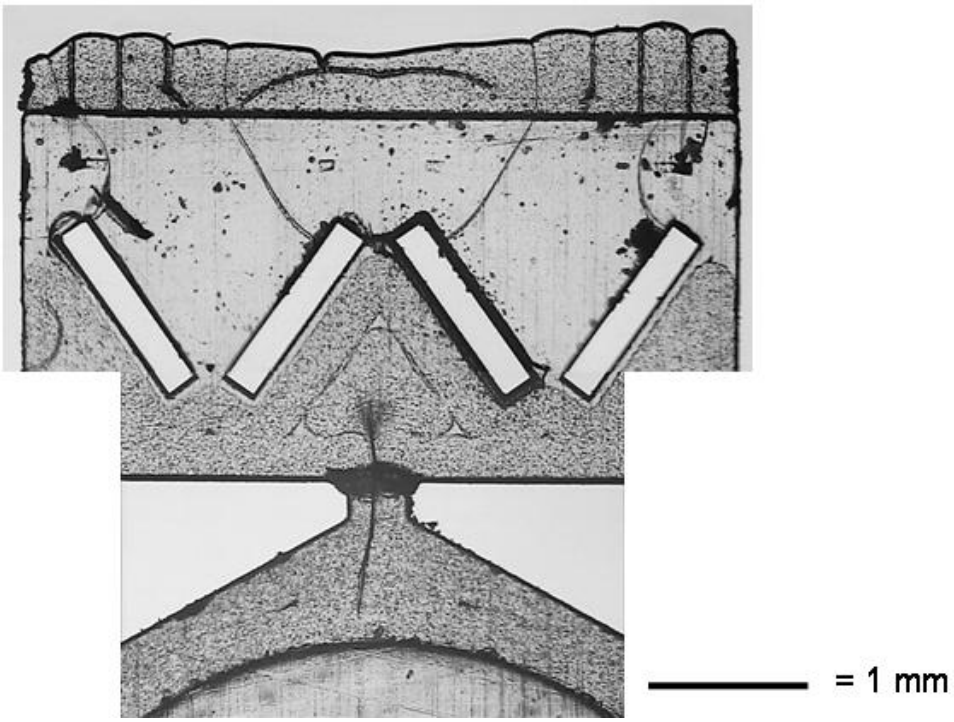

Figure 27 – Experimental short shot showing the flow front straightened by the 150 µm thick plateau.

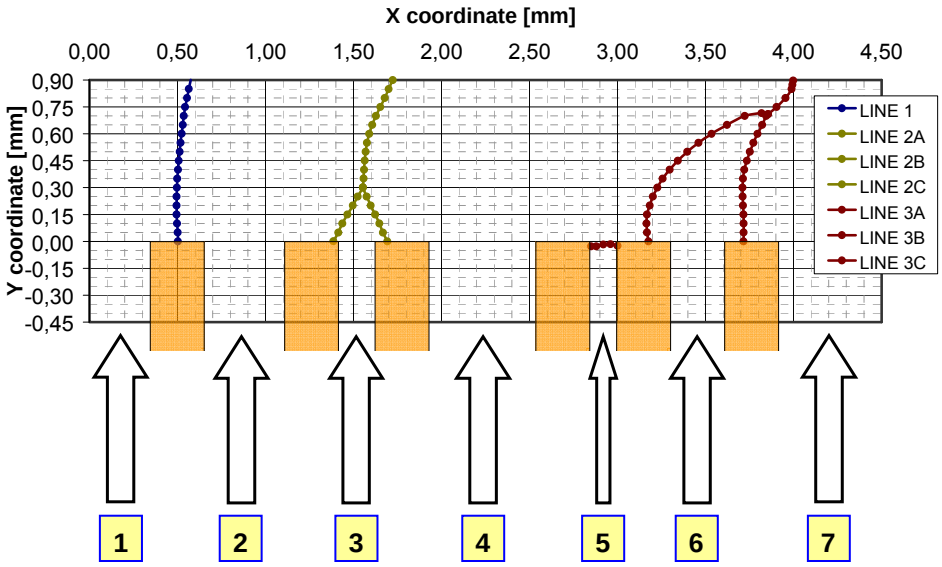

Channel no.	Width [μm]	Depth of filling [μm]	End of cavity
1	400	900	☑
2	450	900	☑
3	200	301	-
4	600	900	☑
5	150	-22	-
6	300	710	-
7	600	900	☑

Table 6 – Experimental depth of filling depending on the channel width.

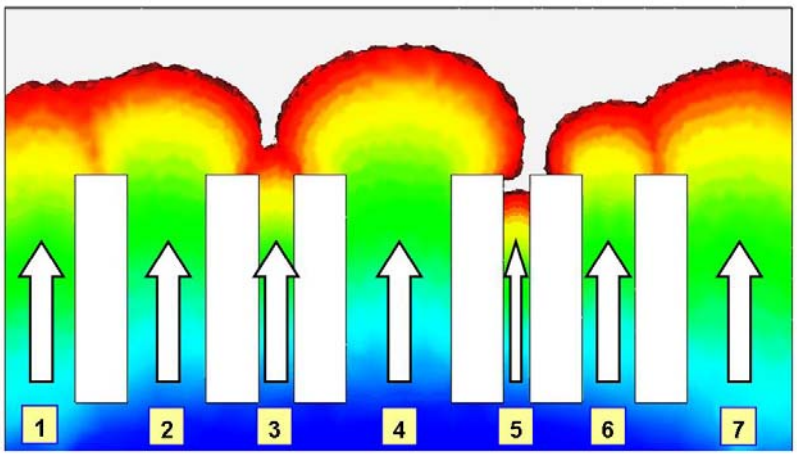

Figure 28 – Simulated flow front pattern to be compared with weld lines used as flow markers.

3.1.4.3 Polymer flow in micro structures

Main effects and two-ways interactions were considered for the statistical analysis of the design of experiment. Main effect plot and Pareto chart were employed to represent which process parameters have a relevant influence on the flow behaviour for the filling of micro cavity. From a manufacturing point of view, it is of great interest to characterize the flow in micro structures and to be able to fill completely miniaturized parts until the end of the cavity. These two crucial aspects were analyzed by considering two different outputs, as described in this section (filling of micro structures) and in the next section (filling of micro parts).

For the optimization of the filling of narrow structures, the weld line created inside the 150 µm wide micro channel was considered (see feature 2 in Figure 29). The factors that lead to a minimum y coordinate (according to the reference system indicated in Figure 29, Y coordinate is negative inside the micro feature 2) will be the factors that enhance the filling capability of the process.

The Pareto chart highlights the most influent factors for this output: injection speed and temperature of the mould (see Figure 30). Effects of the injection speed and of the temperature of the mould extend beyond the reference line (significant at the level of 0.05). The effect of the melt temperature and of the interaction between the injection speed and the temperature are on the limit of significance. All the other interactions are not significant. Moreover, it has to be noted that the effect of the packing pressure is also not significant.

The effect plot of the main factors shows the actual displacement in dimensional unit of the melt flow front due to the different level of the factors. It is interesting to notice that an increase of either the injection speed or the temperature of the mould has the positive effect to extend the filling of the micro feature of 46 µm (see Figure 31).

In Figure 32 the interaction plot for the position of the weld line inside the micro feature shows that the effect of an increase of temperature of the mould at low injection speed is higher of the effect of the same increase of Tmould at high injection speed.

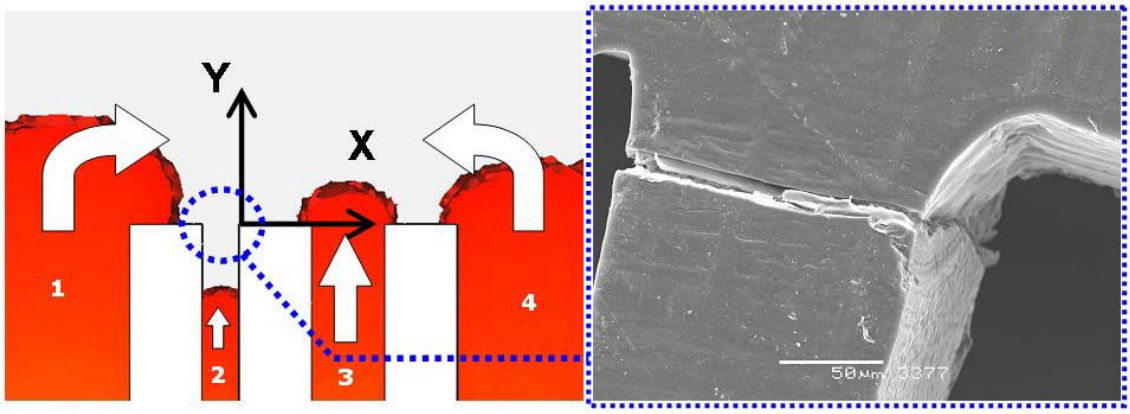

Figure 29 – Layout of weld lines formation in area 3 of the micro moulded part and local reference system (left); SEM picture of the weld lines in the 150 µm wide feature (feature no.2) (right).

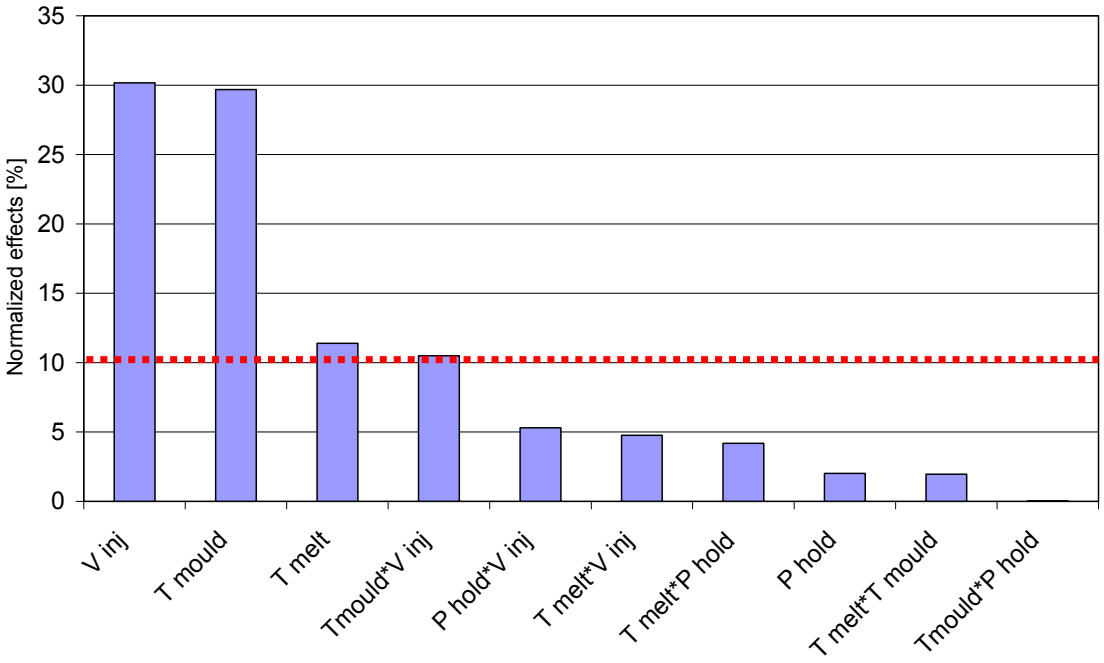

Figure 30 – Pareto analysis of the standardized effects for the analysis of the filling of the micro channel 150 µm wide.

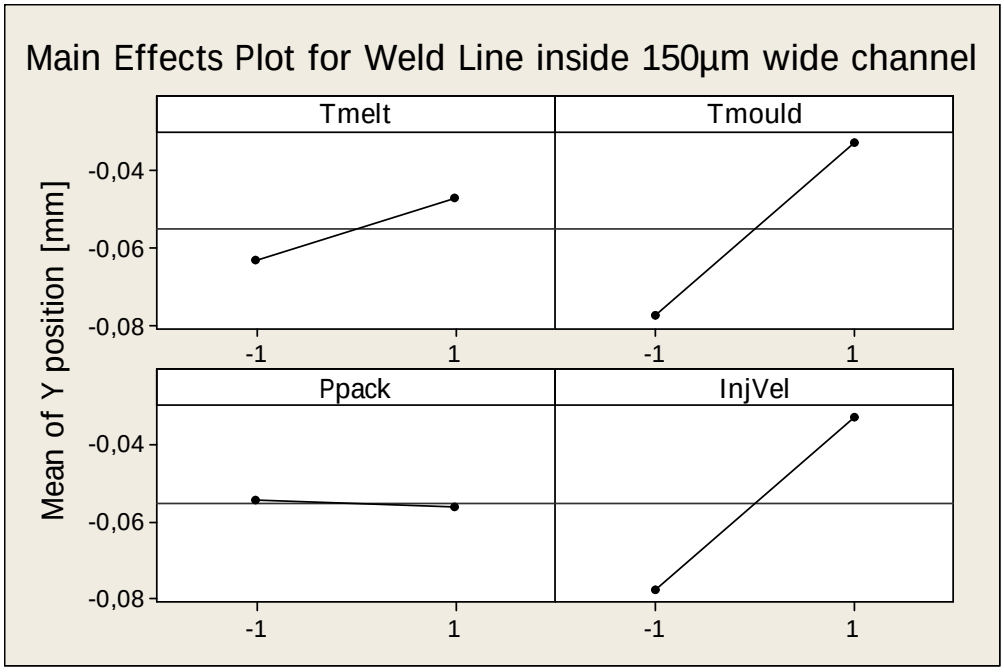

Figure 31 – Main effect plot for the position of the weld line inside the 150 µm wide micro channel.

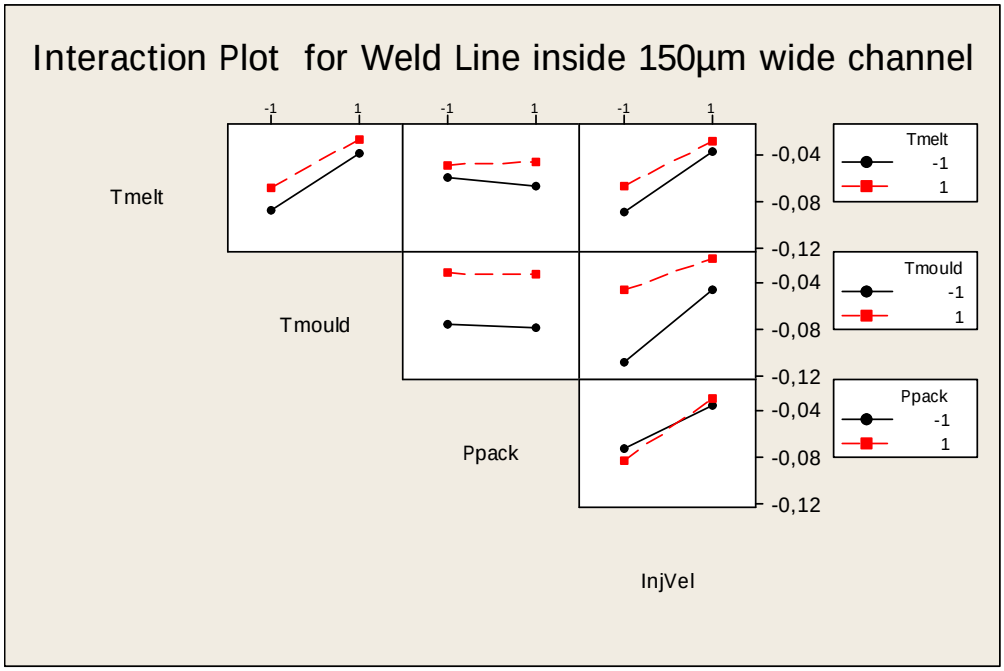

Figure 32 – Interaction plot for the position of the weld line inside the 150 µm wide micro channel.

3.1.4.4 Polymer flow in micro components

Variations of the levels of the process parameters cause changes of the position of the meeting point of weld lines at the end of filling. Hence, the process conditions which improve the flow front path towards the end of the filling of the micro component are investigated (see Figure 33). A particular output was considered for this purpose: the Y coordinate of the meeting point (Ymp) of the weld lines represented in Figure 34. The main factors leading to a maximum Ymp value will be the ones enhancing the filling capability of the process.

The Pareto chart highlights the most influent factors for this output: injection speed and temperature of the mould (see Figure 35). Effects of the injection speed and of the temperature of the mould extend beyond the reference line (significant at the default level of 0.05). All the other interactions are not significant. Moreover, it has to be noted that the effect of the packing pressure as well as of the melt temperature are also not significant.

The effect plot of the main factors shows the actual displacement in dimensional unit of the melt flow front due to the different level of the factors. It is interesting to notice that an increase of the injection speed pushes upward the melt flow front at the end of filling of 202 µm (when passing from the low to the high level). Similarly, an increase of the temperature of the mould has the positive effect to displace the meeting point towards the end of the part (i.e. to extend the filling of the micro part) of 126 µm (see Figure 36).

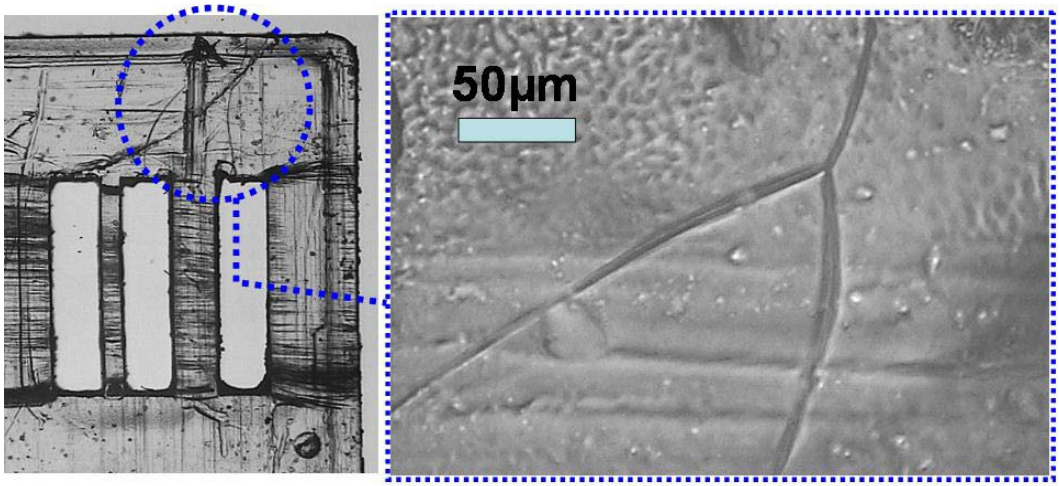

Figure 33 – Optical image of weld lines in area 3 of the micro moulded part.

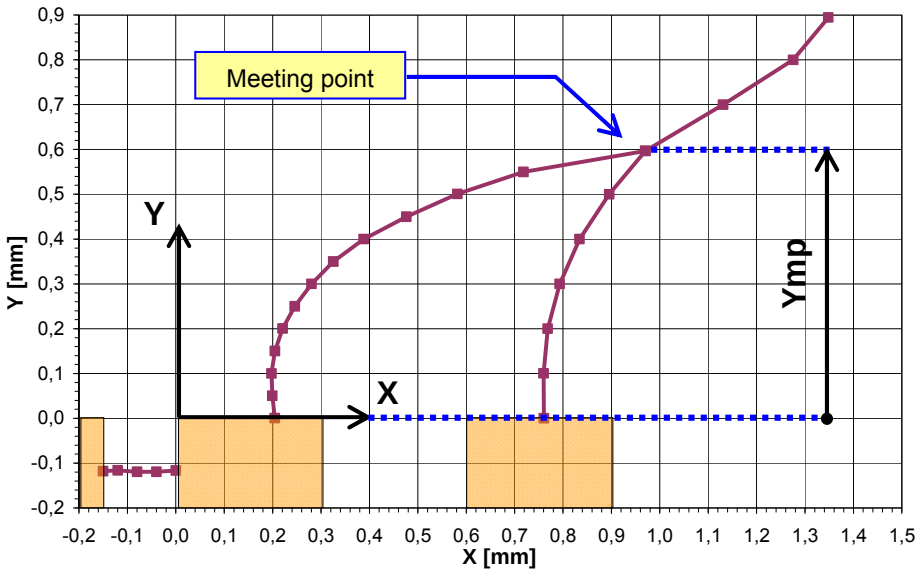

Figure 34 – Weld lines layout and measuring reference system for the evaluation of the melt flow behaviour at the end of filling.

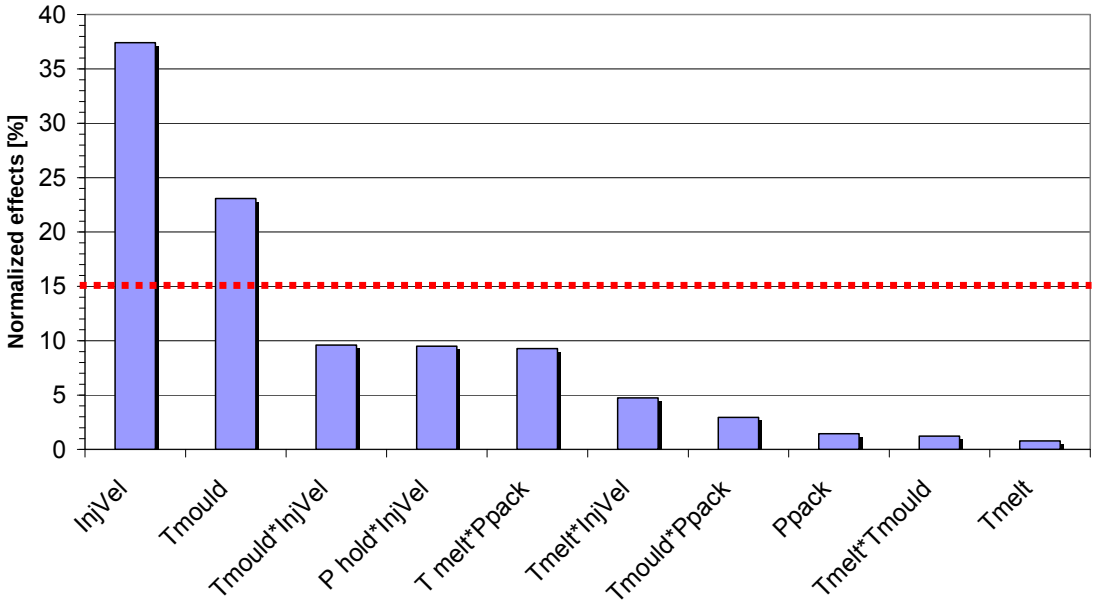

Figure 35 – Pareto analysis of the standardized effects for the analysis of the Y coordinate of the meeting point of weld lines of the polymer micro component.

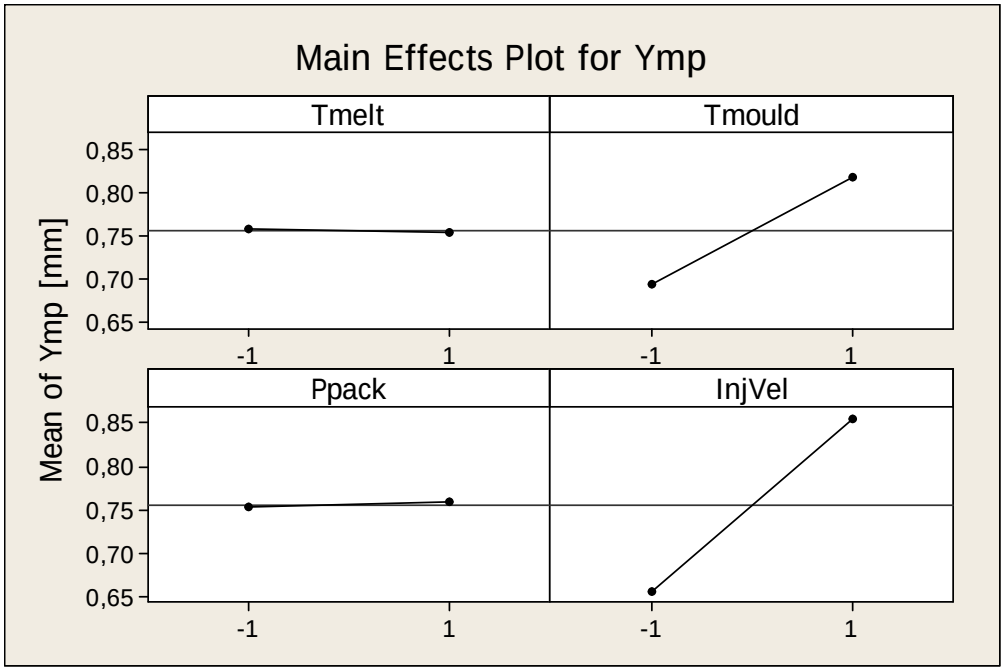

Figure 36 – Main effect plot for the position of the meeting point of weld lines at the end of filling.

3.1.5 Design of Experiment and uncertainty analysis

The dimensional measurements and the quality of measurements are fundamental steps during an experimental investigation in order to obtain reliable data results to be analysed. In micro manufacturing, and especially in the case considered in this project, the following aspects were considered:

- Critical dimensions of the produced micro parts were in the sub-mm range.
- Variations of the position of the weld lines (i.e. of the flow patterns) due to different process conditions were measured to be in the order of 10^1 up to 10^2 µm depending on the location and position considered.
- Measuring uncertainty should be reasonably lower than the effect due to a certain factor variation.

In metrology a tool exists to help deciding what measuring uncertainty should an instrument possess in order to be suitable for a given measuring task. The so-called "golden rule" of metrology, states that the measurement uncertainty shall be less than 10% of the tolerance to be verified. As tolerances become smaller, the "golden

rule" of metrology cannot be fulfilled anymore because the lowest level of available uncertainty is reached. Such lower level is due not only to technological limitation, but it also includes the cost of the measurement. The percentage ratio between the uncertainty and the tolerance can be changed to a margin of 20%, but does not solve the problem [Knapp, 2001]. In case of high accuracy processes, as in the in the field of micro manufacturing, the above mentioned uncertainty limit is reached. Especially in the case of micro parts, uncertainty should be accurately estimated in order to verify that the instrument being used is suitable for sub-millimetre dimensional ranges.

In the case of the design of experiment, uncertainty and dimensional measurements play an important role being the link between the process effects on the part and the numerical data to be analysed. As a consequence, a procedure for uncertainty management capable of implementing the measuring uncertainty in the statistical analysis and to verify its reliability is hereby proposed. The procedure can be summarized in the following steps:

- A number of 5 parts was selected for each of the 16 experiments to carry out all the measurements related to the full factorial design of experiments (see section 3.1.3.3);
- Evaluation the uncertainty of the measurements by applying dedicated procedures [ISO, 1995] [ISO, 1999] (see section 3.1.3.5);
- Definition of a set of parameters able to describe the shapes of the weld lines and consequent statistical analysis (see sections 3.1.4.3 and 3.1.4.4);
- Perform the statistical analysis applying the uncertainty of the measurement. This will be carried out by:
    - Defining a Coefficient of Uncertainty (COU);
    - Analysing the influence of the uncertainty on the Pareto analysis result (both for the effects and the reference line of significance);
    - Applying the uncertainty to the main effects plot.

With very accurate measurements (i.e. low measuring uncertainty) the design of experiment will provide reliable results, being the response in large part consequence of the different process settings. Alternatively, with high measuring uncertainty (i.e. low accuracy measurements), the results will be not only affected by the variability

due to the manufacturing process parameter levels, but also by the large spread induced by the measuring process itself. A balance between these two situations has to be found because the former can lead to a very measuring process expensive (in terms of measuring time, cost of the equipment, etc.). On the other hand, the latter will lead to not reliable results and therefore potentially wrong conclusion based on the analysis.

In this research different scenarios have been investigated, relating the uncertainty value to the actual response of each factor considered in the statistical analysis. For the purpose, a coefficient named COU (coefficient of uncertainty) has been defined in order to decide whether the level of uncertainty was adequate to consider reliable the analysis.

- Coefficient of Uncertainty (COU)
  - $COU[\%] = \frac{U}{|effect|} \cdot 100$
  - Where:
    - U is the expanded uncertainty of the analysed output. The average expanded uncertainty from all the 16 blocks was considered;
    - |effect| is the absolute value of the effect of the considered term.

The COU coefficient has been then implemented into a Pareto analysis and into the main effect plots. In case of a Pareto chart of the normalized effects, uncertainty could also be normalized (U(norm,%)) and applied to each of the normalized effect of each term (E(i)).

- Normalized uncertainty of the effect
  - $U(norm,\%) = \frac{U}{\sum_i E(i)} \cdot 100$
  - Where:
    - U is the expanded uncertainty of the analysed output;
    - E(i) is the effect of the i-th term;
    - i indicates the term and it is comprised between 1 and 10 (4 main factor and 6 two-ways interactions for a total of 10 effects).

The spread of results, due to the measurement uncertainty, produced variations on the value of the reference line (see Pareto analyses in section 3.1.4.3). This was also taken into account. For each of the outputs it was calculated a number of virtual measurements having a Gaussian distribution with average and standard deviation equal to the actual measured value and to the combined standard uncertainty respectively. This was implemented by creating a routine (using the Matlab® software platform) which, given the average, the standard deviation and distribution type, was able to choose randomly an amount of values from the distribution. In this way, 5 virtual measurements were obtained for each output of every weld line of all the workpieces of the whole factorial plan. Hence, 5 virtual and 1 real outputs were used to carry out 6 different analyses. Then the characteristic standard deviation of the design of experiment analysis was determined. In particular, an interval of variability of the reference line was observed.

Finally, all the information could be summarized in an up-to-date Pareto chart of the normalized effects including the following information (see Figure 37 and Figure 38):

- The effects of the terms, ordered depending of their magnitude effect;
- The range of variability of each effect (normalized uncertainty of the effect);
- The percentage COU for each of the terms' effect;
- The variability of the reference line due to the uncertainty of measurements.

3.1.5.1 COU and effect

With this procedure, it was possible to observe that the two main contributors for an optimized filling of micro structures (injection speed and temperature of the mould) had a Coefficient of Uncertainty much lower (12.0% and 12.2% respectively) than the other terms (see Figure 37). Therefore the reliability of the result was proven by a low experimental measuring uncertainty compared to the effect. This is also shown by the fact that the effect, taking into account the uncertainty range, does not intersect the reference line (considered with its variability due to the uncertainty). The two terms with COU just above 30% (temperature of the melt and the interaction between Tmould and InjVel) are now overlapping the reference line range with their

uncertainty bandwidth, resulting in a not reliable evaluation of their effect. All the others term are not significant from a statistical point of view.

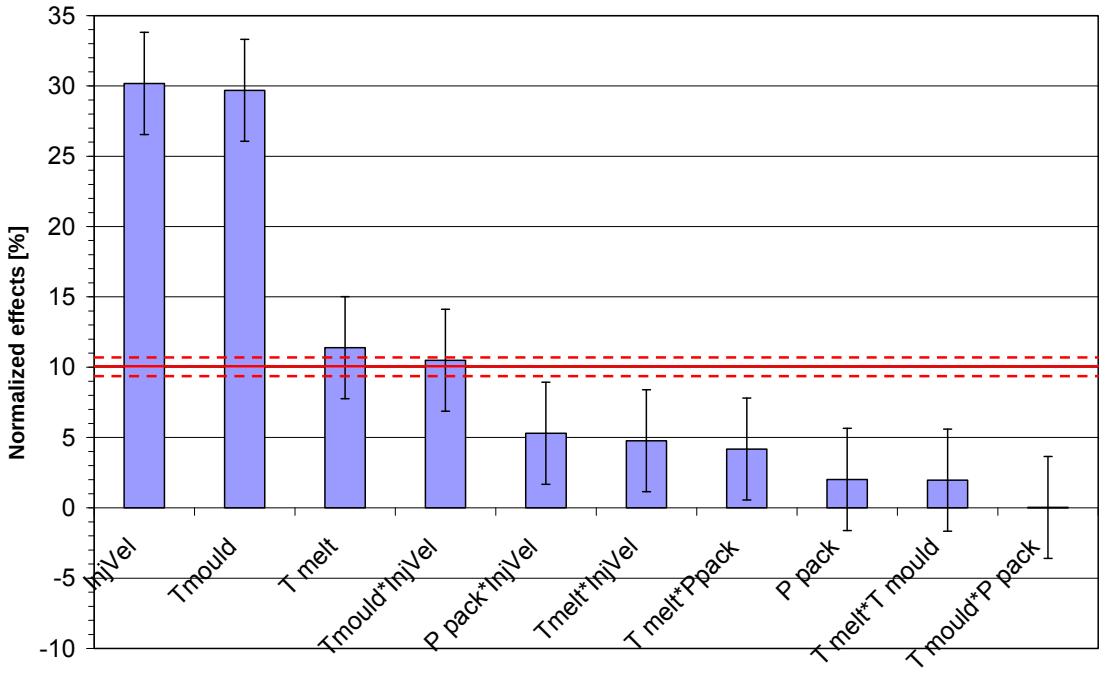

COU [%]	12.0	12.2	31.8	34.6	68.4	76.1	86.7	$>10^2$	$>10^3$	$>10^4$

Figure 37 – Example of up-to-date Pareto chart of the measurements of the melt flow position in the micro channel 150 µm wide [Tosello, 2007(4)].

3.1.5.2 COU optimization

An investigation has been carried out to estimate the optimum COU (and therefore the uncertainty) in order, on one hand, to contain the effort in terms of measuring equipment and procedure, and on the other that still gives reliable results in this particular DOE analysis. A series of DOE analysis has been carried out first with results from the actual measurements (as previously described) and later on by increasing the uncertainty performing a parametric study. The effect of an increase of the measuring uncertainty U (from 14 µm to 40 µm) on the DOE analysis is simulated and shown in the chart depicted in Figure 38.

As a consequence of the increased uncertainty, three distinct phenomena can be observed:

- The COU of a significant factor (Tmould) increases from 11.2% to 31.1% and the effect range partially overlaps the reference line of significance (solid lines represent the range of reference line for the experimental case, dashed lines are related to the simulation).
- The threshold of significance indicated by the reference line increases. A lower accuracy on the measurement brings as consequence a loss of significance of the experiment. It could happen that experimentally significant factors have their effect hidden by the scatter induced by the measurements.
- The range of the reference line increases at the increase of the measuring uncertainty. It makes more probable the overlap between the reference line range and the uncertainty bandwidth, with consequent loss of confidence of the experiment.
- A threshold value of the COU of approximately 25% has been found to be the limit for a significant factor (from a conventional Pareto analysis) before having its effect (enlarged by the uncertainty) overlapping the reference line range (considered with its variability). Therefore, it could be concluded that a COU lower than 25% is a pre-requisite to fulfil in order to obtain reliable and accurate results from the DOE analysis.

3.1.5.3 Uncertainty applied to main effect plot

The measuring uncertainty can also be applied to the main effect plot. This analysis clearly shows that the significant factors with low COU have their uncertainty ranges not overlapping proving the reliability of the result of the design of experiment analysis (see for example Tmould and InjVel in Figure 39).

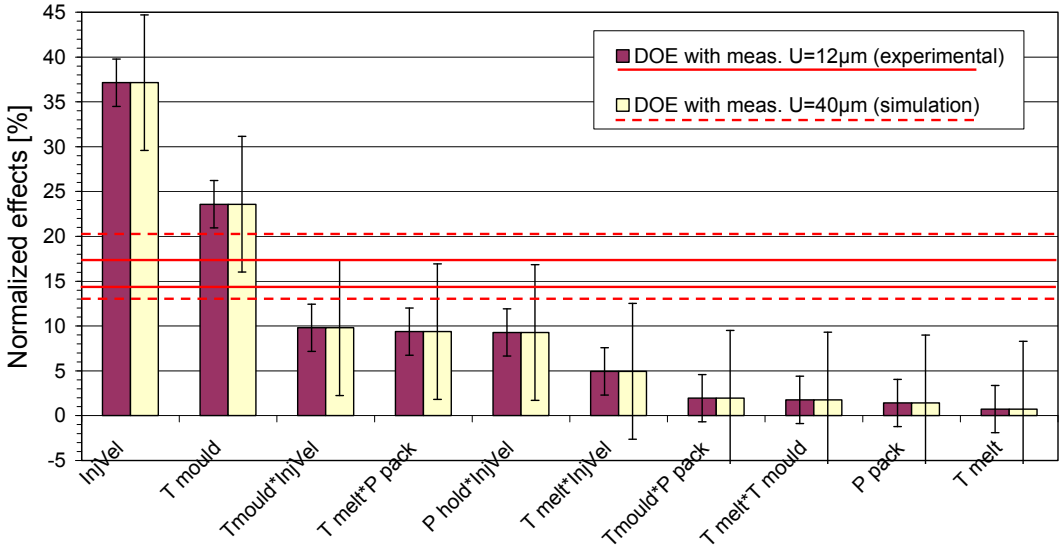

COU		7.1	11.2	26.9	28.1	28.4	53.3	$>10^2$	$>10^2$	$>10^2$	$>10^2$
[%]		20.5	31.1	76.8	81.9	85.7	$>10^2$	$>10^2$	$>10^2$	$>10^2$	$>10^3$

Figure 38 – Example of up-to-date Pareto chart and uncertainty effect on the measurements of the meeting point of weld lines at the end of filling [Tosello, 2007(4)].

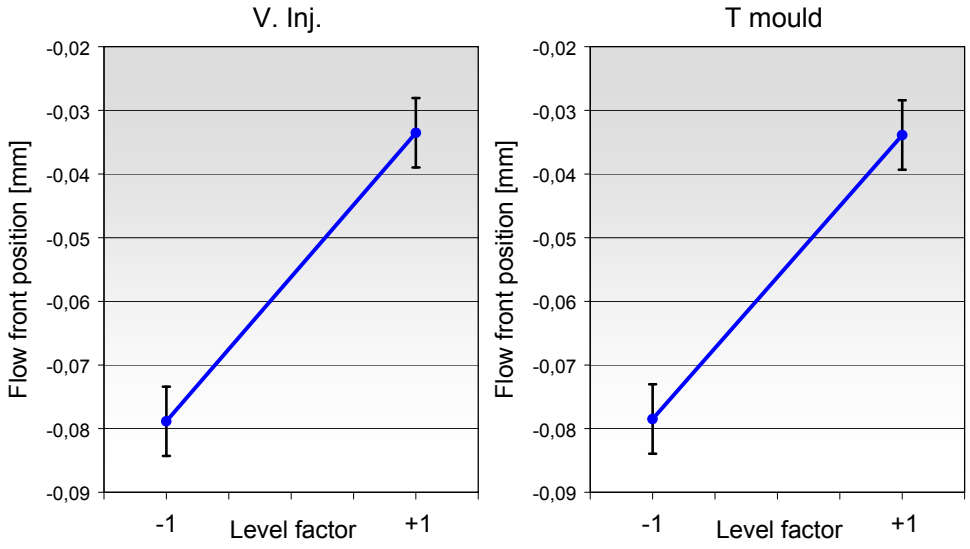

Figure 39 – Uncertainty applied to the main effect plot of the analysis melt flow position in the micro channel 150 µm wide.

3.1.6 Discussion

The result of the statistical analysis is that the final position of the flow front at the end of filling could be extended by increasing the temperature of the mould and the injection speed. On the other hand, increases of temperature of the melt and packing pressure do not influence significantly the filling behaviour.

Hence, it can be concluded that complete filling of micro injection moulded features (i.e. a good filling performance) can be therefore obtained by using a high temperature of the mould (which decreases the viscosity of the melt and prevents premature solidification) and high injection speed (which also decreases the viscosity of the melt due to viscous thinning and viscous heating, as well as decreasing the injection time avoiding premature short shots and incomplete filling).

On the other hand, it is not convenient to increase the temperature of the melt, firstly due to the limited benefit on the filling performance, and secondly to avoid material degradation due to material over-heating. An elevated packing pressure is also not advantageous because it can produce high internal tension on the polymer matrix as well as induce high stress on the mould itself.

The influence of the measuring uncertainty on the reliability of the design of experiments results was also investigated. It was observed that the necessary condition to be fulfilled, in order to obtain reliable results from the analysis of the DOE, is the uncertainty of the employed measuring process being lower than the 25% of the term effect of the most effective factors indicated by the Pareto analysis. The quality of results could be proved also by applying the measuring uncertainty to the main factor plot. It was observed that effect produced by the variation of the significant process parameters (injection speed and temperature of the mould) was larger that the measuring uncertainty, confirming the validity of the experimental implementation and of the metrological framework.

3.2 Micro injection moulding process control and analysis

The reliable manufacturing of polymer-based micro components on a mass production perspective is directly connected to the capability of controlling the micro injection moulding process. A crucial step during the process is the filling of the cavity. It is important to understand the influence of the process parameters on the filling of a micro cavity for the optimization of the process and obtain completely filled micro parts complying with the specifications. Therefore, experimental activity was carried out in order to fully understand the process dynamics during the moulding process performed with a micro injection moulding machine.

The influence of process parameters on µ-injection moulding (µIM) and on µ-injection moulded parts has been investigated using the design of experiments technique (DOE). A mould with a sensor applied at injection location was used to monitor actual cavity injection pressure and to determine the cavity filling time. Flow markers positions were measured on the polymer µ-parts to evaluate filling behaviour of the polymer melt flowing through µ-features.

The aim of the investigation was twofold: on one hand, the characterization of the cavity injection pressure at different process conditions, and on the other, the filling behaviour of the melt into the cavity. For both types of result, studies concerning the absolute value of the output (i.e. cavity injection pressure) and the repeatability of the selected output (i.e. cavity injection pressure standard deviation) were carried out.

This section is structured as follows. In section 3.2.1 the micro injection moulding machine is presented. Section 3.2.2 describes the micro moulded parts and the tool. Section 3.2.3 introduces the experimental plan and the µIM execution. Finally, in sections 3.2.4, 3.2.5, 3.2.6 the cavity injection pressure, the cavity injection time and the flow marker position are analyzed respectively.

3.2.1 Micro injection moulding machine

The employed injection moulding machine (Battenfeld Microsystem50) was equipped with a three stages plastication-metering-injection unit (see section 2.2) particularly suited for micro molding (see Figure 40):

- The first stage includes a 14 mm diameter screw (mounted at an angle of 45°) for the homogeneous preparation of the melt;
- The second stage is represented by a vertical metering piston for the accurate metering of the material to be injected;
- The third stage is the injection chamber where a 5 mm diameter servo-electric-driven piston injects the dose coming from the metering unit directly into the cavity.

The piston was capable of a maximum injection speed of 960 mm/s and it was able to inject until the parting line of the micro cavity. In this way no sprue was attached to the moulded part (see Figure 41). This design feature is particularly suitable for mass production of micro injection moulded components due to the following reasons:

- It allows shorter filling time due to the lower volume to be filled.
- It avoids short shots due to premature melt freezing allowing better micro features replication.
- It decreases the cycle time due to shorter cooling time.

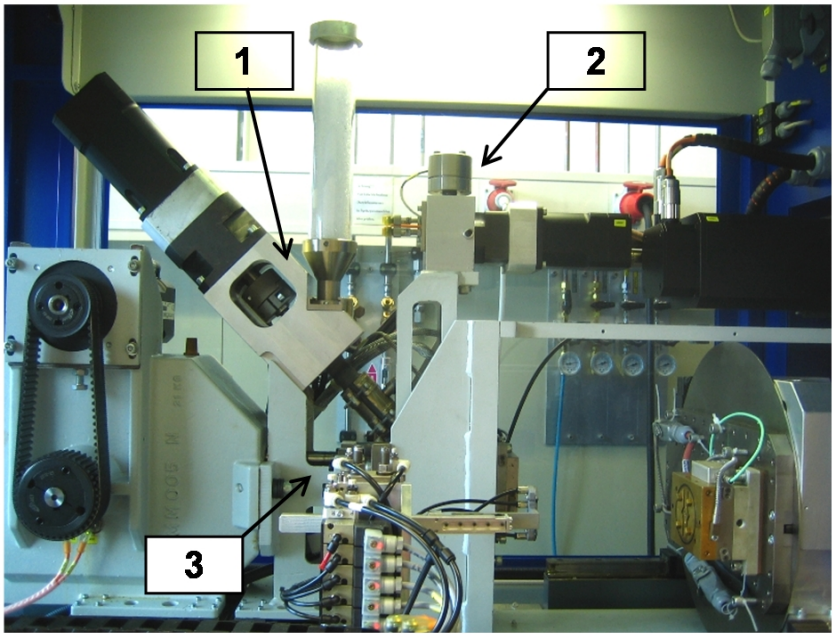

Figure 40 – Micro moulding machine and the three-stage unit: plastication (1), metering (2) and injection (3).

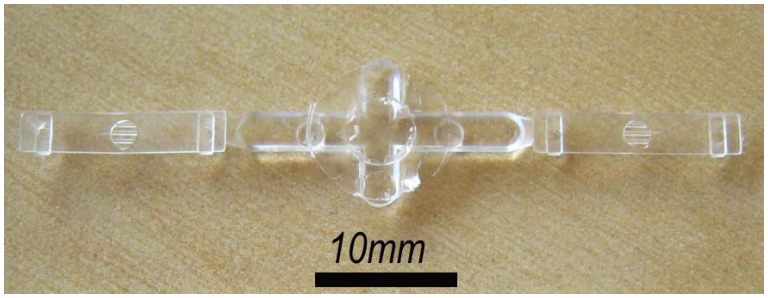

Figure 41 – Micro moulded components and runner systems [Tosello, 2008(1)].

3.2.2 Micro injection moulded part and micro tool

The component chosen for the experiments was a tensile bar test part, shaped as a thin plate (15x3x0.3 mm^3) and including three micro features having semi-circular section (150 µm radius) and lengths from 1500 µm up to 2000 µm (see Figure 42a). The part was moulded with a two-micro-cavity mould (see Figure 43, detail A). The part was moulded using a commercially available polystyrene polymer grade (BASF PS 143E).

The average weight of the complete moulded part was 119mg distributed as follows: 17% for each of the two parts and 64% for the miniaturized runner system. It was calculated that a single micro feature had a weight in the range from 0.14 up to 0.18 mg depending on the length.

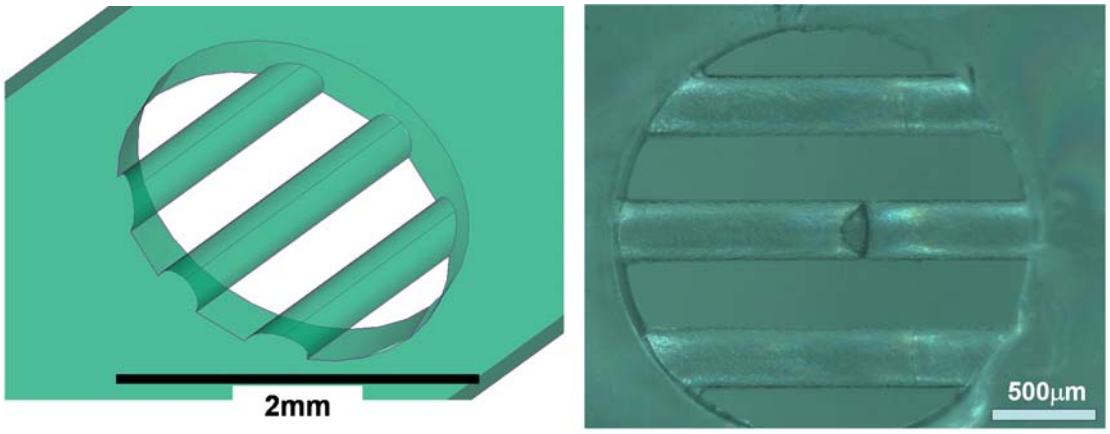

(a) (b)

Figure 42 – Three dimensional CAD model of the 300 µm wide micro features (a) and optical microscope image of the actual moulded micro features (b).

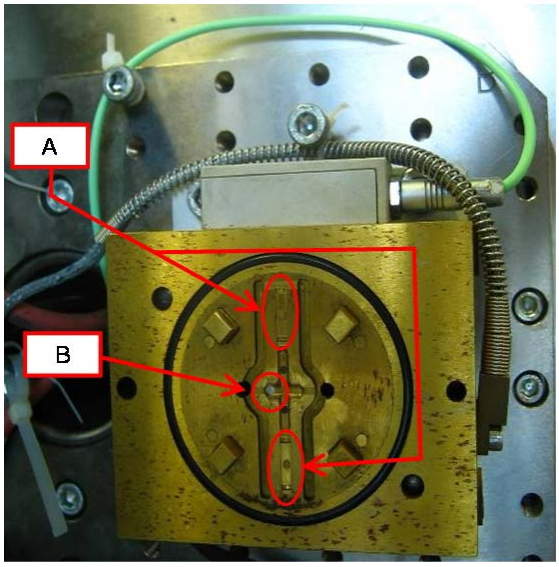

Figure 43 – Two-micro-cavity mould (A) equipped with in-cavity pressure sensor at injection location (B) [Tosello, 2008(2)].

The part design has been especially optimized to obtain weld lines on the micro features during the filling of the parts (see Figure 42b). This revealed to be a very useful feature when flow markers (as weld lines, for example) are employed to investigate filling behaviour of polymer melts.

At the injection location where the melt is pushed into the cavity by the injection piston, a piezoelectric pressure sensor was placed (see Figure 43, detail B). The recording of the in-cavity pressure at injection location over time is one of the methods to monitor conventional and micro injection moulding processes. It allows performing comparative studies on different process conditions and evaluating the process repeatability when moulding in the same process condition. Moreover, especially in the case of micro moulding, it is a powerful method to calculate the cavity filling time which would not be possible by other means since filling of micro cavities takes place in time in the order of tens of milliseconds.

3.2.3 Process parameters settings and execution

The entire process windows for the micro moulding of polystyrene was explored by means of a three factor-three levels full factorial design of experiments for a total number of 3^3=27 experiments (see Figure 44).

Three different process parameters were investigated in order to determine their influence on the micro injection moulding process:

- Melt temperature (Tmelt);
- Mould temperature (Tmould);
- Injection speed (InjVel).

Maximum and minimum values for the three selected process parameters where set taken into machine capability, physical properties of the material, and process feasibility. In particular the following was taken into considerations:

- Tmelt(max) = 260 °C was the maximum temperature before polymer material degradation was observed at plastication stage;
- Tmelt(min) = 220 °C was the lowest temperature allowing the process to be realized, avoiding premature solidification at the injection point, especially at low mould temperature and low injection speed;
- Tmould(max) = 85 °C was set in order to be slightly lower than the glass transition temperature (88 °C) and was therefore the highest temperature which still allowed complete cooling and successful demoulding of the part from the cavity;
- Tmould(min) = 55 °C was the lowest temperature allowing micro feature replication and complete filling of the cavity at the slowest injection speed;
- InjVel(max) = 900 mm/s was limited by the capability of the machine and was chosen close to the maximum injection speed of the machine (approximately 95% of the maximum value);
- InjVel(min) = 100 mm/s was the lowest speed allowing complete filling of the cavity and micro features replication (i.e. to avoid short shots) at low levels of both melt and mould temperatures;
- Intermediate levels were set as average between the minimum and the maximum values.

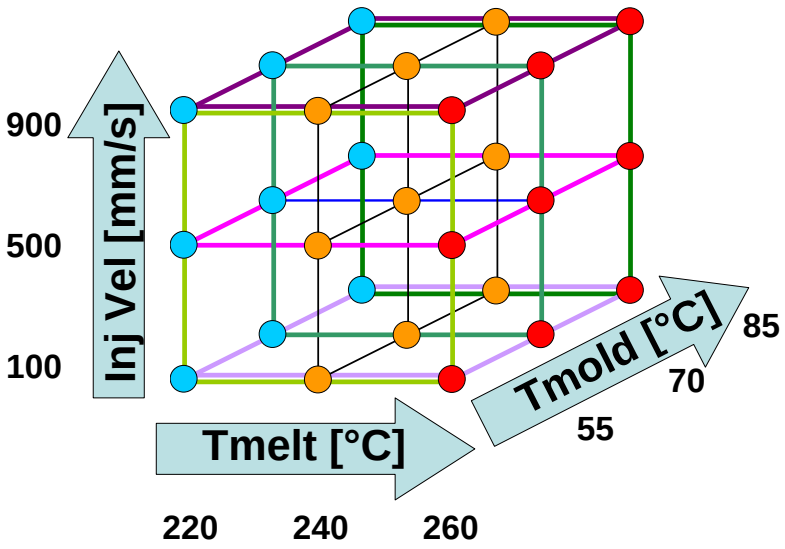

Figure 44 – Three factors-three levels full factorial design of experiments (27 experimental different settings) [Tosello, 2008(1)].

During the moulding, an automatic execution of the process (including ejection and handling of the polymer micro parts) was performed for each of the 27 experiments. Firstly, 50 cycles where carried out to stabilize the process in the current process parameter set-up. Subsequently, 50 parts obtained from the following 100 cycles were randomly collected and the related injection pressure measurements were carried out. Finally, three parts where randomly selected from the 50-pieces production batch for flow marker measurements and subsequent filling behaviour evaluation. During the whole investigation, 4000 micro moulded parts were produced.

3.2.4 Cavity pressure analysis

The cavity pressure profile, in µIM as well as in precision injection moulding, is a factor directly correlated to the quality of the part [Varela, 2000]. The cavity pressure control, expressed in terms of both absolute value and repeatability (i.e. standard deviation), is fundamental for an optimized part and process realization and it is the critical process parameter for the precision moulding of high accuracy thermoplastic parts [Kazmer, 1997] as micro moulded components. For example, an excessive value of the cavity pressure will lead to defects such as flashes (see Figure 45); whereas a large value of the standard deviation of the pressure indicates a poor

cycle-to-cycle process repeatability (i.e. different filling conditions) and therefore different properties of the moulded part. The maximum cavity injection pressure was recorded for all the 27 experiments (including average value, standard deviation and coefficient of variance). The coefficient of variation (COV) is the ratio between the standard deviation and the average, expressed in percentage value.

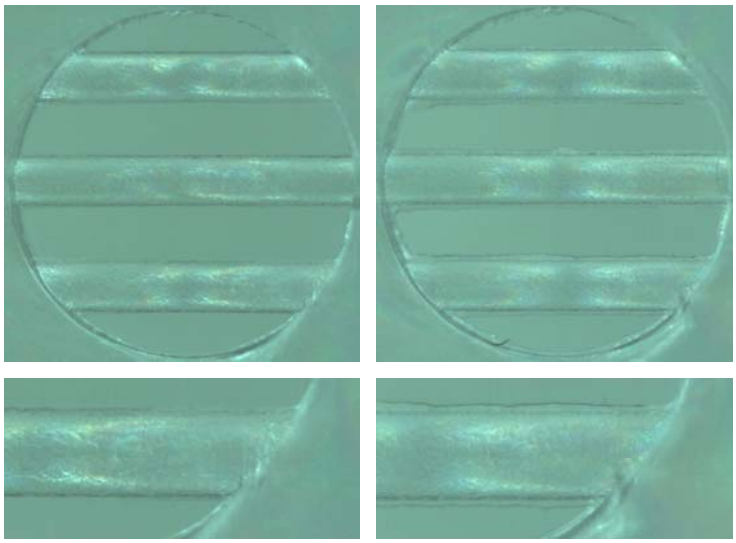

(a) (b)

Figure 45 – Effect of cavity injection pressure: micro flashes do not occur at lower pressure (553 bar, a) and appear at higher pressure (778 bar, b). Tmelt, Tmould and Inj.Speed were 260 °C, 70 °C, 100 mm/s and 260 °C, 70 °C, 900 mm/s respectively.

Results of the statistical analysis of the DOE could be effectively summarized using a main effect plot (see Figure 46) and show that an increase of the temperature of the melt causes an increase of the cavity injection pressure. This is due to the fact that higher temperature reduces the melt viscosity, which has as consequence the reduction of the pressure drop through the nozzle and runners, resulting in higher cavity injection pressure. To attain higher injection speed, a higher injection pressure must be applied, which in turn increases the cavity injection pressure. The influence of the temperature of the mould shows two different behaviours depending on the level. At higher mould temperature (Tmould = 85 °C), close to the glass transition temperature of the polymer, the melt viscosity is decreased, which in turn reduces the pressure drop resulting in a higher cavity injection pressure. At lower temperature

of the mould (Tmould = 55 °C) also high cavity pressure is recorded. This is due to the fact that cooling was occurring, especially at the gate location (i.e. gate freezing), and therefore higher injection pressure was required to force the polymer melt through the gate into the micro cavity. This phenomenon decreases with the increasing of the temperature of the mould, determining a lower injection pressure at intermediate mould temperature (Tmould = 70 °C).

The cavity injection pressure standard deviation over the whole design of experiments was comprised in the range of 7 and 57 bar, which corresponded to a COV between 1% and 7% respectively. In particular, increasing the injection speed leaded to a more repeatable process (lower standard deviation) as well as the use of the intermediate melt temperature (i.e. 240 °C), as shown in Figure 47.

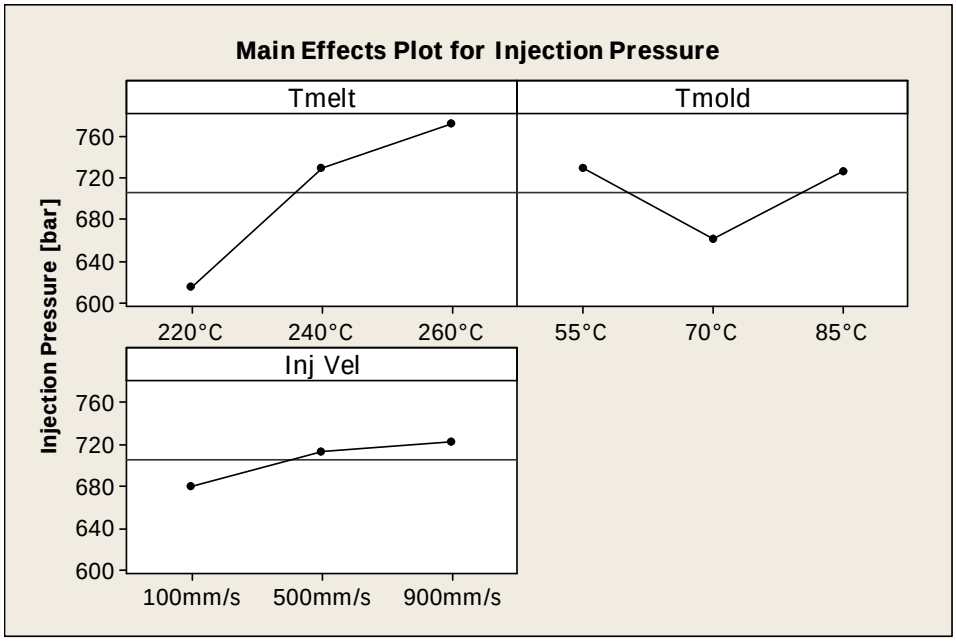

Figure 46 – Main effect plot for cavity injection pressure.

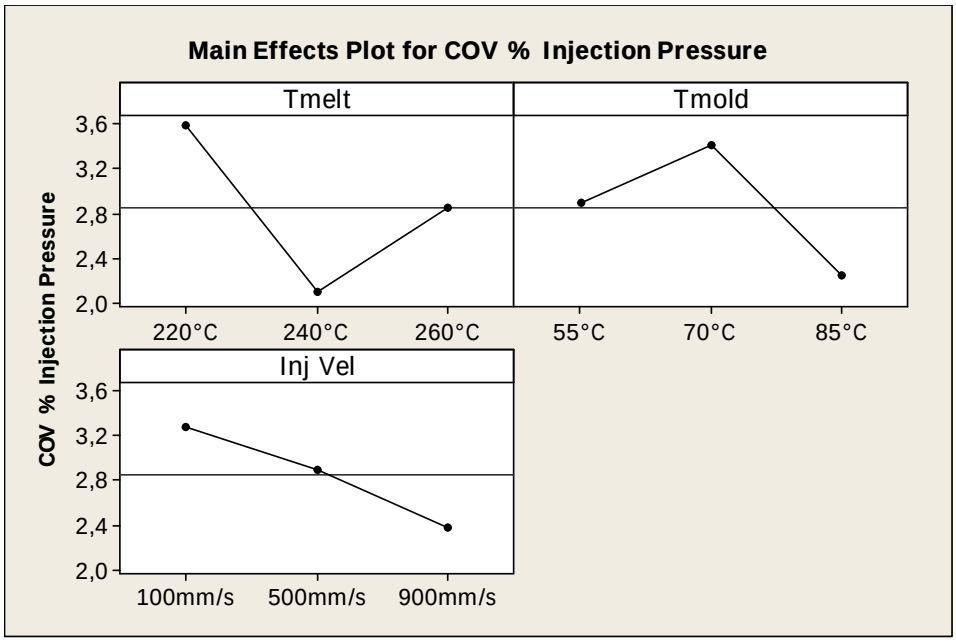

Figure 47 – Main effect plot for coefficient of variation (COV) of the cavity injection pressure.

3.2.5 Cavity filling time analysis

The injection pressure rise at the injection location and the subsequent reaching of the maximum cavity pressure were employed to determine the cavity injection time (see Figure 48) in different process conditions of the design of experiments. In the experimental set-up used during the present research, sample rate up to 25 kHz (i.e. one pressure sampling every 0.04 ms) was employed.

Results show that an increase of both temperature of the mould and of injection speed leads to a shorter cavity injection time. In particular, the injection speed has the highest influence, decreasing the cavity injection time of 47%, whereas a mould temperature variation has effect of decreasing the cavity injection time of 19%. The melt temperature appears to have no influence, producing a decrease of the cavity filling time of only 3% (see Figure 49). Standard deviation of the cavity injection time in the range between 1 and 3 ms were obtained during moulding in different process conditions (which corresponded to a COV from 0.2% to 0.7%).

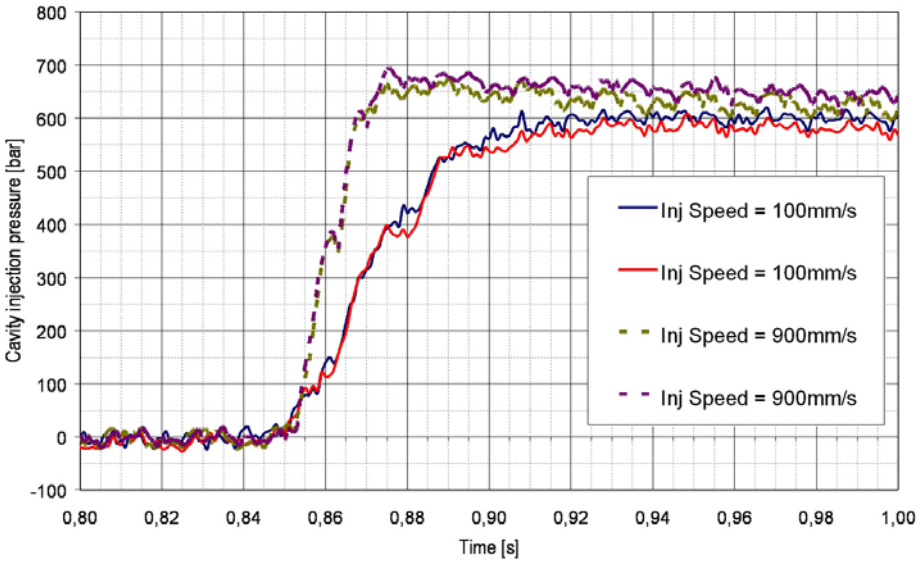

Figure 48 – Pressure vs. time curves from the in-cavity sensor. Mouldings at two different injection speeds (100 mm/s and 900 mm/s) are shown. Temperatures of the melt and of the mould were 220 °C and 55 °C respectively. In the chart, two curves sampled from the same moulding, carried out under the same processing conditions, are shown. The increase of the injection speed produced a decrease of the average cavity injection time from 67 ms to 30 ms and an increase of the average maximum cavity injection pressure from 612 bar to 672 bar [Tosello, 2008(2)].

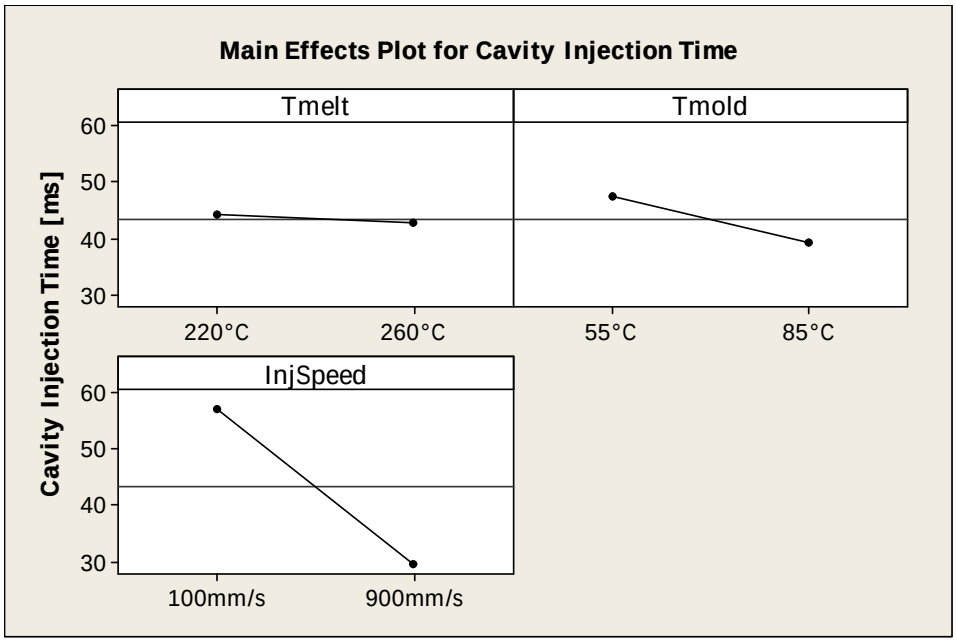

Figure 49 – Main effect of process parameters on the cavity injection time.

3.2.6 Flow marker analysis

The method of using weld lines as flow markers for the analysis of filling of micro cavities during μIM (as described in section 3.1.2) was applied to the micro moulded tensile bar test parts. Weld lines were visible on the surface of the part and due to the particular design of the component they were placed on each micro feature (see Figure 50). As previously explained, weld lines are a clear trace of the development of the flow melt during the filling of the cavity, and in particular they represent the position of the flow front at the end of filling in a certain area of the moulded part.

Weld lines can be used as flow markers to evaluate the influence of different process conditions (see Figure 51) because their position depends on the thermo-mechanical history of the melt in the cavity. For this purpose, high resolution images of the area with the micro features were taken using a calibrated optical microscope (calibration uncertainty U = 1 μm, standard coverage factor k = 2 corresponding to a confidence level of 95%). Subsequently, the images were post-processed to convert distances represented by pixels in the image in actual distances in length (see Figure 52, [Image Metrology, 2005]). The output parameter was defined as the position of the flow marker divided by the length the considered micro feature (expressed in percentage).

Results from the statistical analysis of the design of experiments show that an increase of all three process parameters leads to an extension of the distance covered by the melt flow when filling micro features (see Figure 53). In particular, the injection speed is the most effective process parameter. The position of the flow markers could be extended of 16% by the increase of injection speed. Measurements on different moulded parts were carried through the whole experimental plan. An average standard deviation of the flow markers position of 31 μm was found (equal to a general COV within the 27 experiments of 2.2%).

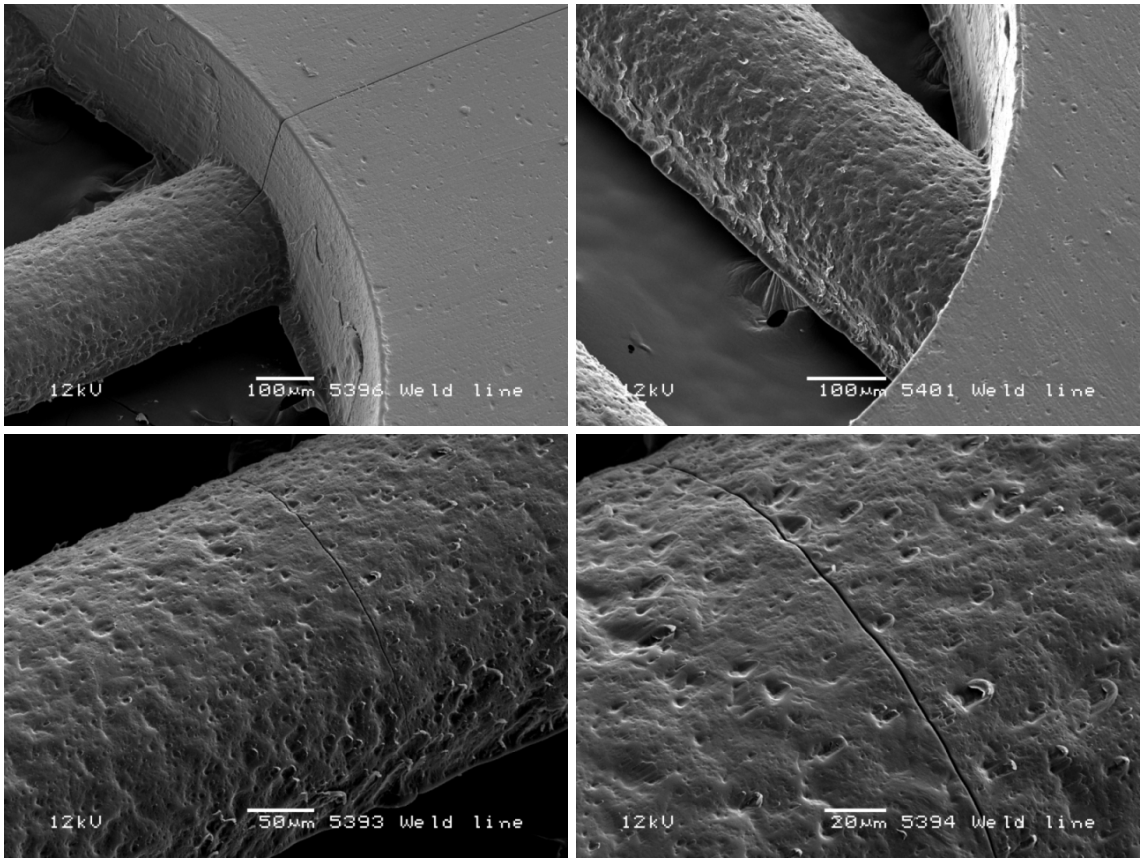

Figure 50 – Scanning electron microscope (SEM) images of weld lines on the surface of the 300 µm wide micro features.

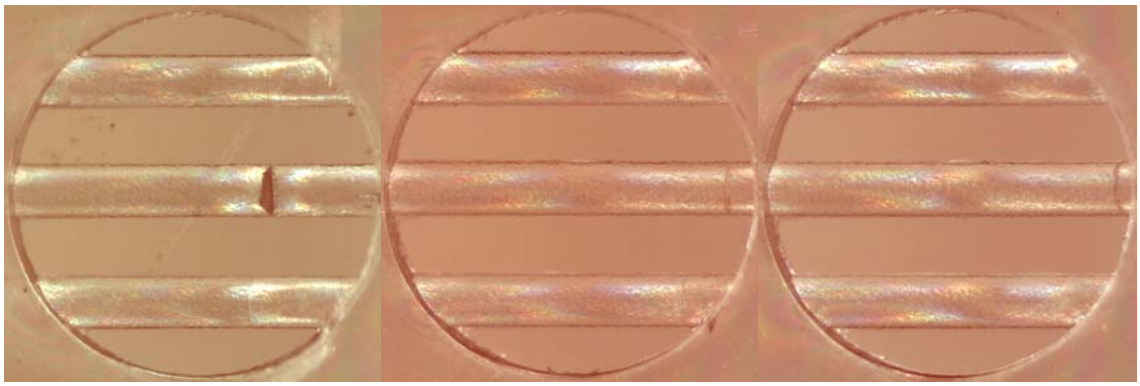

100 mm/s	500 mm/s	900 mm/s

Figure 51 – Optical microscope images of the flow front position shift due to an increase of injection speed (injection direction from left to right, Tmelt = 220 °C, Tmould = 55 °C).

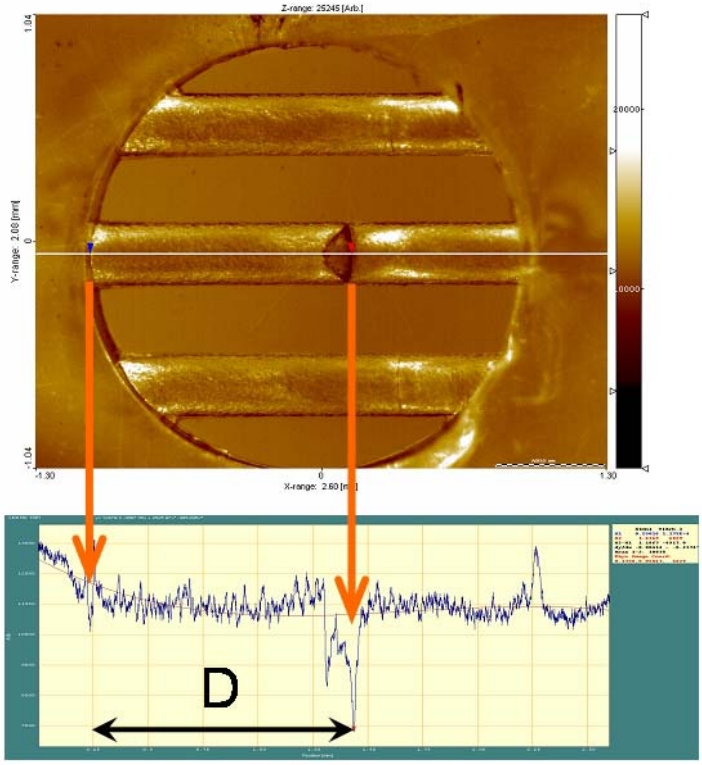

Figure 52 – Weld lines as flow markers: the length D represents the distance covered by the melt flow towards the end of the micro feature (melt flow moving from left to right).

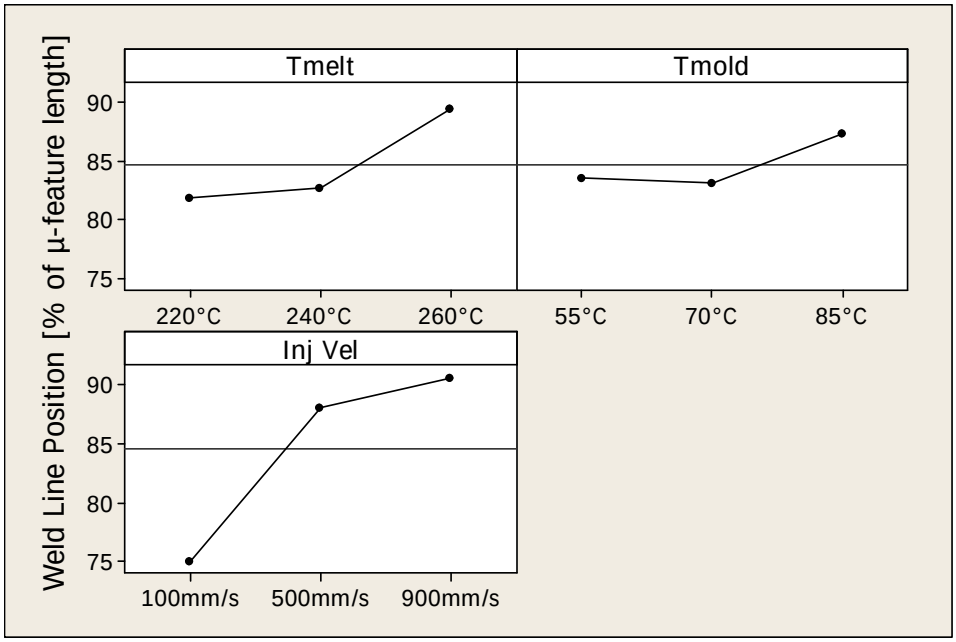

Figure 53 – Influence of process parameters on the position of weld lines.

3.2.7 Discussion

Cavity injection pressure and cavity injection time were assessed using high sampling rate in-cavity injection pressure measurements during micro injection moulding. Moreover, melt flow behaviour during the filling of cavity was characterized by studying flow markers positions under different process conditions.

Injection speed was found to have the largest influence on the repeatability of the process, on the cavity injection time, and on the position of the melt flow during the filling of the micro cavity. On the other hand, temperature of the melt and of the mould had a limited effect. Absolute values and repeatability of both cavity injection pressure and time over a broad range were studied and related to process parameters levels. The effect of the process parameters on the injection pressure and was highlighted.

Firstly, it has been demonstrated that both a high temperature of the melt and of the mould produce an increase of the cavity injection pressure, which in turn produces undesirable defects such as micro flashes. A high melt temperature can also result in the degradation of the polymer which is obviously a situation to avoid.

Moreover, a low temperature of the mould promotes a premature freezing of the gate contributing to a rise of the cavity injection pressure. Therefore an intermediate mould temperature (i.e. 70 °C) and is recommendable because can minimize the cavity injection pressure.

Secondly, despite the fact that a high injection speed can actually enhance the filling performance of the polymer melt flow and shorten the cavity filling time (which would avoid short shots due to premature freezing of the polymer melt), it should not be pushed to an excessive level to avoid too high cavity injection pressure that could damage the micro structures and could produce micro flashes.

Finally, process repeatability was assessed over the whole production batch: injection pressure could be reproduced within a range of 7 bar up to 57 bar, injection time within a range between 1 and 3 ms.

3.3 Conclusion

The injection moulding process analysis has been presented in this chapter. Polymer micro parts were produced using both conventional and micro injection moulding machines.

For the purpose a new process analysis method based on the measurement of the position of weld lines (i.e. flow markers) on the surface of the plastic component has been developed, implemented and validated.

Conclusions regarding the effect of different process parameters on the filling of the polymer melt into micro cavity were obtained. For both investigations, the importance of the injection speed and of the temperature of the mould was highlighted. It was also concluded that when moulding polystyrene, the melt temperature should not be increased to avoid polymer degradation and high cavity pressure. Moreover, the very limited advantage on replication performance due to an increase of melt temperature was demonstrated.

Furthermore, a new approach on uncertainty management when using design of experiments was presented. As a conclusion, the validity of the whole experimental plan was confirmed.

3.4 References

[Del Vecchio, 1997] Del Vecchio R.J. (1997) Understanding design of experiments, Hanser ed., München (Germany), pp.1-175.

[EA, 1999] EA (European co-operation for Accreditation) (1999) Expression of the Uncertainty of Measurement in Calibration, EA-4/02.

[Fellahi, 1995] Fellahi S., Meddad A., Fisa B., Favis B.D. (1995) Weld lines in injection molded parts: a review, Advances in Polymer Technology, Vol.14, No.3, pp.169-195.

[Han, 2006] Han X., Yokoi H. (2006) Visualization analysis of the filling behaviour of melt into microscale V-groove during the filling stage of injection molding, Polymer Engineering and Science, Vol. 46, No. 11, pp.1590-1597.

[Image Metrology, 2005] Image Metrology A/S (2005) Scanning Probe Image Processor (SPIP™).

[ISO, 1993] ISO (International Organization for Standardization) (1993) International Vocabulary of Basic and General Terms in Metrology, 2nd edition.

[ISO, 1995] ISO (International Organization for Standardization) (1995) GUM (Guide to the Expression of Uncertainty in Measurement).

[ISO, 1999] ISO (International Organization for Standardization) (1999) Geometrical Product Specifications (GPS) - Inspection by measurement of workpieces and measuring equipment - Part 2: Guide to the estimation of uncertainty in GPS measurement, in calibration of measuring equipment and in product verification, ISO/TS 14253-2.

[Jaworski, 2003] Jaworski M.J., Yuan Z. (2003) Theoretical and experimental comparison of the four major types of mesh currently used in CAE injection molding simulation software, Society of Plastic Engineers (SPE) - Proceedings of the 61st Annual Technical Conference ANTEC, Nashville (TN, USA), Vol.1, pp.642-646.

[Kazmer, 1997] Kazmer D., Barkan P. (1997) The process capability of multi-cavity pressure control for the injection molding process, Polymer Eng. and Science, Vol.37, Issue 11, pp.1880-1895.

[Knapp, 2001] Knapp, W. (2001) Tolerance and uncertainty, Fifth International Conference on Laser Metrology, Machine Tool, CMM and Robot Performance, LAMDAMAP 2001, Birmingham (UK), 17th-20th July 2001, pp.357-366.

[Montgomery, 2001] Montgomery D.C. (2001) Design and Analysis of Experiments, 5th edition, John Wiley & Sons.

[Park, 2004] Park K., Ahn J.H. (2004) Design of experiment considering two-way interactions and its application to injection molding processes with numerical analysis, Journal of Materials Processing Technology, Vol.146, Issue 2, pp.221-227.

[Sha, 2005] Sha B., Dimov S.S., Pham D.T., Griffiths C.A. (2005) Study of Factors Affecting Aspect Ratios Achievable in Micro-injection Moulding, 1st International Conference on Multi-Material Micro Manufacture (4M), Karslruhe (Germany), 29th June-1st July 2005, pp.107-110.

[Sha, 2007] Sha B., Dimov S., Griffiths C., Packianather M.S. (2007) Micro-injection moulding: Factors affecting the achievable aspect ratios, International Journal of Advanced Manufacturing Technology, Vol.33, Issue.1-2, pp.147-156.

[Tosello, 2007(1)] Tosello G., Gava A., Hansen H.N., Lucchetta G., Marinello F. (2007) Characterization and analysis of weld lines on micro injection moulded parts using Atomic Force Microscope, 11th International Conference on Metrology & Properties of Engineering Surfaces (Met & Props 2007), Huddersfield (UK), 16th-20th July 2007, pp.166-170.

[Tosello, 2007(2)] Tosello G., Gava A., Hansen H.N., Lucchetta G. (2007) Influence of process parameters on the weld lines of a micro injection molded component, Society of Plastics Engineers (SPE) – 65th Annual Technical Conference (ANTEC), Cincinnati (OH, US), 6th-10th May 2007, pp.2014-2018.

[Tosello, 2007(3)] Tosello G., Gava A., Hansen H.N., Lucchetta G., Guarise M. (2007) Filling analysis in micro injection moulding using weld lines as flow markers, 3th International Conference on Multi-Material Micro Manufacture (4M), Borovets (Bulgaria), 3rd-5th October 2007, pp.259-262.

[Tosello, 2007(4)] Tosello G., Gava A., Hansen H.N., Lucchetta G., Guarise M. (2007) Measuring uncertainty applied to design of experiment analysis: a micro injection moulding case study, Joint ENBIS-DEINDE 2007 Conference (European Network for Business and Industrial Statistics & DEsign of INDustrial Experiments) “Computer Experiments versus Physical Experiments”, Turin (Italy), 11th-13th April 2007, pp.202-213.

[Tosello, 2008(1)] Tosello G., Hansen H.N., Schoth A. (2008) Process and part filling control in micro injection molding, Society of Plastics Engineers (SPE) – 66th Annual Technical Conference (ANTEC), Milwakee (WI, USA), 4th-8th May 2008 (in press).

[Tosello, 2008(2)] G. Tosello, A. Schoth, H. N. Hansen (2008) In-cavity pressure and injection time measurements during the micro injection moulding process, 10th Anniversary International Conference of the European Society for Precision Engineering and Nanotechnology (Euspen), Zurich (Switzerland), 18-22 May 2008 (in press).

[Varela, 2000] Varela A.E. (2000) Self-tuning pressure control in an injection moulding cavity during filling, Chemical Engineering Research and Design – Trans IChemE, Vol.8, Issue A, pp.79-86.

[Whiteside, 2005] Whiteside B.R., Martyn M.T., Coates P.D. (2005) In-process monitoring of micromoulding – Assessment of process variation, International Journal of Polymer Processing, Vol. XXI, Issue 5, pp.162-169.

[Wu, 2005] Wu C.H., Liang W.J. (2005) Effect of geometry and injection-molding parameters on weld line strength, Polymer Engineering and Science, Vol. 45, Issue 7, pp.1021-1030.

[Yang, 2002] Yang, S.Y., Nian, S.C., Sun, I.C. (2002) Flow visualization of filling process during micro-injection molding, International Polymer Processing, Vol.17, Issue 4, pp.354-360.

[Zhao, 2003] Zhao J., Mayes R.H., Chen G., Xie H., Chan P.S. (2003) Effects of Process Parameters on the Micro Molding Process, Polymer Engineering and Science, Vol.43, Issue 9, pp.1542-1554.

4 Part defects control and optimization

The quality control of products is an essential step during the manufacturing process in the macro as well in the micro world. During this project, the quality control was devoted to the investigation and the optimization of typical defects of injection moulded parts such as weld lines (as described in section 4.1).
Defect inspection and dimensional measurements of weld lines were performed using scanning electron microscope (SEM) and atomic force microscopy (AFM) respectively. The aim was to establish the relation between geometrical properties of the weld lines (namely width and depth) and the injection moulding parameters (as presented in sections 4.2 and 4.3). The uncertainty of the AFM measurements was also analyzed (section 4.4).

4.1 Defects of micro injection moulded parts: weld lines

Weld lines are a reality of the injection moulding of complex parts. Multiple gating, splitting of the melt flow due to inserts in the cavity or through holes, as well as changes of thickness give rise to points within the structure where the flowing fronts will recombine and weld. An imperfection is observed as a line on the surface of the moulded part (see Figure 54). In the moulding of very complex components a multiplicity of weld lines is generated. The weld lines are formed as the mould is being filled. Weld lines reduce the mechanical strength of components in the macro [Fellahi, 1995] as well as in the micro [Wu, 2005] dimensional range. In particular, an area whose properties are different from the bulk is created. Weld-line factors (defined as the ratio between the strength of workpieces containing a weld line and workpieces with the same geometry but without weld lines) as low as 20% were found on micro injection moulded tensile strength specimen. Main causes are incomplete molecular entanglement or diffusion, formation of V-notch at the weld

surface, presence of contamination of microvoids at the weld line interface, and unfavourable molecular or fibre orientation at the weld [Wu, 2005].

It is therefore of great importance to optimize the injection moulding process, and especially the filling phase, in order to decrease the entity of such defects. In the following, an investigation devoted to the determination of the influence of typical injection moulding parameters is presented. Depth and width of weld lines have been chosen as parameters to be optimized.

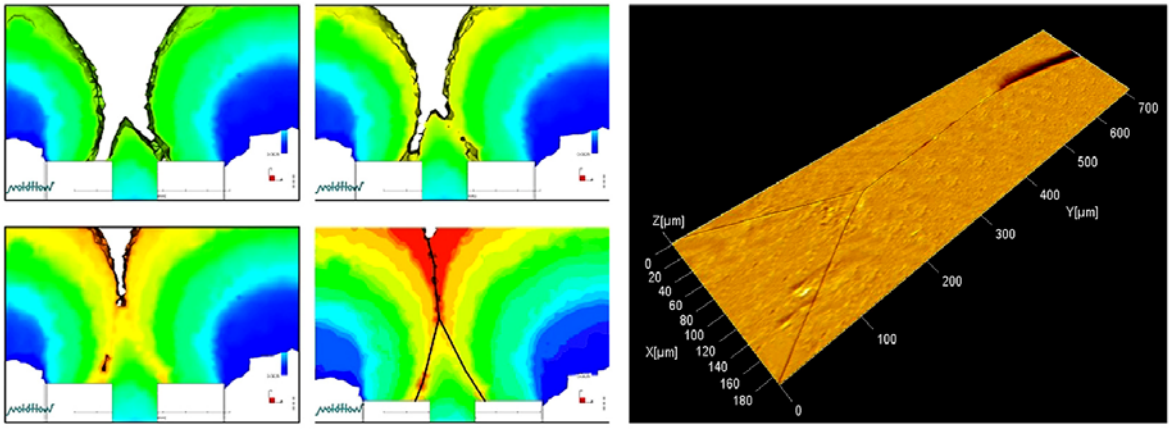

Figure 54 – Simulation of the formation of a weld line due to the presence of 2 micro features and the meeting of 3 melt flow fronts (left) [Gava, 2007] and large-range AFM scanning of the actual meeting area on a polystyrene micro moulded part (right). The large range scanning of 700 µm x 200 µm was obtained using a software tool for stitching three dimensional surface topography data sets [Marinello, 2007]: 18 different scannings 50 µm x 100 µm were employed for the reconstruction.

4.2 Experimental

A micro-cavity manufactured by µEDM (Electro Discharge Machining) with a design specifically developed to obtain the formation of weld lines was employed (see description in section 3.1.3.1).

To investigate the influence of process parameters on the weld lines formation in the micro cavity, a series of statistically designed experiments have been carried out. Four different process parameters were varied in order to determine their influence on the micro injection moulding process: melt temperature, mould temperature,

injection speed and packing pressure. A half factorial design has been carried out performing 2^{4-1}=8 moulding experiments (each parameter being varied between two levels) with 5 injection moulding replications. A fraction of the complete factorial experiment was used because it was assumed that second and higher interactions were negligible for the purpose (as described in section 3.1.3.2). At the same time, the number of experiments was drastically reduced, allowing a decrease of the measuring time. The injection moulding details are given in sections 3.1.3.1 and 3.1.3.2 and 3.1.3.3).

	Low level	High level	Design of Experiment - Trials							
Process parameters	-	+	1	2	3	4	5	6	7	8
Melt temperature	240 °C	270 °C	+	+	+	+	-	-	-	-
Mould temperature	45 °C	70 °C	+	+	-	-	+	+	-	-
Injection speed	200 mm/s	350 mm/s	+	-	-	+	-	+	+	-
Packing pressure (hydraulic)	10 bar	100 bar	+	-	+	-	+	-	+	-

Table 7 – Process parameters settings and half-factorial 4-factors 2-levels Design of Experiment (DOE).

4.3 Weld lines measurement strategy

To analyse the influence of process parameters on the characteristics of the weld lines of the micro injection moulded part, a three-dimensional surface topography investigation was carried out. In particular, the average depth and width of weld lines were chosen as representative parameters to be analysed by means of the design of

experiment. The employed instrument was an atomic force microscope (AFM) DME DualScope 4000.

The AFM was mounted on a coordinate measuring machine (CMM). The CMM was employed as a positioning system for the sensor: both the X and Y axis were provided with measuring scale with output resolution of 0.1 µm [Bariani, 2005]. Moreover, a CCD camera was co-axially mounted along the Z axis of the AFM, providing direct visual feedback for the positioning of the probe sensor on the part. The system allowed accurate repositioning of the scanner on different micro parts. This was a fundamental requirement in order to measure the same portion of features (i.e. weld lines) obtained with different process conditions.

AFM DME-DS 95-200	
Scanning mode:	Non-contact (AC) and contact (DC)
Max. Scanning area:	200 x 200 μm^2
Z range	15 µm
Z resolution	<0.5 nm
X, Y resolution	< 1nm
Z-linearization	0.5% (on full scale scan)
Optical system	
Magnification	100 X
Optical axis	Infinite corrected
Transmission bandwidth	400 - 600 nm

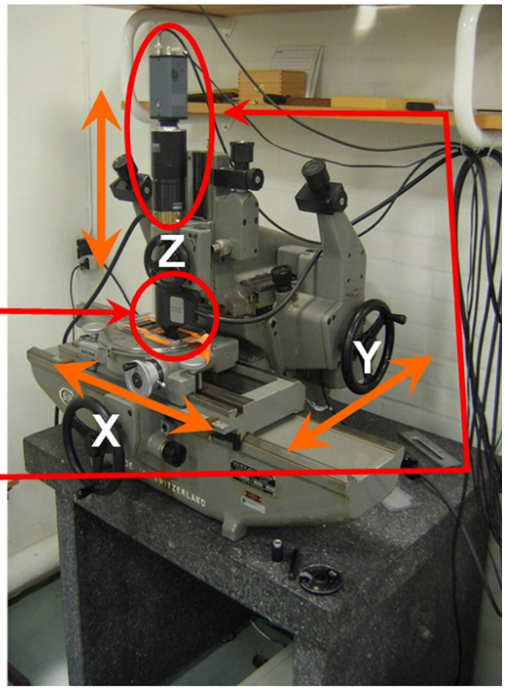

Figure 55 – AFM and CMM integrated measuring equipment.

Weld lines were measured on 3 different locations on the surface of the micro injection moulded part (see Figure 56). For each of the 8 process set-ups of the half-factorial design of experiment, 2 samples were randomly selected from the production batch and then measured. A total of 48 scannings were performed. The scanning was 50 µm wide along the fast-scan direction (i.e. X direction) with a step size of 24,4 nm (2048 pixels) and 100 µm long along the slow-scan direction (i.e. Y

direction) with a spacing between two adjacent lines of 1587 nm (64 profiles) for area 1 and 3 (see Figure 57 and Figure 59 respectively). For the weld line area 2, a higher scanning density along the Y direction was chosen (512 profiles over a measuring range of 100 µm, resulting on a spacing between two consecutive scanning lines of 195 nm). This setting increased the measuring time sensibly; on the other hand it allowed a better resolution on the surface measurement of the meeting point of the three melt flows (see Figure 58).

After the measurement, a post-processing of the measuring data was performed: a 1st degree alignment in the vertical Z direction, a profile alignment along the correlation direction of the weld lines, and finally the average X profile was calculated. The depth and width measurements were carried out on this final two-dimensional profile. The base line for both measurements was the mean height of the profile. The depth was defined as the Z distance between the mean height line and the deepest point of the weld line. The width was defined as the X distance between two points placed on the two sides of the weld lines at the intersection between the average profile and the mean height line.

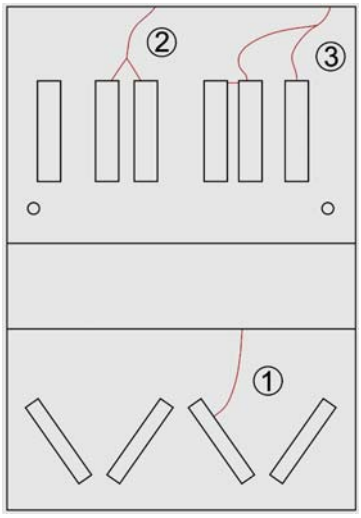

Figure 56 – Locations of the 3 different weld lines investigated areas on the surface of the micro injection moulded part.

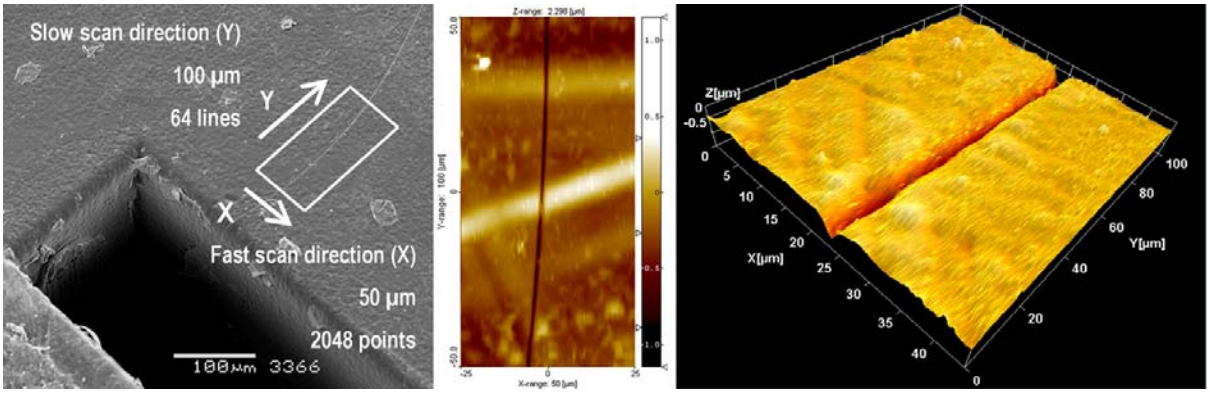

Figure 57 – Measurement layout for weld lines area 1.

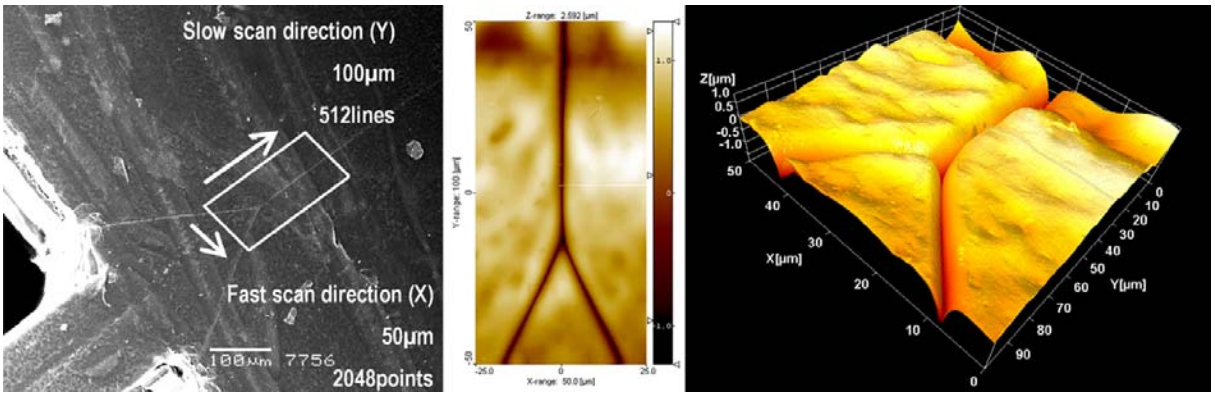

Figure 58 – Measurement layout for weld lines area 2.

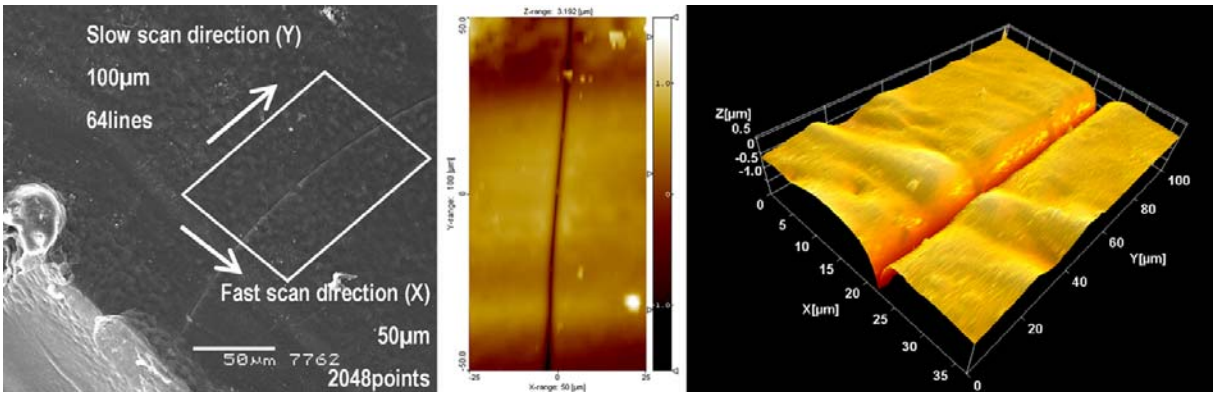

Figure 59 – Measurement layout for weld lines area 3.

4.4 Measurement uncertainty

When performing design of experiment, uncertainty and dimensional measurements play an important role being the link between the process effects on the part and the numerical data to be analysed (see section 3.1.5).

Uncertainty of measurements for both depth and width was assessed and implemented on the statistical analysis to verify the reliability of the obtained results. In the following, the considered contributors and the related standard uncertainties in the measurements of the micro moulded with the AFM are presented and discussed [Tosello, 2008(3)].

4.4.1 Measurement of depth

- Vertical calibration uncertainty [u(C(z))] – Vertical measurements are compensated by using the calibration factor C(z), whose value is obtained by repeated measurements on a reference object (i.e. step height). Uncertainty on such calibration was considered having a linear behaviour. The uncertainty of calibration (u(cal)) of the reference object is included in the uncertainty of the calibration factor.
    - u(C(z)) = 1% of the measurand (with Gaussian distribution)
    - u(cal) = 1 nm (with Gaussian distribution)
- Uncertainty due to the background noise [u(noise)] – Repeated measurements on an optical glass were performed in order to determine the background noise of the instrument.
    - u(noise) = 0.5 nm (with Gaussian distribution)
- Repeatability of the measuring process [u(rep)] – The repeatability of the measurement was estimated by measuring 5 times the same plastic sample, calculating the depth as previously described (see section 4.3) and finally considering the standard deviation of the results. The standard deviation was normalized to the actual measured depth. This value, on percentage, was considered as u(rep), assuming a linear behaviour of this uncertainty contributor: higher the measurand, higher the spread of the measurement.
    - u(rep) = 0.62% of the measurand (with Gaussian distribution)

- Effect of the X resolution on the Z measurement [u(res)] – The resolution along the fast scan direction is clearly half of the step size, considered with a step distribution. This resolution is a source of uncertainty when determining the Z coordinates of points, especially in case of features with inclined profiles (as in the case of the weld line). It is worth to mention that such contributor is far larger than the actual Z resolution of the scanner (1.5pm) that is therefore neglected in the uncertainty budget.
    - u(res) = 0.5% of the measurand (with Step distribution)
- Uncertainty due to the scanning speed [u(speed)] – Measurements performed at different speeds (2 µm/s, 5 µm/s, 10 µm/s, 20 µm/s) along the fast-scan direction resulted on different measuring results. A trade-off between speed (to minimize the measuring time) and accuracy (closest result obtained with the slowest scanning speed of 2 µm/s) was found: a scanning speed of 10 µm/s was chosen.
    - u(speed) = 0.5% of the measurand (with Gaussian distribution)

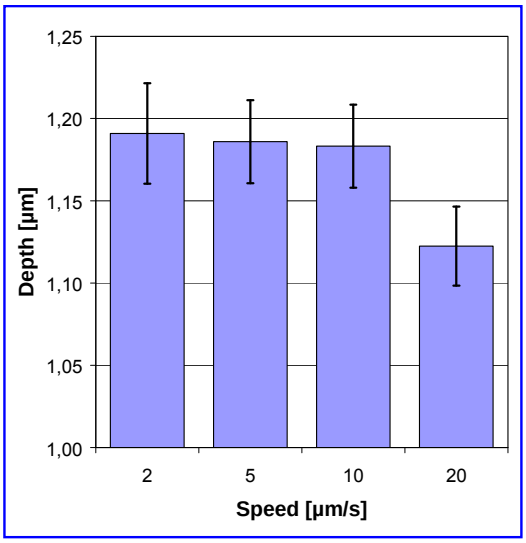

Figure 60 – Optimization of the measuring scanning speed along the X direction.

- Uncertainty of the micro injection moulding process [u(µIM)] – Different samples lead to different measuring results and this has to be taken into account in order to verify the reliability of the design of experiment analysis. Each batch was affected by its own process repeatability that was calculated

accordingly. A representative average value is reported below. By considering measurements from two different samples, the area localization and the re-positioning error are also taken into account.

  - u(μIM) = 4.4% of the measurand (with Gaussian distribution)

- Effect of the scanning force – Measurements using different scanning forces (5nN, 10nN, 15nN) have been performed. Both the lowest and the highest forces resulted in a smaller depth of the weld line. On the other hand, the measurements performed using a force of 10 nN resulted on a larger depth of the weld line. Hence, a force of 10 nN was chosen because it optimized the measurement (see Figure 61). Because of the optimization, it was decided to not include the scanning force in the uncertainty budget.

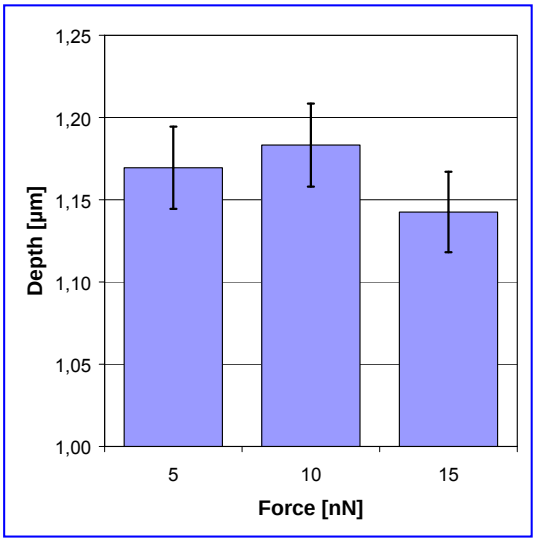

Figure 61 – Optimization of the scanning force for measurement of depth.

Once all the uncertainty sources have been analysed and the standard uncertainty evaluated for each source, the combined standard uncertainty u_c was calculated. The expanded uncertainty U was obtained by multiplying the combined standard uncertainty u_c by the coverage factor k (k=2 for a confidence of approximately 95%). Representative average values of standard uncertainty contributors, combined standard uncertainty (u_c) and expanded uncertainty (U) for depth are reported in Table 8.

Unc. contrib.	u(C(z))	u(noise)	u(rep)	u(res)	u(speed)	u(μIM)	Comb. std. unc. (u_c)	**Exp. unc. (U)**
[μm]	0.0044	0.0005	0.0055	0.0035	0.0044	0.038	0.039	**0.08**

Table 8 – Average values of standard uncertainty contributors, combined standard uncertainty and expanded uncertainty for depth measurements of weld lines.

4.4.2 Measurement of width

Analogue considerations as in section 4.4.1 for the single uncertainty contributors for the width measurements were carried out and are presented in the following. Main differences regarded the magnitude of uncertainty components related to the calibration along the X scanning direction, the scanning speed, the repeatability of the μIM process as well as of the measuring process. All these contribution were found to be larger for width measurements than in the case of depth measurements. Representative average values of standard uncertainty contributors, combined standard uncertainty (u_c) and expanded uncertainty (U) for depth are reported in see Table 9.

- Horizontal calibration uncertainty [u(C(x)) and u(cal)] – Horizontal measurements are compensated by using the calibration factor C(x), whose value is obtained by repeated measurements on a reference object (i.e. grating). Main source of uncertainty is the non-linearity on the measured range along the fast-scan direction. Uncertainty was considered to be proportional to the measured length.
    - u(C(x)) = 1% of the measurand (with Gaussian distribution)
    - u(cal) = 1 nm (with Gaussian distribution)
- Uncertainty due to the background noise [u(noise)] – Repeated measurements on an optical glass were performed in order to determined the background noise of the instruments.
    - u(noise) = 0.5 nm (with Gaussian distribution)
- Repeatability of the measuring process [u(rep)] – The repeatability of the measurement was estimated by measuring 5 times the same plastic sample,

calculating the width as previously described (see section 4.3) and finally considering the standard deviation of the results. The standard deviation was normalized to the actual measured depth. This value, on percentage, was considered as u(rep), assuming a linear behaviour of this uncertainty contributor.

  - u(rep) = 0.20% of the measurand (with Gaussian distribution)

- Resolution along the X direction [u(res)] – The resolution along the fast scan direction is half of the step size, considered with a step distribution.
  - u(res) = 3.5 nm (with Step distribution)
- Uncertainty due to the scanning speed [u(speed)]
  - u(speed) = 2.0% of the measurand (with Gaussian distribution)

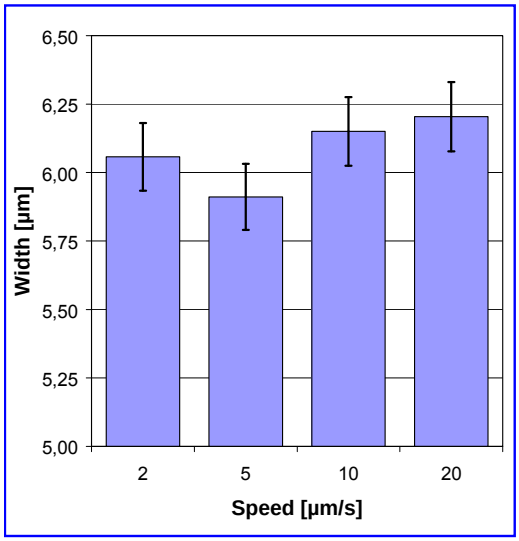

Figure 62 – Verification of the selected scanning speed along the X direction after optimization for depth measurements.

- Uncertainty of the micro injection moulding process [u(µIM)]
  - u(µIM) = 5.2% of the measurand (with Gaussian distribution)
- Effect of the scanning force – The force of 10nN was chosen because optimized the depth measurement and was verified for the width measurement.

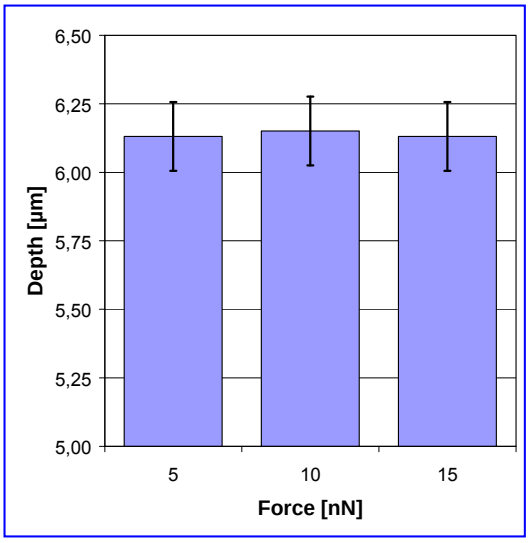

Figure 63 – Verification of the selected scanning force for width measurements after optimization for depth measurements.

Representative average values of standard uncertainty contributors, combined standard uncertainty (u_c) and expanded uncertainty (U) for width are reported in Table 9.

Unc. contrib.	u(C(x))	u(noise)	u(rep)	u(res)	u(speed)	u(µIM)	Comb. std. unc. (u_c)	**Exp. unc. (U)**
[µm]	0.0477	0.0005	0.0085	0.0035	0.0954	0.246	0.268	**0.54**

Table 9 – Average values of standard uncertainty contributors, combined uncertainty and expanded uncertainty for width measurements of weld lines.

4.5 Design of Experiment analysis

The statistical analysis results for both the depth and the width of the micro weld lines are represented in Fig. 3 in the form of a Pareto chart. The Pareto chart is employed to show the effects of the main factors studied and to plot them in a descending order according to their magnitude. In this way the significance of each main factor is clearly identified. The statistical analysis has been performed on the average depth

of the weld lines on the different areas shown considered on the same processing conditions (see Figure 56, Figure 57, Figure 58 and Figure 59).

The most influencing process parameters on the weld lines depth were the temperature of the mould and the injection speed. On the other hand, the most affecting parameter on the weld lines width is the temperature of the mould as shown in the Pareto chart in Figure 64.

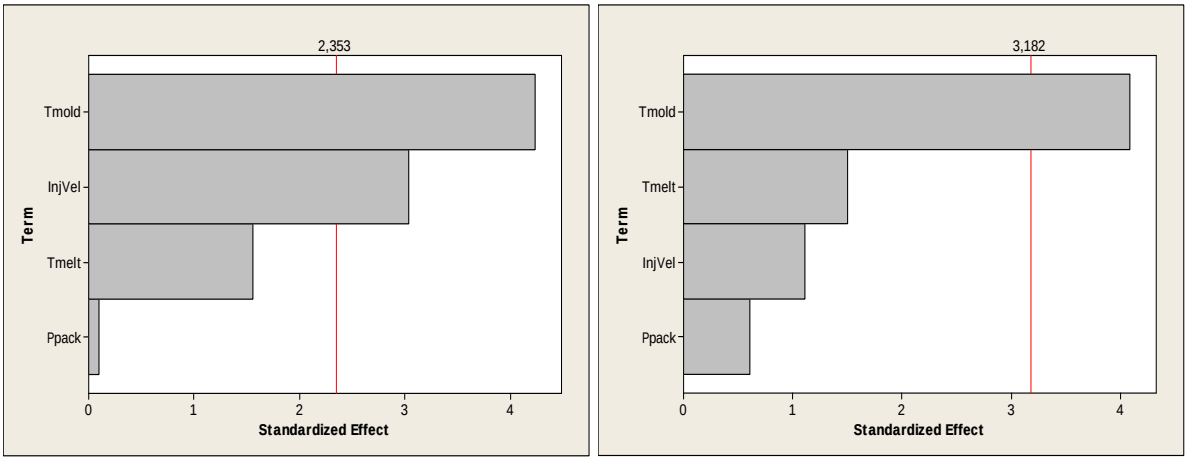

(a) (b)

Figure 64 – Pareto charts for depth (a) and width (b) of weld lines.

4.5.1 One-factor at-the-time analysis

Once the most important process parameters have been individuated, it has been possible to visualize their effect by means of a one-factor at-the-time analysis. It was also possible to relate their effect directly to the result they produce on the weld lines, considering both an averaged profile along the slow scanning direction (i.e. Y direction, as shown in Figure 65 and Figure 66) and a three dimensional rendering produced by post-processing of AFM measurements (see Figure 67). The effect of the temperature of the mould and of the injection speed is clearly visible.

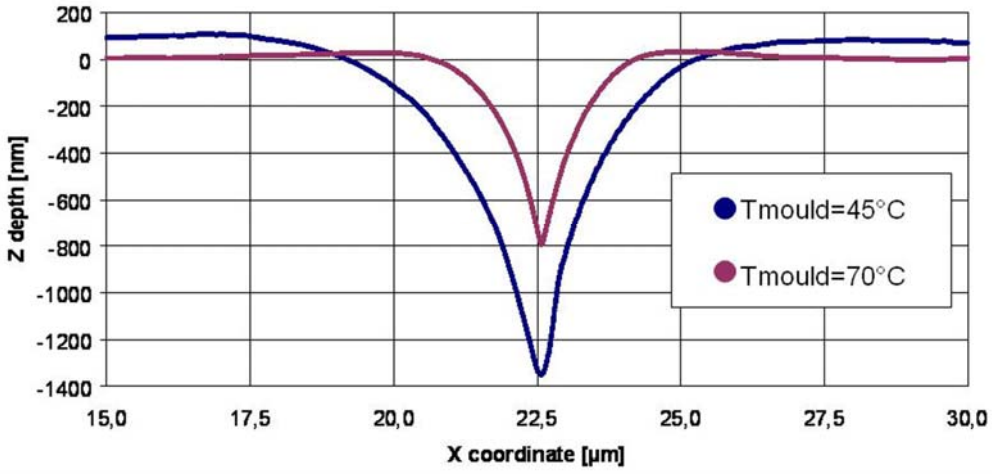

Figure 65 – Effect of the temperature of the mould on the weld line profile.

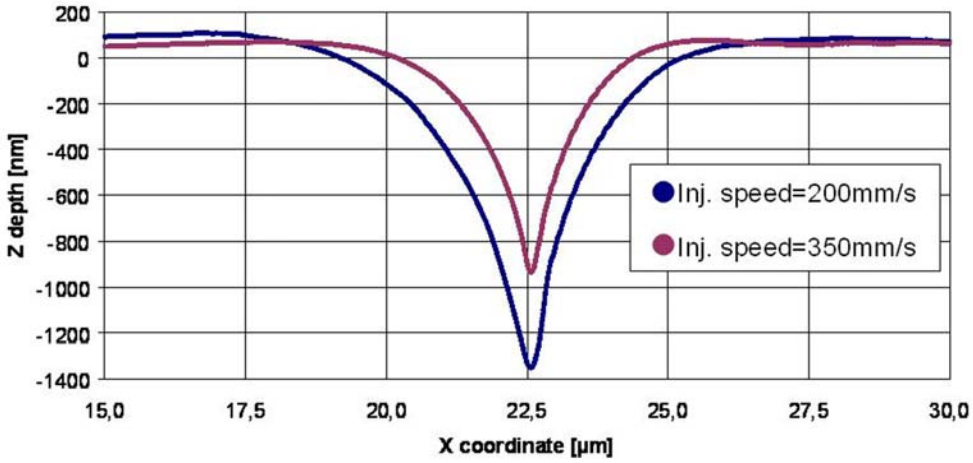

Figure 66 – Effect of the injection speed on the weld line profile.

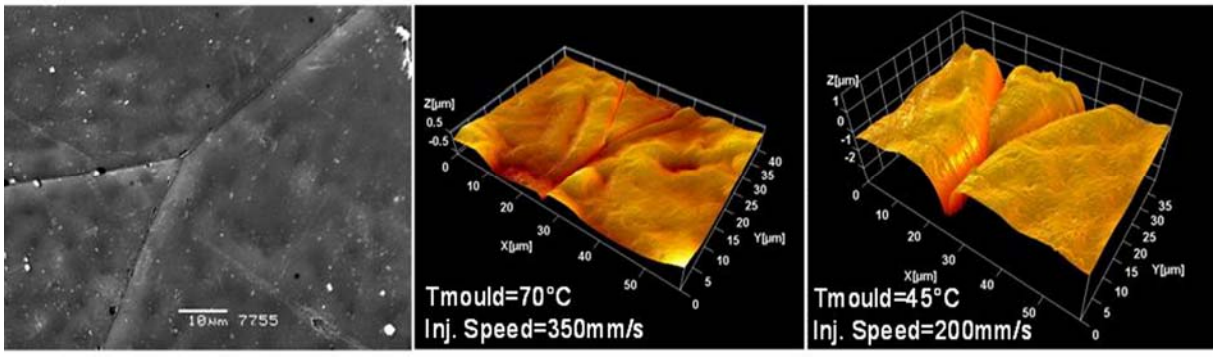

Figure 67 – Three dimensional visualization of the effect of temperature of the mould and of injection speed on weld lines topography [Tosello, 2007(5)].

4.5.2 Main effects and uncertainty

An increase of the temperature of the mould and of the injection speed produces a decrease of the depth of the weld lines of 0.45 µm and 0.32 µm respectively. Regarding the width, the main factor with statistical significance (at 95% of confidence) is the temperature of the mould: higher level of this factor produces a decrease of width of 2.6 µm.

The variations produced by the different levels of the process parameters are larger than the estimated measuring uncertainties presented in section 4.4. In particular, the measuring uncertainty was calculated to be within 18% and 25% of the variation of the response. As a consequence, the reliability of the experiments, of the measurements as well as of the results has been confirmed (see Figure 68 and Figure 69).

4.5.3 Gate location effect

A further investigation based on the previously introduced measurements was carried out by including as variable the position of the gate with respect to the considered weld line on the part. In particular, to the weld line in the area 1 was assigned level of the gate location ‘low’ (i.e. weld line near the gate); on the other hand, to weld lines belonging to areas 2 and 3, was assigned gate location level ‘high’ (i.e. weld line far from the gate).

In this way, the design of experiment became a 32-runs full factorial design, with 5 factors (Tmelt, Tmould, InjSpeed, Ppack and gate location) and two-levels for each factor. The statistical analysis, expressed as main effect plot, clearly shows that a larger distance between the gate and the considered area produces deeper and wider weld lines. In other words, in order to decrease the entity of defects such as weld lines, the flow path length has to be as short as possible (see Figure 68 and Figure 69). This can be achieved, for example, by a special design contemplating multi-gating system (see Figure 72).

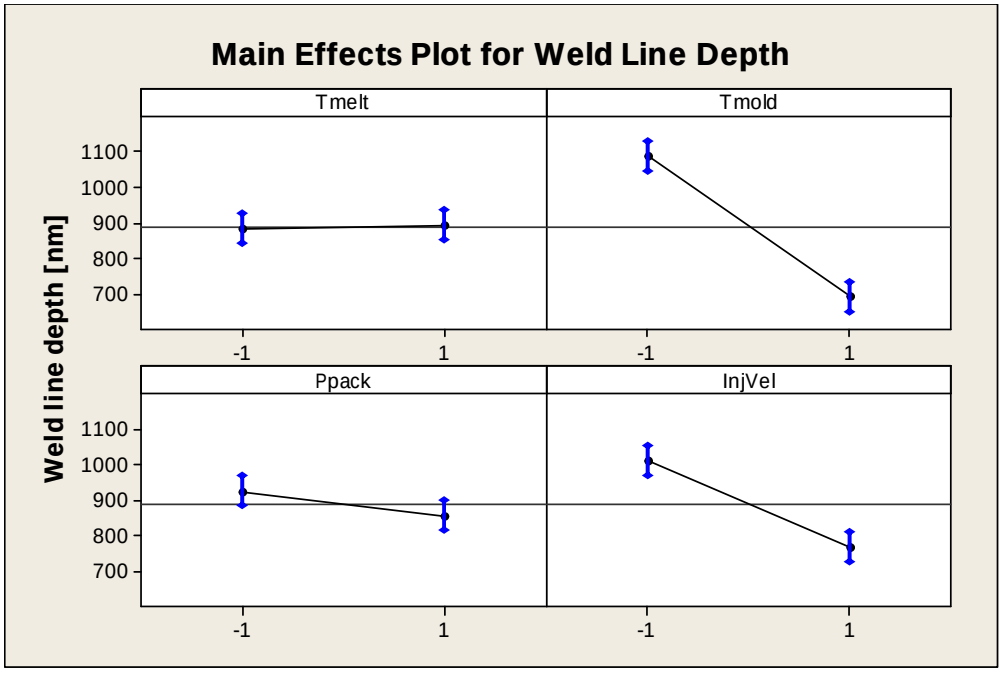

Figure 68 – Main effect plots for weld line depth including measuring uncertainty.

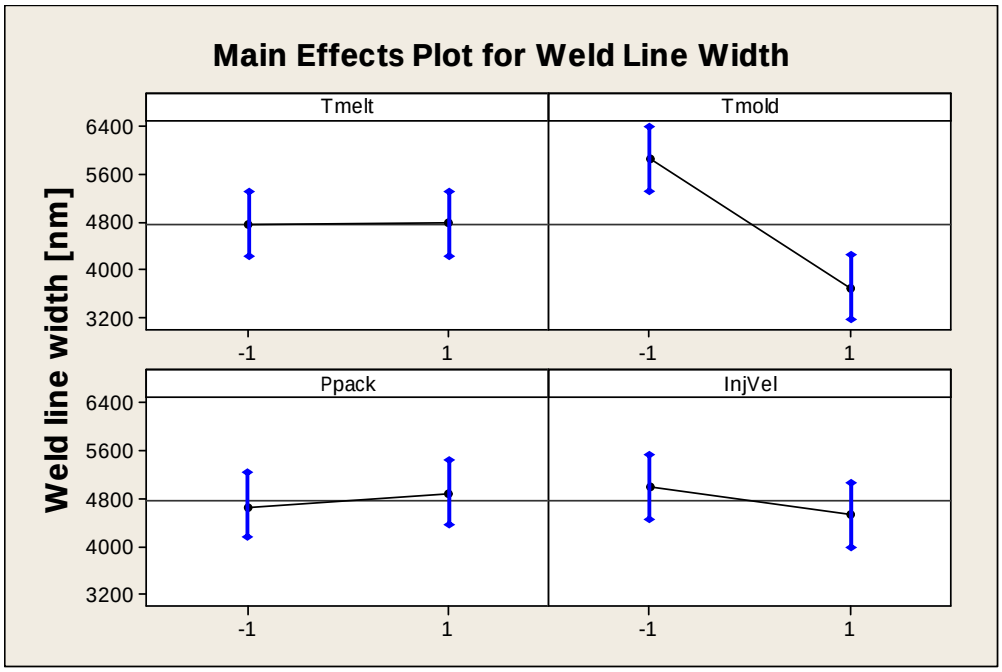

Figure 69 – Main effect plots for weld line width including measuring uncertainty.

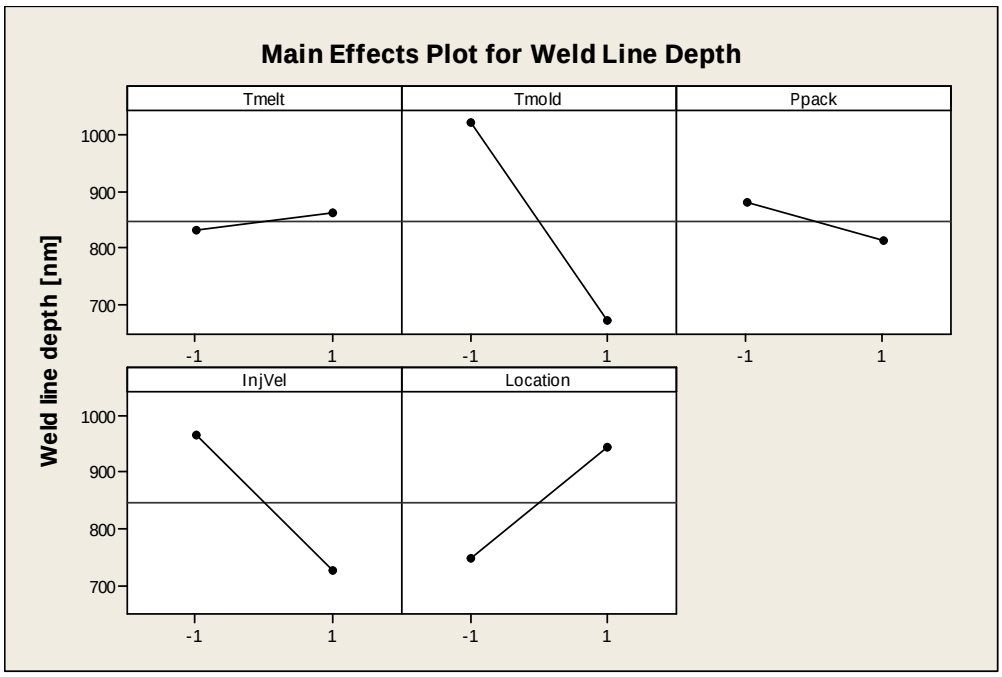

Figure 70 – Main effect plot for weld line depth considering location also as a variable.

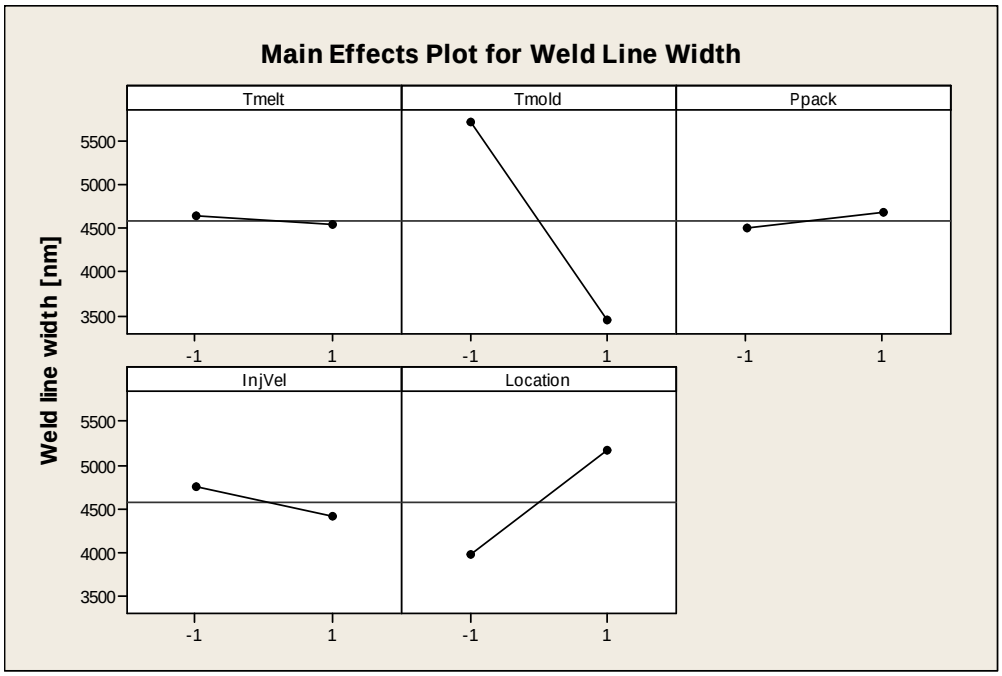

Figure 71 – Main effect plot for weld line width considering location also as a variable.

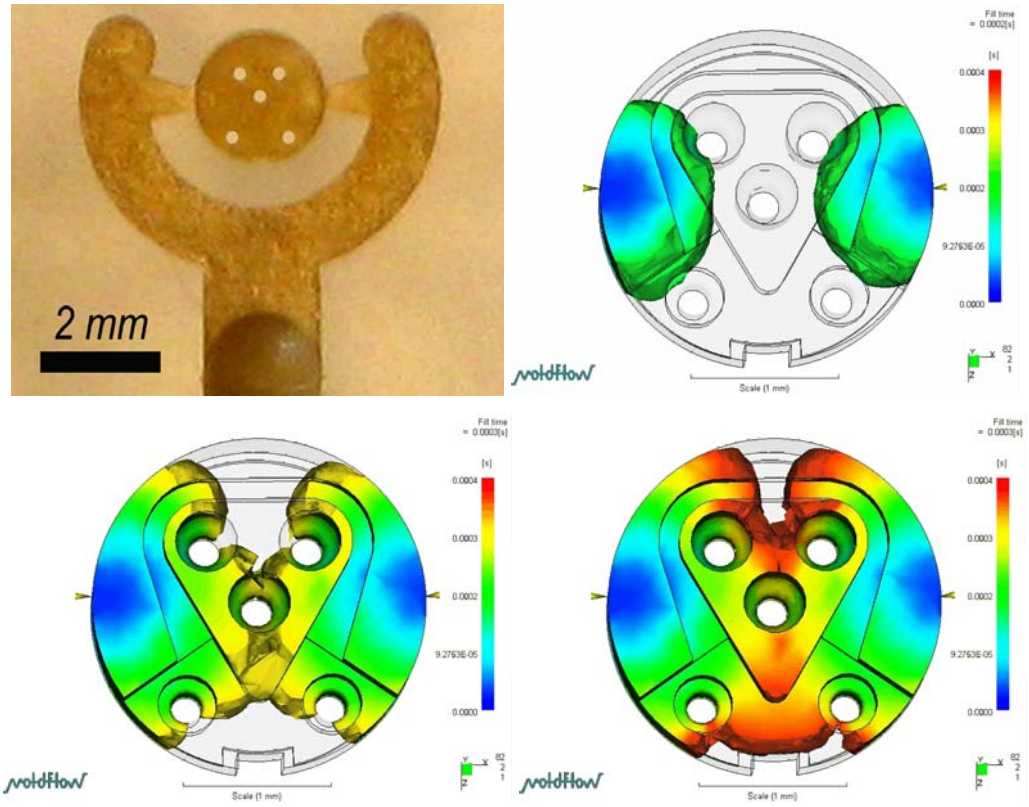

Figure 72 – Multi-gating design of a polymer micro product produced by injection moulding (holes diameter is 300 µm).

4.6 Conclusion

In this chapter, the defects of micro injection moulded parts such as weld lines were investigated. The effect of micro injection moulding process parameters on the weld lines depth and width were analyzed by applying design of experiments techniques. Atomic force microscopy was applied for the three-dimensional characterization of the weld lines. Temperature of the mould and injection speed were found as the most important factor influencing the weld lines on the polystyrene micro injection moulded component.

A higher temperature of the mould allows a higher molecular mobility (i.e. lower viscosity) which permits to obtain smaller weld lines. Higher injection speed causes a decrease of the injection time, which has as consequence to avoid premature freezing of the polymer melt, allowing higher mobility of the polymer at the interface melt front / mould surface. As a conclusion, higher temperature of the mould and

higher injection speed are preferable when moulding micro components with polystyrene polymer grade in order to decrease the importance of weld lines.
On the other hand, the low effect of both melt temperature and packing pressure gives also important indication for the injection moulding of micro components and for the minimization of defects such as weld lines. The former because the melt temperature should not be increased: this will bring to polymer degradation and will not produce a sensible decrease of weld lines dimensions. The latter because higher packing pressure will induce stresses on the polymer matrix as well as on the micro structures of the mould (which has to be avoided to preserve structural integrity of both the plastic part and the mould features).
Finally, it was demonstrated that weld lines dimensions (i.e. depth and width) increase when the distance from the gate increases. Solution to this issue can be represented by a proper multi-gating design which can shorten the flow path length of the polymer melt during the filling of the cavity.

4.7 References

[Bariani, 2005] Bariani P. (2005) Dimensional metrology for micro technology, Ph.D. thesis, Department of Manufacturing Engineering and Management, Technical University of Denmark.

[Fellahi, 1995] Fellahi S., Meddad A., Fisa B., Favis B.D. (1995) Weld lines in injection molded parts: a review, Advances in Polymer Technology, Vol.14, No.3, pp.169-195.

[Gava, 2007] Gava A., Tosello G., Lucchetta G., Hansen H.N., Salvador M. (2007) A new approach for the validation of filling simulations in micro injection moulding, Proceedings of 9th International Conference on Numerical Methods in Industrial Forming Processes (NUMIFORM), pp.307-312.

[Marinello, 2007] Marinello F., Bariani P., De Chiffre L., Hansen H.N. (2007) Development and analysis of a software tool for stitching three dimensional surface topography data sets,

Measurement Science and Technology, Vol.18, pp.1404-1412.

[Tosello, 2007(5)] G. Tosello, A. Gava, H. N. Hansen, G. Lucchetta, F. Marinello (2007) Micro-Nano integrated manufacturing metrology for the characterization of micro injection moulded parts, 7th International Conference of the European Society for Precision Engineering and Nanotechnology (Euspen), Bremen (Germany), 20-24 May 2007, pp.377-380.

[Tosello, 2008(3)] Tosello G., Gava A., Hansen H.N., Lucchetta G., Marinello F. (2008) Characterization and analysis of weld lines on micro injection moulded parts using Atomic Force Microscopy (AFM), Wear Journal (Accepted).

[Wu, 2005] Wu C.H., Liang W.J. (2005) Effect of geometry and injection-molding parameters on weld line strength, Polymer Engineering and Science, Vol.45, Issue 7, pp.1021-1030.

5 Tooling technology

The increasing employment of micro products, of products containing micro parts and of products with micro-structured surfaces calls for mass fabrication technologies based on replication processes. In many cases, a suitable solution is given by the use of polymer micro products, whose production is based on replication technologies such as injection moulding, micro injection moulding, hot embossing, injection compression, etc.

Mass fabrication processes pose the highest challenges in terms of the realization of high quality and high performance micro parts, which depend mainly on the quality and performance of the corresponding micro mould.

Polymer replication technology gives high design freedom and opens opportunities to use 2½D and 3D micro features, free forms features, as well as high aspect ratio micro structures. Mass fabrication of polymer micro components with high aspect ratio and free form micro structures requires high performance micro tools. This makes the manufacturing of the tool a crucial step of the process chain, bringing to the limit the use of single micro machining technologies (e.g. micro milling), especially if the continuous trend towards further miniaturization is considered.

Additionally, the mould and die industry in Europe has more than 5.500 companies, with an average size of 23 employees and total sales of 10.000 M€. Therefore, mould making is an important industry in Europe, dominated by SMEs, and having a strong competition from USA, Japan and other Asian countries [ISTMA, 2004]. Therefore, due to micro product-driven needs for further miniaturization and the strategic importance in the European competitiveness, micro tools manufacturing has been investigated in order to propose innovative solution to improve the performance of the existing micro machining processes.

During the Ph.D. research project, an extensive study on micro tooling processes benchmark integration (i.e. hybrid tooling) has been conducted.

First, a systematic analysis of European partners' expertise in different technologies for processing tool inserts for replication in polymers was conducted within the Network of Excellence (NoE) 4M (Multi-Material Micro Manufacturing, www.4m-net.org). The 4M partners current capabilities in individual tooling processes are presented, and also the expected capabilities for year 2010 are analysed for each of the following processes: micromilling, micro-wire electrodischarge machining (μWEDM), micro sinking electrodischarge machining (μSEDM), laser micromachining, electrochemical micromilling (μECM), and electrochemical milling with ultrashort pulses (ECF).

Later the concept of hybrid tooling as different process chains for tooling fabrication is introduced. Several examples of hybrid tooling within 4M partners are presented. Considered materials are nickel for electroforming, stainless steel for ECF, and tool steel for the other processes, all suitable for the production of micro tools for polymer replication. Current limitations of these technologies concerning feature sizes, surface finish, aspect ratios, etc. are identified. The main conclusion drawn is the imperative requirement to combine individual processes (hybrid tooling) to produce mould inserts required outside research laboratories.

This chapter is structured as follows. Section 5.1 describes the most important micro machining processes for the manufacturing of micro tools, their characteristics and limitations. Section 5.2 introduces the definition of hybrid tooling and examples of hybrid tooling process chains from the literature are given. In section 5.3 a new hybrid tooling process chains realized during the Ph.D. project is presented. This innovative hybrid tooling route, based on micro electrical discharge machining (μEDM), electroforming and selective etching, was realized for the fabrication of a micro tool for the production of polymer micro fluidics platform by injection moulding. Section 5.4 deals with the micro tooling round robin performed within the Polymer Technology Division of the Network of Excellence 4M (Multi-Material Micro Manufacturing). Finally, section 5.5 discusses the metrology benchmark performed to compare the performances of the different tooling technologies employed to produce the micro tools introduced in section 5.4.

5.1 State-of-the-art in micro tooling and future trends of individual processes

The data contained in Table 10 summarise the information collected from 4M partners in order to highlight the limits of each process for producing mould inserts for polymer replication by micro machining. Although in specific cases these limits are surpassed due to current research and development activities, the figures correspond to most common materials used for mould inserts. Table 11 summarize the expected new limits in the same processes for year 2010 according to 4M partners' comments. Although no actual breakthroughs are expected in the near future, trends can be highlighted showing that there is a tendency towards an increase of accuracy, of aspect ratio and towards further miniaturization. On the other hand, nearly no productivity improvements are expected.

	µmilling	µWEDM	µSEDM	µLASER	µECM	ECF
Maximum mould insert external dimensions (mm)	200x200x200	200x200x100	300x300x150	200x200x200	200x200x30	20x20x10
Maximum micro structured area (mm)	100 x 100	200 x 200	200 x 150	200 x 150	40 x 30	20 x 20
Minimum tool size (mm)	0,1	0,02-0,05	0,05	-	-	-
Minimum feature dimension (µm)	50 - 100	20-50	10 - 50	5	50	10
Accuracy (µm)	3-10	2	3	1	8	2
Aspect ratio	2-5	10-50	3-10	2-50	-	10
Roughness (µm Ra)	0,2	0,1	0,1	1	0,1	
Material removing rate (mm^3/min)	20	0,1	0,01	0,04	-	6×10^{-6}

Table 10 – Micro machining capabilities within the European NoE 4M in 2006.

	µmilling	µWEDM	µSEDM	µLASER	µECM	ECF
Maximum mould insert external dimensions (mm)	300x300x200	200x200 x100	300x300x160	200x200x200	300x300x30	100x100x50
Maximum micro structured area (mm)	150 x 150	200 x 200	200 x 150	200 x 150	100 x 100	100 x 100
Minimum tool size (mm)	0,04	0,01	0,005	-	-	0,0005
Minimum feature dimension (µm)	10 – 25	5-20	4 – 10	1	10	0,5
Accuracy (µm)	1	0,5	0,5	0,5	2	0,5
Aspect ratio	5-10	100	50	> 50	20	100
Roughness (µm Ra)	0,1	0,05	0,05	0,4	0,05	
Material removing rate (mm^3/min)	20	0,1	0,01	0,04	1	4×10^{-3}

Table 11 – Expected limits to be reached in 2010 according to NoE 4M.

At present time, micro machining processes currently employed for the manufacturing of micro moulds show limitations

- Micro milling is problematic with sizes below 0.1 mm in tool steels, and repeatable feature sizes below 50 µm (even with the newest 40 µm tools for milling and drilling) are not possible. Smaller tools down to 20 µm are also available but are limited to drilling and with low quality in the cutting edges.
- Wire-EDM (Electro Discharge Machining) with thin wires, smaller than 50 µm (20-30 µm), allows better accuracy and surface roughness but is limited to ruled geometries. Micro-die sinking EDM is also very problematic for obtaining features sizes below 50 µm, and the roughness is still poor for replication purposes.
- Micro EDM milling is a promising new technology in the field of EDM [Fleischer, 2005] [Uhlmann, 2005]. Flexible and suitable for three-dimensional feature machining, the process needs investigation in order to assess parameters for electrode wear compensation. Electrode diameters down to 15-20 µm can be obtained by means of a micro wire-EDG (electro discharge grinding) unit.
- Laser milling is most suitable for machining parts with one-sided geometry or for partial machining of components from one side only. Complete laser milling of parts is also possible but difficulties in accuracy of re-positioning for additional set-ups have to be addressed. The influence of the process parameters is complex and must be optimized to obtain the highest part quality [Pham, 2004].
- A new technology called electrochemical micro milling (ECF, where F is the German acronym for milling) has been recently introduced to machine hard materials like stainless steel and other electrochemical active materials. Feature dimension below 50 µm have been obtained [Staemmler, 2006]. The very small removal rate ($6x10^{-6}$ mm^3/min) allows for high resolution in machining and therefore is suitable to manufacture the finest details in a pre-machined structure.

Clearly, with the increase of miniaturization and integration of different micro features, only a combination of processes can lead to an accurate manufacturing of micro moulds. The concept of hybrid tooling is therefore introduced (see section 5.2).

5.2 Hybrid tooling

Hybrid tooling is defined as the ***capability of producing a mould insert combining two or more processes in sequence***. Most of the cases are based on the combination of conventional and energy assisted micro machining processes like micromilling, μEDM, μECM or laser machining. Other processes such as electroforming and photolithography are also included.

According to a recent review on hybrid tooling [Azcarate, 2006], a number of different process chains has been already established at research level and are briefly introduced in the following.

- μEDM + USM or + μECM
    - This hybrid tooling process chain consists on the generation of the main shape by μEDM on a conductive material. As second step, μ-ultrasonic machining (μUSM) for improving surface roughness or μECM for improving material removal rate and resolution are applied. In some cases, the μEDM process is used for electrode preparation. The electrode is machined down to the required dimensions, and is then used in μECM process, where no wear occurring on the electrode, onto the same machine. In this case, to overcome surface roughness limits of μEDM, ultrasonic machining for surface finishing is required.
- Micro milling + electroforming + etching
    - This process chain combines a material-removal process by mechanical machining (i.e. micro milling), with electroforming (indirect tooling, alternative A in Figure 73) and etching, and should be considered as a viable alternative to direct mould insert machining (direct tooling, alternative B in Figure 73). The process chain starts with the micro milling in a ‘soft’ material like aluminium or zinc, following by the electroforming on milled surfaces to form a nickel layer with the

negative geometry. It requires a conducting surface for electroplating purpose. Final dissolution of the aluminium substrate by selective etching will free the nickel surface of the tool insert and thereby negative geometry. It requires a true selective etching process that only attacks the base material: aluminium or zinc, but not nickel. Its main advantage is based on the easier machining of a positive structure in 'soft' material, with minimum tool wear and good surface quality. It allows combining a true 3D process as micro milling with clean room technologies. It is critical a good cleaning and activation between steps 1 and 2, and also to achieve a stable and low stress electroforming process. Other cases with a similar configuration chain are presented in Table 12. In this case to overcome the limits imposed by the complexity of some features it is necessary to use an indirect way for producing mould inserts.

(1)

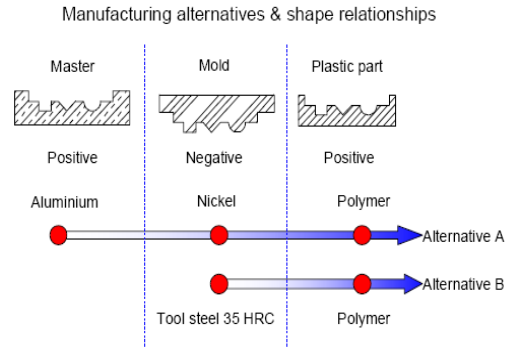

(2)

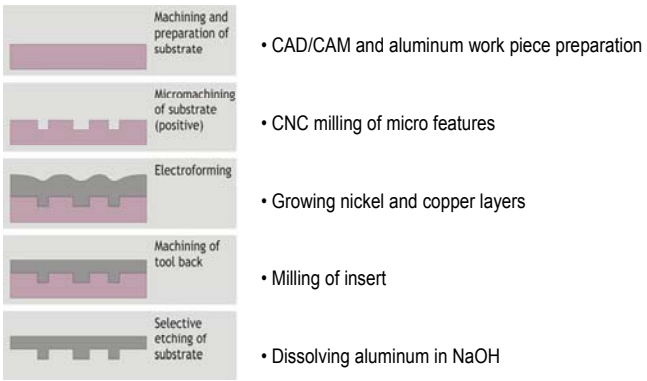

Figure 73 – Indirect hybrid (alternative A) and direct (alternative B) process chain for micro tool inserts manufacturing (1) [Azcarate, 2006]; process chain steps for the indirect hybrid tooling (alternative A) (2) [Bissacco, 2005].

Hybrid indirect tooling (a) → Si etching + electroforming + etching	
Process 1	Advanced silicon etching of a silicon wafer
Process 2	Electroforming to form the tool insert
Process 3	Selective etching of silicon without damaging the master structure
Remarks	It is much easier to dissolve silicon than aluminium since silicon is very pure and dissolved readily in potassium hydroxide. A metallization step is required between process 1 and 2, in order to make the silicon master sufficiently conducting for the electroforming process.

Hybrid indirect tooling (b) → Laser machining + electroforming + etching	
Process 1	Laser micromachining in polymer
Process 2	Electroforming to form the tool insert
Process 3	Selective etching
Remarks	Polymers like ABS are easily dissolved in acetone which will not attack electroforming metals as Ni or Cu. Also a metallization step is required to make the polymer master sufficiently conducting for electroforming.

Hybrid indirect tooling (c) → Photolithography + electroforming + photoresist removal	
Process 1	Photolithography in SU8
Process 2	Electroforming to form the tool insert
Process 3	Photoresist removal without attacking the electroformed metal
Remarks	Potential problems with side wall angles and the removal of the SU8. Solving the photoresist removal by introducing intermediate layers will often result in problems elsewhere.

Table 12 – Different hybrid indirect tooling solutions including micro machining of a soft substrate such as silicon (a) and polymer (b)(c), electroforming and selective etching of the substrate [Azcarate, 2006].

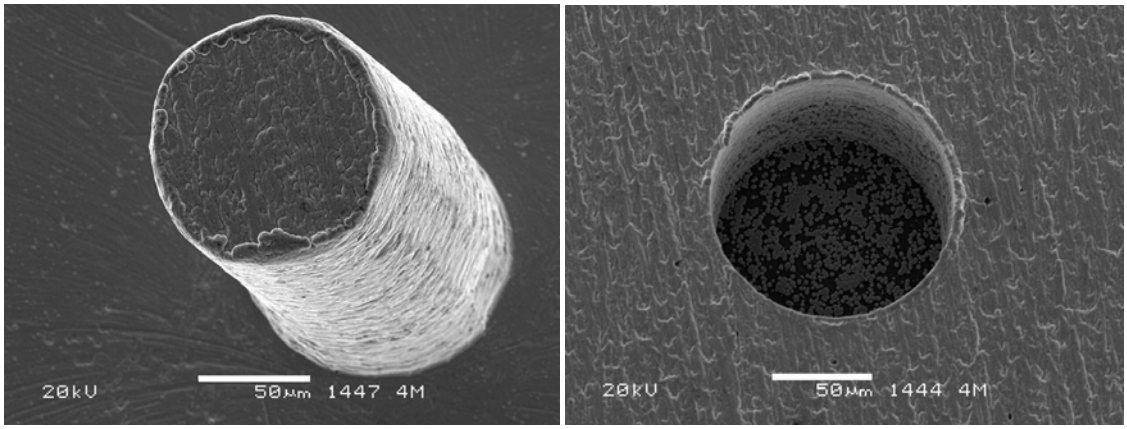

(a) (b)

Figure 74 – Two examples of micro features on micro tool for obtained by electroforming of micro machinined aluminium substrate: a 150 µm diameter pin (a) (which was first a hole in the aluminium substrate) and a 150 µm hole (b) (which was first a pin in the aluminium substrate) [Tang, 2006].

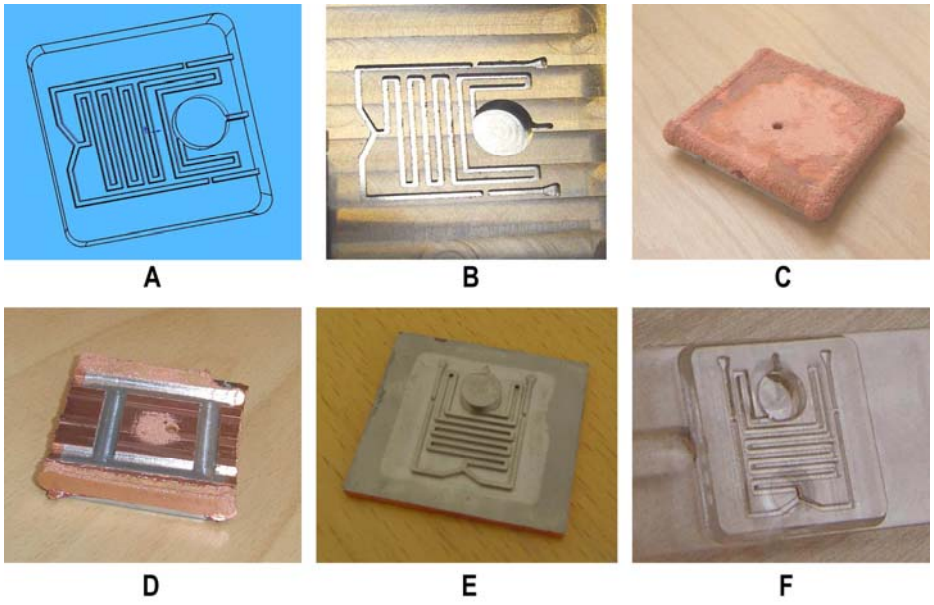

Figure 75 – Complete process chains for the manufacture of a polymer micro fluidic platform from design to final polymer part based on an indirect hybrid tooling method: (A) part design, (B) micro milling of the micro features positive geometry on aluminium substrate, (C) nickel and copper deposition by electroplating, (D) insert machining for dimensional fitting, (E) insert obtained after aluminium dissolution (with

negative geometry), (F) injection moulded part with micro channels [Tosello, 2005(2)].

- Micromilling + ECF
    - This hybrid tooling route combines material-removal by mechanical processes (micro milling), with ECF (electro chemical milling). In principle the rough machining and the shaping of the larger features (down to 100µm) of the tool insert are machined by micro milling, usually in steel. Consequently the ECF process is used where higher resolution, sharper edges and smaller radius than the micro mill are required. The main advantages of this technique are the small tools available (down to 5-10 µm), the absence of tool wear and no generation of burrs. Examples of structures obtainable with this hybrid tooling technique are long and thin ribs with high aspect ration (up to 5) as shown in Figure 76: each rib is 100µm deep, 1 mm long, and from 20 µm to 100 µm wide. The outer contour was micro milled and the grooves between ribs were ECF-processed into stainless steel 1.4301. This hybrid tooling technology is particularly suitable for the manufacturing of metal micro features without burrs at the edges.

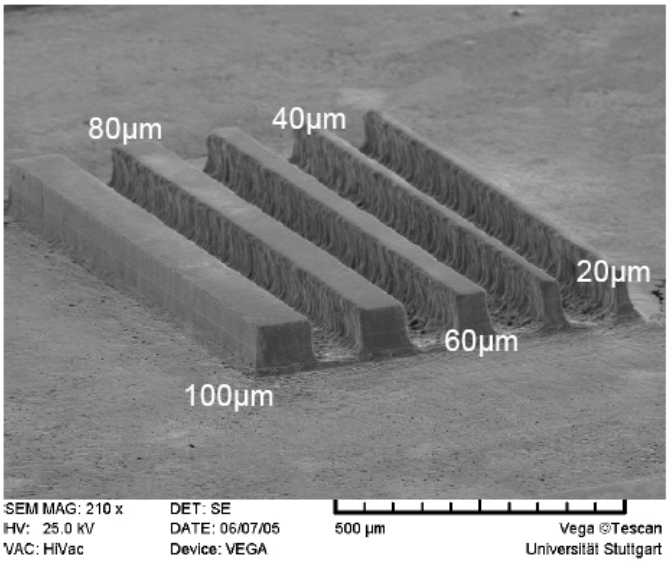

Figure 76 – Test part with micro features machined by a combination of micromilling and ECF [Staemmler, 2007].

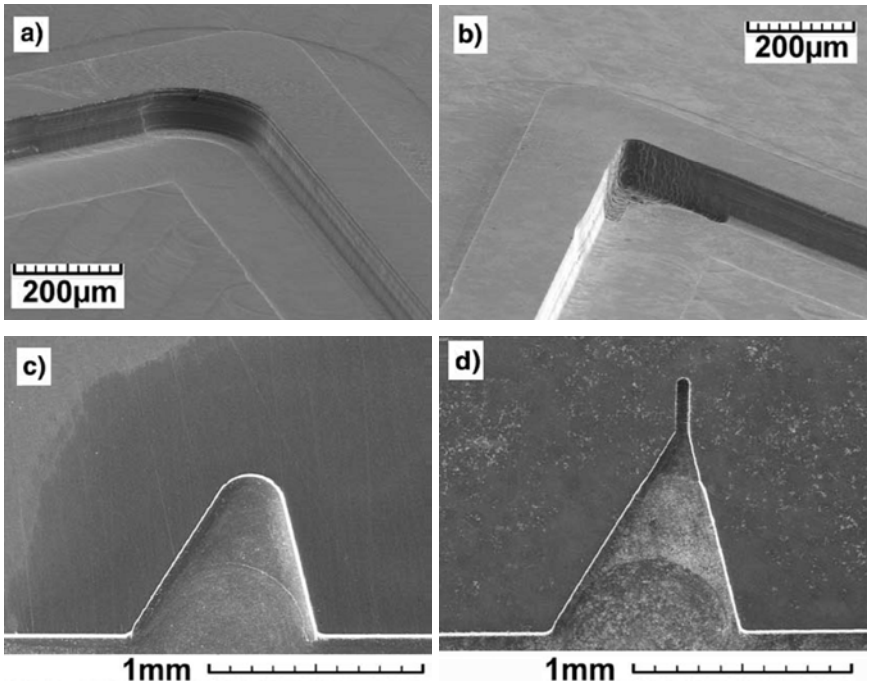

Figure 77 – Two examples of micro hybrid tooling for micro fluidics application where the milled main shape (details (a) and (c)) is finished with an ECF machining step (details (b) and (d)) [Staemmler, 2007].

5.3 Hybrid indirect tooling using µEDM, selective etching and electroforming

Mass fabrication of polymer micro components with high aspect ratio micro structures (i.e aspect ratio higher than 2-3) requires high performance micro tools compatible with low cost replication processes such as micro injection moulding or hot embossing. To this respect the realization of the tool poses the greatest challenges in terms of costs, achievable geometry, accuracy, surface topography and minimum obtainable feature size. Manufacturing methods based on photolithographic processes enable the realization of silicon masters with sub-micrometric features and high aspect ratios. They require however the use of clean room facilities and preparation of a lithographic mask, making the process expensive and inflexible. Furthermore this method is limited to the realization of 2½D features. Alternatively, the tools can be realized by direct machining using material removal processes such as micro milling or micro electrical discharge machining. As seen in section 5.1,

micro milling shows limitations in terms of minimum feature size and obtainable aspect ratio. The smallest mills capable of machining high aspect ratio structures have a diameter of 100 µm, posing limits for example to minimum radius obtainable (50 µm).

Micro structures by micro electro discharge machining (µEDM) depend on the chosen configuration. Wire-µEDM with thin wires (diameter down to 20 µm) allows the machining of small and accurate micro structure but it is limited to 2½D geometries. Sinking µEDM needs the prior manufacturing of an electrode having a negative geometry with respect to the part. Consequently, the employed process is usually micro milling, whose limitations have already been mentioned.

When the focus is on micro tooling and especially for micro fluidic production purposes, a direct tooling strategy is time consuming because of the machining of the protruding walls and plateaus (which will create channels and reservoir chambers respectively in the polymer product).

Indirect tooling, instead, refers to a tooling technology where a master structure produced by machining is the positive geometry and it is identical in shape to the final product. This strategy reduces enormously the amount of material to be removed (especially in case of micro fluidic systems): channels and reservoir chambers will be directly machined. Subsequently, by electro-deposition of a solid layer of metal on top of the machined master and its selective etching, the final micro tool with negative geometry is obtained [Tang, 2006].

In order to investigate the possibility to overcome the limitation of the mentioned micro tooling technologies and to extend the application of hybrid tooling with even further miniaturization and higher aspect ratio, a micro fluidic design has been selected. For this reason, a newly developed technology, named µEDM-milling, which allows the machining of three-dimensional micro structures with high aspect ration and lateral dimension down to 20 µm, has been selected [Uhlmann, 2005].

The aim of the study was to manufacture a micro tool for polymer-based micro fluidic fabrication and consequently to employ the micro tool for polymer replication by mean of the injection moulding process.

5.3.1 Part design

In order to investigate the feasibility of application of the selected of the hybrid tooling process chain a micro fluidic device has been chosen (see Figure 78).

The micro fluidic system design was defined within the activities of the European Network of Excellence 4M (Multi Material Micro Manufacturing) and included a blood/plasma separation unit based on micro channel bend structures [Blattert, 2005]. The system contained large reservoirs chambers (diameter of 3 mm), long channels (length of 2.88 mm) with a minimum width of 20 µm and a total depth of 90 µm (realizing a maximum aspect ratio of 4.5) as well as radius of 25 µm on the meeting point of the three ribs in the mould.

The challenges represented by this geometry were the following:

- Channels 20 µm, 50 µm, 75 µm wide.
- Radius down to 25 µm.
- Depth of 90 µm (i.e. aspect ratio up to 4.5).
- Presence of features having dimensions both in the millimeter as well as in the sub-millimeter range (channel length of 2,88 mm, reservoir chamber with diameter of 3 mm).
- Sub-micrometer roughness (suitable for micro fluidic applications).

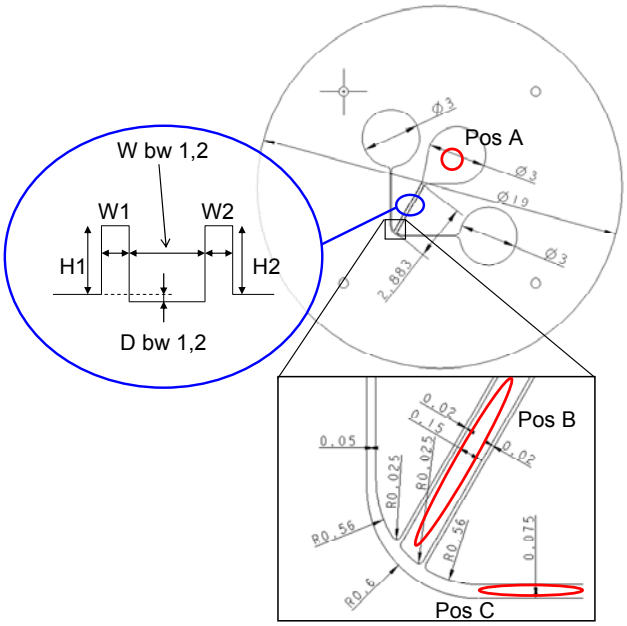

Figure 78 – Micro fluidic system layout and dimensions [Tosello, 2007(6)].

5.3.2 Process chain

The µEDM-milling process was selected as starting micro machining process. The material substrate (or master) needed to be suitable for both µEDM-milling (to be conductive or semi-conductive, i.e. with an electrical resistivity lower than 10 ohm-cm) and for selective etching after the electroforming is completed. Moreover, due to the micro fluidic application, it was preferable to have a flat and smooth substrate surface to ease the sealing during the packaging of the final product (i.e. bonding of a lid on top of the micro fluidic system). For these reasons, an 8 inches silicon wafer (1000 µm thick) was used as a substrate to be machined by µEDM-milling.

The process chain was composed by the following steps:

- µEDM of micro structures on the silicon substrate (master).
- Laser cutting of the Si wafer to the specified size and shape to fit into the holder for the electroforming bath.
- Pre-treatments including cleaning and deposition of a thin layer of Ti/Cu by PVD coating.
- Electroforming of nickel and copper for the insert fabrication.
- Selective etching of silicon in a warm alkaline solution.
- Mechanical machining of the back of the insert and of the external shape.
- Final cleaning and selective etching of the Ti/Cu layer.

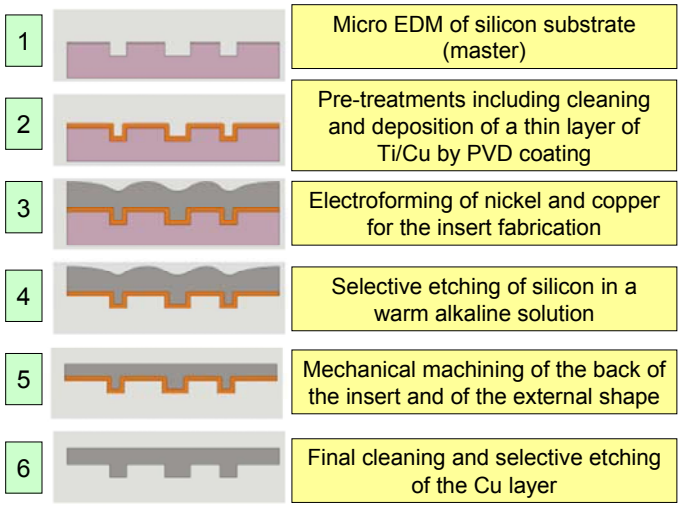

Figure 79 – Micro tool manufacturing by hybrid tooling process chain [Tosello, 2007(7)].

In the following sections, a detailed description of the implementation of the employed processes is given.

5.3.3 μEDM of silicon

The μ-EDM milling process was selected for the generation of the channels and reservoirs on the wafer surface. Micro electrical discharge milling consists in a recent evolution of the electrical discharge machining (EDM) process that overcomes the limitations of the more conventional sinking and wire EDM. In micro EDM, the machining of conductive materials is performed by a sequence of electrical discharges occurring in an electrically insulated gap between a tool electrode and a workpiece. During the discharge pulses, a high temperature plasma channel is formed in the gap, causing local melting and evaporation of both workpiece and electrode material. The machining forces are negligible compared to those in mechanical material removal processes.

Micro EDM milling combines the advantages of the EDM process, as insensitivity to workpiece material hardness, absence of burrs and capability to machine brittle materials, with the flexibility of conventional 3 axes milling strategy and allows the generation of complex 3D micro geometries with no need for complex electrode preparation as in the case of sinking EDM. In fact, in micro EDM milling, circular electrodes of the desired diameter, and down to less than 10 μm, are driven by a CNC controller interfaced with a dedicated CAM module. The electrodes can be shaped to the desired diameter by means of a wire electro discharge grinding (WEDG) unit. The material is removed layer by layer, with layer thickness ranging from a few microns down to 0.1 μm, depending on the diameter of the electrode and on the discharge energy. As the process erodes both the workpiece and the electrode, it is necessary to compensate for the electrode wear. In this respect, the simple electrode geometry realized in the micro EDM milling process, combined with the small layer thickness enables uniaxial wear compensation. Thus, the implementation of an electrode wear compensation algorithm allows controlled material removal with machining accuracy of less than 2 μm [Bissacco, 2007(1)]. The machine tool used in this investigation was a Sarix SX-200, having 3 controlled axes and equipped with a WEDG unit for electrode preparation. Although electrical

discharge machining relies on the electrical conductivity of the workpiece material, the range of machinable materials is not limited to metals and alloys, but includes semiconductors as for instance silicon [Feng-Tsai, 2006]. The application of micro EDM to the machining of silicon has some remarkable advantages like high material removal rate and low electrode wear (when compared to the machining of steel or tungsten carbide), in addition to the advantages given by the characteristics of the substrate (flatness, low surface roughness, low cost, etc). However there are also a number of issues that need to be solved. A dedicated vacuum clamping system, capable of working in presence of oil, was developed in order to ensure the position of the substrate throughout the processing. Furthermore, the position of the silicon wafer in the machine tool working volume must be defined. This is normally done by touching the workpiece surface with the rod electrode while applying a low voltage difference between tool and workpiece. Due to the lower conductivity of silicon compared to metals and the higher contact resistance, no short circuit occurs and the machine is therefore unable to detect the surface. In order to overcome this problem, it was necessary to coat the wafer's surface with a conductive metallic layer of Ti/Au by means of PVD (Figure 80).

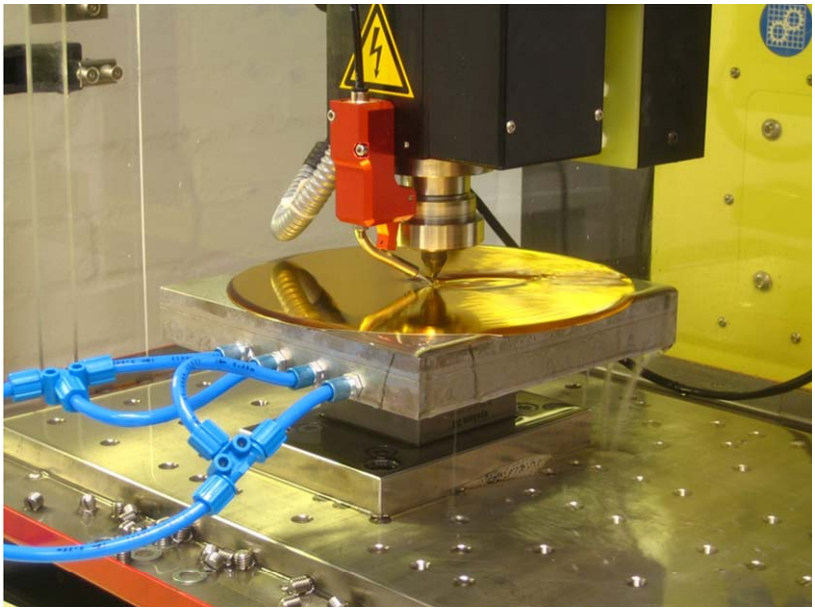

Figure 80 – Micro electric discharge machining (μEDM) of the Ti/Au coated silicon substrate attached to the vacuum clamping system.

Another problem was the lack of data in the literature concerning micro EDM milling of silicon. The accuracy of the machined structures strongly depends on the accuracy of the dressed electrode diameter, the knowledge and stability of the discharge gap and the accuracy of electrode wear compensation. The optimal settings for process stability, both in terms of engagement conditions and pulse characteristics, strongly depend on the electrode diameter as well as on the desired surface roughness. In order to ensure high accuracy of the dressed electrode diameter, a calibration of the WEDG process was performed, in stabilized thermal conditions, for a tungsten carbide electrode with diameter of 15 μm; this is the smallest electrode diameter intended to be used in the realization of the master, achieving electrode dressing accuracy of ±2 μm. For the same diameter, a dedicated process parameter optimization was performed, with respect to gap size and process stability [Bissacco, 2007(2)]. In this respect, one noticeable feature present in most of the process parameters combinations considered in this optimization study is the formation of banks of recast material at the sides of the machined grooves (Figure 81). As a consequence of these preliminary experiments, an optimized process parameter configuration in connection with 15 μm electrodes was employed. For larger diameters, no optimization was performed, and the parameter settings were extrapolated by adaptation of those known for steel. No optimization was conducted with respect to wear compensation. However in-process corrections were performed by means of the frequent automatic wear checks set up in the CAM program.

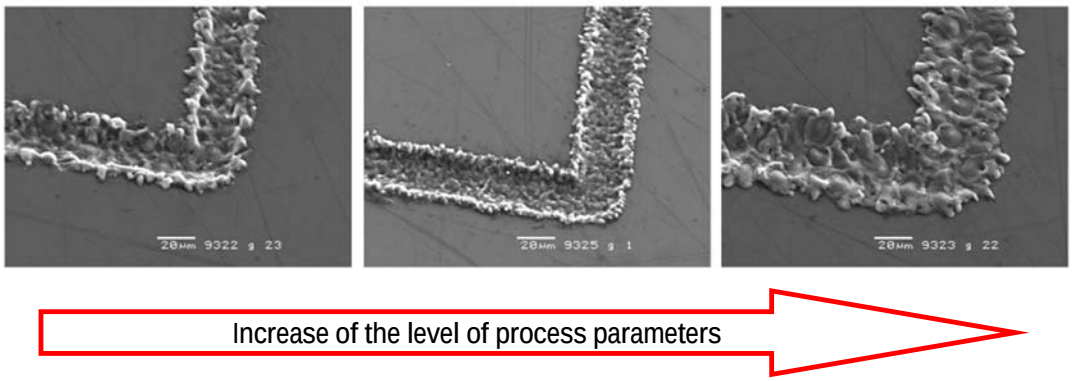

Figure 81 – Effect of μEDM process parameters (energy, voltage, average voltage on a spark cycle, frequency) levels on the machining of silicon substrate. Nominal test grooves width is 20 μm, electrode diameter is 15 μm [Tosello, 2008(4)].

Besides the high accuracy and the ability to generate true 3D geometries, important advantages of this process – as compared to conventional methods used for the preparation of silicon masters – are represented by its high flexibility, no need for masking and the CAD-CAM interface compatibility. Any design change of the insert can be readily implemented simply by modifying the CAM file. Furthermore the process does not require to be operated in a clean room environment, with a consequent reduction of the manufacturing costs.

For the generation of the 20 µm, 50 µm, 75 µm wide and 90 µm deep channels, electrodes with diameters of 15 µm, 45 µm and 68 µm were used respectively. SEM images of the machined features are shown in Figure 82 along with the nominal and measured dimensions.

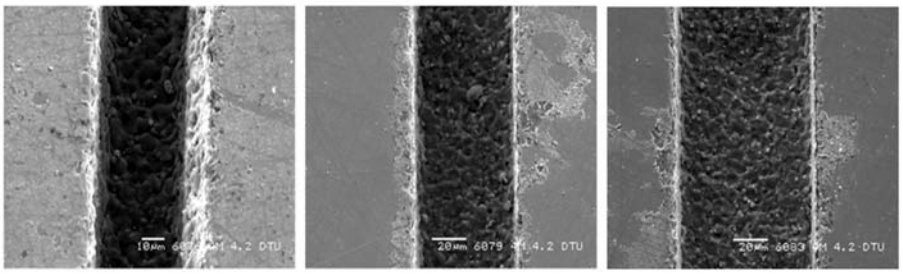

Width – Nominal (±T)	(20 ± 5) µm	(50 ± 5) µm	(75 ± 5) µm
Width – Measured (±U)	(38 ± 3) µm	(57 ± 2) µm	(76 ± 3) µm
Depth – Nominal (±T)	(90 ± 5) µm	(90 ± 5) µm	(90 ± 5) µm
Depth – Measured (±U)	(113 ± 3) µm	(106 ± 3) µm	(89 ± 3) µm

Figure 82 – Micro channels produced by µEDM in a silicon substrate. Nominal widths (20 µm, 50 µm, 75 µm) and depths (90 µm), with the tolerance (T) of 5 µm defined by the design specifications, are compared with actual measured dimensions. Width measurements (performed with scanning electron microscope (SEM) and image post-processing) and depth measurements (carried out with autofocus 3D laser profilometer) are indicated with the respective measuring uncertainty (U, expressed with a coverage factor k=2 for a confidence level of 95%).

Although the machining parameters for the smallest electrodes were optimized through a set of dedicated experiments, the smallest channels show a relatively large deviation from the nominal geometry consisting mainly in the presence of a draft

angle (particularly evident on one side). This is reckoned to be caused by unfavourable flushing conditions, forcing the erosion debris towards one side of the channels and thereby locally enlarging the sparking gap. The phenomenon is not visible for larger channels and a possible solution is to force the flushing along the longitudinal direction of the channels.

5.3.4 Electroforming

After µEDM milling, the silicon master was cut out from the wafer in a circular shape using an Nd:YAG laser and a pre-treatment process was applied in order to carry out the subsequent advanced electroforming process. The pre-treatment consisted of two steps. First a chemical etching [Enthone, 2007] of the Au layer that was originally on the silicon wafer. In the areas affected by the µEDM-milling the Au had already been removed, and therefore – in order to avoid problems with different electrochemical behaviour of the various materials – it was decided to remove the Au layer everywhere. In the second step a thin layer of Ti/Cu was applied by PVD DC-magnetron sputter coating. Titanium is often used as an under-layer or adhesion layer due to its good adhesion to many materials [Plummer, 2000]. The 50 to 100 nm thick layer is sufficient for achieving good adhesion between the wafer and the Cu layer. After the deposition of the Ti layer an estimated 300 nm thick Cu layer was deposited as a conduction layer, without breaking the vacuum of the chamber, in order to avoid any oxidation of the Ti. In order to apply the coating to the side walls, the sputtering process was optimized for maximum step coverage. For higher aspect ratios, or negative slopes, problems can occur as sputtering generally is a line-of-sight process. To overcome this, the wafer can be tilted and rotated inside the deposition chamber. This step is necessary in order to create a uniform electrically conducting plating base for the electroforming process.

Electroforming of nickel and, after that, of copper was then performed. In particular, the nickel deposition was carried out by immersing the master for 5h in a specially optimized low-stress nickel bath. The bath was based on nickel sulphamate and operated at 32 °C with a relatively low current density of 1.0 A/dm^2 (corresponding to a deposition rate of 0.18 µm/minute), resulting in a deposited thin nickel layer (54 µm) for tool wear resistance. The relatively low temperature of the nickel-sulphamate-based bath nearly avoids the introduction of thermal stresses induced by the

difference of the thermal expansion coefficient of silicon ($2.49 \cdot 10^{-6}$ 1/°C) and of the nickel ($13.1 \cdot 10^{-6}$ 1/°C). The decrease of the effect of the internal stresses induced by the electrochemical deposition, was one of the reasons for choosing the 8" wafer, as the thickness of a standard Si wafer increases with increasing size. Having a relatively thick substrate made the stresses unable to bend the substrate.

After the deposition and a surface re-activation, the nickel plated silicon master was immerged in the copper bath which was mainly composed by an aqueous solution of $CuSO_4$ and H_2SO_4 at room temperature. In addition to that, a commercially available organic solution [Enthone, 2006] was added in a concentration of 40 ml/l. With a deposition time of 168 hours, a 2.75 mm thick layer of copper could be deposited. The advantage of using copper deposition as the second and thicker layer is that the bath can run at room temperature which means only low stresses were induced on the workpiece. Moreover, the cold bath is also significantly easier to manage: it does not require external heat and water does not evaporate. From the point of view of the micro tool, the copper layer has a higher thermal conductivity than nickel (385 W/m·K and 60.7 W/m·K respectively) which for a mass-production application could turn out to be an important feature since the better thermal conductivity enables fast application and removal of heat and thus faster cycle times in the injection moulding process.

5.3.5 Selective etching

The next step was the silicon dissolution, which was performed using a NaOH (60 g/l) solution. Mechanical agitation of the solution was applied to remove dissolute silicon from the wafer surface and convey forward new silicon to be dissolved in contact with the solution. Furthermore, mechanical agitation ensures homogeneity of the solution's temperature. The temperature of the solution was 60 °C and the process lasted 24 hours to make sure that all the silicon was dissolved.

Once the Ti/Cu surface appeared (previously deposited by PVD as a plating base) due to the silicon being dissolved, it was removed using a patented selective etching solution [Tang, 2006(2)] which will only remove Cu and not attack the Ni tool surface in any way (Figure 83). The thin Ti layer (estimated thickness was between 50 and

100 nm) will most likely not be attacked by the etching solution. Instead, it will most likely oxidize to TiO_2 when coming into contact with air or water. The relatively soft Cu layer is mainly removed to avoid wear of the tool surface during injection moulding. If the Cu is removed in a non-uniform way because of wear it will lead to dimensional changes of the polymer products.

5.3.6 Post-processing

The manufacturing of the insert was finally completed by precision milling of back side of the block. A flat surface on the copper side is machined parallel to the nickel surface. Moreover, wire-EDM of the insert was used to give the insert the desired circular shape (Figure 84). Final dimensions were a thickness of 2.875±0.005 mm and a diameter of 18.95±0.01 mm.

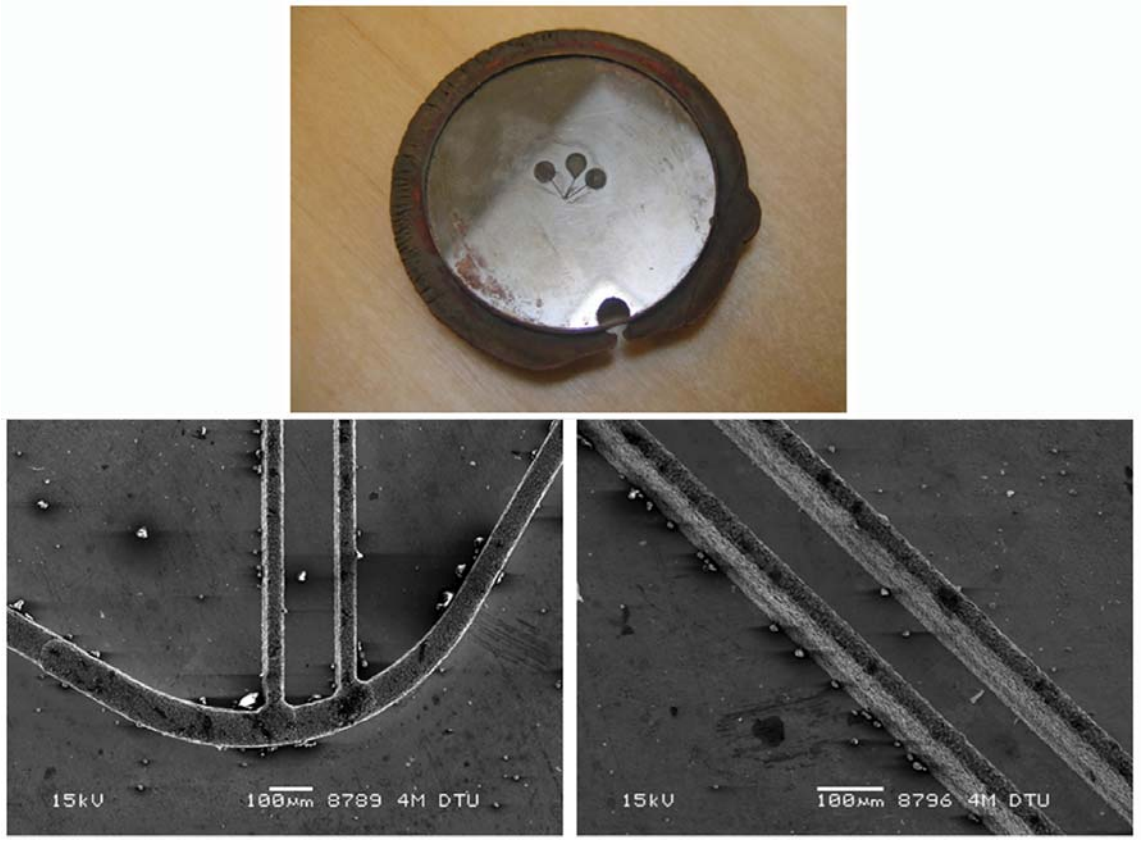

Figure 83 – Nickel substrate after electroforming and selective etching (above). SEM images of the micro walls obtained after nickel electro deposition and silicon etching (below).

Figure 84 – Milling of the back side of the tool (left) and wire-EDM cut for final shape definition (right). The double layer composed by Cu and Ni is visible from the side of the micro tool.

5.3.7 Injection moulding

The micro tool was employed for polymer replication by means of the injection moulding process. A commercially available polypropylene grade (from the manufacturer Basell) was used as polymer material.

Process parameters suitable for the replication of the microstructures (high injection speed = 350 mm/s, temperature of the mould = 75 °C, temperature of the melt = 260 °C) were employed. The tool has demonstrated a good mechanical resistance (sign of good filling of the micro ribs by the electroforming process). A batch of more than 200 injection moulded components was produced on a Ferromatik Milacron K60 injection moulding machine (see Table 3 for machine charactristics).

Dimensional correspondence with the tool and good definition of the edges were verified by means of dimensional measurements and qualitative inspection using scanning electron microscopy and subsequent image post-processing for width measurements. The depth of the injection moulded channels was measured with an optical CMM, whereas heights of the micro walls on the tool were measured using a 3D mechanical stylus roughness tester.

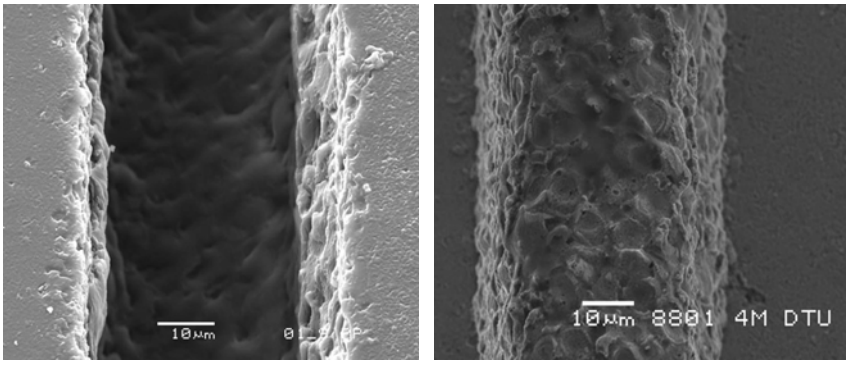

Width	(38±3) µm	(37±3) µm
Depth	(110±1) µm	(110±6) µm

Figure 85 – Comparison between µ-tool and polymer part for replication capability assessment: results regarding the feature 20 µm wide and 90 µm high (nominal).

The different manufacturing processes involved in the hybrid tooling process chain resulted in different surface topographies on different locations of the tool. The electroformed surface of the wafer presented a roughness in the nanometre scale, whereas the surface firstly obtained by µEDM and then electroplated had a roughness in the sub-micrometre range. Moreover, the traces left by the wafer polishing are still visible in the nickel tool (due to the high resolution of the electroforming process) and in the polymer replica. On the other hand, the µEDM surface appears as a random surface. Due to the optimized injection moulding process parameters, sub-micrometre and nano-features of both types of surfaces could be replicated from the master tool to the polymer replica. Surface topography measurements were carried out using an atomic force microscope (AFM) in order to evaluate the replication of both roughness types:

- Replication of the polished Si-wafer's surface substrate (Figure 86):
  - Nickel tool: Sa = 14 nm, Sq = 22 nm;
  - Polymer part: Sa = 14 nm, Sq = 19 nm;
  - Measuring uncertainty estimate = ±15% (k=2, conf. 95%).
- Replication of the µEDM-ed Si-wafer's surface substrate (Figure 87):
  - Nickel tool: Sa = 314 nm, Sq = 392 nm;
  - Polymer part: Sa = 341 nm, Sq = 432 nm;
  - Measuring uncertainty estimate = ±15% (k=2, conf. 95%).

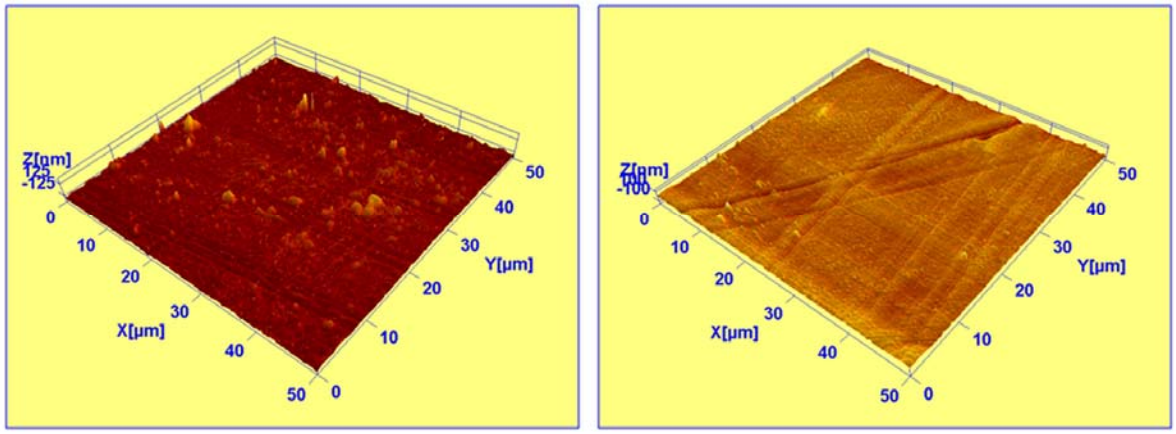

Figure 86 – AFM scanning of the polished Si-wafer surface replicated by electroforming on the tool (left) and by injection moulding on the polymer part (right) [Tosello, 2008(4)].

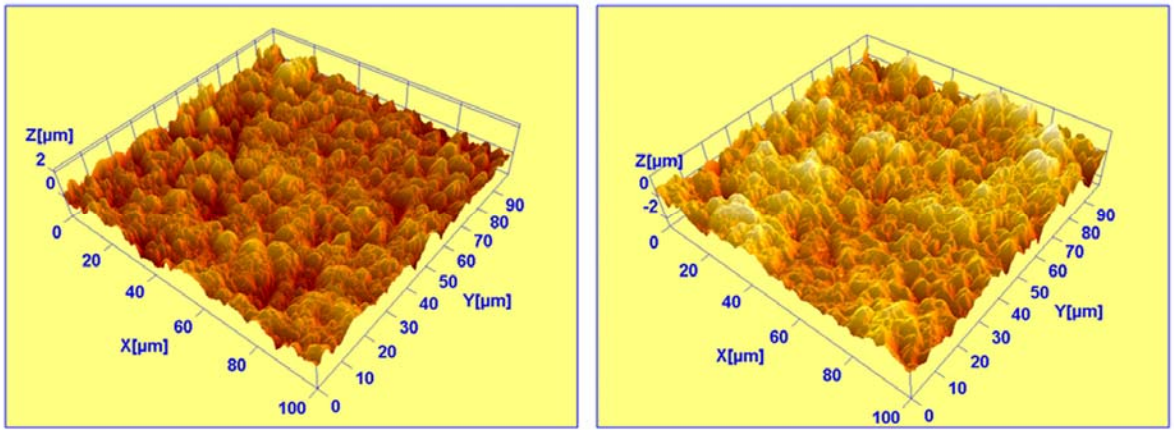

Figure 87 – AFM scanning of the µ-EDM-ed Si-wafer surface replicated by electroforming on the tool (left) and by injection moulding on the polymer part (right) [Tosello, 2008(4)].

5.4 Micro tooling round robin

Within the framework of the activities of the NoE 4M, a benchmark activity was carried out in order to evaluate the performance of hybrid tooling (both direct and indirect) when compared with conventional micro direct machining for micro tooling purposes. The benchmark consisted on the manufacturing of different micro tools for the polymer replication of the micro fluidic system described in section 5.3.1 [Tosello,

2007(8)]. Five inserts have been produced, based on the same geometry, using the following different tooling strategies:

- µTool_1 = direct tooling with an optimized 4 steps micro milling operation (insert material: Stainless Steel AISI 304) (see Table 13);
- µTool_2 = direct tooling with an optimized 4 steps micro milling operation (insert material: tool steel EN30B) (see Table 13);

Micro tool	µTool_1	µTool_2
Milling step	Mill diameter [mm] / Rotational speed [rpm] / Depth of cut [µm]	
1	3 / 18000 / 18	3 / 8000 / 84
2	0,6 / 25000 / 10	0,6 / 30000 / 15
3	0,3 / 35000 / 7	0,15 / 39000 / 7
4	0,1 / 75000 / 2	0,1 / 40000 / 3

Table 13 – Milling steps and machining parameters for micro tools manufacturing.

- µTool_3 = indirect hybrid tooling with µEDM milling of silicon, deposition of nickel-copper by electroforming, selective silicon substrate etching, final cut by µWire-EDM (insert material: nickel with copper substrate) (described in section 5.3) (see summary in Table 14);

µTool_3	Indirect tooling
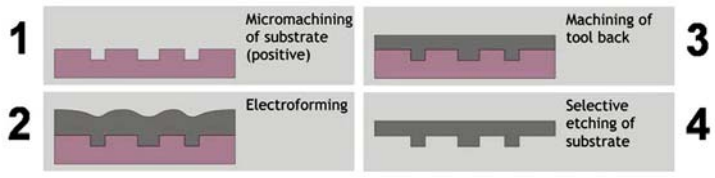	
• Substrate = silicon • Micromachining = µEDM milling • Electrodes diameter [µm] = 20, 50, 68, 300 • Silicon dissolution = NaOH 60g/l solution	

Table 14 – Main features of the indirect hybrid tooling process chain for the manufacturing of micro tool 3 based on µEDM and electroplating.

- µTool_4 = direct hybrid tooling with micro milling and ECF (insert material: Stainless Steel 1.4441) (see Table 15);
- µTool_5 = direct hybrid tooling with micro milling (as for µTool_2) and laser milling (insert material: tool steel EN30B) (see Table 16);

µTool_4	Electrochemical micro milling
• Tool = tungsten wire, diameter 40 µm • Pulse width = 120 ns and 80 ns • Pulse amplitude = 3 V • Feedrate = 0.0005 mm/s • Depth of cut = 0.1 mm	

Table 15 – Main features of the direct hybrid tooling process chain for the manufacturing of the micro tool 4 based on micro milling and µECM.

µTool_5	Laser micro milling
• Laser type = Nd:YAG • Wavelength = 1064 nm • Pulse = 10 µs • Frequency = 40 KHz • Speed 400 mm/s • Spacing = 10 µm	

Table 16 – Main features of the direct hybrid tooling process chain for the manufacturing of micro tool 5 based on micro milling and laser micro machining.

Two of the main issues of the micro structure to be machined were to produce the 25 µm radius and to manufacture the two 20 µm wide ridges meeting the dimensional requirements (width, height, aspect ratio) as well as having the walls straight with no bending involved.

With a conventional approach, e.g. direct tooling by micro milling, the smallest obtainable radius is directly related to the minimum micro mill diameter available (100 µm) as shown in Figure 88 for both the micro mould and the micro moulded part. On

the other hand, hybrid technologies can provide a viable solution to decrease the smallest obtainable dimension of micro structure (see Figure 89 and Figure 90).

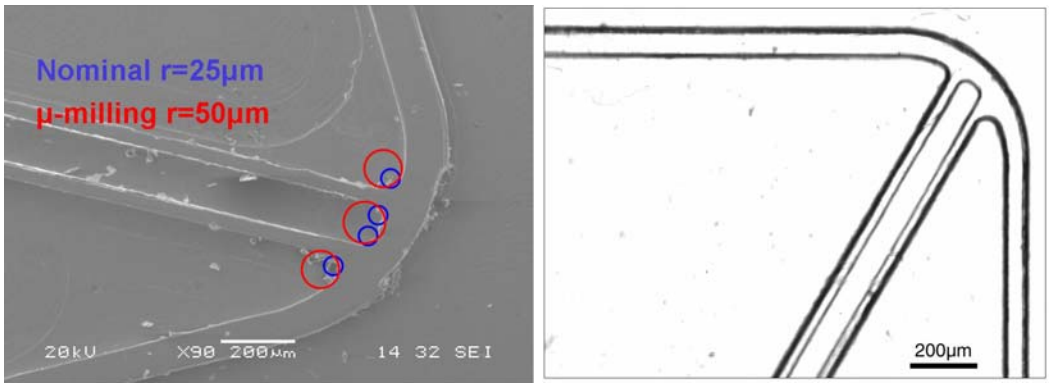

Figure 88 – Micro tool manufactured by micro milling (left) and injection moulded part (material: polycarbonate) (right).

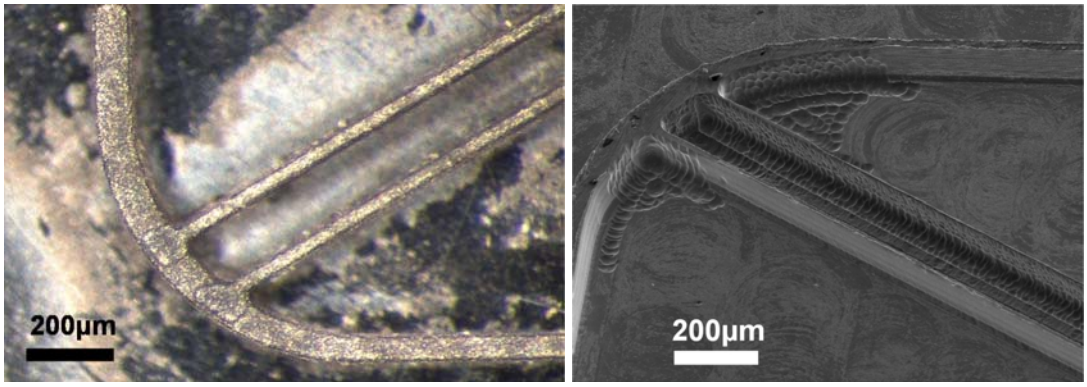

Figure 89 – Hybrid micro tools 3 (left) and 4 (right).

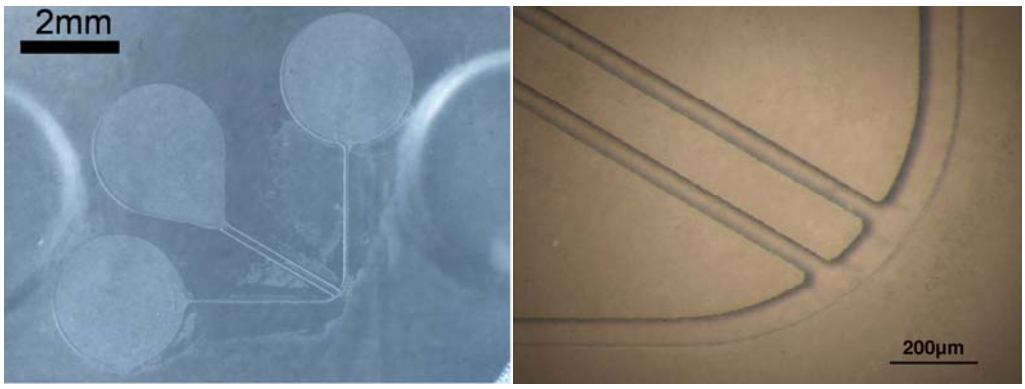

Figure 90 – Injection moulded micro fluidic system using the tool number 3 (material: polypropylene).

To obtain the required 20 µm ridges different approaches were used.

When micro milling was employed, very thin walls were bended by the cutting forces. The width of the ribs had to be increased in order to obtain straight walls, compromising dimensional accuracy respect to the tolerances. Effect of such optimization is shown in Figure 91.

With indirect tooling a channel was machined in the master's substrate and the ridges were manufacture as channels (as it will be in the moulded part) (Figure 92, left) therefore the micro toll resulted on having straight walls.

With electrochemical milling, where cutting forces (responsible for walls' bending) are not involved, straight and thin walls can be manufactured (see Figure 92, right).

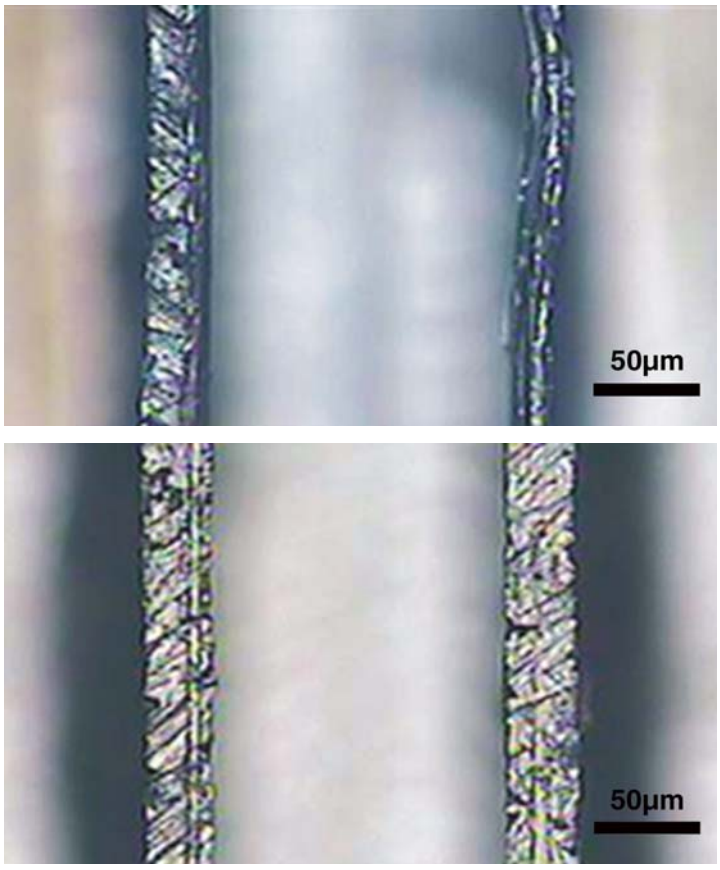

Figure 91 – Micro milling of 20 µm ridges: bended wall (above) and optimized milling for straight wall manufacturing (below).

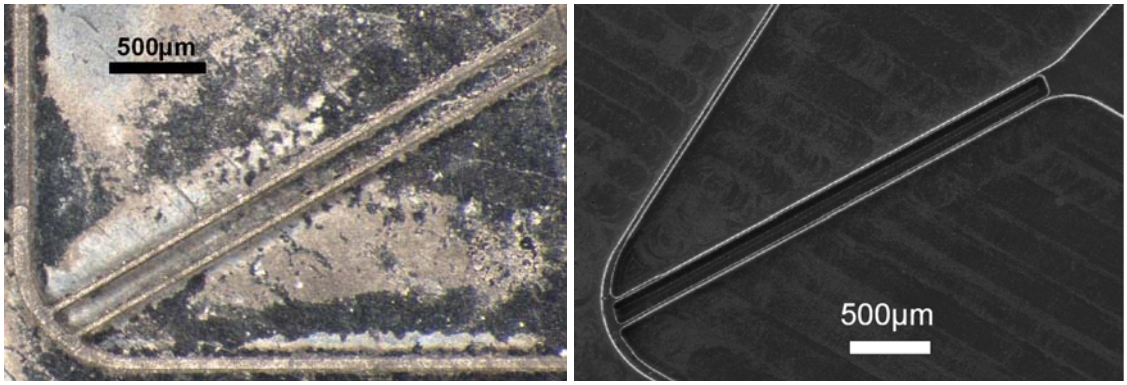

Figure 92 – 20 µm wide ridges manufactured by hybrid tooling: micro tool 3 (left) and micro tool 4 (right).

5.5 Metrology benchmark of direct and hybrid tooling

After manufacturing, the different micro insert moulds have been measured using different instruments. With this investigation, two results were obtained. On one hand, the performances of the different tooling technologies were assessed. On the other, the measuring capabilities of the available measuring technologies were determined for both dimensional and surface topographical measuring tasks. In particular, the following quantities were measured (see Figure 78):

- Width of the two 20 µm ribs (W1, W2).
- Distance between the two 20 µm ribs (W bw 1,2).
- Height of the two 20 µm ribs (H1, H2).
- Difference on depth of the middle area between the two 20 µm ribs (D bw 1,2).
- Roughness of the bottom part of reservoir chamber placed in the middle of the micro fluidic system (Ra Pos A).
- Roughness of the area between the two 20 µm ribs (Ra Pos B).
- Roughness of the 75 µm wide rib (Ra Pos C).

Metrological investigations of the different micro tools showed that the required height H1 and H2 of 100 µm for the ridges could be met in most cases within a tolerance of 15% (see Figure 93). A challenge was represented by the ridges width (20 µm), which could not be manufactured with a sufficient accuracy. The micro tool 5 was close within an interval of ±20%. The others exhibited ridges of width 40% up

to 100% larger than the nominal dimension (see Figure 94). The area between the two ridges could be machined with accuracy depending on the technology. The hybrid tooling method (µ_Tool3), starting from a silicon wafer with almost perfect planarity, resulted on the smallest error (H bw 1,2 < 1 µm). The distance of the ridges was manufactured with a tolerance lower than 8% (see Figure 95).

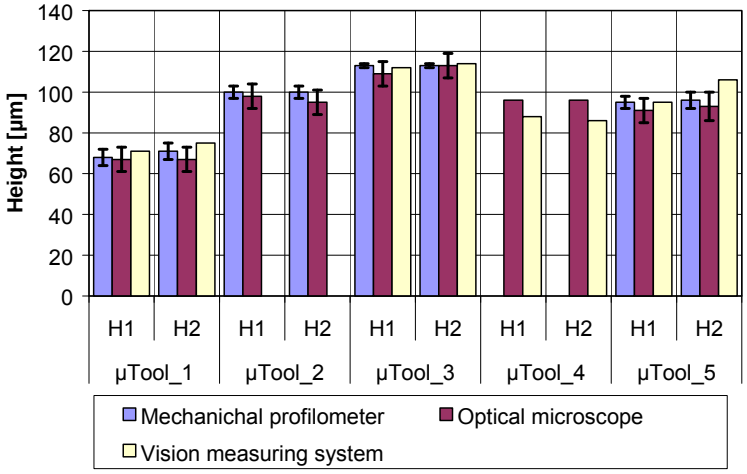

Figure 93 – Height of ridges 1 and 2 (H1, H2).

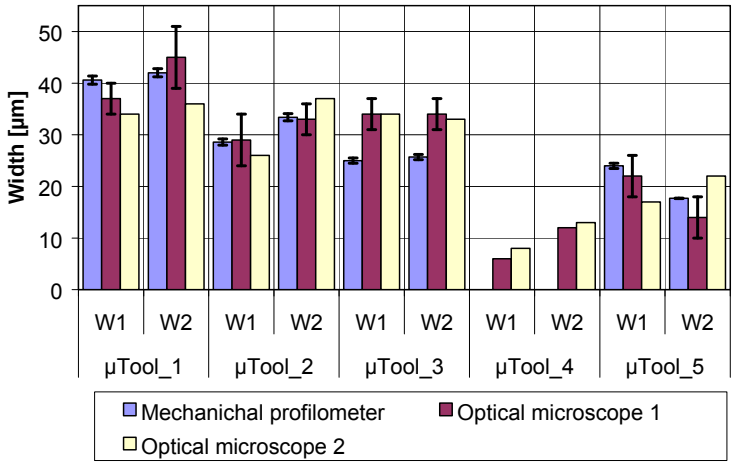

Figure 94 – Width of ridges 1 and 2 (W1, W2).

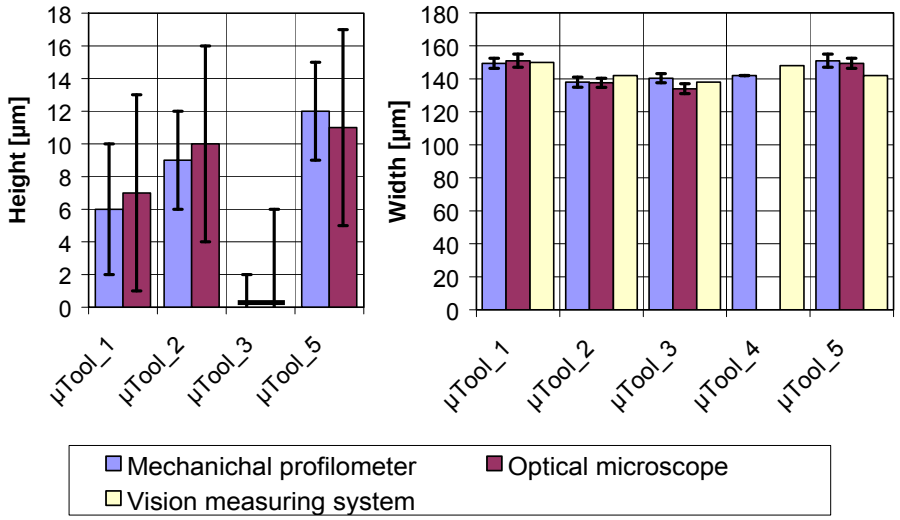

Figure 95 – Height of mid range between ridges (H bw 1,2) (left); width between ridges (W bw rid1,2) (right).

The surface roughness was measured in three positions (see Figure 96) and was in almost all cases below 0,5 µm. The smoothest surfaces have been obtained by micro milling: roughness surface ranges between 0.07 µm and 0,37 µm, with an average value of 0,21 µm. The µEDM milling surface also created smooth surfaces (Ra between 0,14 µm and 0,33 µm), but less uniform if compared with the others. In fact, a higher standard deviation from repeated measurements in different areas of the same feature was encountered. The electrochemical milled surface exhibited a quite rough surface (Ra=0,61 µm) if compared with conventional processes.

5.6 Conclusion

Hybrid tooling was presented and defined in this chapter. It has been demonstrated that hybrid tooling opens new possibilities in terms of miniaturization of features in micro tools for polymer micro replication. Moreover, hybrid tooling has the potential to enable the production of tool inserts with real 3D free-form micro features.

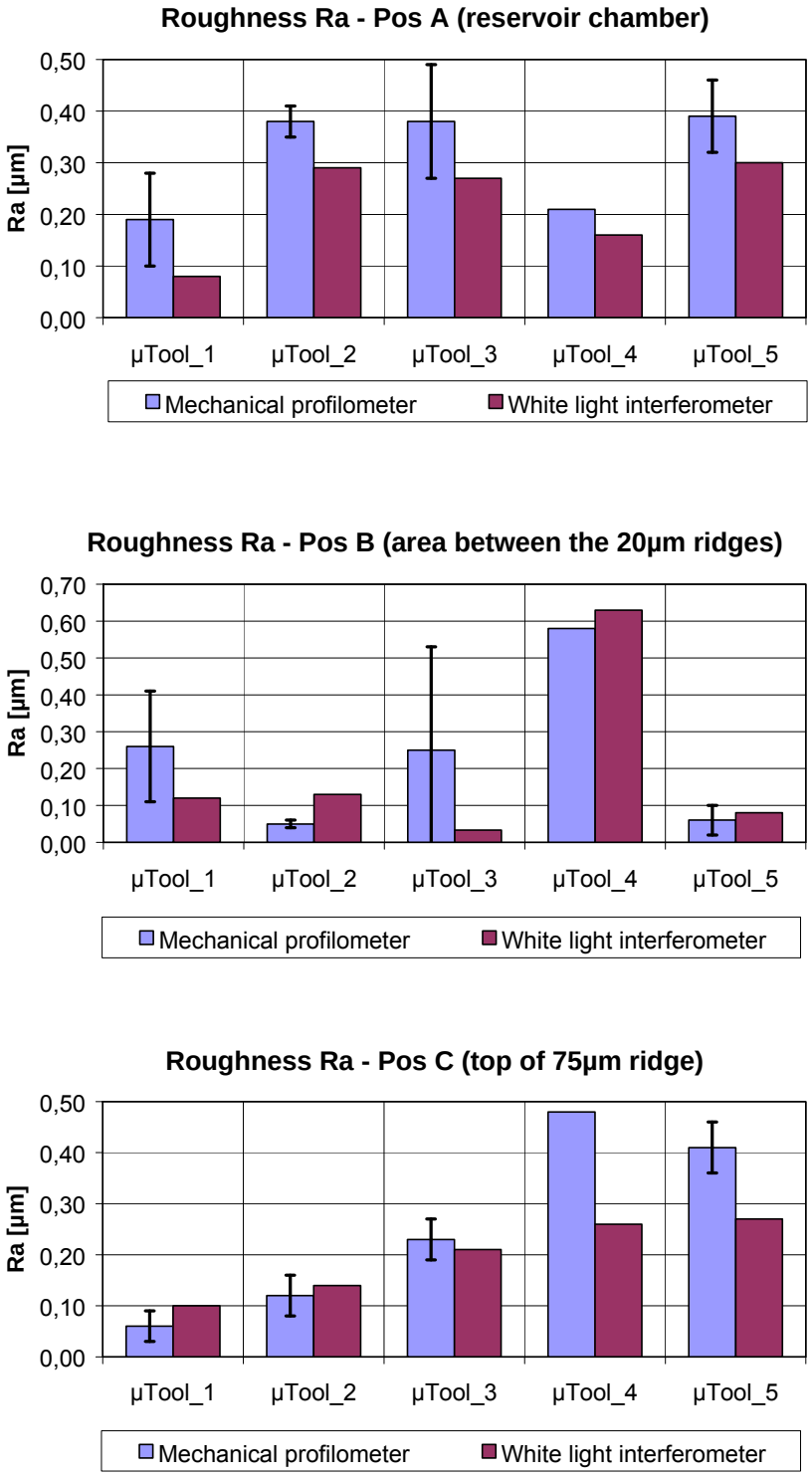

Figure 96 – Roughness measurements results for positions A, B, and C.

A review of hybrid tooling capabilities within 4M partners has been presented, and this can be considered as the current state of the art on hybrid tooling. Some of the technologies mentioned are well established with potential industrial application, and continuous improvements are developed. Some others are more in a research phase looking for industrial partners to make the step towards industrialization.

The most attractive advantage of such combination of processes is the possibility to produce 3D free-form micro structures in hard metals with accuracy, resolution and quality only available today by clean room technologies.

In particular, concerning the study case investigated during the Ph.D. project, the potential of micro EDM process of a soft substrate suitable for electroplating and subsequent selective etching has been demonstrated. Significant advancement in terms of miniaturization (micro features down to 38 µm of width), accuracy and multi-scale integration (3 mm long and straight micro ribs, planarity), high aspect ratio (up to 3) and surface roughness (Sa = 0.31 µm of the micro EDM machined areas and Sa = 14 nm on the Si-Ni-electroplated areas). Optimization is still needed in order to produce the smallest micro features within the specified tolerances. To this respect, the µEDM should be optimized in order to reach the foreseen capabilities of the process. Areas that will require further work are particularly the optimization of the electrode diameter dressing process and of the electrode wear compensation.

The manufacturing of micro tools using an innovative hybrid indirect tooling process chain has been demonstrated to be a feasible solution for polymer micro fluidic fabrication by means of polymer replication process such as injection moulding (see Figure 97).

Finally, a metrology benchmark was performed within the European Network of Excellence 4M (Multi-Material Micro Manufacturing) in order to evaluate the performance of the newly developed hybrid tooling technology when compared to conventional micro machining direct tooling. Results in terms of surface finishing, miniaturization, obtainable aspect ratio, wall straightness and mould flatness showed that the proposed indirect hybrid tooling technology is competitive when compared with for example micro milling.

(a)

(b)

(c)

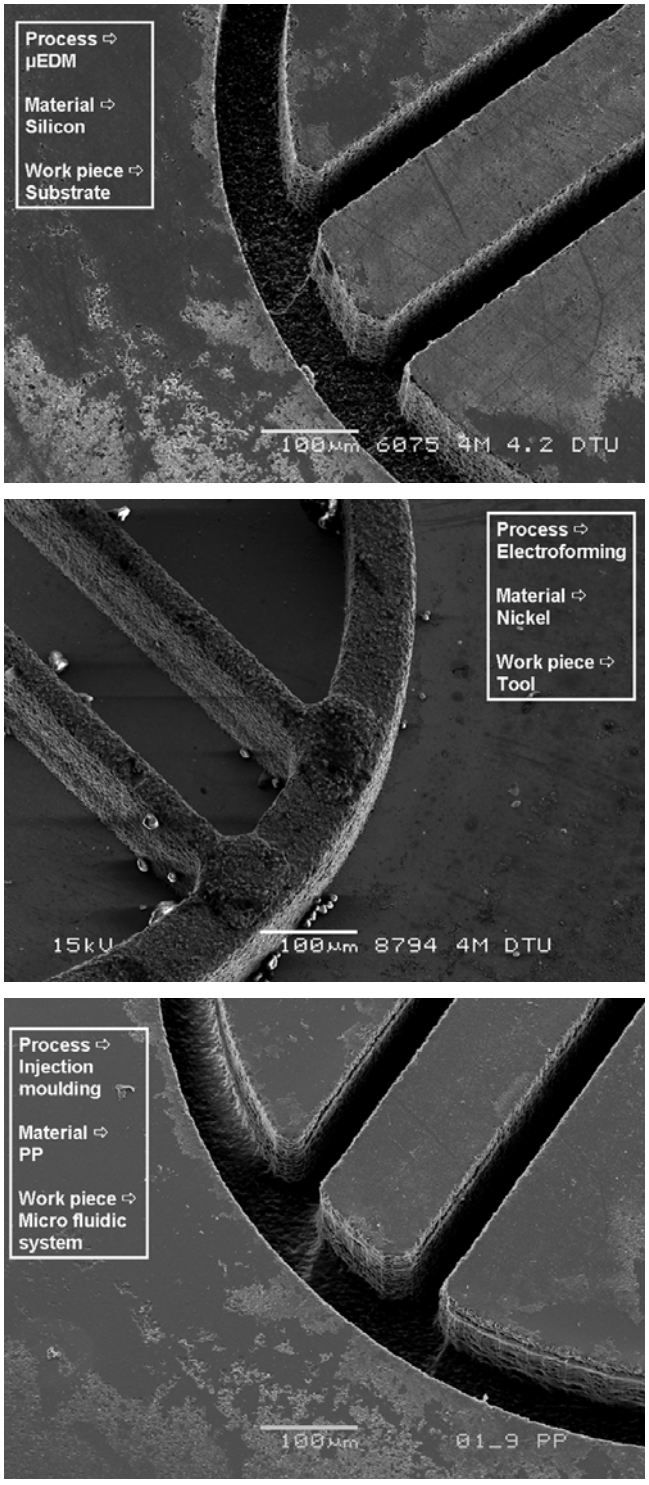

Figure 97 – High aspect ratio micro structures replication: indirect hybrid tooling including µEDM of silicon substrate (a), electroforming of nickel (b) and polymer injection moulding (right) [Tosello, 2008(4)].

5.7 References

[Azcarate, 2006] Azcarate S., Uriarte L., Schoth A., Bigot S., Tosello G., Roth G., Staemmler L. (2006) Hybrid Tooling: A Review of Process Chains for Tooling Microfabrication within 4M, Proceedings of 2nd International Conference on Multi-Material Micro Manufacture (4M), Grenoble (France), 20th-22nd September 2006, pp.305-308.

[Bissacco, 2005] Bissacco G., Hansen H.N., Tang P.T., Fugl J. (2005) Precision manufacturing methods of inserts for injection molding of microfluidic systems, ASPE Proceedings of Spring Topical Meeting on Precision Micro/Nano Scale Polymer Based Component & Device Fabrication, Columbus (OH, USA), 18th-19th April 2005, pp.57-63.

[Bissacco, 2007(1)] Bissacco G., Hansen H.N., Wiwe B.D. (2007) Micro EDM milling for silicon based tooling, Proceedings of the 9th International Conference on Management of Innovative Technologies, Fiesa (Slovenia), 8th-10th October 2007, pp.126-130.

[Bissacco, 2007(2)] Bissacco G., Valentincic J., Wiwe B.D., Hansen H.N. (2007) Characterization of pulses in micro EDM milling based on wear and material removal, Proceedings of the 3rd International Conference on Multi Material Micro Manufacture (4M), Borovets (Bulgaria), 3rd-5th October 2007, pp.297-300.

[Blattert, 2005] Blattert C., Jurischka R., Tahhan I., Schoth A., Kerth P., Menz W. (2005) Microfluidic blood/plasma separation unit based on microchannel bend structures, Proceedings of the 3rd Annual International Special Topic Conference of the IEEE EMBS on Microtechnology, Oahu (HI, USA), 12th - 15th May 2005, pp.38-41.

[Enthone, 2006] Enthone (2006) Cuprostar – commercial Cu plating solution.

[Enthone, 2007] Enthone/Rohm&Haas (2007) Entreat 100 – commercial Au

etching solution.

[Feng-Tsai, 2007] Feng-Tsai W., Chen-Siang H., Wen-Feng L. (2006) Fabrication of micro components to Silicon wafer using EDM process. Materials Science Forum, Progress on Advanced Manufacture for Micro/Nano Technology, Trans Tech Publications Switzerland, 505-507, pp.217-222

[Fleischer, 2005] Fleischer J., Kotschenreuther J. (2005) Manufacturing of micro moulds by conventional and energy assisted processes, Proceedings of the 1st International Conference on Multi-Material Micro Manufacture (4M), Karlsruhe (Germany), pp.9-17.

[ISTMA, 2004] International Special Tooling and Machining Association (ISTMA) (2004) Annual Report.

[Pham, 2004] Pham D.T., Dimov S.S., Ji C., Petkov P.V., Dobrev T. (2004) Laser milling as a rapid micro manufacturing process, Journal of Engineering Manufacture, vol. 218, pp.1-7.

[Plummer, 2000] Plummer J.D., Deal M.D., Griffin P.B. (2000) Silicon VLSI Technology, Prentice Hall, Upper Saddle River, New Jersey.

[Staemmler, 2006] Staemmler L., Hofmann K., Kim M.H., Warkentin D., Kück H. (2006) Adapting ECF to steels used for micro mould inserts, Proceedings of the 2nd International Conference on Multi Material Micro Manufacture (4M), Grenoble (France), 20th-22nd September 2006, pp.309-312.

[Staemmler, 2007] Staemmler L., Hofmann K., Kück H. (2007) Hybrid tooling by a combination of high speed cutting and electrochemical milling with ultrashort voltage pulses, Microsystem Technologies, Vol.14, Issue 2, pp.249-254

[Tang, 2006(1)] Tang P.T., Fugl J., Uriarte L., Bissacco G., Hansen H.N. (2006) Indirect tooling based on micromilling, electroforming and selective etching, Proceedings of the 2nd International

Conference on Multi Material Micro Manufacture (4M), Grenoble (France), 20th-22nd September 2006, pp.183-186.

[Tang, 2006(2)] Tang P.T. (2006) A method of manufacturing a mould part, Patent WO2006026989 (A1), US2007298173 (A1), EP1807553 (A0).

[Tosello, 2005(2)] Tosello G., Jensen J.D., Friis K., Islam A., Wiwe B.D. (2005) Micro Mechanical Product Development and Manufacture – Design, Manufacturing, and Testing of Micro Fluidic Device, Internal report, Technical University of Denmark (DTU), Department of Manufacturing Engineering and Management (IPL), pp.1-81.

[Tosello, 2007(6)] Tosello G., Fillon B., Azcarate S., Schoth A., Mattsson L., Griffiths C., Staemmler L., Bolt P.J. (2007) Hybrid tooling technologies and standardization for the manufacturing of inserts for micro injection molding, Society of Plastics Engineers – 65th Annual Technical Conference (ANTEC), Cincinnati (OH, US), 6-10 May 2007, pp.2992-2996.

[Tosello, 2007(7)] Tosello G., Bissacco G., Tang P.T., Hansen H.N., Nielsen P.C. (2007) Micro tools manufacturing for polymer replication with high aspect ratio structures using μEDM of silicon, selective etching and electroforming, 7th International Workshop on High-Aspect-Ratio Micro-Structure Technology (HARMST007), Besançon (France), 7th-9th June 2007, pp.43-44.

[Tosello, 2007(8)] Tosello G., Fillon B., Azcarate S., Schoth A., Mattsson L., Griffiths C., Staemmler L., Bolt P.J. (2007) Application of different process chains for polymer microfluidics fabrication including hybrid tooling technologies, standardization and replication: a benchmark investigation within 4M Polymer Division, 3rd International Conference on Multi-Material Micro Manufacture (4M), Borovets (Bulgaria), 3rd-5th

October 2007, pp.77-80.

[Tosello, 2008(4)] Tosello G., Bissacco G., Tang P.T., Hansen H.N., Nielsen P.C. (2008) High aspect ratio micro tool manufacturing for polymer replication using μEDM of silicon, selective etching and electroforming, Microsystem Technologies, DOI: 10.1007/s00542-008-0564-9, Vol. 14, Issue 9-11, pp.1757–1764.

[Uhlmann, 2005] Uhlmann E., Piltz S., Doll U. (2005) Machining of micro/miniature dies and moulds by electrical discharge machining-Recent development, Journal of Materials Processing Technology, 167:2-3, pp.488-493.

6 Process simulation

Simulation programs in polymer micro replication technology are applied with same purposes as in conventional injection moulding. To avoid the risks of costly re-engineering, the functions of the final products as well as the manufacturing steps are simulated extensively before starting the actual manufacturing process: important economic factors are the optimization of the moulding process and of the tool using different simulation techniques.

In polymer micro manufacturing technology, software simulation tools adapted from conventional injection moulding can provide useful assistance for the optimization of moulding tools, mould inserts, micro component designs, and process parameters.

Simulation tools can work adequately from a qualitative point of view and numerical values cannot be calculated as precisely as necessary. In addition to that, most programs have difficulties in simulating exactly the filling of microstructures with high aspect ratio. The reason is that commercial software tools developed for macroscopic applications do not consider microscopic aspects properly.

However, a proper implementation strategy employed during the set-up of the simulation can greatly improve the quality (i.e. the accuracy) of the simulated results.

To this respect, the main challenge which was addressed during the Ph.D. research work is represented by the difficult to establish reliable terms of reference in order to perform an accurate and quantitative comparison between the simulated and experimental results at micro scale. As it will be explained in this chapter, to face this challenge a new method for the validation of software simulating the micro injection moulding process was developed. Moreover, additional studies were conducted employing established methods and eventually they were combined with the new procedure in an integrated solution. The experimental data base was developed during the process analysis of the research project and was based on both injection moulding and micro injection moulding (μIM) of micro parts (see chapter 3).

Simulations were carried out using a commercially available code. The aims of the study have been to evaluate whether the available software was able to simulate the μIM process and to study the influence of different simulation factors on the software accuracy to possibly optimize the quality of the simulated results.
In particular the influence of the following factors was investigated:

- At the machine/software interface boundary:
    - The implementation of the actual injection speed profile during the filling stage of the cavity.
    - The implementation of the actual cavity injection pressure profile developed during the filling stage.
    - The use of the actual cavity injection time.
- Concerning part modelling and meshing:
    - Three dimensional modelling of the whole moulded component including sprue, runner, gate, part and micro features.
    - To consider the meshing tolerance compared to the actual dimensions of the micro features and therefore using micro-sized elements with edge length between 20 and 90 μm.
    - To optimize meshing accuracy for high precision modelling of the part and of the micro features with surface and edge definition within 5 to 10 μm.
- Regarding the material characterization:
    - The use of experimental micro rheological data of the polymer material instead of the default rheology available in the software database.

Results were compared in a quantitative study to indicate the methods leading to the most accurate results and to highlight specific applicable optimization trends and strategies. Performance indicators such as cavity injection pressure, injection cavity time and flow front position have been selected for the optimization analysis.
The chapter is structured as follows. Section 6.1 introduces the finite element method for the simulation of the injection moulding process. In section 6.2 the meshing of micro moulded parts is discussed. Sections 6.3 and 6.4 deal with the implementation of the actual (i.e. experimental) conditions into the simulation program, in terms of injection speed profile and cavity injection time respectively. In section 6.5 the

validation of filling simulation in μIM is presented. Finally, section 6.6 contains a discussion on the use of a rheology model suitable for micro injection moulding for the improvement of simulation accuracy.

6.1 Injection moulding process simulation and introduction to finite element analysis

Finite element analyses are identified with the acronym FEM (finite element modelling) or FEA (finite element analysis).

They are based on the idea to discretize the model to be analyzed in simple parts (i.e. meshing elements, see Figure 98). The geometry of every element that composes the mesh is characterized by a certain number of nodes placed in the vertexes of the element itself.

Beam mesh	Mid-plane mesh	Dual Domain™ mesh	3D Solid mesh
	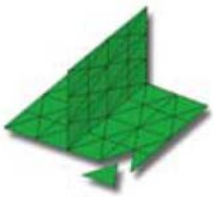	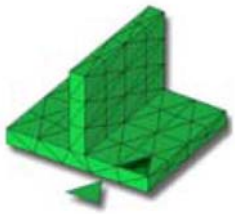	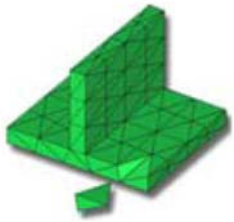

Figure 98 – Example of mesh types [Jaworski, 2003].

The equations describing the flow of the melt in the mould are calculated in every node of the mesh.

The characteristics of the analysis of the flow of a polymer melt in a mould are:

- The properties of the material are not linear (i.e. during the flow the polymer viscosity changes continuously because of thermal effects).
- The boundary conditions change with the flow of the polymer.

The FEM analysis requires the knowledge of the boundary conditions which are fixed only for a steady flow that is not the one typical of the filling of a mould during injection moulding. In the filling simulation of a cavity, almost no steady phenomenon

occurs because the melt accelerates or decelerates depending on the mould characteristics.

The best solution requires a dynamic analysis with hypothesis of the position of the flow front and of the magnitude of the flow rate in every moment. The 3D simulation based on the Navier-Stokes equations offers results that are more accurate than a 2D or 2½D simulation and it is therefore more suitable for the purpose [Yu, 2004] [Lee, 2006].

The Navier-Stokes, mass conservation and energy conservation governing equations are given by the following equations [Shen, 2002].

- Continuity equation
  - $$\frac{\partial \rho}{\partial t} + \frac{\partial (\rho u)}{\partial x} + \frac{\partial (\rho v)}{\partial y} + \frac{\partial (\rho w)}{\partial z} = 0$$
- Momentum Equation
  - $$\rho\left(\frac{\partial u}{\partial t} + u\frac{\partial u}{\partial x} + v\frac{\partial u}{\partial y} + w\frac{\partial u}{\partial z}\right) = -\frac{\partial p}{\partial x} + \eta\left(\frac{\partial^2 u}{\partial x^2} + \frac{\partial^2 u}{\partial y^2} + \frac{\partial^2 u}{\partial z^2}\right) + \rho g_x$$
  - $$\rho\left(\frac{\partial v}{\partial t} + u\frac{\partial v}{\partial x} + v\frac{\partial v}{\partial y} + w\frac{\partial v}{\partial z}\right) = -\frac{\partial p}{\partial y} + \eta\left(\frac{\partial^2 v}{\partial x^2} + \frac{\partial^2 v}{\partial y^2} + \frac{\partial^2 v}{\partial z^2}\right) + \rho g_y$$
  - $$\rho\left(\frac{\partial w}{\partial t} + u\frac{\partial w}{\partial x} + v\frac{\partial w}{\partial y} + w\frac{\partial w}{\partial z}\right) = -\frac{\partial p}{\partial z} + \eta\left(\frac{\partial^2 w}{\partial x^2} + \frac{\partial^2 w}{\partial y^2} + \frac{\partial^2 w}{\partial z^2}\right) + \rho g_z$$
- Energy Equation
  - $$\rho c_p\left(\frac{\partial T}{\partial t} + u\frac{\partial T}{\partial x} + v\frac{\partial T}{\partial y} + w\frac{\partial T}{\partial z}\right) = k\left(\frac{\partial^2 T}{\partial x^2} + \frac{\partial^2 T}{\partial y^2} + \frac{\partial^2 T}{\partial z^2}\right) + \eta\dot{\gamma}^2$$
- Where:
  - P = pressure
  - g_x, g_y, g_z = gravity acceleration along the x, y, z axes
  - ρ = density
  - u = melt speed in the x direction
  - v = melt speed in the y direction
  - w = melt speed in the z direction
  - c_p = specific heat at constant pressure
  - T = temperature of the melt in the evaluating point

- k = thermal conductivity
- $\eta \dot{\gamma}^2$ = viscous heating term

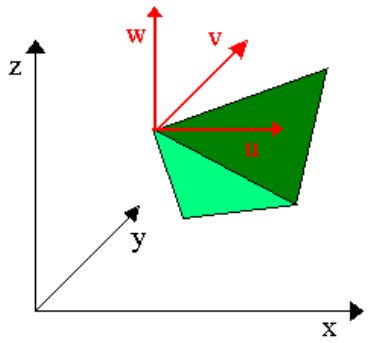

Figure 99 – Three dimensional coordinates (x, y, z) and melt speed versors (u, v, w).

The commercially available software Moldflow® (versions 4.1 and 6.1) was employed during the investigation. It is a CAE (computer aided engineering) simulation software based on the finite element method (FEM). This software allows the simulation of the injection moulding phases such as:

- Filling of the cavity;
- Packing;
- Cooling.

Particular attention has to be paid during the pre-processing of the solid model of the part to guarantee an accurate simulation. To avoid numerical problems (i.e. inaccurate results, lack of convergence of the numerical solving) the mesh has to be adjusted in order not to have stretched triangles, holes, overlapping elements, intersections, free edges and different element orientation.

Commercial simulation tools such as Moldflow® are generally characterized by the following capabilities:

- Filling analysis – The software simulates the injection phase to define the behaviour of the thermoplastic material with the aim of obtaining high quality products. This simulation can underline the necessity of mould design changes or of changes in the process conditions or in the used materials in order to obtain a good compromise between quality, costs and cycle time. The results that are obtainable with this analysis are:

  - Visualization of the flow front;
  - Determination of the injection pressure;
  - Optimization of the thickness of the moulded part to obtain a uniform melt flow;
  - Decrease of the cycle time to reduce the costs;
  - Identification of air traps;
  - Optimization of the process conditions as the injection time, speed profile, melt and mould temperature, packing pressure etc. ;
  - Determination of the gate freeze time.
- Packing and cooling analysis – By controlling the packing phase, it is possible to control the residual tensions and the subsequent deformations and shrinkage. The cooling simulations permit to optimize the design of cooling channels to obtain a uniform temperature on the moulded part, to optimize the cycle time and to predict the deformations due to non-uniform cooling. The results that are obtainable with this analysis are:
  - Observation of the difference of the temperature between the inner part of the mould and the surface;
  - Minimization of the unbalanced cooling and the consequence minimization of the residual stresses;
  - Determination of all the temperatures of the injection channels and cooling channels;
  - Determination of the cooling time of the moulded part.
- Shrinkage and deformations analysis – During this analysis, the material characterization is the most sensible parameter. The predictions of the deformations are reliable regarding the direction and the order of magnitude of the deformation itself. The results that are obtainable with these analysis are:
  - Evaluation of the final part of the moulded part before the realization of the mould;
  - Optimization of the mould design, of the material and of the process parameters to minimize the deformations;
  - Separation of the deflection along the x, y, z directions.

The use of FEM simulations, especially in the case of the injection moulding process is particularly advantageous because it allows:

- To reproduce of real phenomena and different solutions without the need of experimental tests;
- To isolate some parameters and develop their specified setup: this is very difficult and expensive to achieve by means of actual experiments;
- To investigate and optimize in a relatively short time the most affecting parameters;
- To improve the productivity and lead time due to the possibility to simulate several alternative configurations in a short time.

It is therefore desirable that simulation software tools are fully integrated in the process chain (from concept until product manufacture) for the fabrication of micro products. Due to compatibility with CAD design tools and framework, as well as the present knowledge on the use of available commercial programs, optimization of the performance of existing software when simulating the micro injection moulding process is of outstanding importance. In the following sections, research carried out with the aim to improve simulation results based on actual comparison with experimental results is presented.

6.2 Mesh analysis

This section deals with the optimization of the meshing phase which is a fundamental requirement when performing FEM simulations. In particular two different scenarios where considered, following the experimental injection mouldings as described in chapter 3:

- A first scenario was represented by the case in which a micro injection moulded component is produced using a conventional injection moulding machine (i.e. with a plastification screw): the actual moulded part included a large sprue and runner system (i.e. volume in the range of few cm^3), and the micro part's volume was a small fraction of the total injected volume (i.e. max 1%).

- A second scenario was represented by a micro injection moulded part produced using a micro injection moulding machine. In this case, the volume of the whole injected part was in the range of few hundreds of mm^3, the runner system still constituted a major part of the injected volume but the actual part represented a volume in the range of at least 10-20% of the total volume.

Different meshing strategies had to be adopted, depending on the considered scenario, as described in the following sections.

6.2.1 Micro moulded part with large runner system

Conventional injection moulding machines can be employed to mould polymer micro component. In this case, large sprue and runner system (i.e. with sizes encountered in conventional injection moulded part) are produced in order to achieve the filling of micro cavities.

It is common practice in simulating such injection moulded system, to mesh with one-dimensional elements the sprue and runner system and to mesh with three-dimensional elements the part (see Figure 100). The sprue-runner system is usually meshed using simplified one-dimensional elements in order to save computational time. In conventional injection moulding, the volume of the sprue-runner system is very low when compared to the part volume, i.e. to 1 to 5%, and it is safely assumed it is not going to affect the results of the simulation sensibly. With this method a total number of 31142 elements were necessary to mesh the geometry.

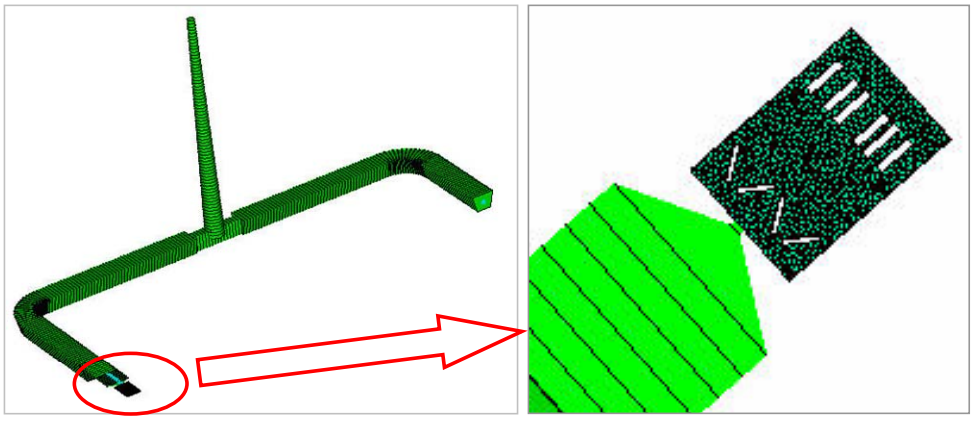

Figure 100 – One-dimensional elements to mesh the runner system and three-dimensional meshing of the cavity.

An optimized meshing strategy was implemented in order to increase simulation accuracy. The method consists on the complete three-dimensional of the whole system (sprue, runner, part) (see Figure 101). In this case 196344 elements were employed.

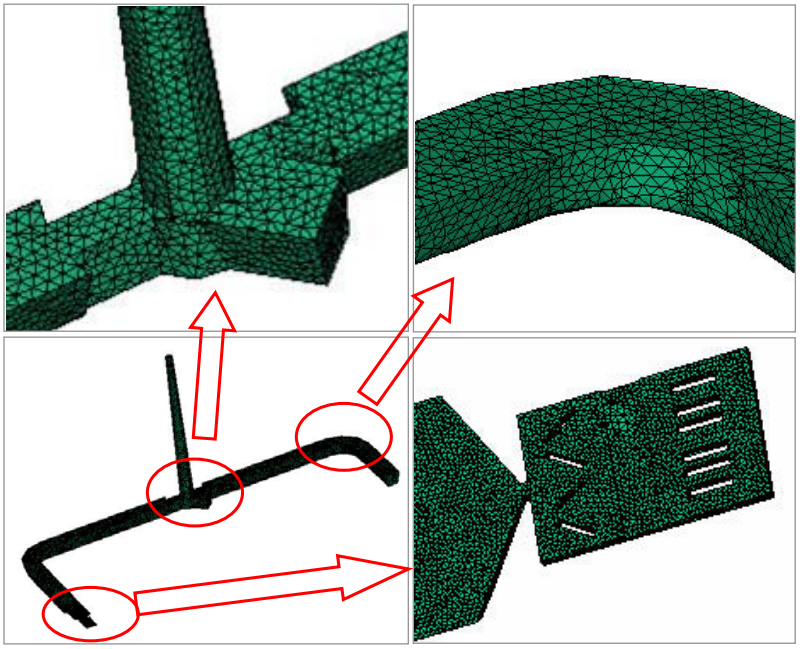

Figure 101 – Complete three-dimensional meshing of the model: sprue, runner, part.

A comparison of the two methods was then performed. Limitations in terms of closeness of the modelled geometry when compared with the actual geometry were found for the hybrid 1D-3D meshing:

- The use of one-dimensional elements brings the software to calculate an equivalent hydraulic radius of the runner system, introducing an approximation.
- The effect of introducing the hydraulic radius is found on the difference in the system volume when compared with the real part (see Figure 102).
  In particular:
  - Actual part volume = 7.3 cm^3
  - Complete 3D meshed volume = 7.2 cm^3
  - Hybrid mesh (1D runner system and 3D cavity) = 5.1cm^3

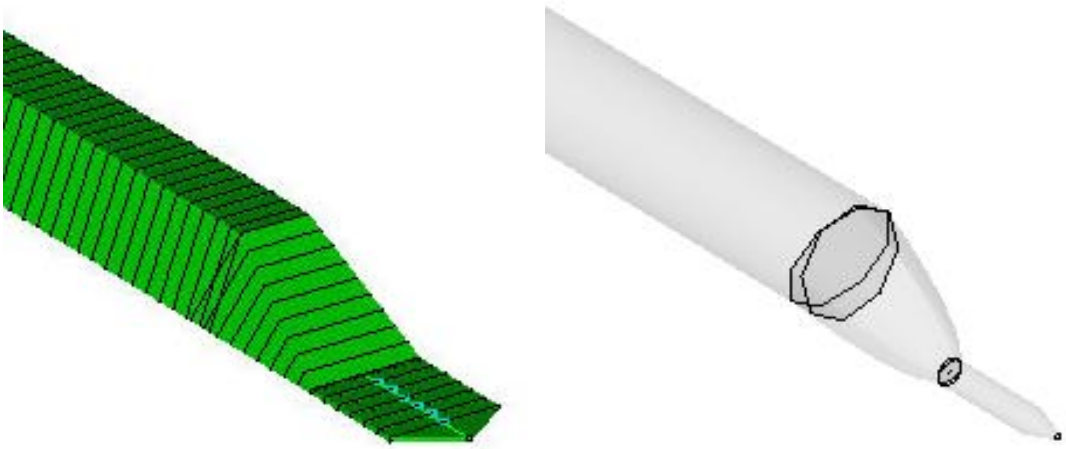

Figure 102 – One-dimensional runner system approximation: model mesh (left), considered geometry underlying the mesh (right).

As result, it is advisable to adopt a full three-dimensional meshing of the complete model including sprue, runner and part. On the other hand, mesh size has to be carefully tuned in order to contain the total number of elements, the requested computational power and therefore the simulation time. Considering the complete 3D model, different dimensions of the mesh elements have to be adopted, in particular:

- Coarse mesh – Mesh size of about 0.88 mm for sprue and runner system.
- Medium mesh – Mesh size of about 0.16 mm for the micro part. The cavity mesh size was decrease compared to the one of the runner system because of the small thickness of the cavity itself (from 250 μm down to 150 μm). However, the size of the mesh in the cavity here employed is not fine enough to permit an accurate analysis of the filling of the micro structured cavity.
- Fine mesh – To trace the melt flow pattern accurately, the mesh size has to be further refined. Mesh sizes have been decreased down to 30 μm in the micro channels and in the parts of the cavity where experimentally melt flows were joining in order to increase the accuracy of the subsequent analysis based on the use of flow markers. The difference between the medium and the fine mesh can be observed in Figure 104.

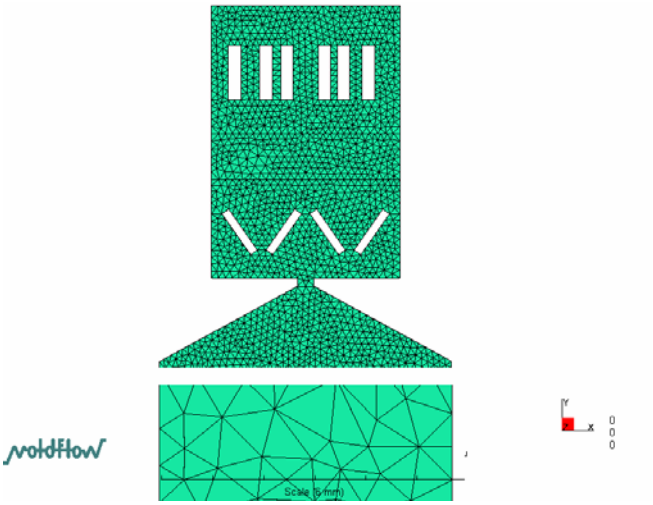

Figure 103 – Comparison of runner and cavity mesh size of the complete 3D model.

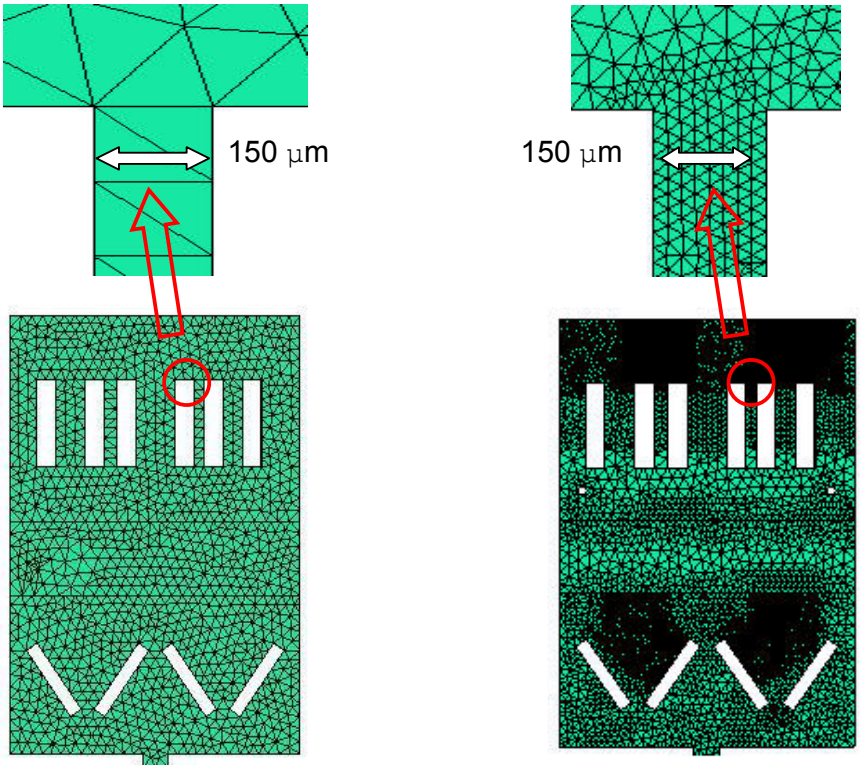

31142 elements (a)

269472 elements (b)

Figure 104 – Medium mesh-size employed for the development of the cavity filling time and zoom of the mesh in the channel of 150 µm (a). Fine mesh-size employed for the study of the flow inside the micro cavity zoom of the mesh in the channel of 150 µm (b).

A complete 3D meshing using very fine elements as shown in Figure 104b would lead to an enormous number of elements which would make the simulation extremely time consuming. A viable solution could be to use a combination of two different simulations:

- A first simulation of the complete model is run using coarse and medium mesh. This simulation is performed in order to estimate the cavity injection time and the flow conditions near the gate before the cavity.
- These conditions are then implemented in a second simulation in which only the cavity with a very fine mesh is employed. The results of this simulation are used to study the flow characteristics in the micro cavity.

6.2.2 Micro moulded part with miniaturized runner system

On micro injection moulding simulation the runner system can easily account for more than 50% of the injection volume. The thermo-mechanical history of the melt flow is heavily influenced by the dynamic evolution through the whole runner, gate and finally the cavity. Therefore, a full three-dimensional meshing of the whole system composed by the runner and the two gates (see Figure 105, detail (a) and (b) respectively) and the two parts considered as a one complete moulded part was carried out. Furthermore, actual volume left on the surface by the ejectors and the pressure sensor were solid-modelled as part of the moulded product (see Figure 106 detail (c) and (d) respectively).

Mesh tolerances should also be analyzed and optimized to fit the need for accuracy of the μIM application. In particular, an average length of the side of a single element (i.e. tetrahedron) of 90 μm was adopted. Moreover, a tolerance between the meshed model and the CAD solid model of 30 μm was used. These settings were chosen as trade-off between the accuracy of the part modelling (especially needed for the micro features modelling, see Figure 107) and the resulting number of elements (i.e. the computational time). The model had a volume of 107 mm^3 and was modelled using 1215156 tetrahedrons 3D solid elements.

In this case, due to the small volume of the part (i.e simulation of micro moulded part) it was not necessary to split the simulation in two steps and to have different mesh

scale sizes to shorten computation time. A fine mesh was applied to the whole system (sprue, runner, part) and the simulation could be run in a reasonable time.

(a)

(b)

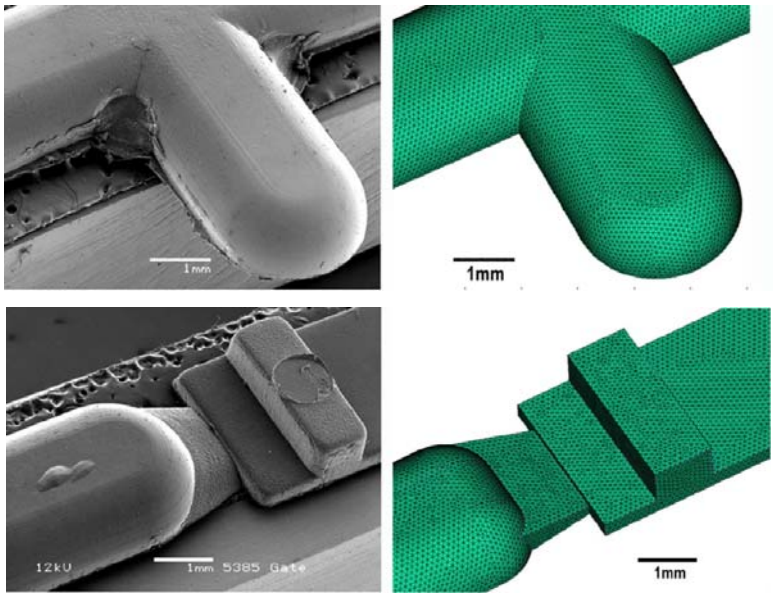

Figure 105 – accurate 3D meshing of runner system and gate of micro injection moulded part [Tosello, 2008(5)].

(a)

(b)

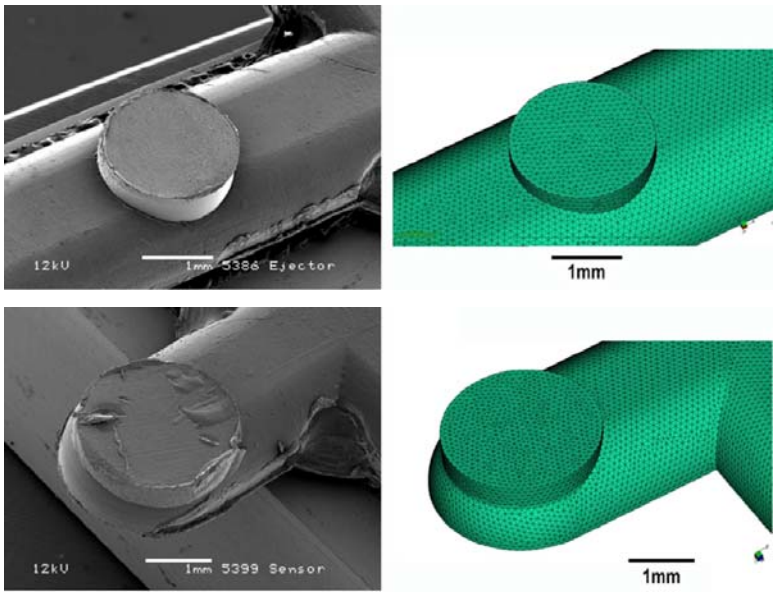

Figure 106 – Extra volume on the surface of the moulded part due to the presence of ejector and pressure sensor [Tosello, 2008(5)].

(a)

(b)

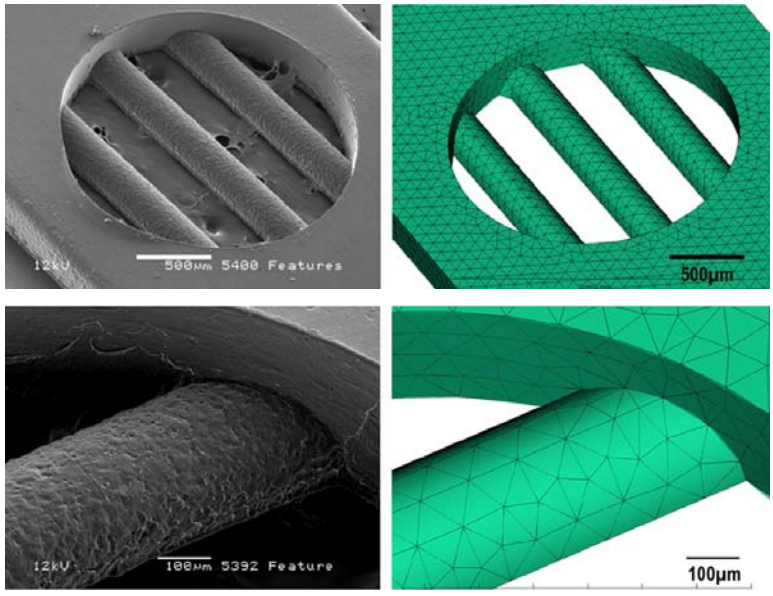

Figure 107 – Micro features 3D meshing (a) and accurate surface matching at micro dimensional level (b) [Tosello, 2008(5)].

6.3 Injection speed analysis

The injection speed is usually set up in the moulding machine with a rectangular profile. The aims are on one hand to achieve the highest injection speed in the shortest time, consistently with the acceleration which can be provided by the machine; on the other hand to set the injection speed in order to obtain an opportune level of the injection pressure to ensure complete filling of the cavity.

In the experiments, the low level of injection speed has been chosen to ensure complete filling of the cavity in conditions of minimum mould and melt temperature. Experimental tests established a value of 200 mm/s (40% of maximum injection speed). The higher level has been selected in order to not exceed the 90% level of the maximum injection pressure of the machine in conditions of minimum mould and melt temperature. Experimental tests established a value of 350 mm/s (which correspond to the 70% of maximum injection speed). Details of the processing conditions, tooling system and the machine are given in section 3.1.3.

The considered part to be filled in this analysis is represented in Figure 108 and it comprises sprue, runner and actual part. The total volume of the moulding was 7.3cm^3 (detail (a)), whereas the micro moulded part volume was 6 mm^3 (detail (b)).

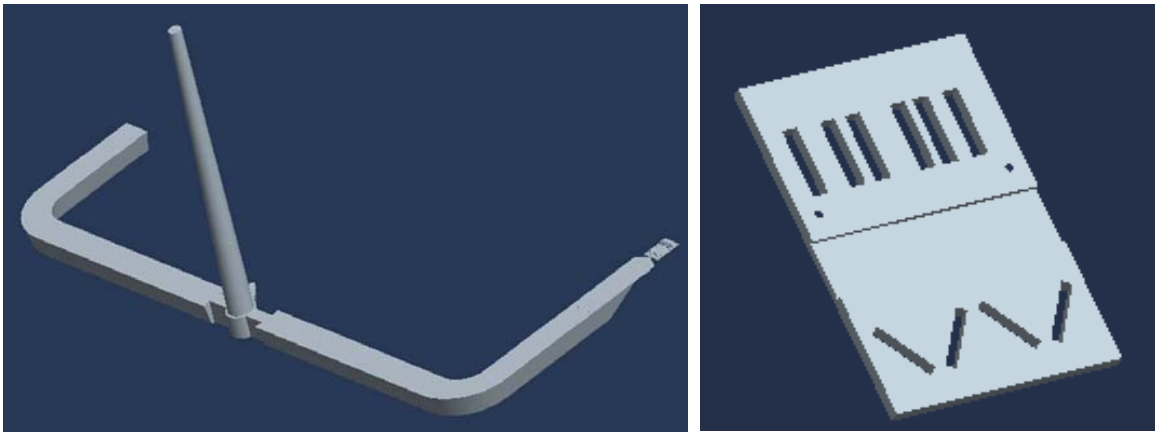

(a) (b)

Figure 108 – Complete moulded part including sprue, runner and micro component (a). Detailed view of the micro injection moulded part (b).

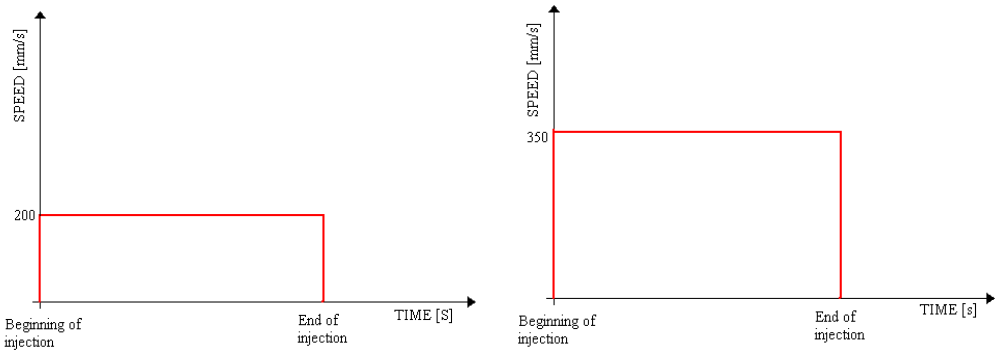

Figure 109 – Injection speed profiles implemented during the injection moulding: 200 mm/s (left) and 350 mm/s (right).

The rectangular speed profile can be considered realistic in the macro moulding process, due to the fact that the injection time is much larger than the time of the transitory (i.e. screw acceleration time). On the other hand, in the micro moulding the transitory time is comparable with the injection time, mainly because of two reasons. Firstly, the injection time is short due to the limited part volume; secondly, when traditional plastification screw moulding machines are employed, the screw acceleration is not high enough to provide high speed in such short time. In this study, the transitory was considered as the elapsed time between the moment when

the ram starts to move and the moment when it reaches its stabilized speed as explained in the figure below.

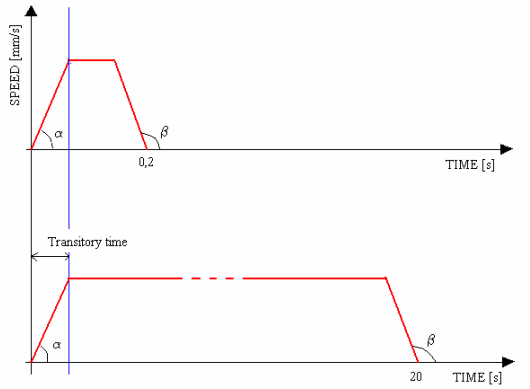

Figure 110 – Injection transitory injection time: micro injection moulding (above), conventional injection moulding (below).

In case of conventional injection moulding, the actual injection speed profile can safely be approximated to a rectangular profile and be directly implemented into the simulation software. As far as the micro injection moulding process is concerned, the actual injection speed has to be determined in order to execute an accurate set-up of the simulation.

The actual injection speed profile was calculated from the screw displacement Vs time data given by the injection machine sensor. The ram (i.e. screw) speed can be obtained by derivation of the ram position Vs time, which was given along with injection pressure Vs time by the machine.

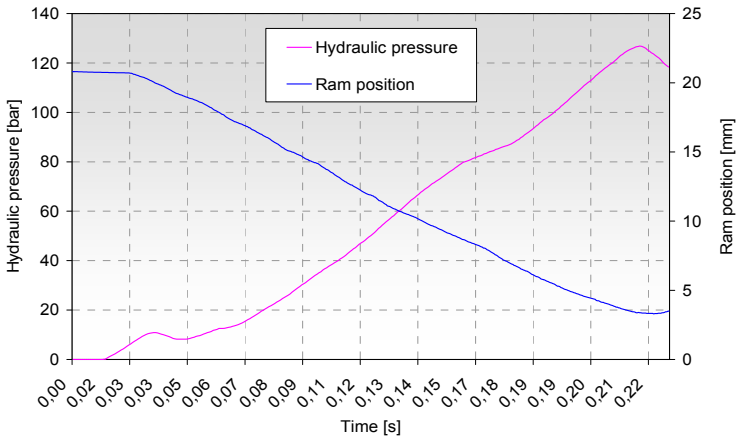

Figure 111 – Ram position and injection pressure actual profile for injection mouldings performed at 200 mm/s.

6.3.1 Determination of the actual injection speed profile

The objective of the analysis was to analyze the ram position Vs time in order to obtain the real ram speed Vs time. The following strategy was employed:

- The displacement Vs time profile data set (Figure 112A) was divided in different sub-sets of points (Figure 112B).
- Each subset had the characteristic to be described by either a linear function or a spline curve with an accurate interpolation (Table 17).
- Each sub-sets' function was then derived. Displacement derivation gave as result the ram speed in the considered injection time interval (Table 18)
- The analysis was performed for both 200 mm/s and 350 mm/s injection speed set-ups (see actual injection speed profiles on Figure 113 and Figure 114).

(A)

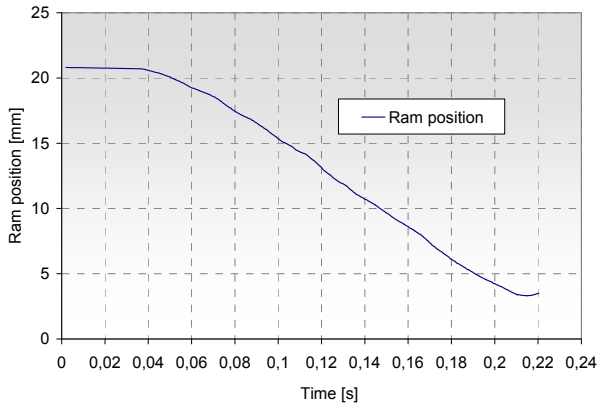

(B)

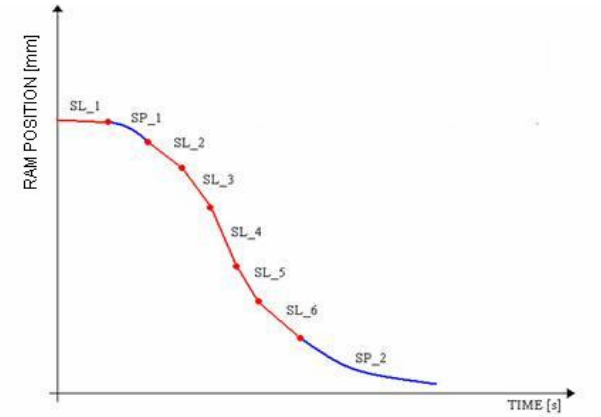

Figure 112 – Injection speed profile determination: (A) ram position Vs time (processing conditions: temperature of the melt = 240 °C, temperature of the mould = 45 °C, injection speed = 200 mm/s); (B) schematization of the ram position VS time graph interpolated with straight lines and splines (SL = Straight line, SP= Spline).

From 5 to 34ms	From 34 to 45ms
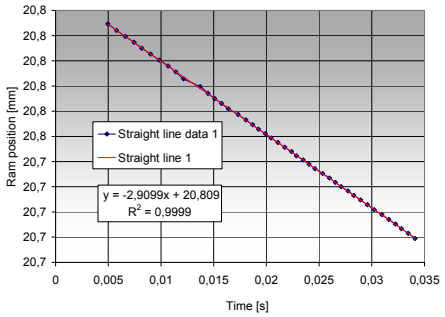	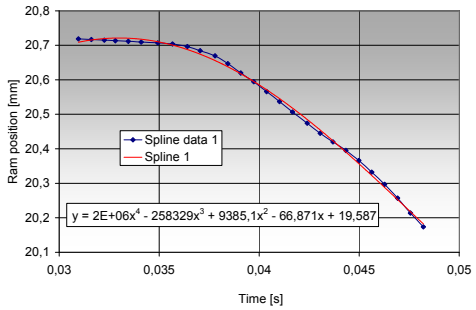
From 48 to 58ms	**From 63 to 111ms**
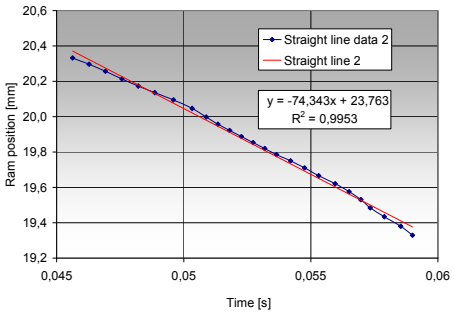	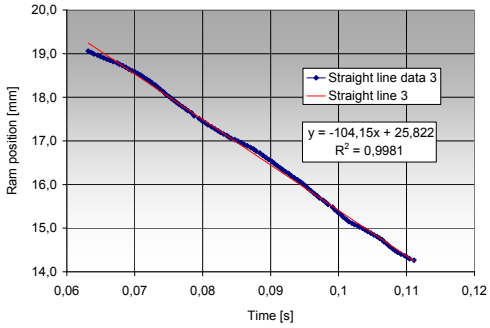
From 114 to 180ms	**From 184 to 197ms**
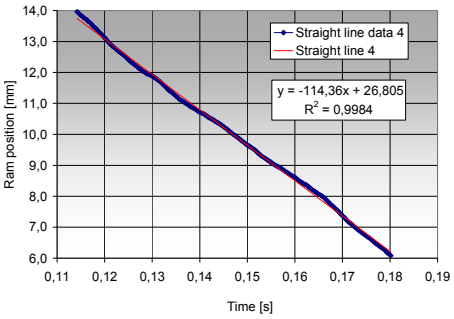	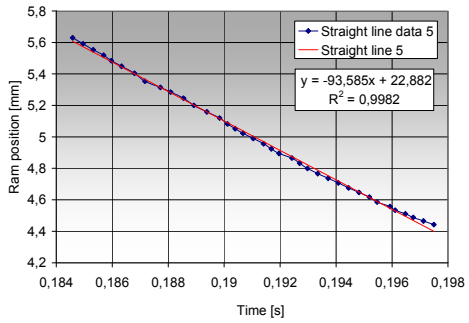
From 197 to 208ms	**From 208 to 215ms**
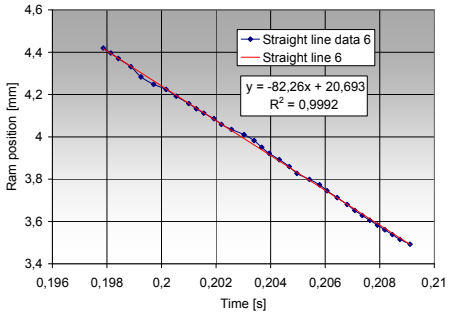	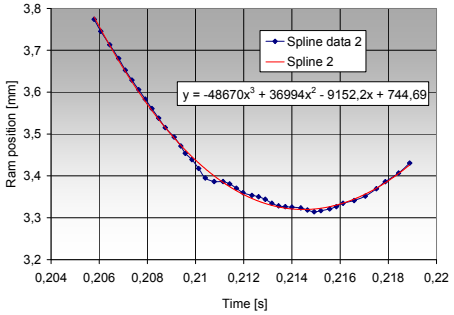

Table 17 – Discretization and interpolation of the ram position Vs time profile.

Step No.	Time [s]	Inj. Vel. [mm/s]	Step No.	Time [s]	Inj. Vel. [mm/s]	Step No.	Time [s]	Inj. Vel. [mm/s]
1	0,005	2,9	9	0,049	74,3	17	0,208	77,2
2	0,034	2,9	10	0,059	74,3	18	0,210	55,7
3	0,035	15,8	11	0,063	104,2	19	0,211	39,5
4	0,036	24,7	12	0,111	104,2	20	0,212	24,9
5	0,038	32,5	13	0,114	114,4	21	0,213	15,1
6	0,040	45,8	14	0,181	114,4	22	0,214	8,6
7	0,043	56,8	15	0,185	93,6	23	0,214	5,5
8	0,046	63,9	16	0,197	93,6	24	0,215	1,2

Table 18 – Actual values of the injection speed, determined after functions derivation.

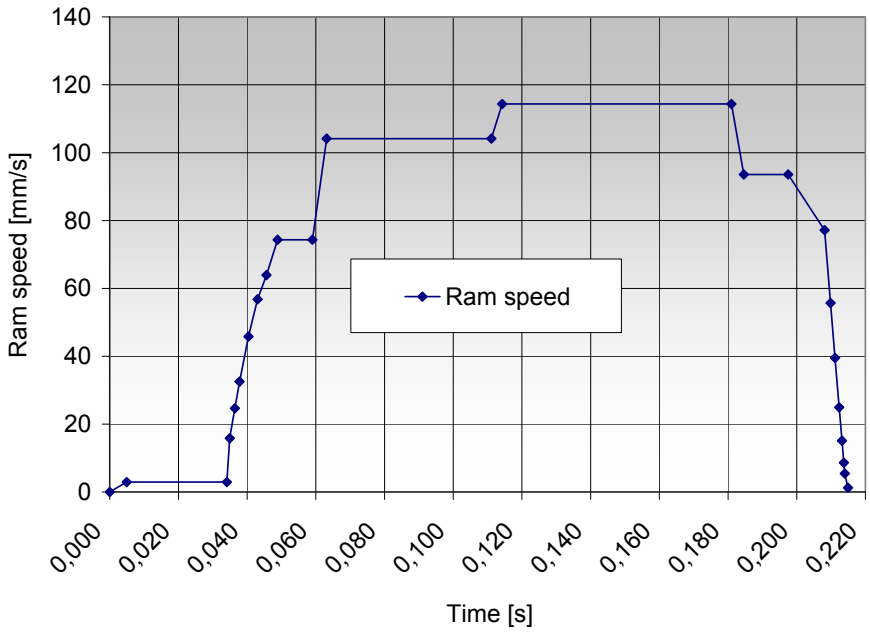

Figure 113 – Actual injection speed profile for the nominal speed set-up at 200 mm/s.

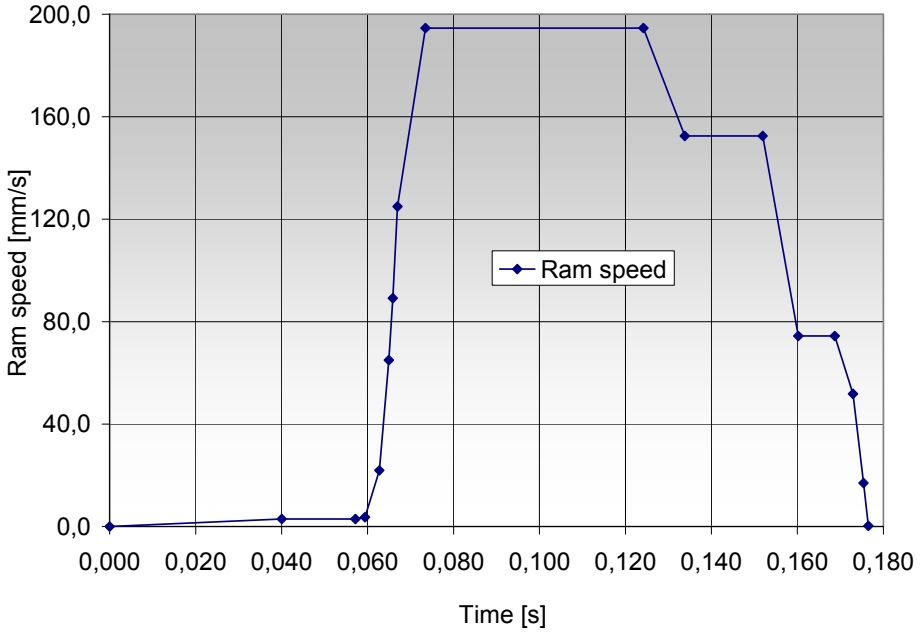

Figure 114 – Actual injection speed profile for the nominal speed set-up at 350 mm/s.

From the experimental investigation, it was found that the maximum speed reached by the ram is lower than the one set with the step speed profile, the transitory played an important role within the actual injection time and the overall profile was far from having a sharp rectangular shape. Therefore, it was not possible to inject at the desired injection speed. This is due to the fact the screw acceleration was not sufficiently high to permit to reach the set injection speed in a very short time if compared to the actual injection time (due to very limited part volume) as previously described.

In conclusion, it is of great importance to implement this experimentally determined boundary condition in the software in order to increase the simulation accuracy.

6.3.2 Validation of actual speed profile and optimized mesh

The actual increased accuracy in terms of injection time is investigated in this section. The actual injection time was determined during injection moulding experiments as reported in Table 19.

Experiment	Melt temperature [°C]	Mould temperature	Injection speed [mm/s]	Injection time [s]
Case 01	270	70	350	0.177
Case 08	240	45	200	0.215

Table 19 – Processing conditions investigated during experiments and simulation (the nomenclature “Case 01” and “Case 08” refers to the design of experiments as indicated in section 3.1.3.3).

Four types of simulations were conducted for both processing conditions:

- Simulations using the rectangular step speed profile and the nominal injection speed set on the injection moulding machine (see Figure 109).
- Simulation using the actual injection speed profile determined from the displacement Vs time profile (see Figure 113 and Figure 114).
- Each of this speed set-up was simulated using the two different meshing strategies described in section 6.2.1:
    - Hybrid meshing 1D and 3D for runner system and part respectively.
    - Full 3D meshing for the complete moulding: sprue, runner, part.

Results are summarized in the following (see Table 20).

Experiment	Model and mesh type	Simulated filling time [s]		Experimental filling time [s]
		Step injection speed profile	Experimental speed profile	
Case 01	1D + 3D	0.022	0.106	**0.177**
	Full 3D	0.031	**0.120**	
Case 08	1D + 3D	0.042	0.119	**0.215**
	Full 3D	0.054	**0.142**	

Table 20 – Filling time depending on mesh type, processing conditions, speed profile, experiments and simulations.

It can be observed that by using the experimental speed profile and a full 3D meshed geometry, the most accurate results in terms of injection time could be obtained.

Considering the improvement due to the employed speed profile, it was observed that there is a substantial difference between the filling time obtained with a step speed profile and with the experimental speed profile. The two main reasons of this remarkable difference are that:

- The ram speed never reaches the set injection speed, i.e. the injection is slower than the desired machine set-up.
- The ram needs a certain amount of time to reach the maximum speed and this amount of time is of the same order of magnitude of the filling time itself.

Considering the increase in the simulated injection time due to the employed model (complete 3D meshed model or 3D meshed cavity and 1D runner system), it can be observed that there is a difference between the filling time estimation. This difference is believed to be mostly due to the difference in the injected volume between the two models.

Despite the final difference still existing between the simulated and the experimental injection time, it can be concluded that:

- In micro injection moulding the real ram speed profile must be considered. It is not advisable to neglect the transitory between the start of the injection to the moment with maximum speed.
- The simulated injection times with a step speed profile are of one order of magnitude shorter than the experimental ones. It is not possible to consider the ram speed constant during the filling phase of the part. Therefore, an accurate ram speed study is needed in order to increase the accuracy of simulations of the micro injection moulding process.
- Improvements are obtained using a complete 3D meshed model instead of 1D meshing elements. Considering 1D runner system a certain volume is neglected due to the hydraulic radius calculation. This neglected volume has no influence in macro injection moulding due to the fact that the moulded part is much bigger than the runner system, whereas in micro injection moulding has to be considered.

Differences still existing between the experimental and the simulated filling time can be attributed to:

- Material characterization – Differences between the rheological database implemented in the software and the actual rheology of the employed polymer.
- Process characterization – Lack of accuracy in the determination of the ram speed profile.

6.4 Determination of the cavity injection time

The determination of the cavity injection time is of great importance in order to obtain accurate filling simulations. This is due to the fact that an accurate time-dependent produces precise determination of the flow rate which gives the correct value of viscosity of the polymer during the filling of the cavity.

During the project, two different approaches have been used to determine the cavity injection time during the injection moulding experiments:

- In case of micro part moulded with a conventional injection moulding machine and large sprue-runner system, an integrated experimental/simulative was applied.
- In case of micro part moulded with a micro injection moulding machine, an in-line process pressure measurement was carried out and the injection time was determined from the pressure Vs time plot.

6.4.1 µIM with large runner system using injection speed profile

The idea is to simulate the filling of the cavity implementing a simulated cavity filling time that is experimentally acceptable. It is of critical importance to note that the filling time of the cavity is too short to be experimentally defined by using the injection pressure or the ram position plots given by the machine. For this reason the comparison with the experimental data aims to verify if the simulated results are congruent with the reality. Whenever the simulated filling time of the cavity is congruent with the experimental results, it is assumed such filling time can be employed for the setup of the simulations for the analysis of flow during the filling and the consequent evaluation of the factors that mainly influence the software validation.

For the analysis of the simulated cavity filling time the simulations results presented in section 6.3 were analyzed. In particular, after the previously described optimization, the chosen simulation set-up was the following:

- Ram speed profile obtained with experimental data.
- Geometry model completely meshed with 3D elements.

The melt flow pattern was analyzed and the moment when the melt entered in the cavity was observed. The filling time of the cavity was then defines as the difference between the filling time of the entire model and the moment at which the melt reaches the gate (see Figure 115 and Table 21).

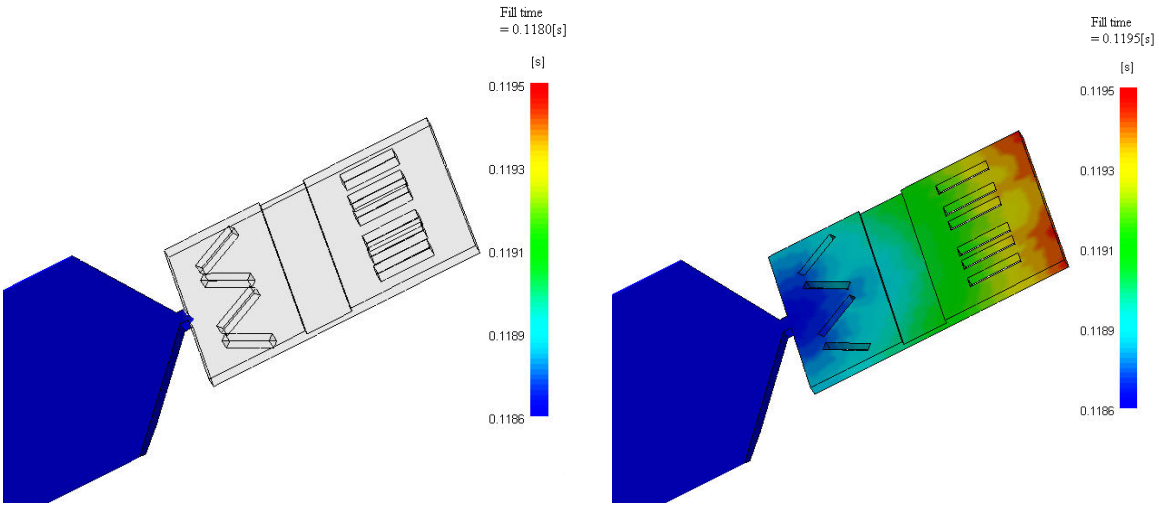

(a) (b)

Figure 115 – Melt flow front at gate location (a) (time = 0.1180s) and flow front at the end of filling (b) (time = 0.1195s).

	Entrance in the cavity	Finish of the filling phase	**Filling time of the cavity**
Case 01 (350 mm/s)	0.1180 s	0.1195 s	**0.0015 s**
Case 08 (200 mm/s)	0.1392 s	0.1421 s	**0.0029 s**

Table 21 – Cavity filling time determination.

These values of cavity injection time are consistent with experimental determination based on the application of the continuity equation. It was decided to estimate the

filling time of the cavity considering the mean values of the screw speed in the last moments of the filling phase (from the experimental injection speed determination as described in section 6.3.1). Given the cavity volume (5.98 mm^3) and the speed, the cavity time was estimated as the cavity was filled at constant flow rate. Cavity injection times of 0.001 and 0.002s were calculated for the experiments at injection speed of 200 mm/s and 350 mm/s respectively. Despite the approximation introduced by the method, the cavity times obtained with the two methods are in the same order of magnitude and they both increase for lower values of the injection speed, confirming the validity of the assumption underlying the investigation.

6.4.2 µIM with miniaturized runner system using injection pressure profile

In order to establish a consistent database to be used for the simulation software validation, experimental micro injection mouldings were produced on a Battenfeld Microsystem50 micro injection moulding machine.

In-cavity injection pressure samplings were executed using a piezoelectric pressure sensor applied at the injection location (where the melt is pushed into the cavity by the injection piston) of a two-cavity micro structured mould (see section 3.2.5). Pressure samplings over time allowed the determination of the cavity injection speed and the punctual value of the cavity pressure during the filling of the cavity.

Micro injection moulding was executed using the following process parameters settings: temperature of the melt of 220 °C, temperature of the mould of 70 °C, injection speed of 100 mm/s, total injected volume of 130 mm^3.

Three different mouldings were randomly selected from a production batch of approximately 100 parts, moulded after 50 parts were produced in order to obtain a stabilized process. Three pressure samplings were collected (see Figure 116), the average cavity injection pressure profile was calculated as well as the point-by-point standard deviation (see Figure 117). The time needed by the flow front to go from the inlet into the cavity (i.e. injection point piston/mould) until the pressure sensor is obviously missing in the raw data plot (see Figure 116). It was calculated after the determination of the flow rate in the runner after the pressure sensor position and added to the pressure plot as shown in the chart below.

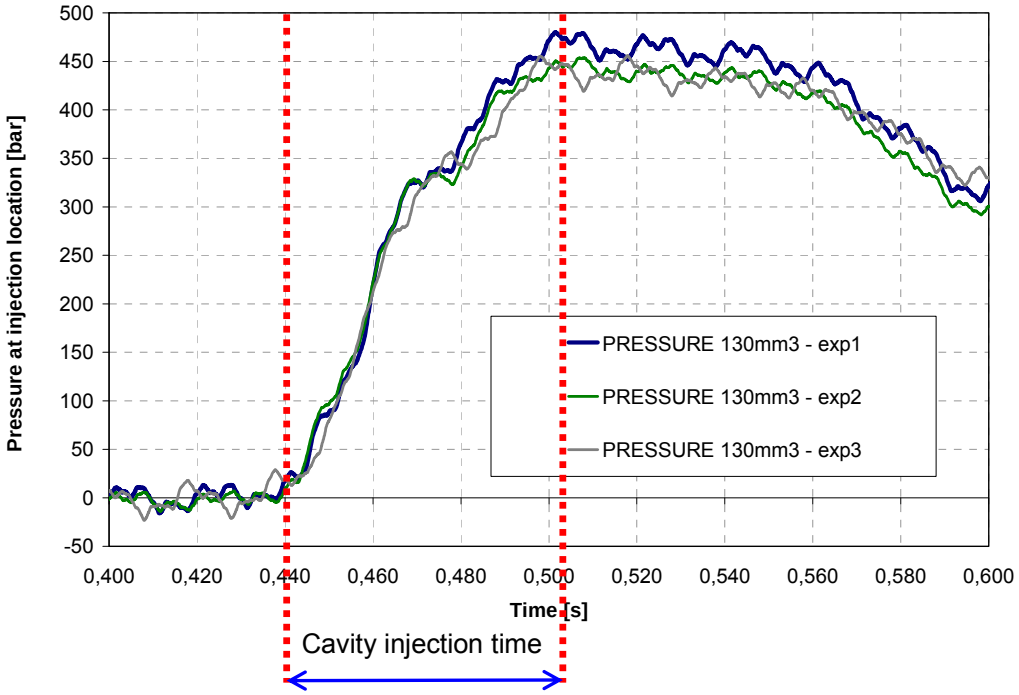

Figure 116 – Cavity injection time determination from the cavity pressure Vs time plot.

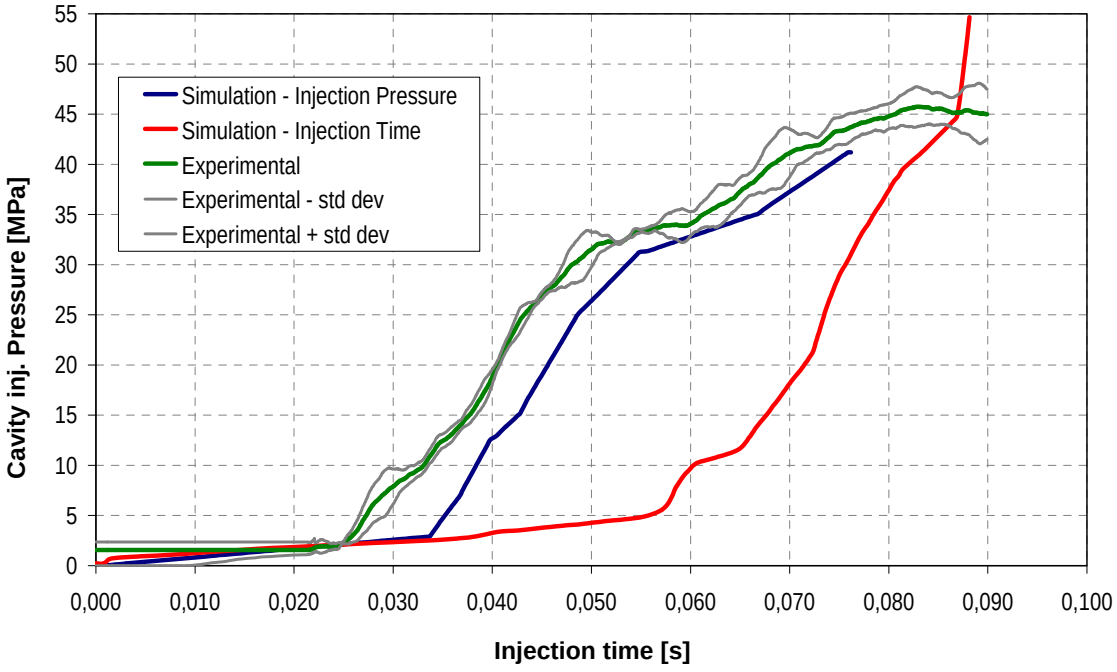

Figure 117 – Comparison of experimental and simulated cavity injection pressure profiles.

When performing the micro injection moulding process, the injection speed (implemented as piston speed) is usually set as parameters to define the evolution over time of the melt to fill the cavity. It is of great importance to implement these conditions on the simulation software with the highest accuracy. A conventional approach is to implement a nominal speed profile. This is a simple but rather inaccurate method because it does not take into account the acceleration of the piston and the fact that the set piston speed is different the actual speed produced by the machine (as discussed in section 6.3). Different approaches can be employed to increase the simulation accuracy. Two methods have been selected and are presented in the following:

- A. Injection time – From the injection cavity pressure plot given by the pressure sensor the actual cavity injection time is determined and implemented into the simulation. The software will calculate the flow in order to fit the given time constrain. In particular, an initial transition time will be allowed to the flow rate to reach a stable value of the flow rate. On the other hand, when such value is reached, is kept constant during the remaining injection time until the complete filling. In particular an experimental cavity injection time of 83±1 ms was determined and implemented.
- B. Cavity injection pressure Vs time – From the injection cavity pressure plot given by the pressure sensor the actual cavity injection pressure over time is determined and implemented into the simulation. In this way, not only the time dependency factor of the flow is constrained, but the physical condition of the polymer (through a punctual value of the injection pressure) is determined. Actual pressure repeatability was calculated for each sampled value through the all cavity injection time for three randomly chosen mouldings. A standard deviation of 1.7 MPa was calculated.

It is interesting to notice that the method (A) is carried out using a filling simulation performed in speed control. On the other hand, to implement the method (B) a packing simulation is carried out (i.e. in pressure control).

The cavity pressure profile is a fundamental process parameter for the precision moulding of high accuracy thermoplastics as micro moulded components. It is therefore of great importance that the injection pressure profile is simulated

accurately in order to obtain reliable results. The comparisons between the experimental pressure plot and the results of the simulation A and B show that:

- The maximum experimental cavity injection pressure (46 MPa) was reached at the cavity injection time of 83 ms, which corresponded to the complete part (injected volume of 130 mm^3).
- Simulation A (i.e. implementation of the cavity injection time) appeared inaccurate in terms of pressure Vs time prediction. The cavity injection pressure was much lower than the experimental for most of the cavity injection time. On the other hand the maximum cavity injection pressure at the very end of filling was of 55 MPa, i.e. 20% larger than in the experiments. Complete part filling happened at 88 ms.
- Simulation B (i.e. implementation of the cavity injection pressure profile) showed a pressure profile following the same trend as the experimental. On the other hand, despite the fact that the entire experimental pressure plot was implemented, the simulation stopped after 76 ms (complete filling of the cavity).

6.5 Validation of filling simulation

Different methods exist for the analysis of the development of the flow front in the cavity during the filling stage in injection mould (see section 3.1.1). The results of such investigations can be employed as experimental term of reference for the validation of filling simulation during injection and micro injection moulding.

During this project, the experimental data base developed with both the thin plate employed for the weld lines investigation (see section 3.1.3) and the tensile bar test part (see section 3.2.2) was used to validate the simulations of the respective moulded parts.

In this section, first the weld lines used as flow marker will be employed to validate the filling simulation of the thin plate (Figure 118a). Then, the flow marker method integrated with the short shots method will be employed for the validation of the filling simulation of the tensile bar test part (Figure 118b).

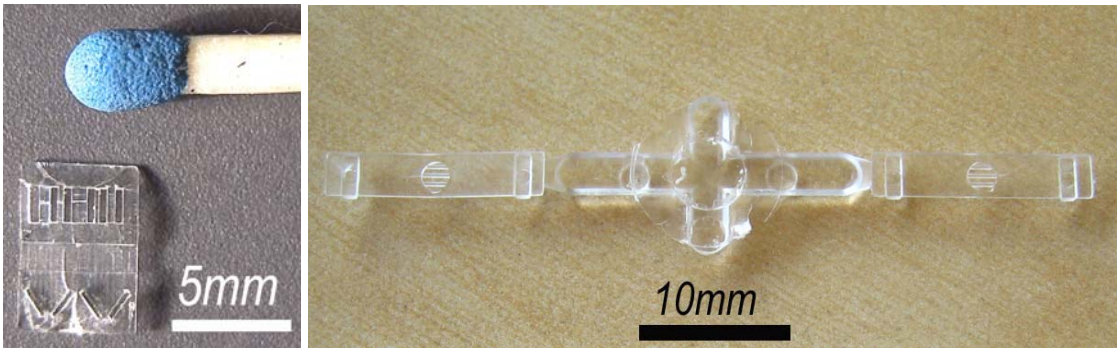

(a) (b)

Figure 118 – Thin plate employed for the weld lines investigation (a) (see section 3.1.3) and micro injection moulded tensile bar test part (b) (see section 3.2.2).

6.5.1 Flow markers method for filling simulation validation

In this section, the employed measurement method to obtain the simulated weld lines position data is analyzed. A particular strategy was developed because the 3D simulation was not provided with a feature giving the position of the weld lines as output. To obtain the weld lines position, data were collected simulating the filling of the cavity. Simulated weld lines were determined reconstructing their path by subsequent simulation steps collection (see Figure 119).

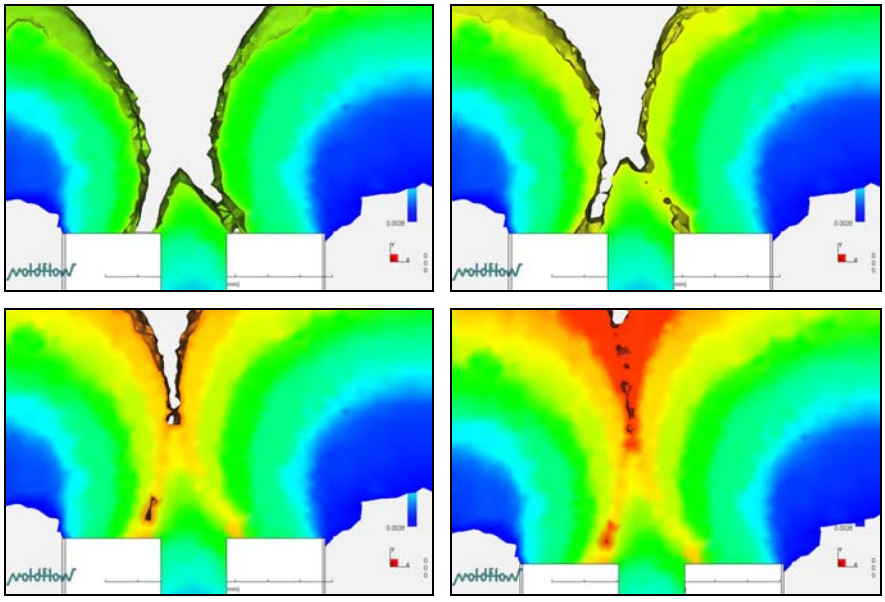

Figure 119 – Flow front advancement and detection of weld line by subsequent simulation steps collection (weld lines area 2 in Figure 121b).

Moldflow® provides a measuring system that gives the X, Y and Z coordinates related to the reference system of the cavity (see Figure 120). The weld lines coordinates were measured in the surface of the moulded part, referred to the workpiece reference system (see Figure 121a) and transferred to local reference systems related to single features (see Figure 121b).
An example of measuring result on a simulated weld lines is shown in Figure 121c.

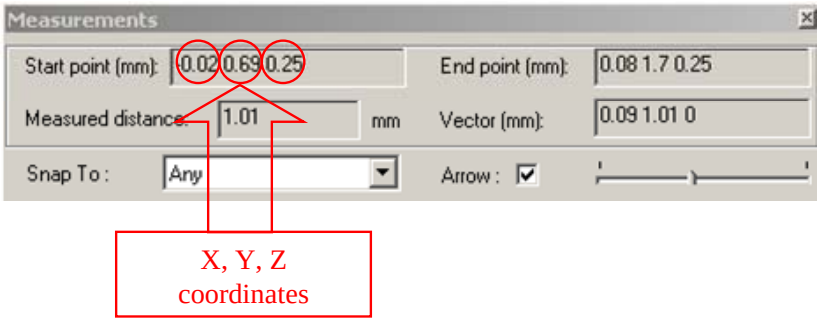

Figure 120 – Moldflow® measuring tool.

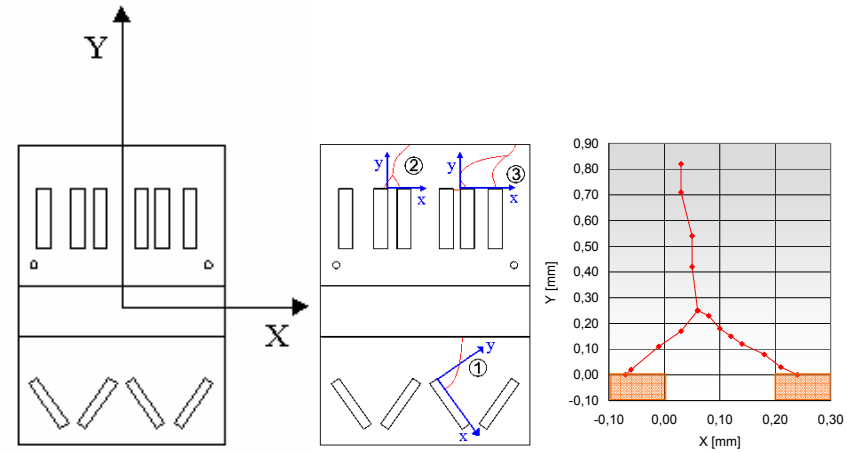

(a) (b) (c)

Figure 121 – Part reference system (a), local reference system related to single weld lines (b) and measuring results of simulated weld lines path on area 2 (c).

The simulated results in terms of weld lines path related to case 01 and case 08 (see Table 19) were compared with the experimental results for the same cases of the factorial plan (see section 3.1.4).

- Comparisons between experimental and simulated weld line area 1, weld line area 2 and weld line area 3 for the case 01 of the factorial plan (Tmelt = 270 °C, Tmould = 70 °C, Inj.Speed = 350 mm/s) are shown in Figure 122, Figure 123 and Figure 124 respectively.
- Comparisons between experimental and simulated weld line area 1, weld line area 2 and weld line area 3 for the case 08 of the factorial plan (Tmelt = 240 °C, Tmould = 45 °C, Inj.Speed = 200 mm/s) are shown in Figure 122, Figure 123 and Figure 124 respectively.

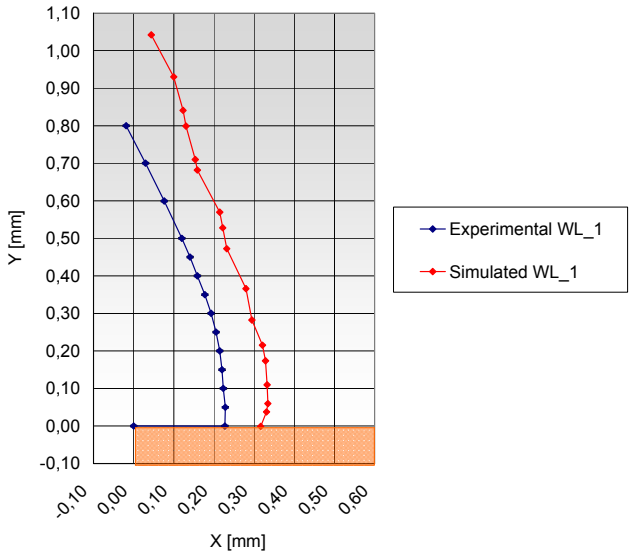

Figure 122 – Case 01: comparison between experimental and simulated weld line 1.

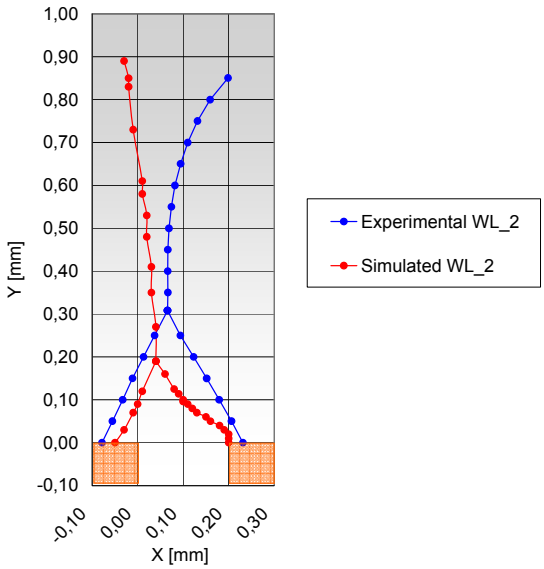

Figure 123 – Case 01: comparison between experimental and simulated weld lines 2.

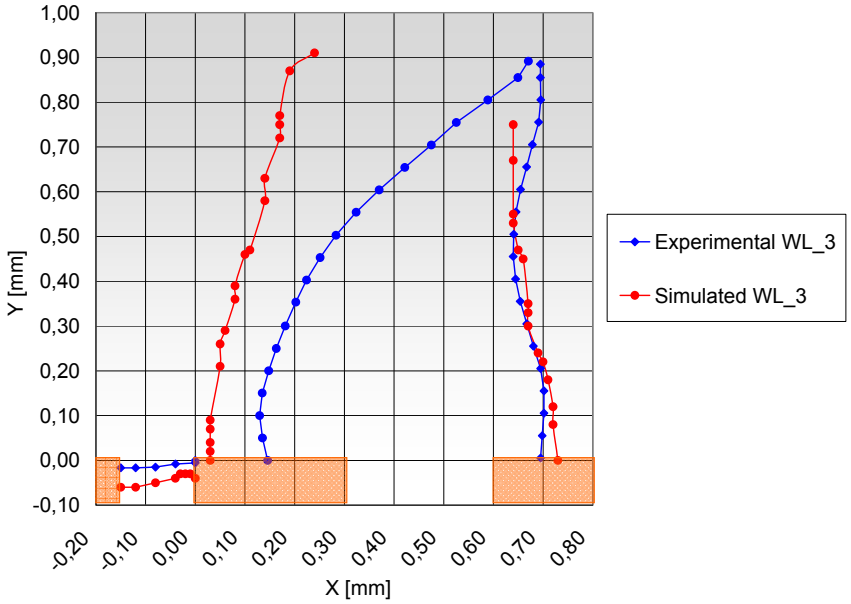

Figure 124 – Case 01: comparison between experimental and simulated weld lines 3.

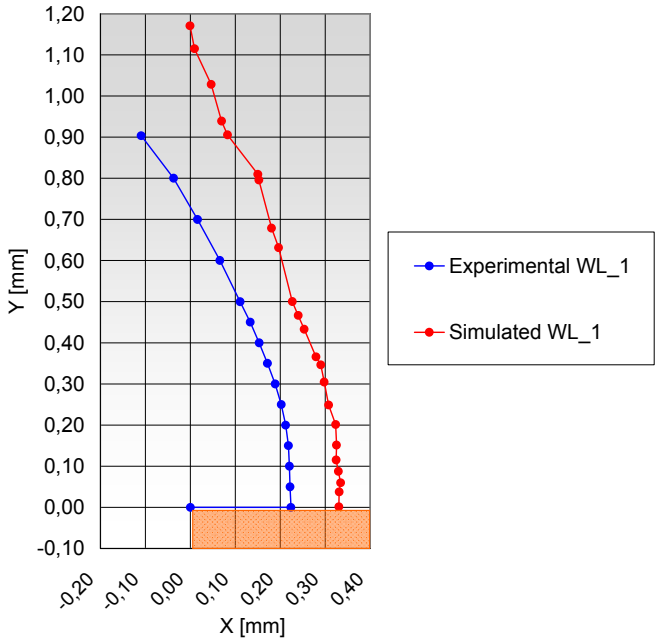

Figure 125 – Case 08: comparison between experimental and simulated weld line 1.

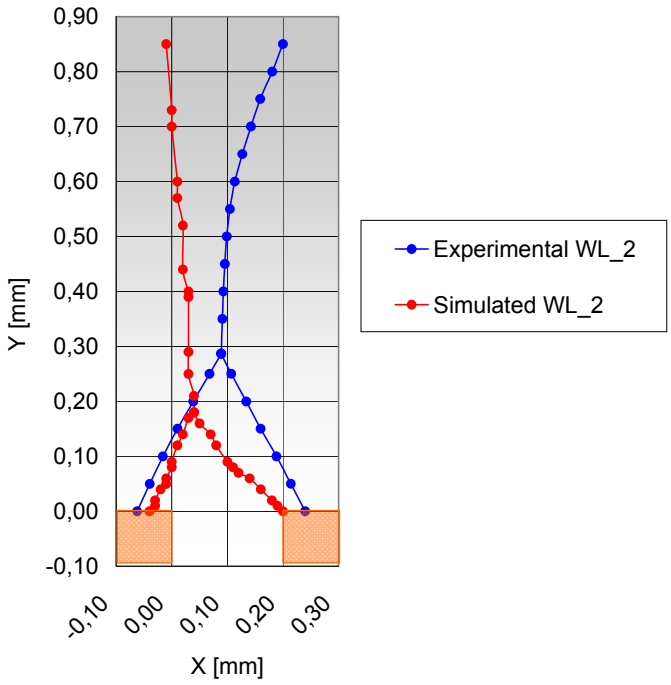

Figure 126 – Case 08: comparison between experimental and simulated weld lines 2.

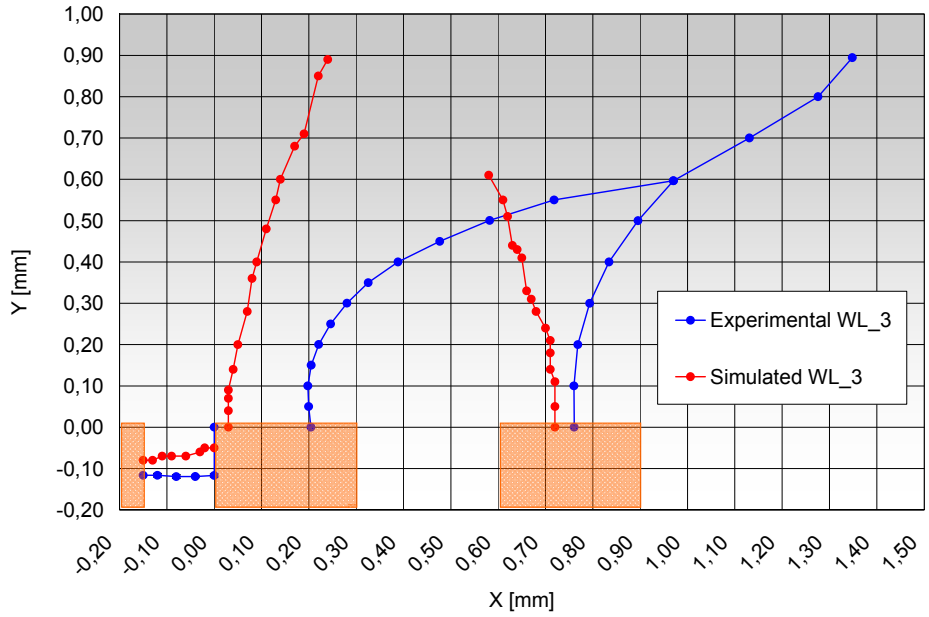

Figure 127 – Case 08: comparison between experimental and simulated weld lines 3.

From this absolute comparison, it is possible to observe that discrepancies do exist between simulated and experimental flow front position at the end of filling as defined by the weld lines (i.e. flow markers). Despite the implementation of the actual injection speed profile, the estimation of a realistic cavity injection time and an accurate meshing of the areas interested by the weld lines formation, predictions of the positions of weld lines do not match experimental results with distance error from 50 µm up 500 µm. This conclusion is verified considering both the uncertainty related to the measurement of the experiments (see section 3.1.3.5) and of the simulated weld lines position as reported in Table 22. Uncertainty was estimated taking into account the measurement repeatability due to the operator (typically $u_{c,rep}$ = 4 µm) and the resolution of the system (e.g. measuring tool, mesh size; typically $u_{c,res}$ = 4 µm).

Uncertainty direction	Combined uncertainty U (k=2, confidence level 95%)	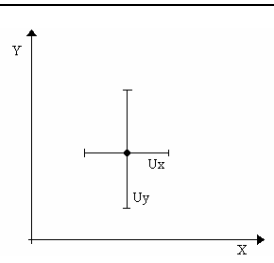
$X \rightarrow U_x$	10 µm	
$Y \rightarrow U_y$	11 µm	

Table 22 – Measurement uncertainties for the simulated weld lines.

6.5.2 Short shots method for filling simulation validation

The short shots method consists on the injection of partial volume of polymer in the cavity, as described in section 3.1.1.1. Previous relevant research work has been published in the specific field of software validation for the simulation of µIM using the short shots method [Mehta, 2003]. However, advancements in term of increased accuracy of the comparison, imaging calibration for flow front position validation, detailed experimental implementation for a true process simulation validation seemed of outstanding priority and needed further investigation. For this reasons an experimental µIM short shots investigation was undertaken, and the results were compared to simulations performed after the implementation of the concepts introduced in the previous sections, especially regarding mesh (size and type), cavity filling time, process dynamics.

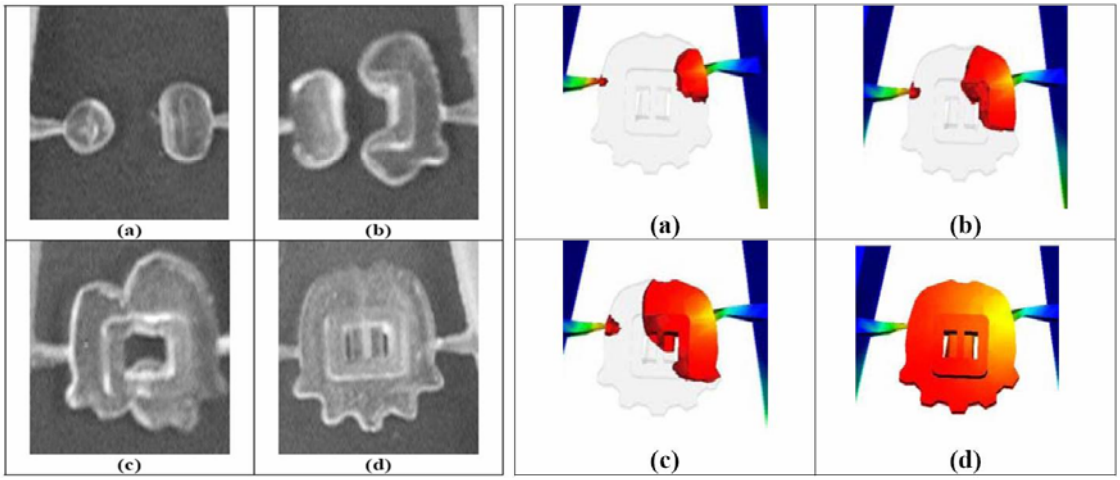

Figure 128 – Micro moulded part filling sequence four subsequent short shots (left). Filling pattern of the micro part using 3D flow simulation reproducing the 4 subsequent steps as in the short shots test (right) [Mehta, 2003].

Micro injection moulding was executed on µIM machine (see section 3.2.1) using the following process parameters settings: temperature of the melt temperature = 220 °C, temperature of the mould = 70 °C, injection speed = 100 mm/s, total injected volume = 130 mm^3. Mouldings were executed increasing the injected volume after each production batch. Partially filled moulded parts (i.e. short shots) were produced by injecting the following volumes (expressed in mm^3): 55, 65, 75, 90, 95, 105, 110, 125, 130 (complete part). For each batch, the cavity injection pressure was recorded with sample rates up to 25 kHz (i.e. pressure samplings at 40 ns interval) (see section 3.2.2).

During the injection moulding process, an automatic execution of the process (including ejection and handling of the polymer micro parts) was performed for each batch. Firstly, 50 cycles where carried out to stabilize the process in the current process parameter set-up. Subsequently, 10 parts obtained from the following 30 cycles have been randomly collected and analyzed. These randomly selected parts have been weighted and inspected with a calibrated optical microscope. During the all investigation, more than 800 micro moulded parts were produced. Moulded part weight, standard deviation and COV are shown in Table 23.

Injected volume [mm^3]	55	65	75	90	95	105	110	125	130
Weight average [mg]	52,1	61,0	70,0	84,0	88,0	96,9	101,2	114,4	118,8
Std dev [mg]	0,5	0,7	0,6	0,3	0,2	0,3	0,2	0,1	0,3
COV [%]	0,9	1,1	0,8	0,4	0,2	0,3	0,2	0,1	0,2
Density [mg/mm^3]	0,947	0,938	0,933	0,933	0,927	0,922	0,920	0,915	0,914

Table 23 – Average weight, standard deviation, COV and density at different injected volumes.

Cavity injection pressure was recorded for each of the short shots moulding batch. This allowed relating the respective injection cavity time for each injected volume at the actual value of the cavity injection pressure creating the conditions for a true step-by-step filling validation of the simulated results (see Table 24).

Injection volume		Cavity inj. Time		Cavity inj. Pressure	
		average	Std dev	average	Std dev
[mm^3]	[%]	[ms]	[ms]	[bar]	[bar]
55	42,3	21,5	0,4	15,9	1,1
65	50,0	25,0	0,5	23,8	3,1
75	57,7	25,3	0,3	26,3	3,3
90	69,2	29,4	0,6	75,6	4,7
95	73,1	30,8	0,8	85,7	5,4
105	80,8	38,4	0,2	161,5	3,4
110	84,6	40,4	0,2	199,5	4,4
125	96,2	51,1	2,0	318,0	8,7
130	100,0	83,1	1,8	463,3	14,6

Table 24 – Maximum cavity injection pressure, cavity injection time and density of moulded parts at different injected volumes.

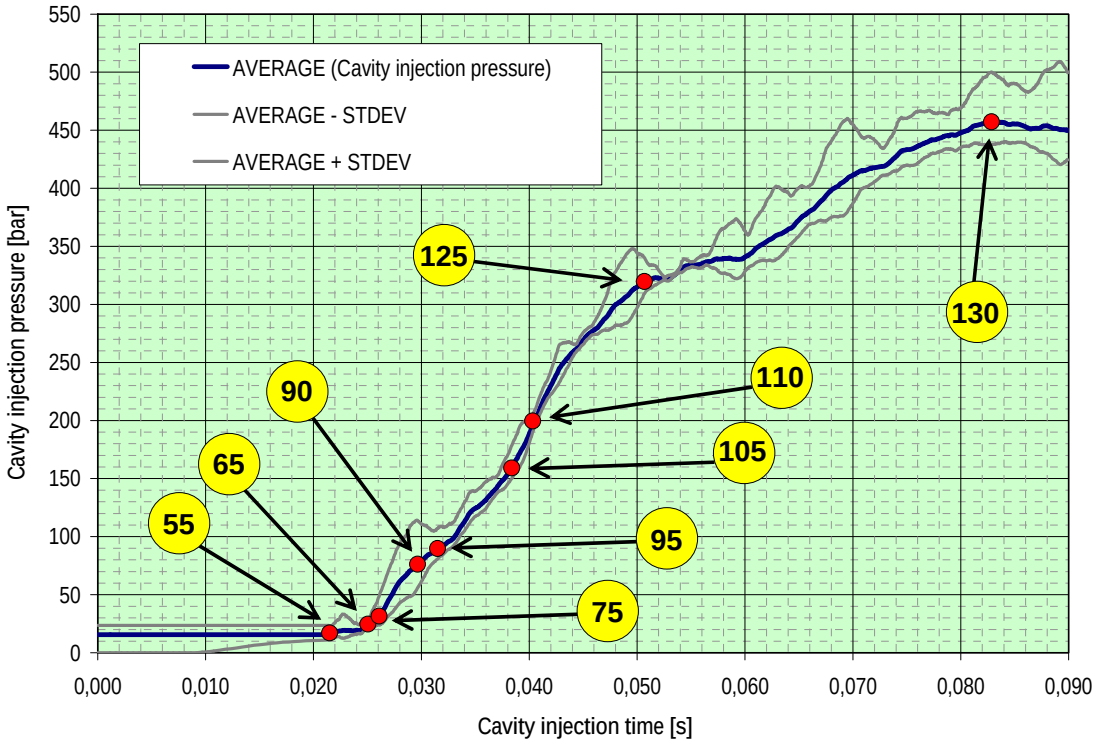

Figure 129 – Cavity injection pressure plot and injection times at different injected volume (expressed in mm^3 in the chart).

Two different simulations have been run using the implementation strategies as described in section 6.4.2:

- A – Injection time.
- B – Cavity pressure Vs time profile.

The simulations results have been post-processed for comparison with the experiments as follows:

For each of the µIM short shots volume (i.e. 55, 65, 75 mm^3 etc.), the corresponding simulated flow front step have been selected (for both simulations A and B) (see

- Figure 130).
- For each simulated short shots, the time frame of the selected simulation step have been then compared to the experimental injection time for the same shots volume (for both simulations A and B) (see Figure 131).

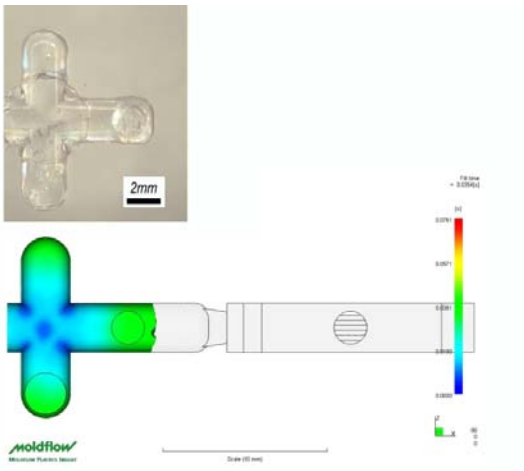

Injected volume = 55 mm^3

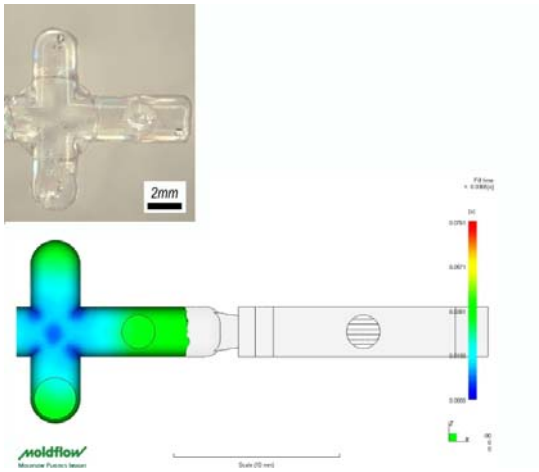

Injected volume = 65 mm^3

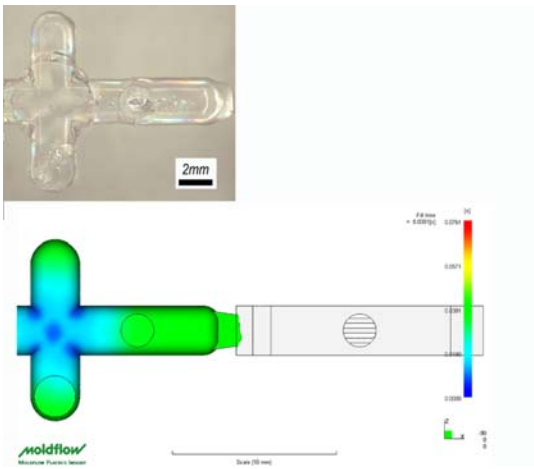

Injected volume = 75 mm^3

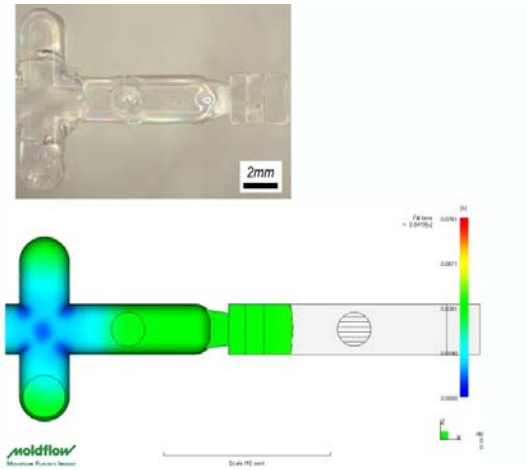

Injected volume = 90 mm^3

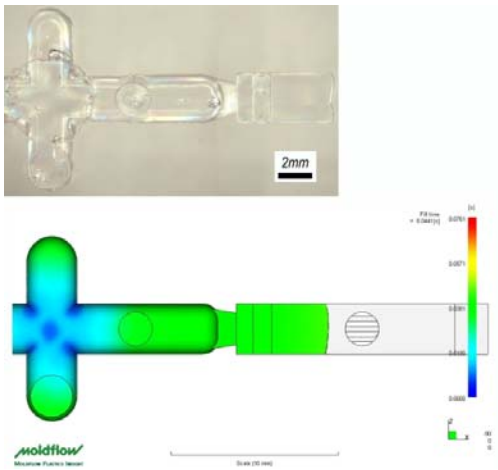

Injected volume = 95 mm^3

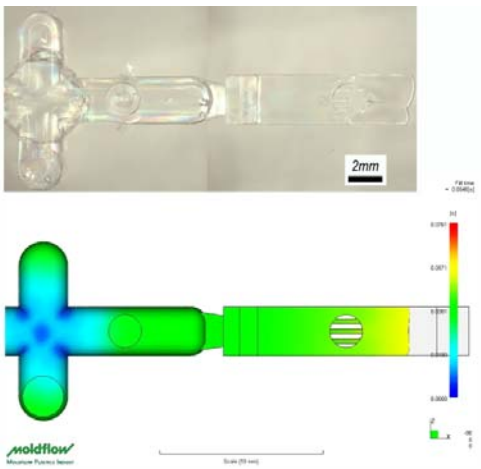

Injected volume = 105 mm^3

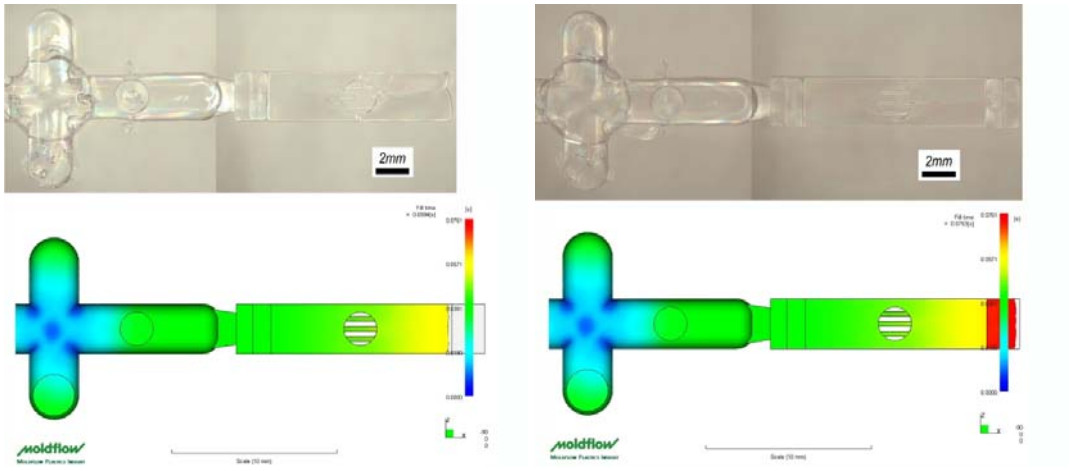

Injected volume = 110 mm^3 Injected volume = 125 mm^3

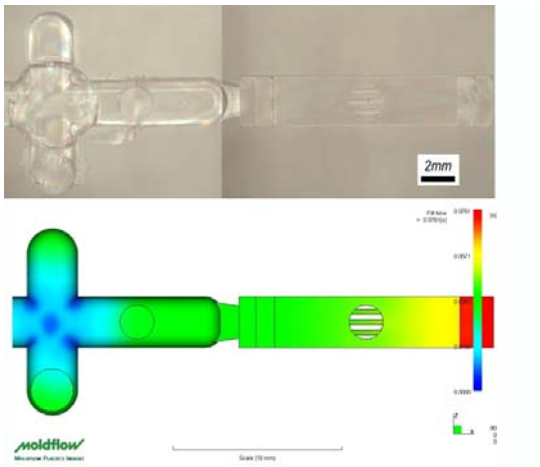

Injected volume = 130 mm^3

Figure 130 – Experimental and simulated short shots method (in this sequence the simulated steps with the cavity pressure Vs time profile implementation method are shown).

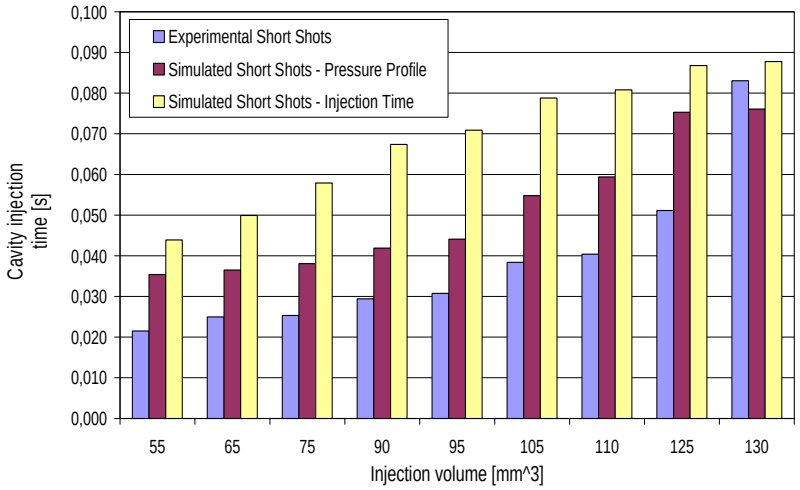

Figure 131 – Comparison of cavity injection times at different injection volumes: experimental short shots, simulation steps with implementation method A and B.

The comparison of the experimental pressure plot and the result of the simulation A and B shows the following:

- Experimental – The experimental short shots corresponding to 125 mm^3 (injection time of 51ms) shows that, despite the fact that the main flow front reached the end of the cavity, one micro feature in the middle of the moulded was not filled yet (see Figure 132). The complete µ-feature filling was obtained during the last 32 ms of the cavity filling time when the polymer could still flow, the piston was applying the needed pressure and the flow rate was very low (160 mm^3/s instead of 2500-3500 mm^3/s calculated during the cavity filling) determining an intermediate flowing condition between a filling and a packing phase.
- Simulation A (i.e. implementation of the cavity injection time) – Simulated short-shots showed that the micro features were completely filled before the main flow front has reached the end of the cavity. Complete micro features filling happened after 75 ms and complete part filling at 88 ms.
- Simulation B (i.e. implementation of the cavity injection pressure profile) – Simulated short-shots showed that the micro features were filled before the flow front reached the end of the cavity (after 50 ms) and the final filling/packing phase could not be predicted.

- In order to assess the accuracy of the two implementation methods, the partial filling times determined with the experimental short-shots and with the simulations were analyzed. The simulations are clearly predicting a slower filling, even though to a different extent depending on the adopted method. An accurate implementation (simulation B) resulted on a reduction of the error on the calculation of the partial filling time. In particular, while the injection time implementation (simulation A) produced an overestimation of the partial filling time of more than 100%, the pressure profile implementation (simulation B) resulted on an overestimation of less than 50%. This means that the dynamic conditions of the flow could be calculated with higher accuracy by using the more advanced approach. This would bring to the fact that the calculation of the shear rate is more accurate and therefore the viscosity values of the material during the filling could be determined closer to the reality.

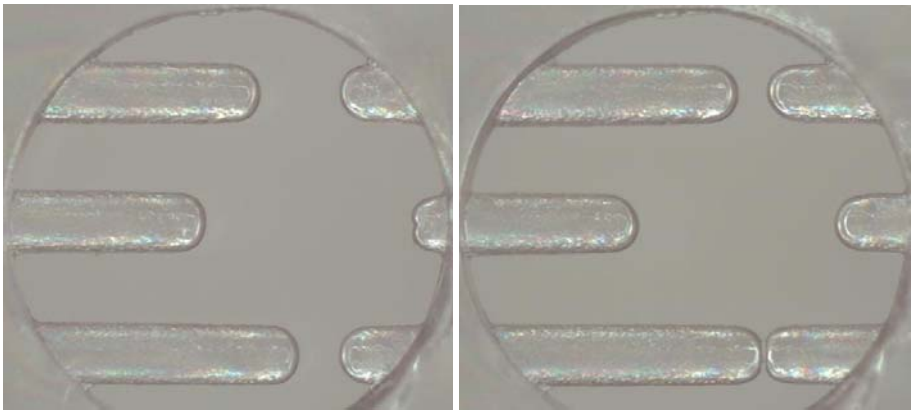

Injected volume = 105 mm^3 Injected volume = 110 mm^3

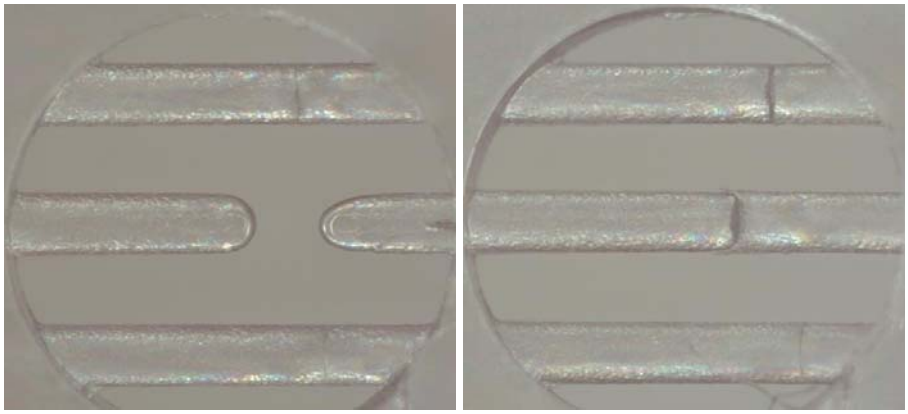

Injected volume = 125 mm^3 Injected volume = 130 mm^3

Figure 132 – Micro features filling steps at different injection volume.

6.5.3 Integrated flow marker-short shots analysis

The method described in section 6.5.1 to validate flow pattern simulation was also applied to the micro injection moulded component presented in the previous section. At the end of filling, the last short shot (i.e. injection volume of 130 mm^3) presented weld lines in the three micro features (see Figure 132). The weld lines represented the position of the flow front at the very end of filling; the same step was reproduced by simulation and position of the weld lines in the three micro features was measured (see method in section 3.2.6 and results in Figure 133). Image post processing and pixel calibration was performed [Image Metrology, 2005], and the comparison between experimental and simulated results was carried out. In particular, the simulation using the pressure Vs time implementation was selected (method B in section 6.4.2).

From this analysis it can be seen that the software overestimated the flow of the molten polymer inside the micro features, despite the accurate implementation in terms of injection pressure and meshing characteristics.

6.5.4 Concluding remarks on validation

Inaccuracies in terms of flow front prediction, step-by-step filling time and cavity injection pressure have been shown in this section, despite the accurate implementation of the simulation. Clearly, the flow behaviour of the polymer melt in micro cavities is not calculated properly.

One of the main reasons for this is believed to be related to the tendency of the polymer to slip (the so-called wall-slip effect) during the filling of micro features, especially at high speed (i.e. during micro injection moulding). The wall-slip effect is not taken into account by the software package, which applies the no-slip boundary condition. Furthermore, the material rheological characteristics present in the software's database are obtained with conventional rheology tests. These tests work in conditions far from the ones encountered during the μIM, causing a lack of accuracy in the simulation results.

During this research project, a solution to these issues has been proposed through the implementation of a rheological database for the material suitable for micro injection moulding (as presented in the next section 6.6).

μ-features	Simulation step for weld line 1 and 3	Simulation step for weld line 2
1 2 3	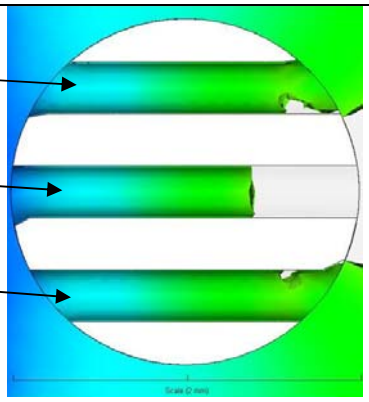	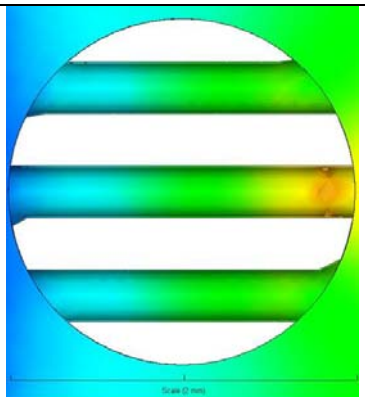
	Image processing for weld line 1 and 3	Image processing for weld line 2
2 mm = 627 pixels →1 pixel = 3.2 μm	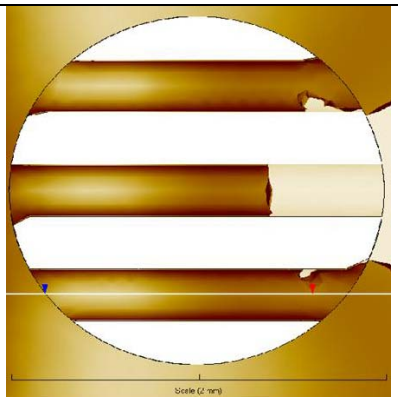	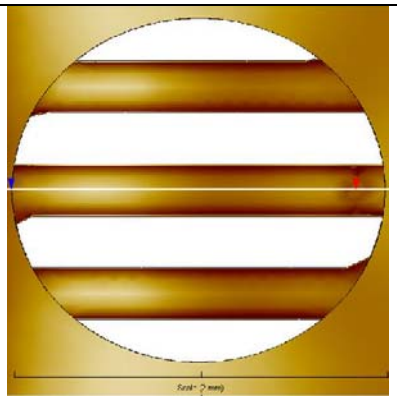

Figure 133 – Simulated weld lines as flow markers: simulation step, image processing, pixel calibration and definition of weld lines position (see blue and red arrows in the processed images).

Weld line	Weld line position	
	Experimental	Simulation
1	1155±43 μm	1378 μm
2	1299 ±38 μm	1856 μm
3	1197±44 μm	1429 μm

Table 25 – Quantitative comparison between experimental and simulated results in term of flow markers (i.e. weld lines) position (average and standard deviation).

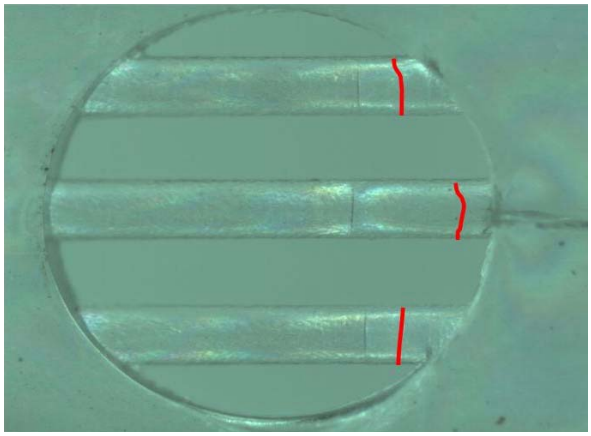

Figure 134 – Direct comparison of flow marker positions: experimental weld lines (in the optical microscope image) and simulated weld lines (red lines) are shown.

6.6 Influence of rheology on µIM simulation

The rheological data used in current packages (e.g. Moldflow) are obtained from macroscopic experiments. These macroscopic data would not be suitable for modelling microscale flows. In this project, using the simulation set-up as described in sections 6.2.1, 6.3.2, 6.4.1 and applying the flow marker validation method (see section 6.5.1), an investigation using a modified rheological model suitable for micro scale polymer melt flow was carried out.

6.6.1 Available rheological model and database

The rheological model represents the behaviour of the polymer melt in terms of viscosity, depending on the shear rate and on the temperature. The material formulation implemented in the Moldflow software is the Cross-WLF (William-Landel-Ferry) model [Kennedy, 1995] [Barnes, 2003].

- Cross viscosity model.
  - $$\eta = \frac{\eta_0}{1 + \left(\frac{\eta_0 \dot{\gamma}}{\tau^*} \right)^{1-n}}$$

- Where:
  - η_0 = pressure and temperature dependent viscosity at zero shear rate [Pa*s]
  - $\dot{\gamma}$ = shear rate [1/s]
  - n = flow index
  - τ^* = shear stress at the transition between the Newtonian and the pseudoplastic behaviour [Pa]

- WLF model which provides the viscosity at zero share rate [Moldflow, 2004].
  - $\eta_0 = D1 \cdot e^{\frac{-A_1(T-T^*)}{A_2+(T-T^*)}}$
  - Where:
    - D1 = material constant used to fit the experimental rheological data with the WLF equation [Pa*s]
    - A_1 = material constant defining the dependence of the rheology from the temperature
    - A_2 = pressure dépendent coefficient [K]
    - T = temperature at which it is wanted to know the rheology of the polymer [K]
    - T* = pressure dependent reference temperature [K]
- The dependence of T* and A_2 to pressure is described as follows [Moldflow, 2004].
  - $T^* = D_2 + D_3 * P$
    $A_2 = A_2 \sim + D_3 * P$
  - Where:
    - D_2 = reference temperature without considering the pressure dependence [K]
    - P = pressure [Pa]
    - A_2 ~= fitting coefficient [K]
    - D_3 = coefficient that describes the viscosity pressure dependence [K/Pa]

Moldflow® material database contains the polymer Polystyrene 143 E from BASF which was used in the µIM experiments (see section 3.1.3.3). The rheological data that are implemented in the software database are obtained with a traditional capillary rheometer. With traditional rheometers, it is possible to test the viscosity of the polymer for shear rates only up to 10^4 1/s. This brings to the fact that the polymer viscosity for shear rate higher than 10^4 1/s is calculated as an extension of the WLF formula for that shear rate for which actual experimental data do not exist. On the other hand, in micro injection moulding, due to the presence of micro features and to the high injection speed, shear rates easily exceed such value (see Figure 135).

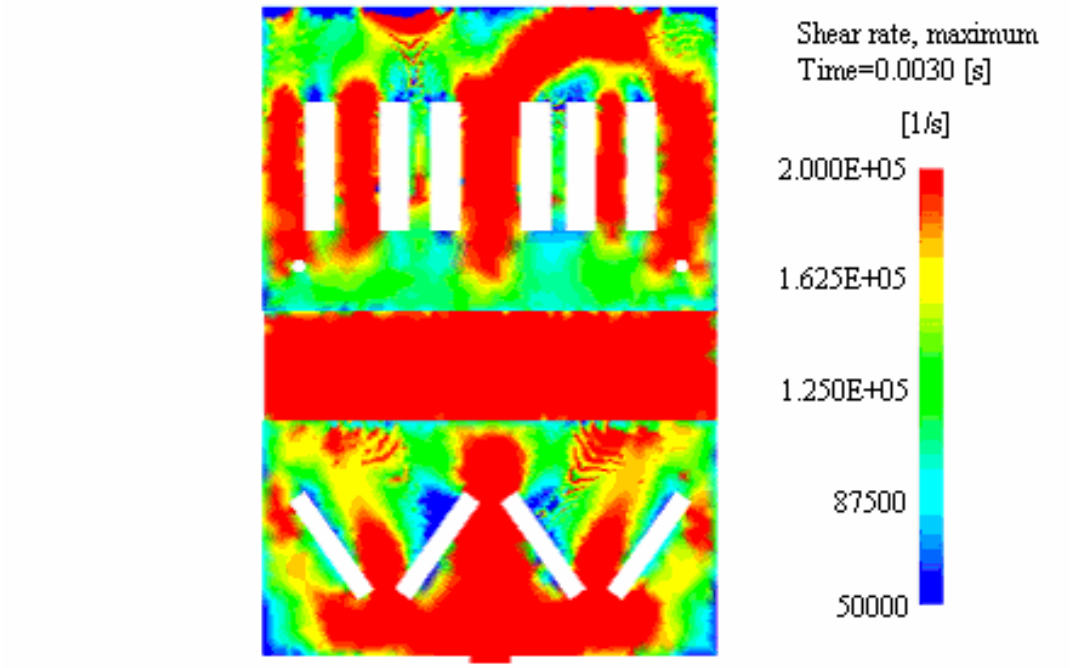

Figure 135 – Simulated shear rate of the investigated micro injection moulded component (Tmelt = 240 °C, Tmould = 45 °C, Inj.Speed = 200 mm/s).

Therefore, when the software solved the finite element problem, in the zones where a shear rate higher than 10^4 1/s occurred, viscosity values whose reliability is not verified are used. This is one of the reasons of lack of accuracy of the flow prediction in the studied micro cavity. In the next sections, a new rheological data set suitable for micro injection moulding simulation is proposed.

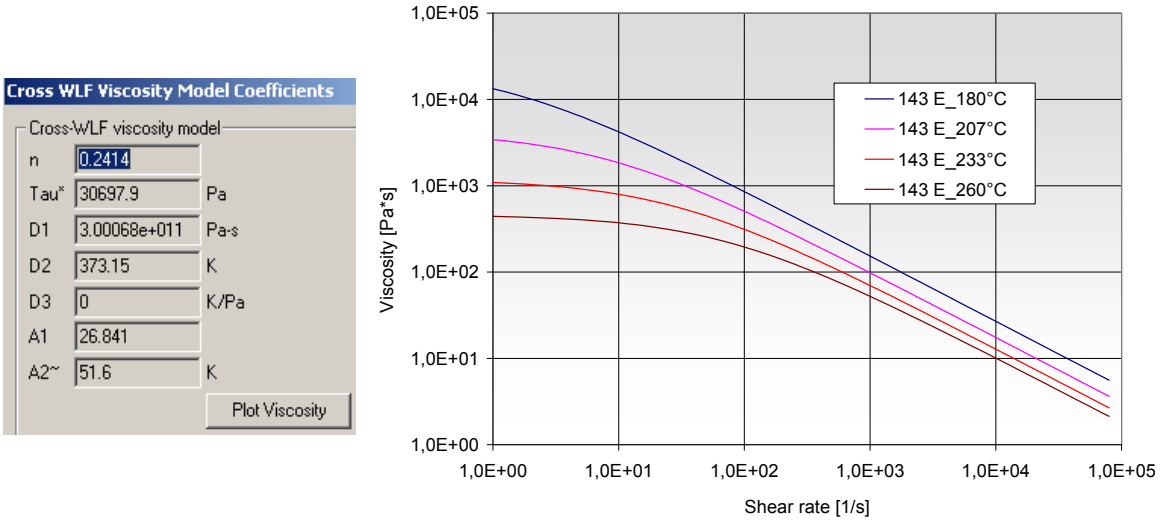

(a) (b)

Figure 136 – Polymer BASF PS (Polystyrene) 143 E: Moldflow Cross-WLF model coefficients (a) and viscosity Vs shear rate plot at four different temperatures (b).

6.6.2 New micro scale rheology data base

This section presents a solution for the determination and implementation in the Moldflow software of a new set of Cross-WLF model coefficients. The new rheological data are based on the experimental findings of a recent research work in the field of micro scale polymer rheology [Chien, 2005]. It is important to note that the use of the data from [Chien, 2005] will allow to:

- Define experimental viscosity values for shear rates up to 10^5 1/s and not only to 10^4 1/s as with macro scale measurements.
- Use rheological data specifically determined to characterize the polymer melt the flow in micro features.

This has been possible because in [Chien, 2005] an injection moulding machine was employed as a plunger and the flow of the melt in an injection moulding tool was studied.

In order to determine the rheological behaviour of the melt flowing through micro-channels, a mould designed with a micro channel of square cross section that allowed sizes varying from 300 µm to 200 µm and 150 µm was used.

The material that was injected in the experiments reported in [Chien, 2005] was a high fluidity class PS (polystyrene) resin (grade PG-22) from CHI MEI.

The injection experiments of the polymer melt were conducted at melt temperatures of 200 °C, 225 °C and 250 °C. The injection speed allowed apparent shear rates ranging from 3×10^3 to 3×10^5 1/s (injection pressures were 15, 30 and 45 MPa, respectively). The mould was operated at the same temperature of the melt.

Two pressure transducers were mounted near the inlet and outlet positions of the micro channels. The difference of pressure between the two embedded sensors determines the total pressure drop.

Finally, from the measured data of flow rate and pressure drop, using the slit flow model, the dependence of the true melt shear viscosity on the shear rate for the polymer melt at the test temperature could be calculated [Chien, 2005].

- Real shear stress at wall in the slit model
  - $\tau_{w(real)} = \frac{h}{2}\left(\frac{-\Delta P_{real}}{L}\right)$
  - Where:
    - h = slit thickness
    - L = slit length
    - ΔP = pressure drop *P* along the slit with length L and thickness h
- Apparent shear rate in the slit model
  - $\dot{\gamma}_{w(app)} = \frac{6Q}{wh^2}$
  - Where:
    - w = slit width
    - h = slit thickness
    - Q = volumetric flow rate through the slit under a pressure drop *P* along the slit
- Walter correction to calculate the shear rate at wall for non-Newtonian liquids
  - $\dot{\gamma}_{w(real)} = \frac{6Q}{wh^2}\left(\frac{2}{3} + \frac{1}{3}b\right)$

- Where:
  - b = the slope of $\log\left(\dot{\gamma}_{w(app)}\right)$ versus $\log(\tau_w)$

- Viscosity
  - $\eta_{(real)} = \frac{\tau_{real}}{\dot{\gamma}_{real}}$

The results the experiments reported in [Chien, 2005] are shown in the following graphs for the three channel sizes and for the three temperatures at which the experiments were conducted. They clearly show the tendency to slip of polymer melt forced in micro channels. This phenomenon results in a viscosity in micro channels which is lower than a viscosity measured by traditional capillary rheometer.

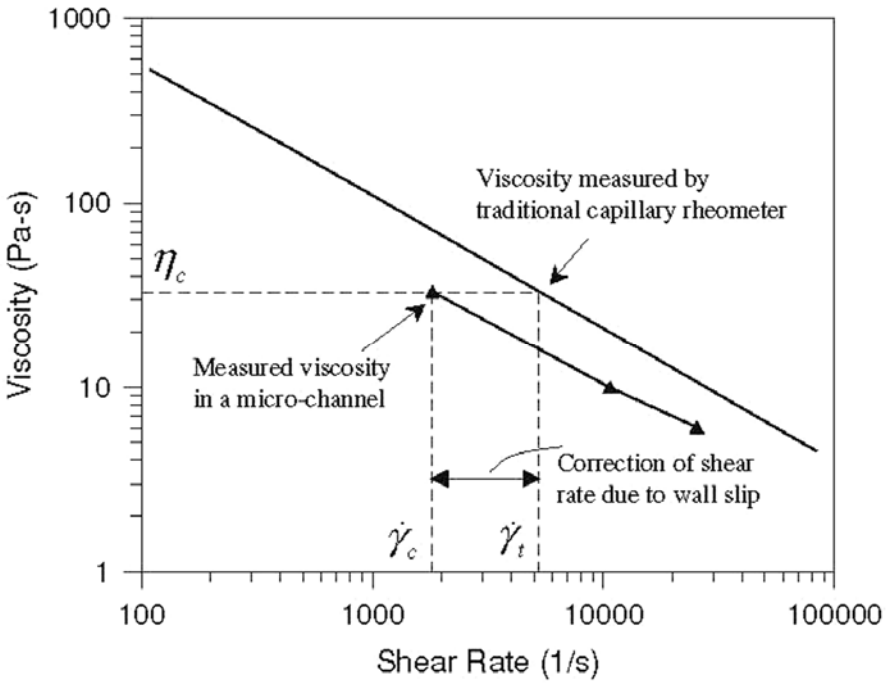

Figure 137 – Measured viscosity in a micro channels compared with viscosity measured by a capillary rheometer [Chien, 2005].

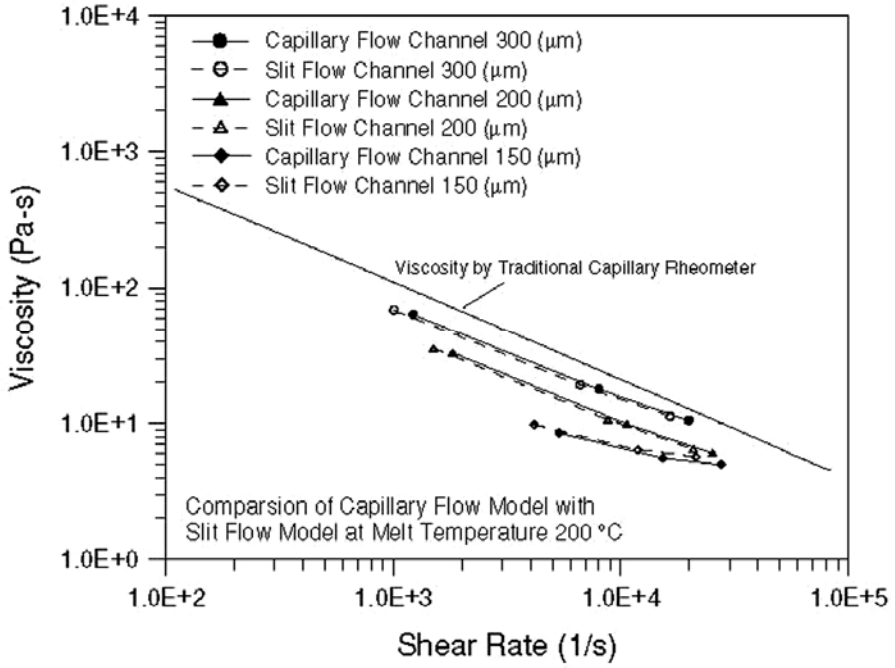

Figure 138 – Micro rheology data for three different channel sizes at melt and mould temperatures = 200 °C [Chien, 2005].

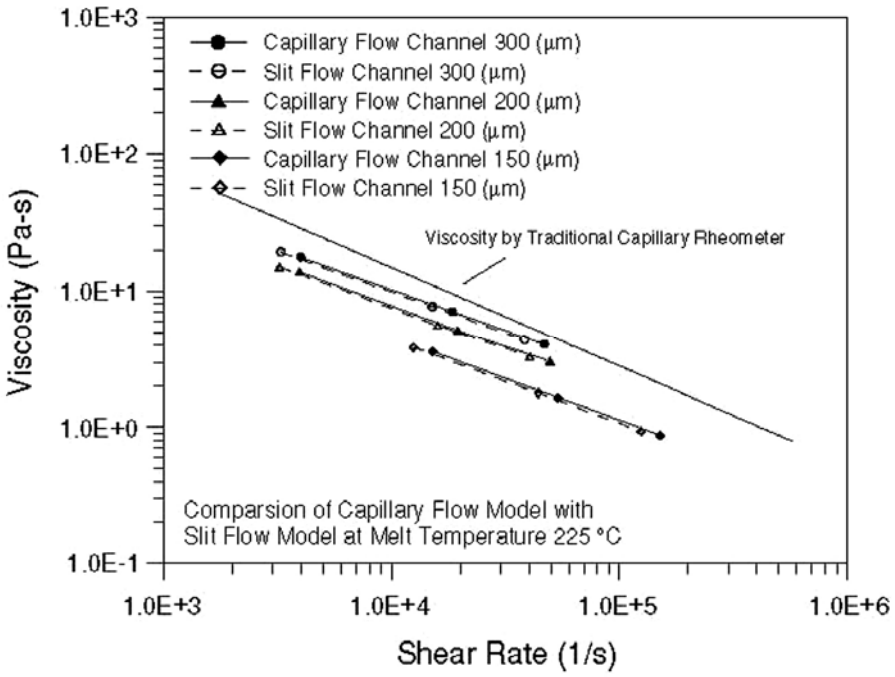

Figure 139 – Micro rheology data for three different channel sizes at melt and mould temperatures = 225 °C [Chien, 2005].

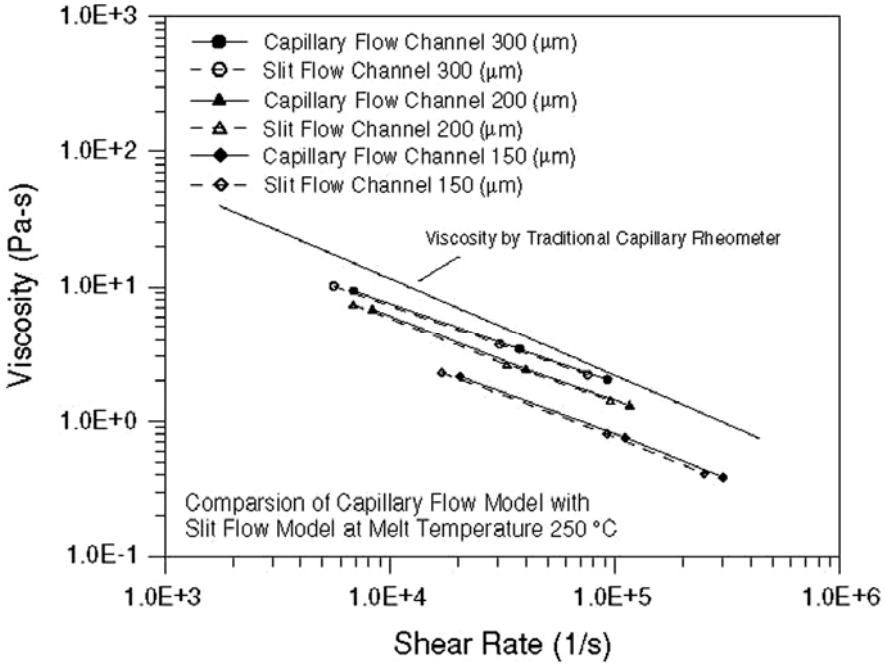

Figure 140 – Micro rheology data for three different channel sizes at melt and mould temperatures = 250 °C [Chien, 2005].

Finally, it was verified that the polystyrene 143 E from BASF was actually very similar to the polystyrene PG-22 from CHI MEI in terms of viscosity properties.

Data of the viscosity of the PG-22 were obtained with a traditional capillary rheometer for 200 °C, 225 °C and 250 °C. The Cross-WLF equation was plotted using the polystyrene 143 E coefficients that implemented in the Moldflow® database for the temperatures of 200 °C, 225 °C and 250 °C. The viscosity measurements of both materials (PG-22 and of 143 E) were executed with the same type of instrument (i.e. traditional capillary rheometer). As a consequence, it was possible to compare the two materials for the same temperatures. The rheological curves for CHI MEI PG-22 and for BASF 143 E at 200 °C, 225 °C and 250 °C were plotted in order to compare the two materials. From Figure 141, it can be observed that the polystyrene CHI MEI PG-22 had rheology curves very similar to the ones of BASF 143 E.

For this reason, it is assumed that the micro rheology data obtained for PG-22 could be employed for the study of the behaviour of 143 E in micro cavities. This reasonable assumption has to be made due to the absolute lack in literature of experimental data dealing with micro rheology of BASF 143 E.

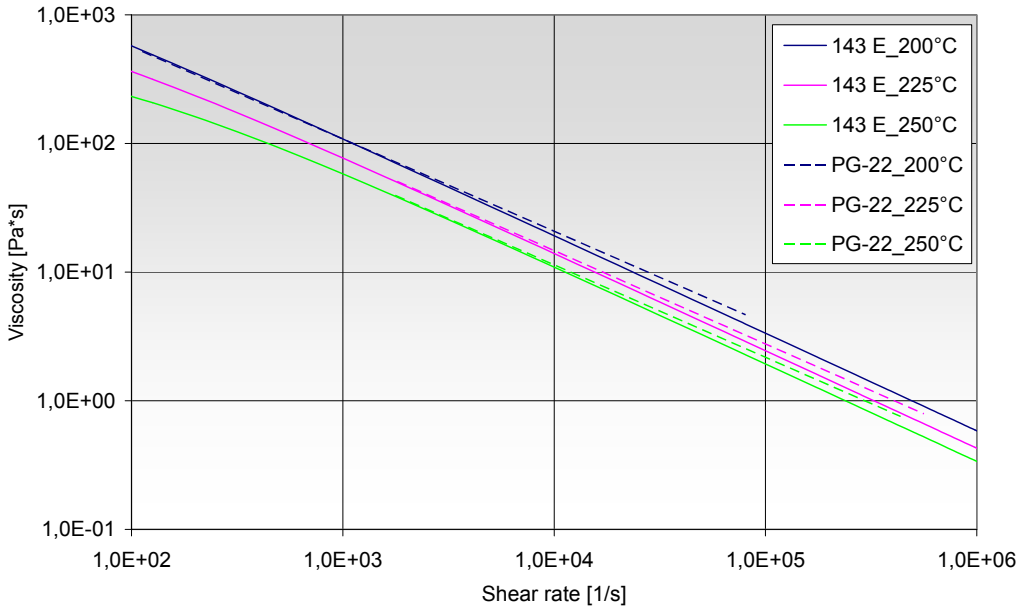

Figure 141 – Comparison between CHI MEI PG-22 and BASF 143 E.

6.6.3 Determination of Cross-WLF model coefficients for micro rheology

A preliminary consideration had to be made prior the determination of the Cross-WLF model coefficients from the viscosity curve. In fact, it has to be noted from Figure 138, Figure 139 and Figure 140 that the rheological data depend also on the channel size. In the WLF model this dependence is not possible to be considered. Therefore, a characteristic dimension that better represents the dimensions of the features of the studied cavity had to be decided. It was decided to consider an average characteristic dimension of 200 μm and to modify the conventional rheology of polystyrene 143 E (defined as *143 E macro*) in order to fit the rheological data of 143 E developed for the channel of 200 μm (defined as *143 E micro*).

Due to this decision and because of the assumption to consider the micro rheological data from [Chien, 2005], the new viscosity curves for polystyrene 143 E are shown in Figure 142). By using these new curves the seven Cross-WLF coefficients (see Figure 136) will be determined, as discussed here below.

6.6.3.1 n – flow index

The flow index represents the slope of the experimental rheological curves obtained for the 200 µm wide channel and for the three considered temperatures (200 °C, 225 °C, 250 °C) (see Figure 142). The interpolation of the three pairs of share rate and viscosity for the three temperatures (see Table 26) it is possible to obtain a value of the n coefficient of n=0,34.

6.6.3.2 A1

A1 represents the influence of the temperature on the viscosity. A first value of A1 was obtained by regression from the experimental data [Gava, 2007]. The obtained value was interactively modified to obtain a good fitting of the experimental data. A value of A1 = 20,7 was obtained.

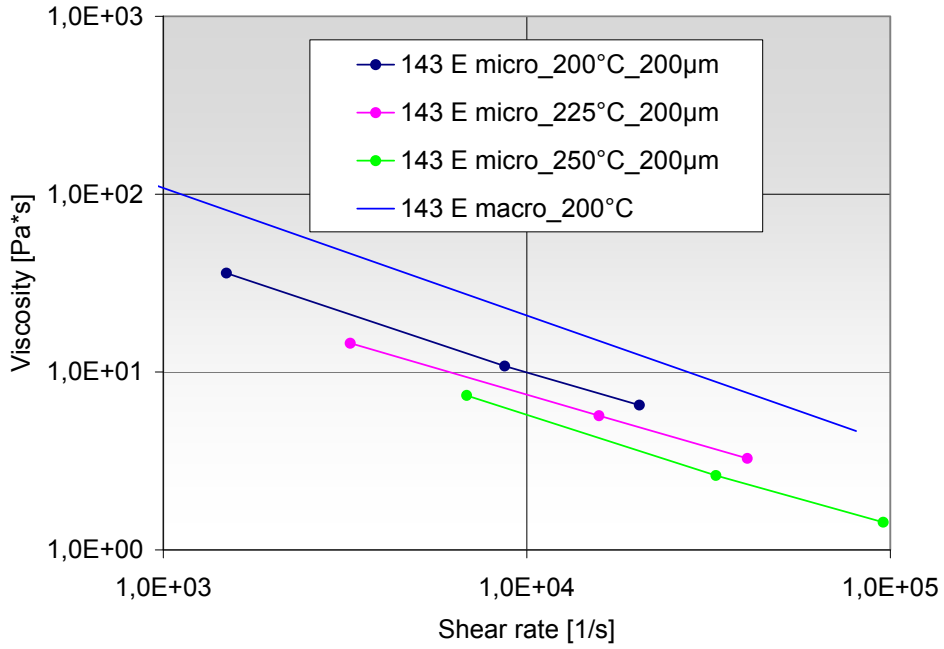

Figure 142 – Polystyrene 143 E micro rheology curves for a channel 200 µm wide at melt temperatures of 200 °C, 225 °C and 250 °C and 143 E macro rheology at 200 °C (i.e. obtained with conventional capillary rheometer).

200 °C		225 °C		250 °C	
Share Rate [1/s]	Viscosity [Pa·s]	Share Rate [1/s]	Viscosity [Pa·s]	Share Rate [1/s]	Viscosity [Pa·s]
1491	35,9	3270,7	14,5	6832	7,3
8696	10,8	15803	5,7	33135	2,6
20399	6,5	40428,7	3,3	95598	1,4

Table 26 – Experimental data for polystyrene 143 E micro rheology: channel 200 µm wide and melt temperatures of 200 °C, 225 °C, and 250 °C.

6.6.3.3 D1

At zero shear rate wall slip does not occur because of the absence of flow rate. This allows assuming that the viscosity at zero shear rate for the micro and macro rheology is the same. In the WLF equation the viscosity at zero shear rate is expressed by η_0.

- Viscosity at zero shear rate.
  - $\eta_0 = D1 \cdot e^{\frac{-A_1(T-T^*)}{A_2+(T-T^*)}}$

In conclusion it is assumed the following condition:

- Constance of viscosity at zero shear rate for 143 E macro and micro rheology.
  - $\eta_{0,macro} = \eta_{0,micro}$

The equation of viscosity at zero shear rate is solved using the following conditions:

- Intermediate melt temperature between the considered interval from 200 °C to 250 °C
  - T = 225 °C = 498,15 K
- Viscosity at zero shear rate of polystyrene BASF 143 E at 225 °C
  - η_0 = 1683,8 Pa·s
- Pressure dependent temperature without considering the viscosity pressure dependency effect (i.e. D3=0)
  - T* = D2 + D3 · P = 373,15 K

- Pressure dependent fitting coefficient without considering the viscosity pressure dependency effect (i.e. D3=0)
  - A2 = A2~ + D3 · P = 51,6 K
- A1 = 20,7 (see previous section)

The result is a D1 coefficient of 3,88E+09 Pa·s.

6.6.3.4 D3

In this investigation the effect of pressure in the viscosity was neglected. For this condition the coefficient D3 must be equal to zero.

- $$T^* = D_2 + D_3 * P$$
  $$A_2 = A_2 \sim + D_3 * P$$
- D3 = 0

6.6.3.5 D2

In this investigation the effect of pressure in the viscosity was neglected, therefore the reference temperature T* is not affected by the term D3 · P.

- T* = D2 = 373,15 K

6.6.3.6 A2~

A2~ is a material constant used to fit the experimental rheological data to the Cross-WLF model.

- A2~ = 51.6 K for polystyrene

6.6.3.7 τ*

τ* is the shear stress value at which the viscosity curve changes from Newtonian to non-Newtonian behaviour. It was calculated by solving the Cross-WLF equation using the requested constant values (n and η_0) as described in the previous sections. The considered melt temperature was of 225 °C.

- Cross-WLF equation
  - $$\eta = \frac{\eta_0}{1 + \left(\frac{\eta_0 \dot{\gamma}}{Tau^*} \right)^{1-n}}$$

Three pairs of values shear rate and viscosity were considered and related τ^* values were calculated (see Table 27). Finally, an average value of τ^* was calculated equal to 4759,8 Pa.

225 °C		
Shear rate [1/s]	Viscosity [Pa·s]	Shear stress [Pa]
3270,7	14,5	4156,5
15803	5,7	4810,7
40428,7	3,3	5312,1

Table 27 – Values of τ^* calculated for the three pairs of shear rate and viscosity values.

6.6.4 Implementation of the micro rheology in the simulation software

After the analysis described in the previous section, the new micro rheology coefficients to be implemented in the simulation software were determined (see Table 28). The new viscosity curves for polystyrene 143 E (micro rheology) were plotted with the PG 22 curves to verify the correctness of the fitting (see Figure 143).

D1	D2	D3	A1	A2~	n	τ^*
[Pa·s]	[K]	[K/Pa]	-	[K]	-	Pa
3,89E+09	373,15	0	20,7	51,6	0,34	4,76E+03

Table 28 – Micro rheology Cross-WLF coefficient to be implemented in the simulation software.

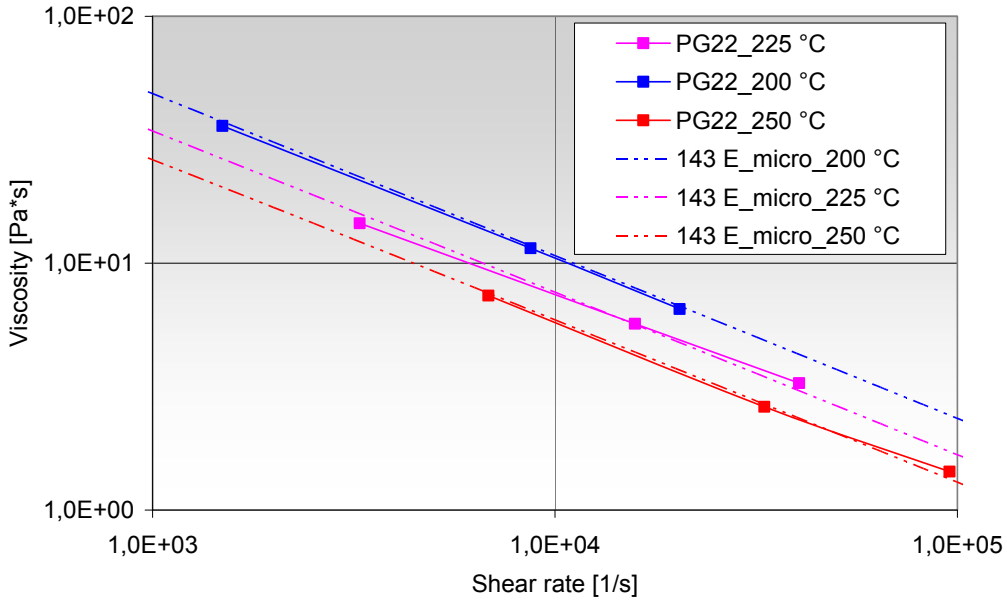

Figure 143 – Fitting results for 143 E micro rheology: channel 200µm wide, melt temperatures of 200 °C, 225 °C and 250 °C.

6.6.5 Simulation results with micro rheology model

The new set of Cross-WLF coefficients suitable for micro scale polymer flow were used to run simulations following the same implementation scheme as previously described in section 6.5.1. Both the experimental cases 01 and 08 (see Table 19) were simulated with the newly developed micro rheology. The flow marker method was used to trace the final simulated position of the flow front and was compared with the findings as in section 6.5.1 and the experimental results.

The implementation of rheology suitable for micro scale polymer flow produces changes on the simulation of flow pattern for both processing conditions 01 and 08 (see Figure 144 and Figure 145). The shifts of the weld lines are dominant when compared with the measuring uncertainty. The fact that the simulated meeting point is closer to the experimental one means that improvements are obtained in the prediction of the filling of the cavity. Therefore micro rheology databases are needed in order to perform more accurate simulations with existing software packages.

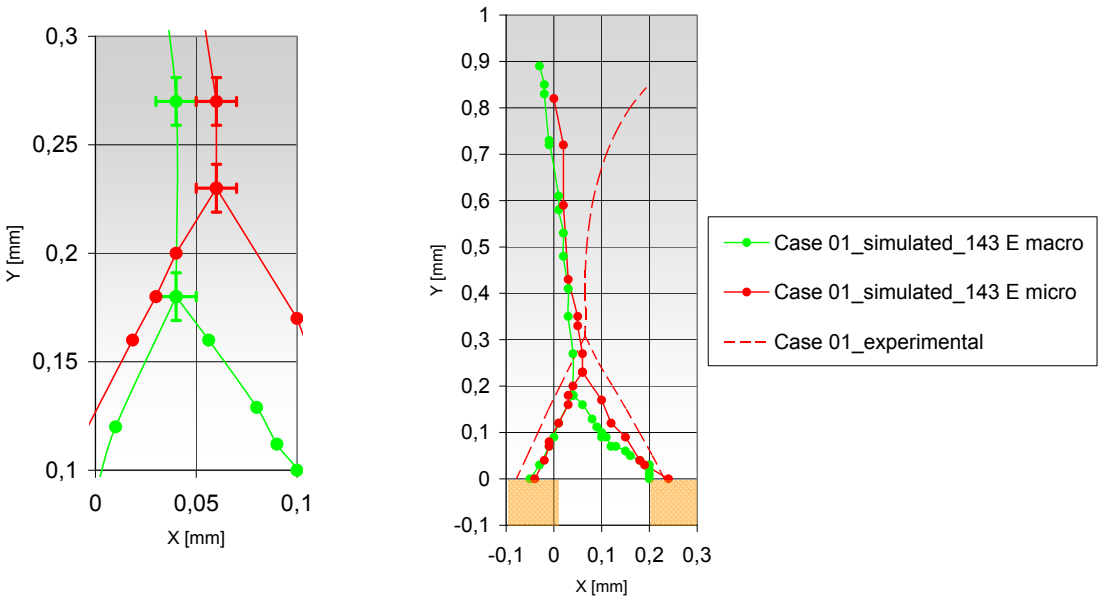

Figure 144 – Case 01: effect of the micro rheology model on the position of weld lines 2.

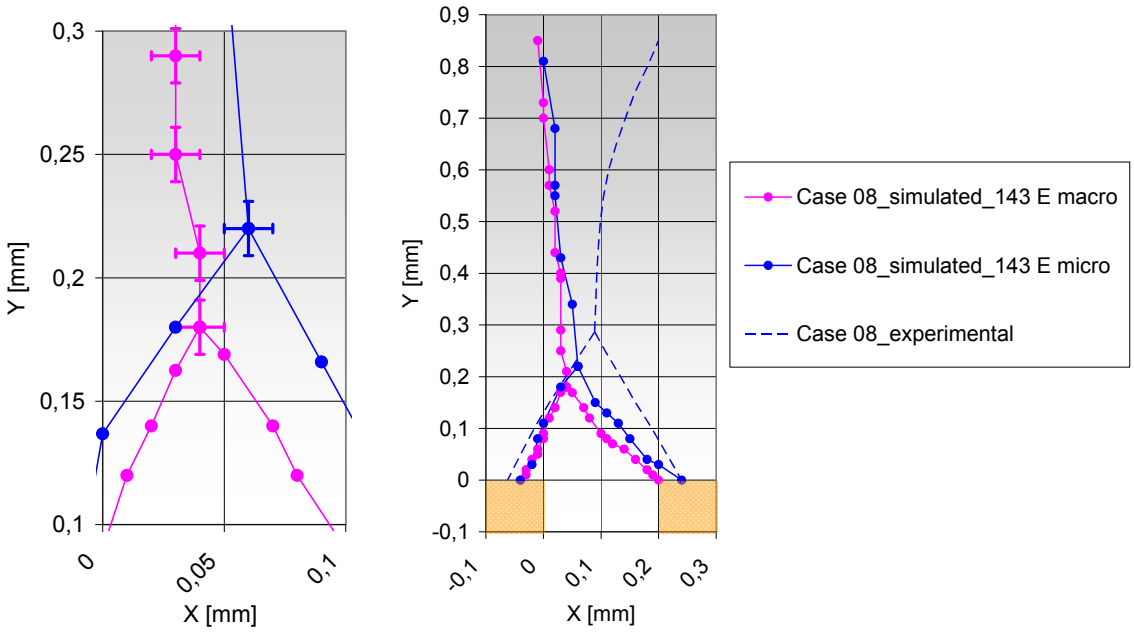

Figure 145 – Case 08: effect of the micro rheology model on the position of weld lines 2.

The weld line position on the micro feature 150 µm was also measured and compared with simulated results obtained with conventional rheology (i.e. macro rheology) and experimental results (see Figure 146 and Figure 147).

The main effect of using the micro rheology model can be seen on the positions of the weld lines which are moved upward in both cases: processing conditions of case 01 and 08. This brings the weld line obtained with the setup of case 01 closer to the experimental weld line obtained with the same setup. On the other hand, the weld line obtained with the setup of case 08 is moved away from the experimental one. The fact that the weld line obtained with the setup of case 08 moves even further from the experimental one evidences the existence of some problems in the simulation software model when dealing with filling of micro features. However, it has to be considered that the rheology was calculated for the channel of 200 µm while the formation of the horizontal part of the weld line 3 occurs in a channel of 150 µm with the obvious lack of accuracy.

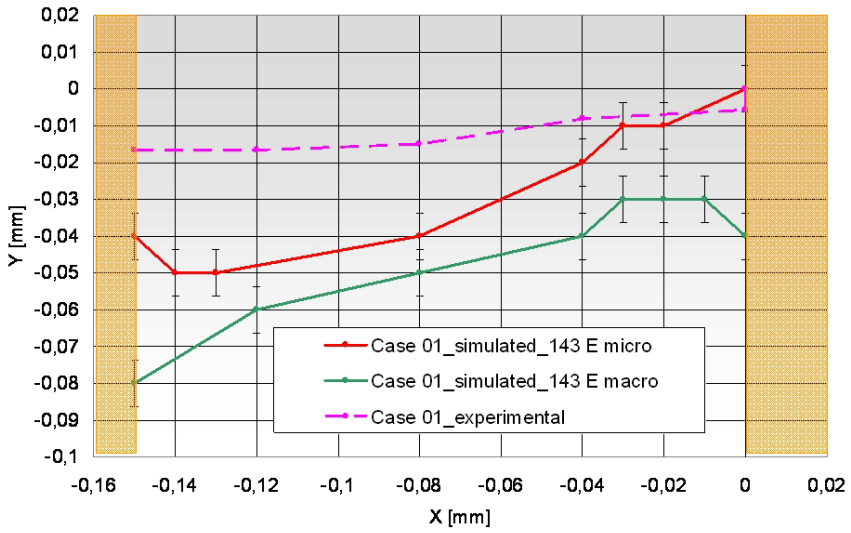

Figure 146 – Case 01: effect of the micro rheology model on the position of weld lines in the 150 µm wide micro feature.

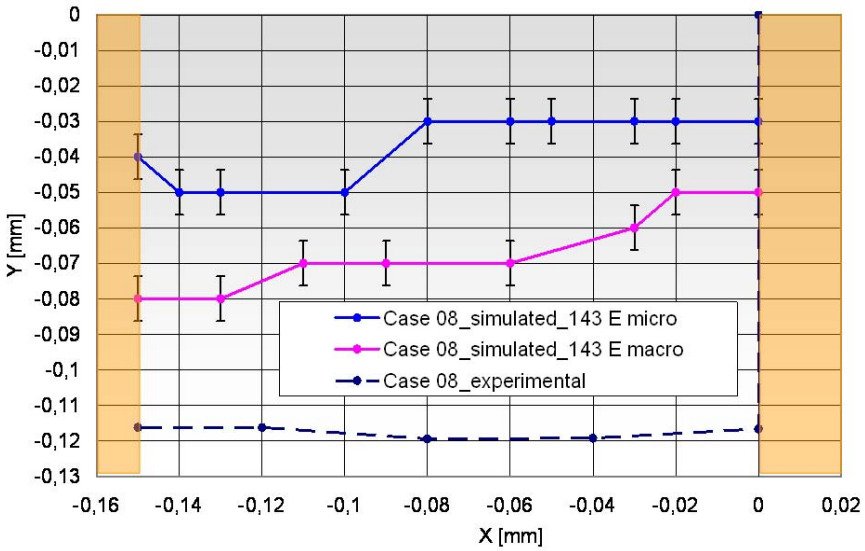

Figure 147 – Case 08: effect of the micro rheology model on the position of weld lines in the 150 µm wide micro feature.

6.7 Conclusion

New advancements in the field of micro injection moulding three-dimensional simulations have been presented in this chapter.

The research focussed on different aspects of µIM: the implementation of the actual machine and process characteristics into the software, the optimization of the three-dimensional meshing of the part, the validation of the filling simulation of micro components and micro features, the formulation of a new material rheological database suitable for micro scale polymer processing.

It was concluded that for a more accurate estimation of the filling time, either the real injection speed or the real cavity injection pressure profile should be implemented into the software. The importance of meshing the complete system composed by sprue, runner, gate and micro part has been demonstrated. Element characteristic dimensions and modelling tolerances were also discussed.

Simulated and experimental flow markers were compared to evaluate the performance of the different simulation settings. Experimental short shots were produced and then simulated resulting on a true step-by-step filling simulation validation.

Finally, a new rheology suitable to describe the polymer melt behaviour during μIM was implemented into the simulation. Actual improvements in terms of accuracy of the prediction of the flow front position were achieved using the newly developed material model.

6.8 References

[Barnes, 2003] Barnes H.A., Hutton J.F., Walters K. (2003) An introduction to rheology, Vol.3, 3rd edition, Elsevier.

[Chien, 2005] Chien R.D., Jong W.R., Chen S.C. (2005) Study on the rheological behaviour of polymer melt flowing through micro-channels considering the wall-slip effect, Journal of Micromechanics and Microengineering, Vol.15, Issue 8, pp.1389-1396.

[Gava, 2007] Gava A., Tosello G., Lucchetta G., Hansen H.N., Salvador M. (2007) A new approach for the validation of filling simulations in micro injection moulding, Proceedings of the 9th International Conference on Numerical Methods in Industrial Forming Processes (NUMIFORM), Porto (Portugal), 17th-27th June 2007, pp.307-312.

[Image Metrology, 2005] Image Metrology A/S (2005) Scanning Probe Image Processor (SPIP™).

[Jaworski, 2003] Jaworski M.J., Yuan Z. (2003) Theoretical and experimental comparison of the four major types of mesh currently used in CAE injection molding simulation software, Society of Plastic Engineers (SPE) - Proceedings of the 61st Annual Technical Conference ANTEC, Nashville (TN, USA), Vol.1, pp.642-646.

[Kennedy, 1995] Kennedy P. (1995) Flow analysis of injection moulds, Hanser (Munich, Germany)

[Lee, 2006] Lee L.J., Yu L., Koelling K.W, Madou M.J. (2006) Theoretical Analysis of Microfeature Injection Molding,

Simulation with Commercial Codes - in Precision Injection Moulding, ed. Greener J. and Wimberger-Friedl R., Hanser (Munich, Germany), pp.215-222.

[Mehta, 2003] Mehta M.N., Barry M.F.C., Bibber T.D., Tully D. (2003) Validation of flow simulation for micromolded parts, Society of Plastic Engineers (SPE) - Proceedings of the 61st Annual Technical Conference ANTEC, Nashville (TN, USA), pp.3550-3554.

[Moldflow, 2004] Moldflow® (2004) v 4.1 Reference Manual.

[Shen, 2002] Shen J.K., Wu W.J. (2002) An analysis of the three-dimensional micro-injection moulding, International Communications in Heat and Mass Transfer, Vol.29, Issue 3, pp.423-431.

[Tosello, 2008(5)] G. Tosello, A. Schoth, H. N. Hansen (2008) Implementation strategies for the optimization of micro injection moulding simulations, 4th International Conference on Multi-Material Micro Manufacture (4M), Cardiff (United Kingdom), 9-11 September 2008 (in press).

[Yu, 2004] Yu L., Lee L.J., Koelling K.W. (2004) Flow and Heat Transfer Simulation of Thin-Wall Injection Molding with Microstructures, Polymer Engineering and Science, Vol.44, Issue 10, pp.1866-1876.

7 Micro insert moulding

New functionalities and smaller dimensions of micro products can be achieved by means of a higher degree of integration of both materials and components. Smart micro assembly techniques (such as on-the-machine assembly) together with hybrid structures (as metal inserts in polymer matrix) are suitable solutions to manufacture new micro products with several integrated functionalities, reduced number of components and assembly phases, as well as the possibility to be replicated in a high number of specimens. In particular, miniaturized devices with increased functionality can be obtained by means of incorporation of metal micro parts in a polymer matrix. They allow achieving both conductive circuits and mechanical functions in the same device, enabling design of MIDs (moulded interconnect devices) with enhanced characteristics.

Innovative manufacturing systems, as well as new design rules and testing methodologies, have to be established in order to be able to develop new and more integrated micro products.

During this project a method for testing the bonding between micro thickened metal inserts and the polymer matrix they were moulded in was investigated. A specific demonstrator has been manufactured by means of a hot embossing-like process, which allowed fast developing time and the possibility of batch process, and over-moulding, for increased productivity.

The bonding strength between the insert and the plastic part was tested by means of a tensile test. A variety of parameters was studied in order to investigate their influence on the bonding: different polymeric and metallic materials, insert thickness, metal surface roughness and texture topography, surface treatment and coating, i.e. metal insert designs to improve polymer/metal interlocking and tensile test speed.

7.1 Introduction to insert moulding

Integration of different materials and components in micro systems production is at the same time an opportunity and a challenge. On one hand, a higher degree of integration brings to smaller dimension, lower number of components, and increased functionality. On the other hand, the production of small and highly integrated devices is complex due to miniaturized dimensions and presents issues on storing, handling, positioning, and joining the micro parts. Alternative techniques to the conventional pick-and-place approach have to be applied.

Miniaturized devices with increased functionality can be achieved by means of integration of polymers and metals in the same components. Polymers are relatively cheap materials; they exist in an enormous variety, in a way they are suitable for virtually any kind of application, and allow good replication capabilities at micro scale. Metals provide additional functions and properties such as stiffness, elasticity, conductivity. Hybrid structures are characterized by properties of both materials, for example providing an insulating matrix with conductive and stiff features. Typical micro devices exploiting such combination of properties in order to achieve higher integration and functionality are micro mechanical actuators, micro regulators, hearing aid components, and integrated sensors for e.g. medical analysis, etc. Because of the extremely wide range of possible applications, it is clear the importance of being able to provide properties and characteristics to design micro products involving integrated metal parts in a polymer based product.

When medium batch or mass fabrication of polymer based products are required, replication processes such as hot embossing and micro injection moulding are suitable to be used. The former primarily is to be employed in laboratory and R&D applications, the latter mostly to produce final products in a larger scale. Depending on the chosen replication manufacturing process, special integrated assembly solutions can be applied:

- Smart assembly techniques as on-the-machine assembly: micro insert moulding and micro assembly injection moulding [Michaeli, 2003] [Michaeli, 2005].
- Parallel assembly techniques: multi-cavity micro injection moulding, hot embossing and pre-adjusted assembly polymer magazine [Ehrfeld, 2001].

- Use of a metal frame connecting all the metal inserts to be overmoulded, to be applied either to multi-cavity micro injection moulding or to a wafer-like approach with hot embossing.
- Automation system in order to feed inserts, pick and place the hybrid (polymer and e.g. metal inserts) moulded or hot embossed parts by handling directly the sprue or the metal frame and not the single micro parts.

7.2 Experimental

Over-moulding processes are characterized by the possibility to position a metal insert into a cavity before the polymer flows in. In this work two different processes have been implemented and investigated: hot embossing and injection moulding.

- Hot embossing for the production of a hybrid miniaturized demonstrator – This process allows fast developing time and it involves limited tooling costs as well as simple moulding equipment (e.g. a hot press), at expense of a low production rate. The hot embossing process is therefore indicated in a prototyping phase and in the production of small batches. Moreover, hot embossing permits quick set-up changes and fast material screening test [Heckele, 2003].
- Injection moulding with insert moulding tool – This process allows higher production speed capability than hot embossing and it is therefore more indicated in an implementation phase of serial production of medium/large batches. The tooling is on the other hand more complex and requires higher investment in terms of design and machining. Moulding equipment (injection moulding machine) is more complex and expensive. In case of mass production, metal inserts are automatically supplied to the cavity by a robot or as a leadframe on a reel [Meeuwsen, 1996].

7.2.1 Design and testing of the hybrid demonstrator

The hybrid polymer/metal part was designed in order to be tested on pull test machine and to be able to evaluate the bonding strength necessary to mutually separate the metal insert and the polymer matrix. The polymer matrix was

represented by a parallelepiped with cross section of 6x4 mm^2 and 6 mm of depth. The insert was position in the middle plane of the polymer part. It measured 16 mm of length and 2 mm of width. The considered thicknesses of the metal inserts were in the micro dimensional range, from 20 µm to 400 µm.

The testing of the hybrid moulded parts was carried by means of a pull test machine. A holding device has been developed in order to support the polymer matrix during the pull test without inducing pressure tensions, while a clamping device was applied to the metal insert (see Figure 148).

The considered output from the pull test was the highest load recorded during the tensile test. This load was defined as the bonding strength of the hybrid moulded demonstrator.

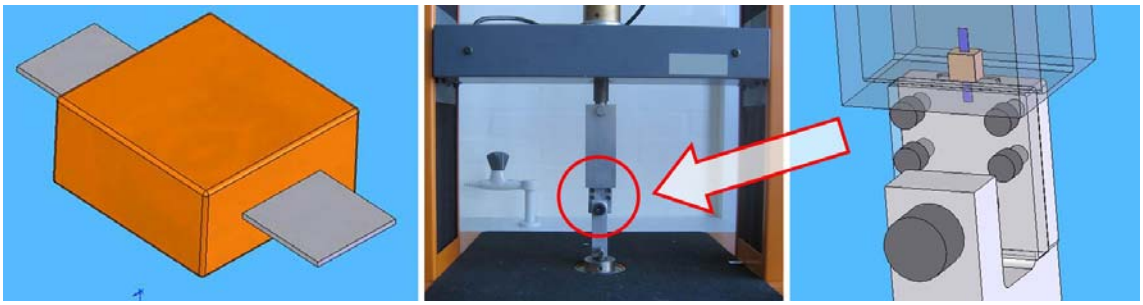

Figure 148 – Schematic view of the hybrid (metal and polymer) demonstrator (left), pull test machine (middle), device for holding the polymer matrix and to clamp the metal insert (right) [Tosello, 2006(1)].

7.2.2 Manufacturing of the hybrid demonstrator by hot embossing

The overmoulding was obtained by means of a steel tool composed by two plates (total thickness 4 mm) and a hydraulic hot press to perform the embossing process (see Figure 149). The cavity of 6x6 mm^2 was manufactured by wire EDM. The housing pocket for the metal insert was then fabricated using sinking EDM on the internal surface of the lower plate (which represents the parting surface of the moulding).

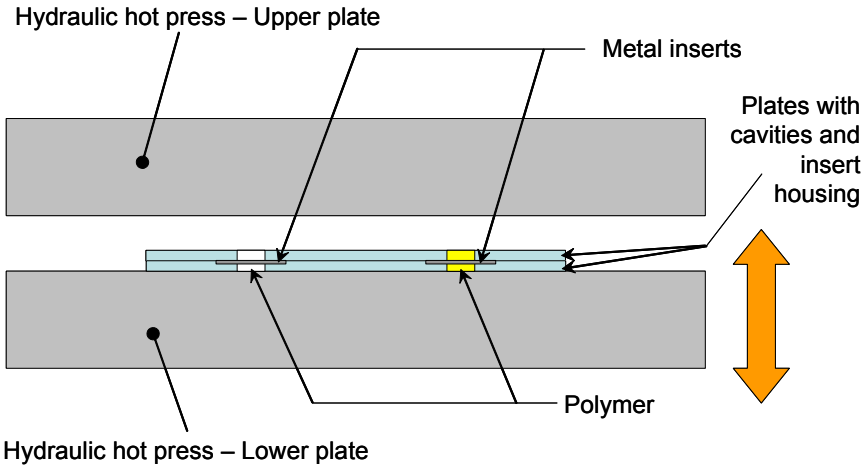

Figure 149 – Hydraulic press and hot embossing set-up.

Polystyrene (PS) and polyoxymethylene (POM) were selected as polymers for the hybrid structure to be produced. The transparency of polystyrene allows to check the inside structure integrity and insert placement. Hot embossing temperature was chosen at 250 °C. POM process temperature was chosen at 180 °C. Both materials are particularly suitable for micro moulding applications due to their very easy flowing. Metal inserts made of rolled steel were used for the experimental batch (see Figure 150). Steel inserts covered by a thin layer of palladium were also used. This particular material combination is used in the production of miniaturized electro-mechanical systems (e.g. micro switches) because it presents both stiffness and high electrical conductivity. Asymmetry of shrinkage with respect to the insert might cause bending. However, due to the symmetry of the demonstrator and a reduced shrinkage because of the smooth temperature cycle, the metal inserts did not show any deformation (e.g. bending) or displacement from the position given by the housing in the cavity.

In a single plate, 6 insert housings with different depths were produced in order to obtain demonstrator with various insert configurations. In particular, it was possible to produce demonstrator with the following insert thicknesses: 20 µm, 40 µm, 80 µm, 100 µm, 200 µm, 400 µm (see Figure 151).

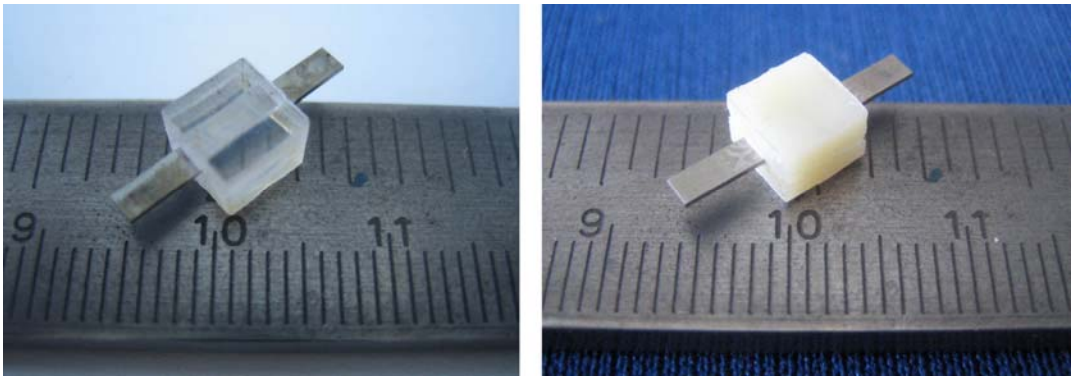

Figure 150 – Over moulded hybrid demonstrator composed of micro thickened steel insert in a polymer matrix (steel, 400 µm / PS on the left; steel and Pd, 80 µm / POM on the right).

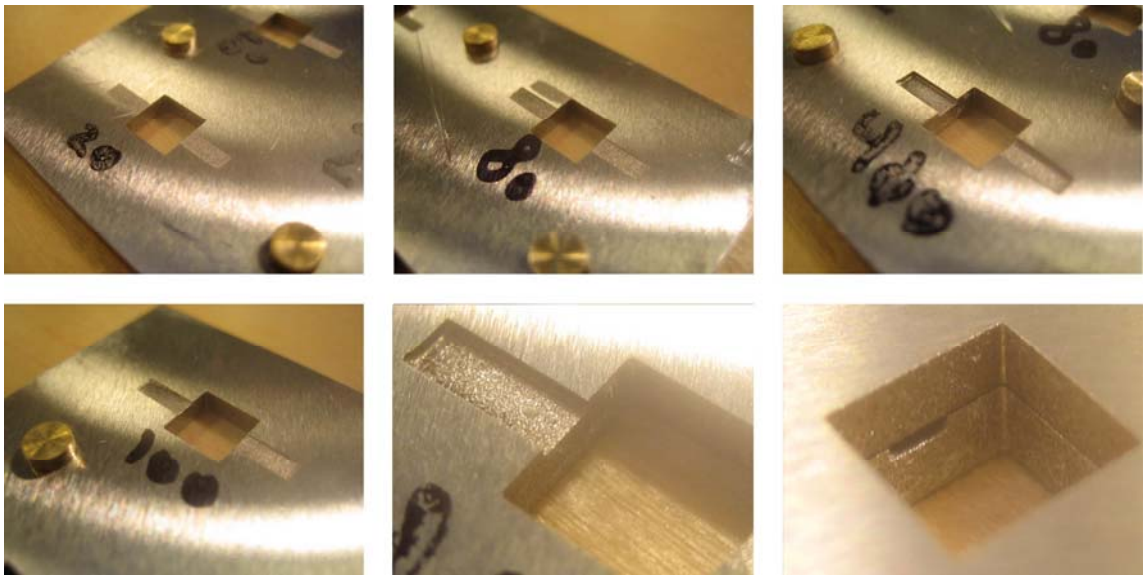

Figure 151 – Hot embossing tool: inserts with different thicknesses can be placed in the respective housings. The assembly of the two plates is shown for the 400 µm insert configuration (down to the right) [Tosello, 2006(2)].

7.2.3 Manufacturing of the hybrid demonstrator by insert moulding

In order to increase the production rate and to assess the hybrid demonstrator bonding strength in case of process conditions closer to a mass-fabrication scenario, insert moulding was implemented and investigated.

The geometry and the dimensions of the moulded part and of the insert were kept as in the hot embossing process. The used injection moulding tool was a two-plate/cold runner tool and the cavity was manufactured using sinking EDM.
In order to investigate metal inserts with different thicknesses, a special device placed inside the mould was designed. It consisted of a sliding feature provided with a spring which keeps the fixture for the metal insert in contact with the metal insert once the mould is closed. In this way an adaptive system was created and metal inserts with different thicknesses could be inserted in their housing. The spring compression force supplies the insert with the needed force to be firmly positioned when the polymer flow reaches the cavity. Metal inserts with any thickness up to 1000 µm can be moulded with such device. Experiments focused on the following thicknesses: 20 µm, 40 µm, 80 µm, 100 µm, 200 µm, 400 µm.

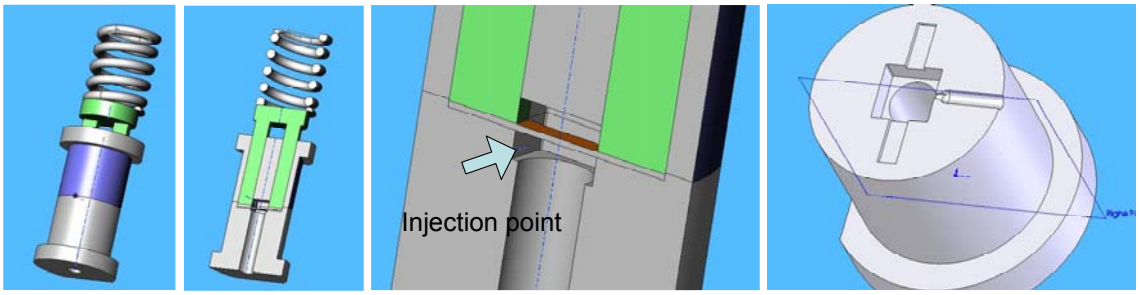

Figure 152 – Movable adaptive device for the insert moulding of hybrid demonstrators with metal inserts having different thicknesses. On the right a close-up of half cavity with gate location on the parting line and metal insert housing are shown [Tosello, 2006(2)].

Polystyrene (PS) and polyamide filled with 50% of glass fibre (PA+GF50%) were used for the insert moulding process. The former was chosen for the easy flowing properties and its transparency. By being the same material as the one used during hot embossing, a comparison between the two processes was carried out. The latter is a glass fibre reinforced injection moulding polymer for moulded parts which combines high rigidity as well as electrical insulating function and high chemical resistance. It is extensively used for micro moulded parts containing conductive micro metal features (e.g. miniaturized hearing aid components). The employed process parameter settings for both PS and PA+GF50% are presented in the Table 29.

Injection moulding was carried with an Arburg 220-15-30 S machine, provided with a plastification screw of 15 mm of diameter.

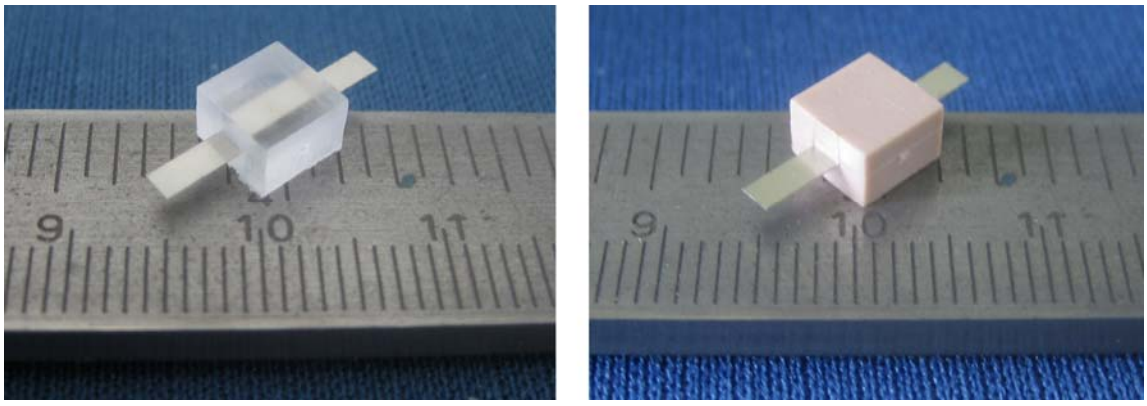

Figure 153 – Insert moulded hybrid demonstrator composed of micro thickened metal insert in a polymer matrix (PS on the left, PA66+GF50% on the right).

Process parameter	Unit	PS	PA66+GF50%
Melt temperature	°C	210	285
Mould temperature	°C	55	90
Flow rate	cm^3/s	15.4	10.0
Holding pressure	bar	1200	300

Table 29 – Injection moulding process parameters.

7.3 Metal inserts selection, surface treatment, and characterisation

During the hot embossing process the polymer flows the very short way from its solid state into the micro structures. High melt and cavity temperatures allow a high degree of replication of the micro surface texture of the insert. Therefore the filling of even the deepest grooves of the surface can be achieved. This brings the insert to be completely surrounded by the polymer, down to the micro dimensional level of the surface texture. Mechanical interlocking at the polymer/metal interface can therefore be obtained. Moreover, higher bonding strength with the polymer matrix can be achieved when such interlocking between the polymer and the metal is increased. This can be obtained by means of a modification of the metal insert surface, e.g. by

increasing its roughness. Hence, the influence of the surface texture of the metal inserts on the mechanical bonding strength of the hybrid structures was investigated.
On the other hand, during injection moulding the surface micro topography replication is more difficult to be completely obtained due to the decreased polymer mobility (due to lower mould temperature, existence of frozen layer at the mould/melt interface, very short injection time). Therefore the polymer will be partially in contact with the surface topography. Typically, the peaks of the mould surface will be replicated and completely surrounded by the polymer. Valleys of the mould surface will be on the other hand more difficult to be filled by the polymer, though in different ways depending on the employed moulding process.
Three materials were selected for the metal inserts: steel, steel covered by a palladium layer as well as German silver. The steel provides stiffness to the metal micro feature and is typically employed in micro mechanical devices. When conductivity is required, a layer of palladium (5 μm) is applied to the steel surface on both sides. German silver is used because of its hardness, toughness, and resistance to corrosion. Typical application for these materials is on the manufacturing of micro electro-mechanical components (e.g. for hearing aid systems and mobile phones) such as: volume controls, micro switches, push buttons, micro plug connectors, micro regulator, etc.
A superficial treatment consisting in a glass blast jet was then applied to the metal insert in order to obtain higher roughness of the metal insert's surface. Glass powder with granules from 40 μm up to 70 μm was used.

Material / Insert thickness: Steel / 40 µm	
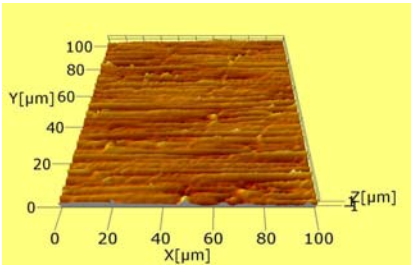	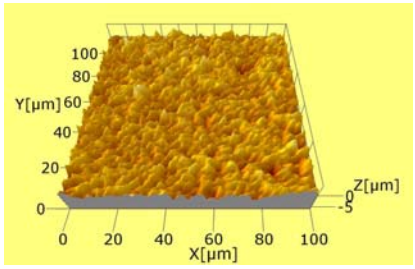
Ra = 0.35 µm	Ra = 0.85 µm
Sa = 0.33 µm	Sa = 0.84 µm
Sdr = 16.6 %	Sdr = 84.7 %
Material / Insert thickness: Steel / 80 µm	
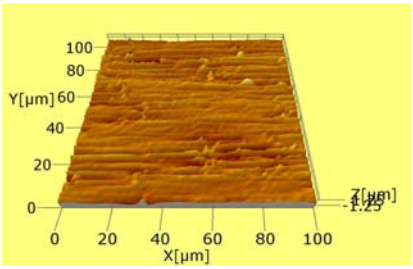	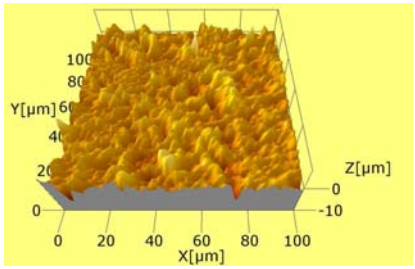
Ra = 0.30 µm	Ra = 0.98 µm
Sa = 0.29 µm	Sa = 1.00 µm
Sdr = 14.2 %	Sdr = 74.5 %
Material / Insert thickness: Steel with Pd layer / 80 µm	
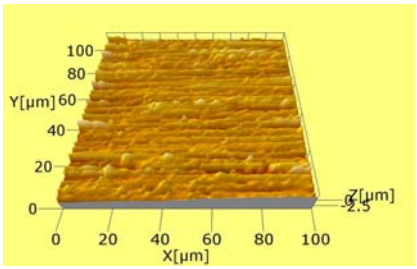	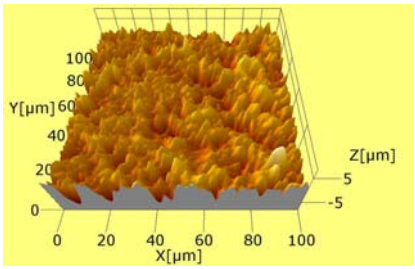
Ra = 0.44 µm	Ra = 1.37 µm
Sa = 0.46 µm	Sa = 1.35 µm
Sdr = 29.2 %	Sdr = 119 %

Table 30 – Surface topography analysis of three metal insert configurations investigated. Measured area is 100x100 µm^2.

The manufactured demonstrator reproduces the case of an actuator in which the two components do not have to change their mutual position. In this case, a surface parameter suitable to be used for surface characterization is the average surface roughness (Ra) [De Chiffre, 2000]. Moreover, though three-dimensional surface parameters are not yet defined by standardization bodies, 3D surface average roughness (Sa) can be obtained by means of calculations based on two-dimensional standards extended to three dimensions [Barbato, 1995]. Hybrid three-dimensional parameter such as the surface area ratio is suitable to be employed as well. The surface area ratio (Sdr) expresses the ratio between the area of the actual measured surface (taking the Z height into account) and the projection of the actual surface on the X,Y plane. For a totally flat surface, the real surface area and the projected area of the X,Y plane are the same and Sdr = 0 %.

Investigation of the surface texture of the micro inserts was carried out with a three-dimensional laser focus detection instrument. Three-dimensional roughness parameters as well as surface mapping of the metal inserts were determined [Image Metrology, 2005]. Results regarding smooth and treated surfaces of 80 μm insert thick made of steel only and covered by a palladium layer, and 100 μm thick insert made of German silver are presented (see Table 30). The same sand blast treatment was applied for all the insert configurations.

7.4 Bonding strength test results

Hybrid structures obtained by hot embossing and injection moulding have been tested using the pull test set-up previously described. A number of factors were investigated in a comparative study:

- Polymer materials: POM, PS, PA66+GF50%.
- Metal insert materials: steel, steel covered with a Pd layer, German silver.
- Metal insert thickness: 20 μm, 40 μm, 80 μm, 100 μm, 200 μm, 400 μm.
- Metal insert thickness: treated and not treated.
- Manufacturing process: hot embossing (HE) and injection moulding (IM).
- Pull test speed: 0.1 mm/min, 1.0 mm/min, 10 mm/min.

Variation of the pull test results was calculated. An average coefficient of variation (COV) of 13% for each experimental configuration was found.

7.4.1 Influence of the insert material and surface treatment

Polystyrene (PS) and polyoxymethylene (POM) hybrid parts were produced by the hot embossing (HE) process, polystyrene (PS) and polyamide (PA66+GF50%) components were insert moulded (IM). In a first experiment steel and steel with a layer of palladium were used. Pull test speed was set to 1 mm/min. The comparison showed bonding strength increasing for higher roughness of the metal insert surface. A lower bonding strength of the insert moulded component compared to the hot embossed one was observed.

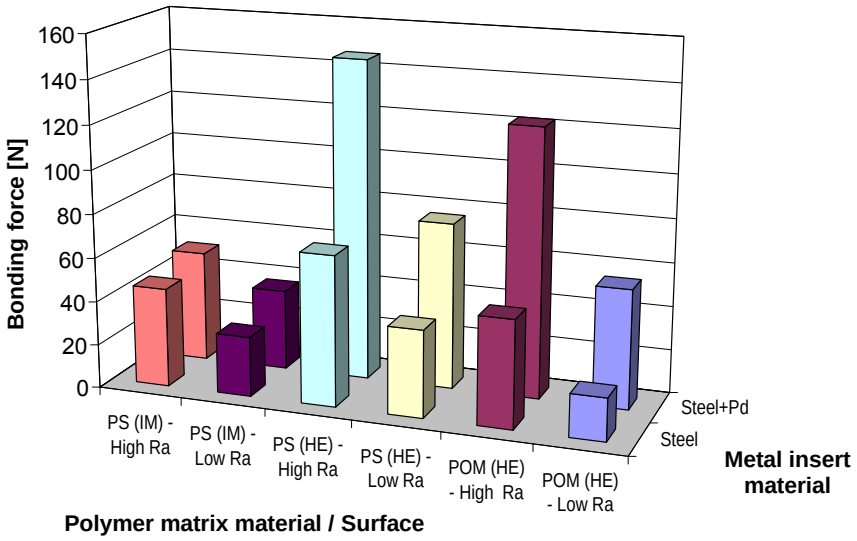

Figure 154 – Bonding strength of hot embossed and injection moulded hybrid demonstrator. Effects of the metal insert surface roughness, of the manufacturing process, and of the different polymer material are shown. Metal insert thickness was 80 µm.

Inserts made of German silver and with thickness of 100 µm were then employed with PS and PA66+GF50% to insert mould hybrid components. An increased bonding strength was found as effect of a higher roughness of the metal inserts. Pull test speed was set to 10 mm/min.

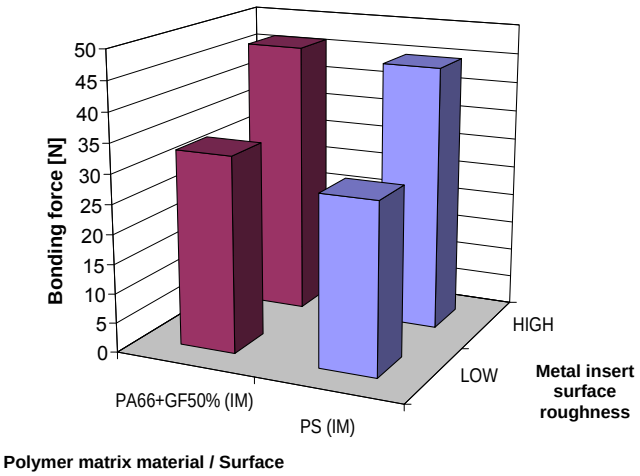

Figure 155 – Insert roughness effect on the bonding strength of insert moulded hybrid demonstrators. Metal: German silver, thickness: 100 µm.

7.4.2 Comparison of different polymer matrix and metal insert materials

Polystyrene (PS) and polyamide (PA66+GF50%) were alternatively insert moulded with inserts (thickness of 100 µm) of different metallic materials: German silver, steel, steel covered with palladium layer. The surface was smooth in all three cases. The bonding strength was found to be independent from the polymer materials. Pull test speed was of 10 mm/min in all cases.

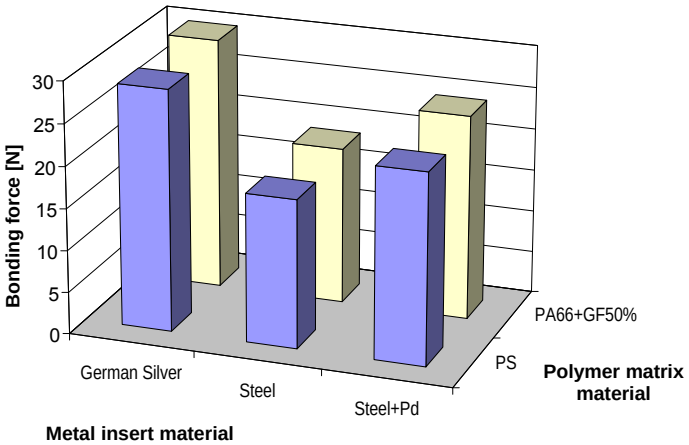

Figure 156 – Comparative study of bonding strength of hybrid demonstrator in different polymeric (PS and PA66+GF50%) and metallic (German silver, steel, steel and palladium) material configuration.

7.4.3 Influence of metal insert thickness

Different inserts made of steel with smooth surface were also tested to evaluate the influence of the insert thickness in a larger range. Hot embossed hybrid demonstrators were manufactured using PS and POM and steel insert with thickness of 100 µm and 400 µm. Insert moulded multi component parts were made of polyamide instead. A variety of steel smooth inserts was then used: 20 µm, 40 µm, 100 µm, 200 µm, 400 µm. A common trend was found: the bonding strength increases with increasing thickness. In particular, a threshold of 100 µm was found for the hybrid parts produced by injection moulding: for thinner inserts the bonding strength is constant and at low level, while for inserts thicker than 100 µm the bonding force increases.

(A)

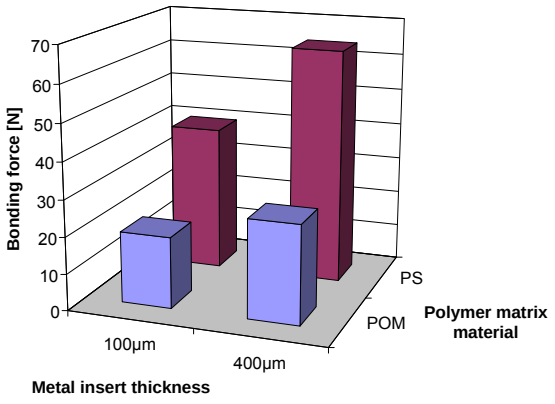

(B)

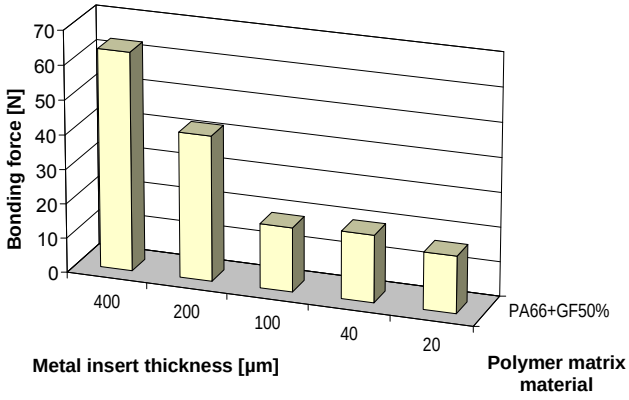

Figure 157 – Insert thickness influence on bonding strength of hybrid demonstrator manufactured by (A) hot embossing (steel + PS, steel + POM, pull test speed = 1 mm/min) and (B) insert moulding (steel + PA66+GF, pull test speed = 10 mm/min).

7.4.4 Influence of pull test speed

A configuration composed by a polymer matrix made of PS and a metal insert 100 µm thick with no treatment (i.e. smooth surface) was chosen and the pull test speed was varied. Three levels were defined: 0.1 mm/min, 1.0 mm/min, and 10 mm/min. Two effects can be observed. On one hand the bonding strength increases with higher pull speed. On the other hand a decrease of one order of magnitude from the standard speed has more effect on the measured bonding strength than when the speed is increased 10 times. This confirms findings of previous research on polymeric materials suitable for micro injection moulding [Haberstroh, 2002].

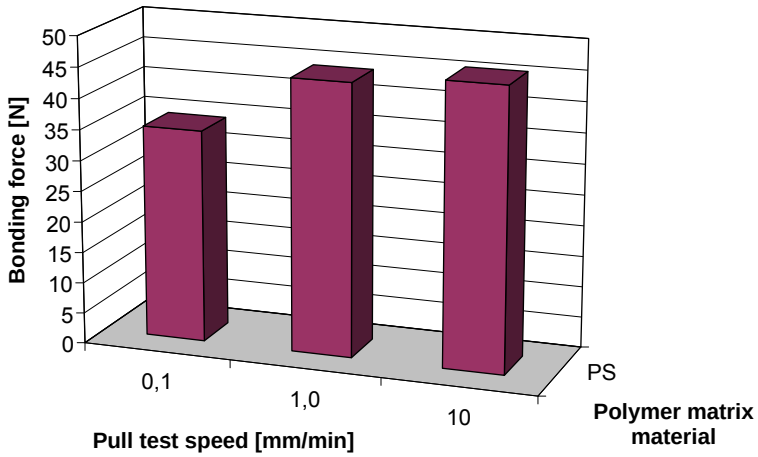

Figure 158 – Influence of pull test speed on the bonding strength of hybrid demonstrator produced by hot embossing.

7.5 Polymer matrix and metal insert interface investigation

Bonding strength of the hybrid components and surface roughness as well as surface area ratio are proportionally related. Because of the almost zero adhesion between polymers and metal, bonding is provided by mechanical interlocking of the metal into the polymer matrix at micro range level. Scanning electron microscopy (SEM) was employed to characterize such interlocking, i.e. penetration of the polymer in the valleys of the metal surface texture.

Due to the favourable hot embossing process characteristics and the easy flowing of the material complete penetration is achieved for both POM and PS. Moreover, by

means of the surface treatment, the depth and the quantity of polymer flowing into the surface texture has been increased. On the other hand, when the injection moulding process is applied, a fine replication of the metal insert's micro surface topography is difficult to be achieved. This results in a lower bonding strength of the hybrid demonstrator (as shown in Figure 154).

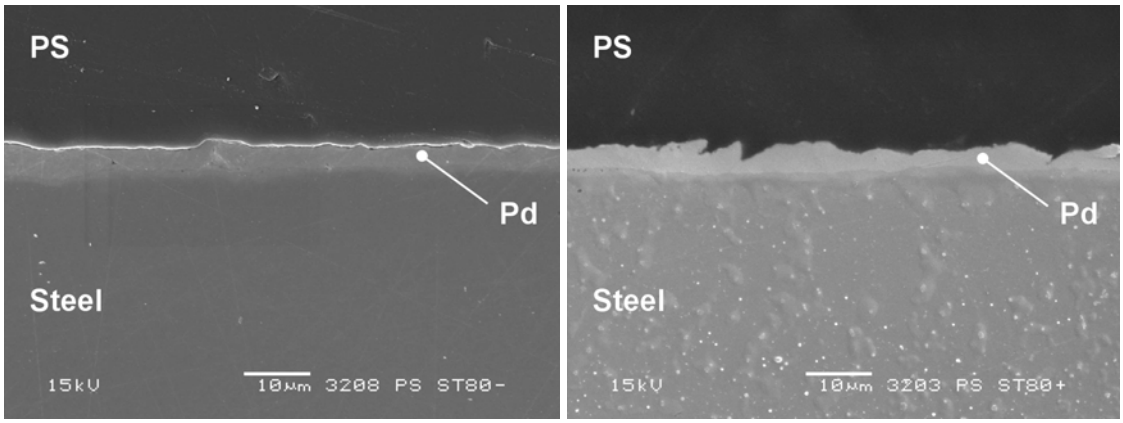

Figure 159 – Full penetration of hot embossed PS in the metal insert surface texture: not treated (left) and treated (right). Insert: steel + Pd, 80 µm thick.

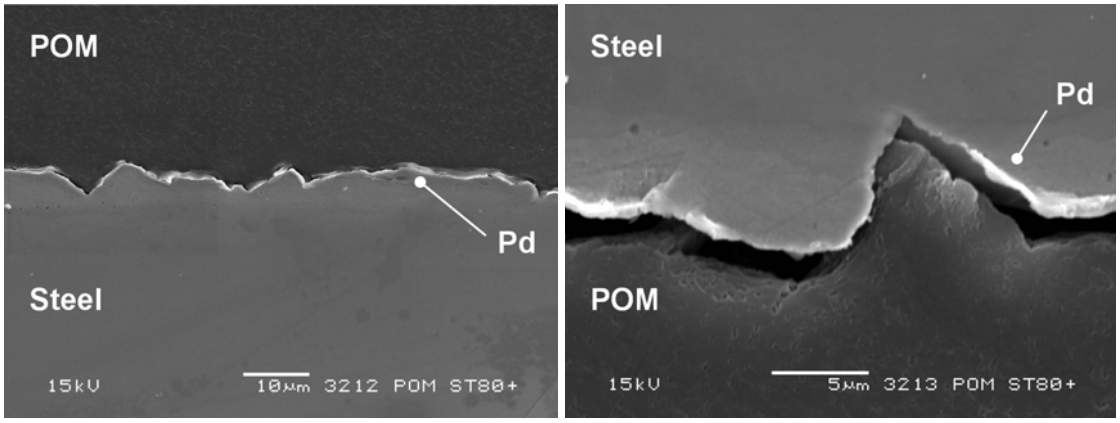

Figure 160 – Full penetration of hot embossed PS in the metal insert surface texture: not treated (left) and treated (right). Insert: steel + Pd, 80 µm thick. Ejection forces show to have pulled apart the polymer from the metal insert creating a gap of 1 µm. Mechanical interlocking is still possible because of mutual embedding.

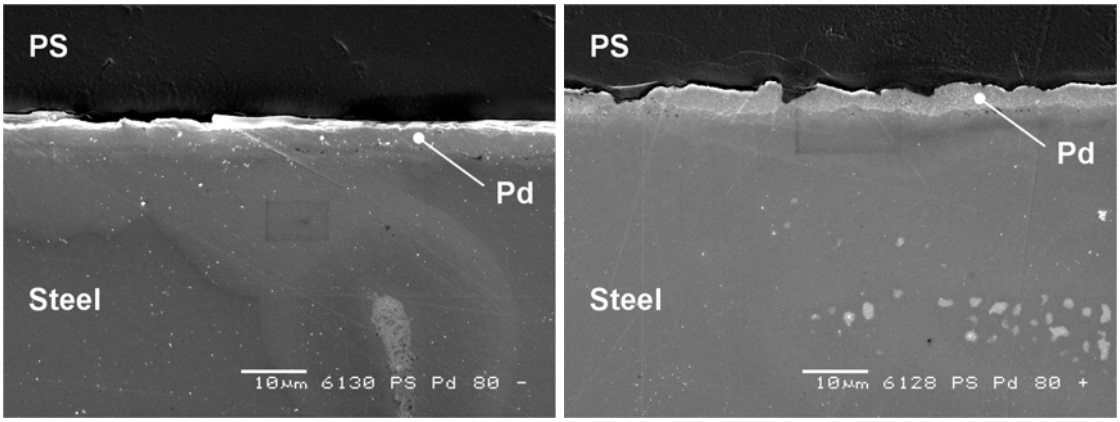

Figure 161 – Partial penetration of injection moulded PS in the metal insert surface texture: not treated (left) and treated (right). Insert: steel + Pd, 80 µm thick.

Cross section of hybrid demonstrator made of polyamide permits to observe the distribution of the glass fibres around the metal insert. The density of glass fibres slightly decreases in the area close to the insert. The polymer flow is hampered by the presence of the glass fibres; therefore low replication of the insert metal surface is obtained. Furthermore is possible to observe the insert is not bended and/or damaged after the injection moulding.

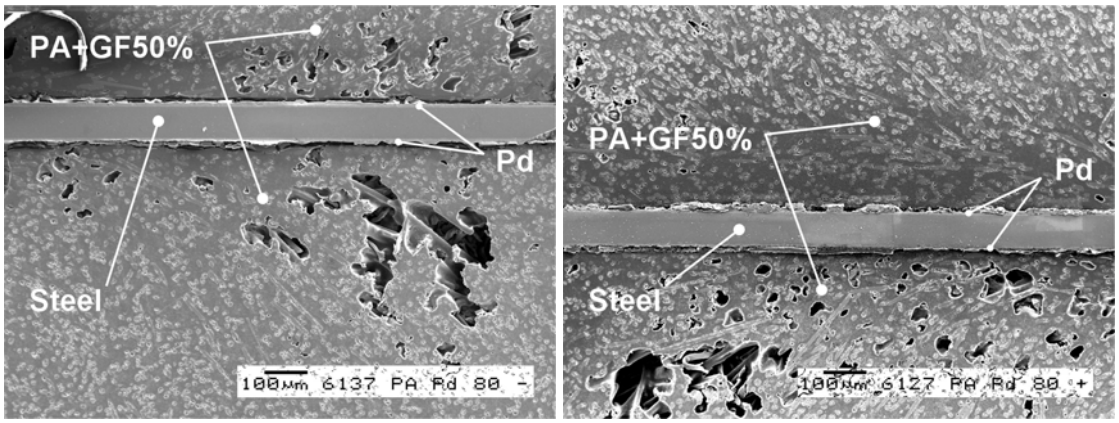

Figure 162 – Partial penetration of injection moulded PA+GF50% in the insert surface texture: not treated (left) and treated (right). Insert: steel + Pd, 80 µm thick.

7.6 Conclusion

Design, production by hot embossing and injection moulding (insert moulding), and testing of hybrid miniaturized components composed by a micro metal insert in a polymer matrix were presented in this chapter.

Different polymers (PS, POM, PA+GF50%) and different metals (steel, steel covered with a palladium layer, and German silver) were tested. Pull tests results showed dependency on the materials, on the metal inserts surface treatment and thickness. In particular, bonding strength was observed to be strongly dependent on metal insert roughness surface. The sand blast treatment applied to the metal insert surface was found to be a very important mean to increase the surface roughness and therefore to enhance the bonding strength of hybrid micro component.

Scanning electron microscopy investigation at the polymer/metal interface showed that penetration of the polymer on the surface texture of the metal part was achieved creating mechanical interlocking between the two components. Hot embossing allowed higher penetration of polymer in the micro surface topography than injection moulding, resulting in a higher bonding strength of the hybrid demonstrator. Mechanical interlocking of polymer at the micro dimensional level of the surface topography depended on the characteristics of flowability of the polymer and on the employed moulding process.

7.7 References

[Barbato, 1995] Barbato G., Carneiro K., Cuppini D., Garnaes J., Gori G., Hughes G., Jensen C.P., Jørgensen J.F., Jusko O., Livi S., McQuoid H., Nielsen L., Picotto G.B., Wilkening G. (1995) Scanning tunnelling microscopy methods for roughness and micro hardness measurements, Synthesis report for research contract with the European Union under its programme for applied metrology, European Commission Catalogue number: CD-NA-16145 EN-C, Brussels Luxembourg, pp.1-109.

[De Chiffre, 2000] De Chiffre L., Lonardo P., Trumpold H., Lucca D.A., Goch G., Brown C.A., Raja J., Hansen H.N. (2000) Quantitative

Characterisation of Surface Texture, Annals of the CIRP, Vol.49/2, pp.635-652.

[Ehrfeld, 2001] Ehrfeld W., Begemann M., Berg U., Lohf A., Michel F., Nienhaus M. (2001) Highly parallel mass fabrication and assembly of microdevices, Microsystem Technologies, Vol.7, Issue 4, pp.145-150.

[Haberstroh, 2002] Haberstroh E., Brandt M. (2002) Determination of mechanical properties thermoplastics suitable for micro systems, Macromolecular Material Engineering, Vol.287, Issue 12, pp.881-888.

[Heckele, 2003] Heckele M. (2003) Hot embossing – a flexible and successful replication technology for polymer MEMS, Proceedings of the SPIE (International Society for Optical Engineering), Microfluidics, BioMEMS, and Medical Microsystems II, San Jose (CA, USA), 26th-27th January 2004, Vol.5345, pp.108-117.

[Image Metrology, 2005] Image Metrology A/S (2005) Scanning Probe Image Processor (SPIP™), http://www.imagemet.com/

[Meeuwsen, 1996] Meeuwsen F. (1996) MID versus metal insert technology, Proceedings of 2nd International Congress Molded Interconnect Devices MID '96, Erlangen (Germany), 25th-26th September 1996, pp.33-41.

[Michaeli, 2003] Michaeli W., Ziegmann C. (2003) Micro assembly injection moulding for the generation of hybrid microstructures, Microsystem Technologies, Vol.9, Issue 6-7, pp.427-430.

[Michaeli, 2005] Michaeli W., Opfermann D. (2005) Micro assembly injection moulding – Potential application in medical science, Proceedings of 1st International Conference on Multi-Material Micro Manufacture (4M), Karslruhe (Germany), 29th June-1st July 2005, pp.79-82.

[Tosello, 2006(1)] Tosello G., Hansen H.N. (2006) In-process assembly of micro metal inserts in a polymer matrix, Proceedings of 2nd

International Conference on Multi-Material Micro Manufacture (4M), Grenoble (France), 20th-22nd September 2006, pp.83-86.

[Tosello, 2006(2)] Tosello G., Hansen H.N., Tang P.T. (2006) In-process assembly of micro metal inserts in a polymer matrix, 7th International Congress Molded Interconnect Devices (MID), Fuerth (Germany), 27th-28th September 2006, pp.279-292.

8 Conclusion

8.1 Summary

Micro injection moulding is recognized as one of the most important manufacturing processes enabling the mass-fabrication of polymer micro components.

The research undertaken during the Ph.D. project has been devoted to further develop the micro injection moulding technology with respect to the process analysis and optimization, to the micro part's defects optimization, to the tooling technology, to the process simulation and to the multi-material (i.e. polymer and metal) integration in miniaturized hybrid components. These five main topics have been the main focus of the research and they reflect the structure of this thesis. The most relevant results are summarized in the following.

- Process analysis and optimization – A series of statistically designed experiments was carried out both on a conventional and a micro injection moulding machine for the production of polymer micro components. Fundamental process parameters such as temperature of the melt, temperature of the mould, injection speed and packing pressure were investigated. Their influence on the filling of the part was determined using a newly developed method based on the analysis of weld lines used as melt flow markers. Furthermore, the process was analyzed by means of in-process cavity pressure measurements. Cavity injection pressure and time were analyzed both in terms of absolute values and of repeatability to fully characterize the process and to find the influence of the different process parameters. The filling of micro part and micro features was analyzed. As a conclusion, recommendations for improved processing were given based on the statistical analysis. Finally, the reliability of the investigation was validated

by using a newly developed method to implement the measurement uncertainty into the design of experiment statistical analysis.

- Part defects control and optimization – Weld lines as defects of micro injection moulded parts were deeply investigated using design of experiment techniques integrated with atomic force microscopy. The micro weld lines were characterized at sub-µm level and the relationship with the most important µIM process parameters was determined. Furthermore, the relation between the weld lines dimensions and their location with respect to the gate position has been established. In particular, it was demonstrated that weld lines dimensions (i.e. depth and width) increase when the distance from the gate increases. Recommendation for improved process and part design are given. As in the previous section, the reliability of the investigation was validated by implementing the atomic force microscope measurement uncertainty into the design of experiment statistical analysis.
- Tooling technology – The concept of hybrid tooling was introduce and defined as the capability of producing a mould insert combining two or more processes in sequence (i.e. in the same process chain). The state of the art of hybrid tooling was presented. During the Ph.D. project a new hybrid tooling process chain has been developed, implemented and validated. The new hybrid tooling strategy includes micro EDM process of silicon, electroplating of nickel and subsequent selective etching. Significant advancement in terms of miniaturization (micro features down to 38 µm of width), accuracy and multi-scale integration (3 mm long and straight micro ribs, planarity), high aspect ratio (up to 3) and surface roughness (Sa = 0.31 µm of the micro EDM machined areas and Sa = 14 nm of the Si-Ni-electroplated areas). The manufacturing of micro tools using an innovative hybrid indirect tooling process chain has been demonstrated to be a feasible solution for polymer micro fluidic fabrication by means of polymer replication process such as injection moulding. Finally, a metrology benchmark was performed within the European Network of Excellence 4M (Multi-Material Micro Manufacturing, http://www.4m-net.org/) in order to evaluate the performance of the newly developed hybrid tooling technology when compared to conventional micro

machining direct tooling. Results in terms of surface finishing, miniaturization, obtainable aspect ratio, wall straightness and mould flatness showed that the proposed indirect hybrid tooling technology is competitive when compared with for example micro milling.

- Process simulation – Different aspects of micro injection moulding three-dimensional simulations were investigated in this chapter: the implementation of the actual machine and process characteristics into the software, the optimization of three-dimensional meshing of the part, the validation of the filling simulation of micro components and micro features, the formulation of a new material rheological database suitable for micro scale polymer processing. A more accurate estimation of the filling time was obtained with the implementation of the real injection speed and of the real cavity injection pressure profile into the software. The importance of an accurate meshing of the micro part and of the complete system (composed by sprue, runner, gate and part) has been demonstrated. Meshing element characteristic dimensions and modelling tolerances were also discussed. Simulated and experimental flow markers were compared to evaluate the performance of the different simulation settings. Experimental short shots were produced and then simulated resulting on a true step-by-step filling simulation validation. Finally, a new polymer rheology database suitable to describe the polymer melt behaviour during μIM was implemented into the simulation. Actual improvements in terms of accuracy of the prediction of the flow front position were achieved using the newly developed material database.
- Micro insert moulding – Design, manufacturing by hot embossing and injection moulding (insert moulding), and testing of hybrid miniaturized components composed by a micro metal insert in a polymer matrix were presented in this chapter. Different polymers (PS, POM, PA+GF50%) and different metals (steel, steel covered with a palladium layer, and German silver) were tested. Bonding strength of the hybrid metal/polymer components was measured and different factors were investigated. A strong dependency on metal insert surface roughness was found. Scanning electron microscopy investigation at the polymer/metal interface showed that penetration of the polymer on the

surface texture of the metal part was achieved creating mechanical interlocking between the two components. Hot embossing allowed higher penetration of polymer in the micro surface topography than injection moulding, resulting in a higher bonding strength than the hybrid component produced by insert moulding. Mechanical interlocking of polymer at the micro dimensional level of the surface topography depended on the characteristics of flowability of the polymer and on the employed moulding process.

8.2 Outlook

The investigations and the achievements of the present work have provided new knowledge and substantial advancements beyond the state of the art in the field of polymer micro replication, with particular focus on current precision injection moulding of polymer micro components.

The undertaken experimental activity concerning process and part analysis, process simulation, micro tooling and multi-material application has opened a variety of new research opportunities which are either on their way to be investigated or are already started, also by virtue of the wide range of collaborations established during the Ph.D. project. Further research works are/will be dealing with the following points.

- The new flow marker method for the analysis of filling of micro cavities can be applied to study the influence of other factors than process parameters, such as micro tool cavity surface roughness and micro features with three dimensional geometries. Different polymers could be studied; in particular the investigation of the filling behaviour in micro cavities of semi-crystalline materials (such as POM and PA) and the influence on the presence of glass fibres and nano fillers are of great interest.
- The integration of the measuring uncertainty into the design of experiment (DOE) can be applied to virtually any manufacturing process optimization statistical study. To this respect, a research work was initiated during the present project with the collaboration of the author for the use of DOE techniques to optimize the measuring uncertainty of point-by-point sampling

complex surfaces using coordinate measuring machines (CMMs) [Barbato, 2007] [Barini, 2008].

- The great potential in terms of three-dimensional machining capabilities and miniaturization of the micro electrical discharge machining (μEDM) has been shown in this project. Research will be undertaken in order to improve the accuracy of the process when machining silicon by the optimization of the electrode diameter dressing process and of the electrode wear compensation.
- Beside silicon, aluminium is also a material of primary importance when performing indirect hybrid tooling. Following the same investigation strategy as described in this thesis, the database for μEDM of aluminium will be soon established at the author's university. To this respect, a research project has recently started on this topic.
- The research regarding the μIM simulation highlighted the limitations of the existing software and the opportunities for improving its simulative accuracy. Further research will focus on micro scale rheology, viscosity pressure dependence, heat transfer coefficient values and more accurate models that define the micro scale flow of polymer materials. The development of reliable procedures for the determination of such parameters will be of outstanding importance. The design and the realization of a micro capillary rheometer will be the key step for the experimental characterization of polymer melt behaviour when flowing in micro cavities. Moreover, the quantitative validation methods developed during the project can be use to benchmark the performances of different software programs when simulating the μIM process.
- In the field of micro manufacturing integration, multi-material μIM is predicted to become the crucial process for micro fabrication and assembly on one single machine and even on a single integrated process. The research will expand in the near future to a European level bringing together research laboratories, universities (including the author's university), large and small/medium enterprises. To this respect, under the coordination of the Network of Excellence 4M (Multi-Material Micro Manufacturing), a group of 4M core partners (namely Cardiff University (United Kingdom), TEKNIKER

(Spain), DTU (Denmark), IMTEK (Germany), FZK (Germany), TNO (The Nederlands), CEA (France)) has initiated a research program supported by the European Community in the field of converging technologies for micro manufacturing as described in [COTECH, 2008]. A polymer micro manufacturing technological platform will be established to link the consortium with leading plastic processing large companies and SMEs.

- The possibility of further downscaling the features obtainable by indirect hybrid tooling is also of primary importance. A preliminary research was undertaken in a project with the collaboration of the author in order to produce sub-µm structured polymer surfaces for micro fluidics applications (4M Cross Divisional Project "MINAFLOT" (Micro- and Nano-structured Surfaces for Liquid and Gas Management in Microstructured Flowfields) supported by 4M and the European Community (Project no. FP6-500274-2)). The replication of the micro-nano structures was performed by hot embossing and the tool was manufactured with a hybrid tooling process chain which included e-beam machining, X-Ray lithography and electroforming of nickel. Due to the sub-µm structuring, a hydrophobic behaviour of the surface can be obtained from a hydrophilic surface [Heckele, 2008(1)] [Heckele, 2008(2)].

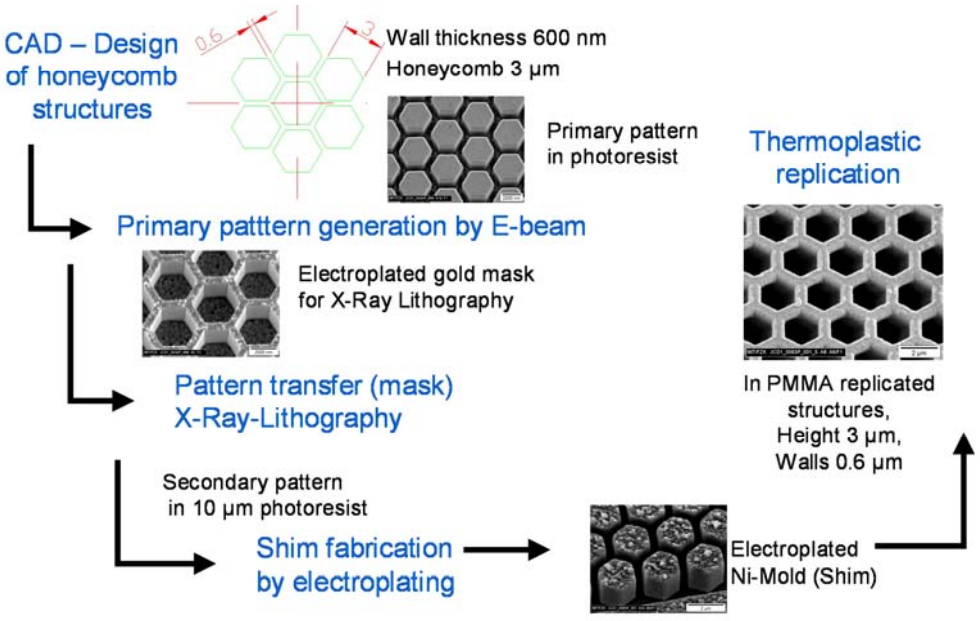

Figure 163 – Schematic of the process chain for the manufacturing of sub-µm structured polymer surfaces [Heckele, 2008(1)].

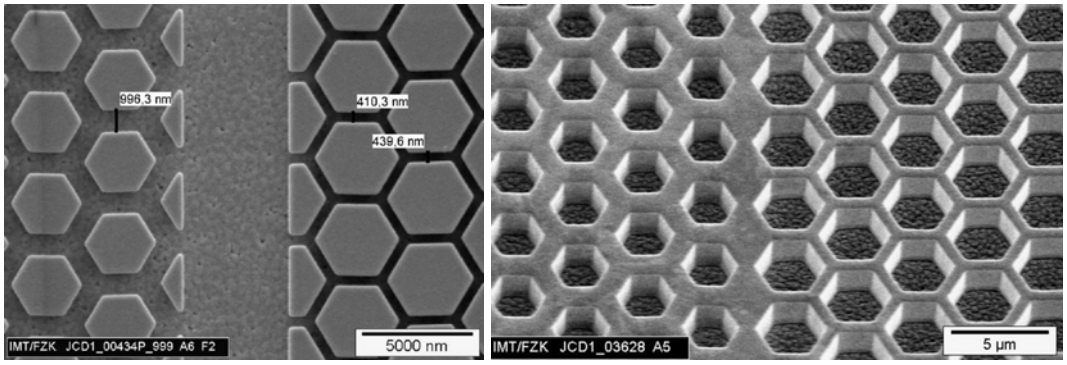

(a) (b)

Figure 164 – Honeycomb structures after E-beam lithography on 3 µm thick resist (PMMA) (a). Electroplated gold mask for X-ray lithography (b). Grooves and thin walls (detail (a) and (b) respectively) are 400 nm and 1000 nm wide [Heckele, 2008(2)].

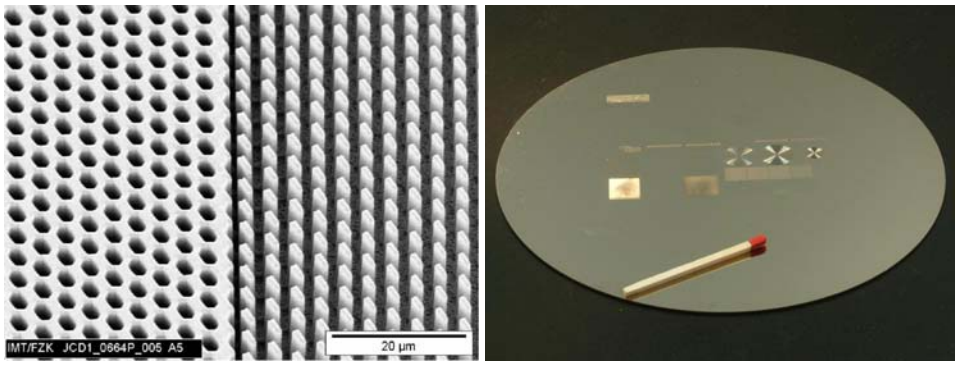

(a) (b)

Figure 165 – Via X-Ray lithography the structures were transferred into 4 µm high resist (a). Electroplated 4 inch nickel shim from the 4 µm thick resist is shown (b) [Heckele, 2008(2)].

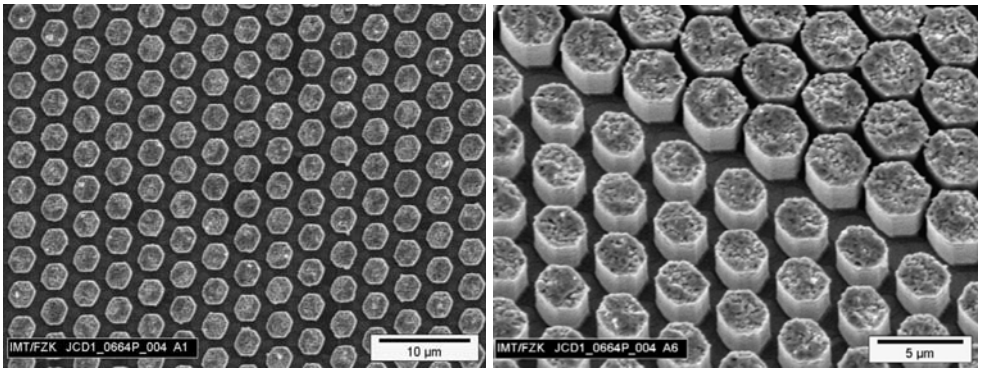

Figure 166 – Honeycomb structures of the micro structured nickel mould insert [Heckele, 2008(2)].

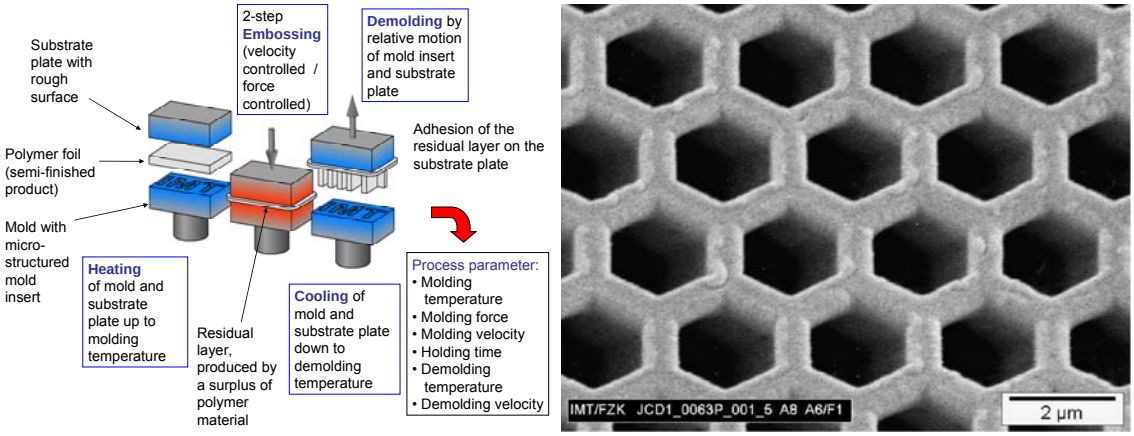

(a) (b)

Figure 167 – Schematic view of the hot embossing process (a). View of sub-µm honeycomb structures replicated in PMMA by hot embossing: pattern pitch is 2 µm and wall thickness is 500 nm [Heckele, 2008(2)].

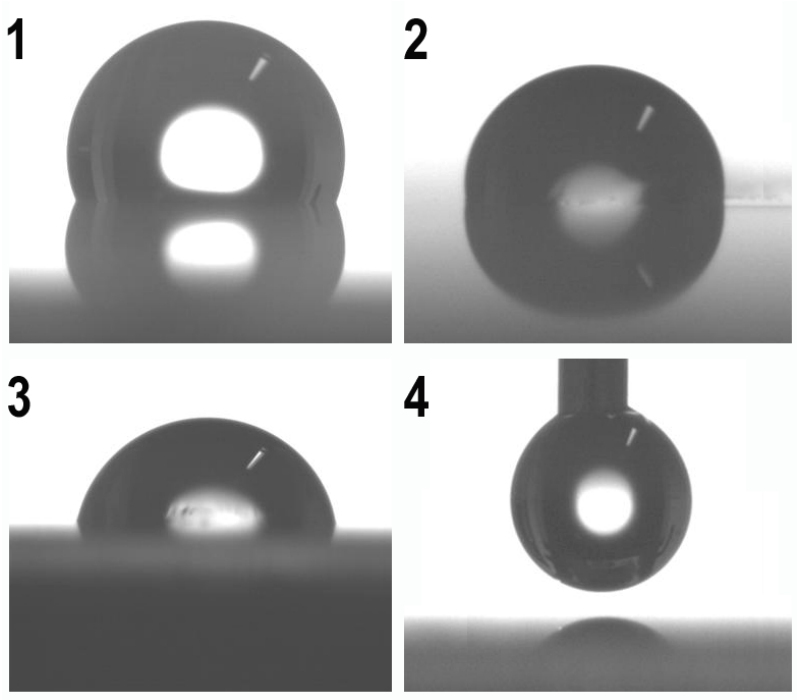

Figure 168 – Different wetting behaviours due to the surface sub-micro structuring of the polymer substrate: honeycomb with wall thickness of 400 nm (1), honeycomb with wall thickness of 1000 nm (2), substrate without structuring (3). In detail (4) a water droplet before the deposition on the surface is shown (diameter = 1300 ± 20 nm and volume = 1.1±0.1 nl) [Heckele, 2008(2)].

8.3 References

[Barbato, 2007] Barbato G., Barini E.M., De Chiffre L., Levi R., Tosello G. (2007) Optimization of a complex surface measurement with touch probe CMM using the design of experiment, Joint ENBIS-DEINDE 2007 Conference (European Network for Business and Industrial Statistics & Design of INDustrial Experiments) “Computer Experiments versus Physical Experiments”, Torino (Italy), 11th-13th April 2007, pp.28-39.

[Barini, 2008] Barini E.M., Tosello G., De Chiffre L. (2008) Uncertainty analysis of point by point sampling complex surfaces using touch probe CMMs, Precision Engineering (accepted for publication).

[COTECH, 2008] COTECH Consortium (2008) Converging technologies for micro systems manufacturing, European Commission, 7th Framework Programme, Large-scale integrating project (CP-IP 214491-2).

[Heckele, 2008(1)] Heckele M., Worgull M., Mappes T., Tosello G., Metz T., Gavillet J., Fugier P., Koltay P., Hansen H.N. (2008) Sub-µm structured surfaces manufacturing using e-beam machining, X-Ray lithography, electroforming and polymer replication for micro fluidics applications, 10th Anniversary International Conference of the European Society for Precision Engineering and Nanotechnology (Euspen), Zurich (Switzerland), 18th-22nd May 2008 (in press).

[Heckele, 2008(2)] Heckele M., Worgull M., Mappes T., Tosello G., Metz T., Gavillet J., Fugier P., Koltay P., Hansen H.N. (2008) Hot embossing of high aspect ratio sub-µm structured surfaces for micro fluidic applications, Society of Plastic Engineers (SPE) – 66th Annual Technical Conference (ANTEC), Milwakee (WI, USA), 4th-8th May 2008 (in press).

9 Appendix

9.1 Glossary

µECF	micro electrochemical milling
µEDM	micro electrical discharge machining
µIM	micro injection moulding
µSEDM	micro sinking electrical discharge machining
µWEDM	micro-wire electrical discharge machining
AFM	atomic force microscope or microscopy
ANOVA	analysis of variance
CAD	computer aided design
CAE	computer aided engineering
CAM	computer aided machining
CMM	coordinate measuring machine
COU	coefficient of uncertainty
COV	coefficient of variation
DOE	design of experiments
DVD	digital versatile disc
FEA	finite element analysis
FEM	finite element modelling
GF	glass fibres
HE	hot embossing
IM	injection moulding
Inj.Speed	injection speed
LIGA	lithographie, galvanoformung, abformung
MIDs	moulded interconnect devices
PA	polyamide

PMMA	poly(methyl methacrylate)
POM	polyoxymethylene
PP	polypropylene
Ppack	packing pressure
PS	polystyrene
PVD	physical vapour deposition
Ra	average surface roughness (2D)
Sa	surface average roughness (3D)
Sdr	surface area ratio
SEM	scanning electron microscope
SME	small/medium enterprise
Sq	surface root mean square (3D)
Tmelt	melt temperature
Tmould	mould temperature
U	expanded measuring uncertainty
WLF	William-Landel-Ferry

10 List of publications

10.1 International ISI journal papers

- Tosello G., Bissacco G., Tang P.T., Hansen H.N., Nielsen P.C. (2008) Micro tools manufacturing for polymer replication with high aspect ratio structures using µEDM of silicon, selective etching and electroforming, Microsystem Technologies, Vol. 14, Issue 9-11, pp.1757-1764.
- Tosello G., Gava A., Hansen H.N., Lucchetta G., Marinello F. (2008) Characterization and analysis of weld lines on micro injection moulded parts using Atomic Force Microscopy (AFM), Wear, Vol.266, Issue 5-6 (Metrology and Properties of Engineering Surfaces), pp.534-538.
- Tosello G., Gava A., Hansen H.N., Lucchetta G. (2008) Study of process parameters effect on the filling phase of micro injection moulding using weld lines as flow markers, International Journal of Advanced Manufacturing Technology (accepted for publication).
- Barini E.M., Tosello G., De Chiffre L., Barbato G. (2008) Complex Surface Verification with Coordinate Measuring Machines: Performance and Uncertainty analysis using Design of Experiment technique, Precision Engineering (accepted for publication).

10.2 Peer reviewed international conference papers as main author

- Tosello G., Schoth A., Hansen H.N. (2008) Implementation strategies for the optimization of micro injection moulding simulations, 4th International Conference on Multi-Material Micro Manufacture (4M), Cardiff (United Kingdom), 9th-11th September 2008 (in press).

- Tosello G., Griffiths C., Azcarate S., Schoth A., Fillon B., Manufacturing routes for disposable blood diagnostic chip (2008) 1st European Conference on Medical Polymers, Belfast (United Kingdom), 2nd-4th September 2008 (in press).
- Tosello G., Schoth A., Hansen H.N. (2008) In-cavity pressure and injection time measurements during the micro injection moulding process, 10th Anniversary International Conference of the European Society for Precision Engineering and Nanotechnology (Euspen), Zurich (Switzerland), 18th-22nd May 2008 (in press).
- Tosello G., Schoth A., Hansen H.N. (2008) Process and part filling control in micro injection molding, Society of Plastics Engineers – 66th Annual Technical Conference (ANTEC), Milwakee (WI, USA), 4th-8th May 2008 (in press).
- Tosello G., Gava A., Hansen H.N., Lucchetta G., Guarise M. (2007) Filling analysis in micro injection moulding using weld lines as flow markers, 3rd International Conference on Multi-Material Micro Manufacture (4M), Borovets (Bulgaria), 3rd-5th October 2007, pp.259-262.
- Tosello G., Fillon B., Azcarate S., Schoth A., Mattsson L., Griffiths C., Staemmler L., Bolt P.J. (2007) Application of different process chains for polymer microfluidics fabrication including hybrid tooling technologies, standardization and replication: a benchmark investigation within 4M Polymer Division, 3rd International Conference on Multi-Material Micro Manufacture (4M), Borovets (Bulgaria), 3rd-5th October 2007, pp.77-80.
- Tosello G., Gava A., Hansen H.N., Lucchetta G., Marinello F. (2007) Characterization and analysis of weld lines on micro injection moulded parts using Atomic Force Microscope, 11th International Conference on Metrology & Properties of Engineering Surfaces (Met & Props 2007), Huddersfield (UK), 16th-20th July 2007, pp.166-170.
- Tosello G., Bissacco G., Tang P.T., Hansen H.N., Nielsen P.C. (2007) Micro tools manufacturing for polymer replication with high aspect ratio structures using μEDM of silicon, selective etching and electroforming, 7th International Workshop on High-Aspect-Ratio Micro-Structure Technology (HARMST), Besançon (France), 7th-9th June 2007, pp.43-44.
- Tosello G., Gava A., Hansen H.N., Lucchetta G., Marinello F. (2007) Micro-Nano integrated manufacturing metrology for the characterization of micro injection

moulded parts, 7th International Conference of the European Society for Precision Engineering and Nanotechnology (Euspen), Bremen (Germany), 20th-24th May 2007, pp.377-380.

- Tosello G., Gava A., Hansen H.N., Lucchetta G. (2007) Influence of process parameters on the weld lines of a micro injection molded component, Society of Plastics Engineers – 65th Annual Technical Conference (ANTEC), Cincinnati (OH, US), 6th-10th May 2007, pp.2014-2018.
- Tosello G., Fillon B., Azcarate S., Schoth A., Mattsson L., Griffiths C., Staemmler L., Bolt P.J. (2007) Hybrid tooling technologies and standardization for the manufacturing of inserts for micro injection molding, Society of Plastics Engineers – 65th Annual Technical Conference (ANTEC), Cincinnati (OH, US), 6-10 May 2007, pp.2992-2996.
- Tosello G., Gava A., Hansen H.N., Lucchetta G., Guarise M. (2007) Measuring uncertainty applied to design of experiment analysis: a micro injection moulding case study, Joint ENBIS-DEINDE 2007 Conference (European Network for Business and Industrial Statistics & DEsign of INDustrial Experiments) “Computer Experiments versus Physical Experiments”, Torino (Italy), 11th-13th April 2007, pp.202-213.
- Tosello G., Hansen H.N., Tang P.T. (2006) Investigation of over-moulded hybrid metal/polymer devices, 7th International Congress Molded Interconnect Devices (MID), Fuerth-Nuremberg (Germany), 27th-28th September 2006, pp.279-292.
- Tosello G., Hansen H.N. (2006) In-process assembly of micro metal inserts in a polymer matrix, 2nd International Conference on Multi-Material Micro Manufacture (4M), Grenoble (France), 20th-22nd September 2006, pp.83-86.

10.3 Peer reviewed international conference papers as co-author

- Mattsson L., Bolt P.J., Azcarate S., Brousseau E., Fillon B., Fowler C., Gelink E., Griffiths C., Khan Malek C., Marson S., Retolaza A., Schneider A., Schoth A., Temun A., Tiquet P., Tosello G. (2008) Reliability of surface roughness measurements of micro-features – Experiences of a Round Robin test within nine 4M laboratories, 4th International Conference on Multi-Material Micro Manufacture (4M), Cardiff (United Kingdom), 9th-11th September 2008 (in press).

- Dimov S.S., Matthews C.W., Brousseau E., Bigot S., De Grave A., Hansen H.N., Bissacco G., Tosello G., Fillon B., Bolt P.J., Engel U., Johander P., Jung E., Kirby P.B., Mattsson L., Richter M., Ritzhaupt-Kleissl H.J., Schoth A., Wenzel C., Matovic J. (2008) 4M Progress Report 2006-2008, 4th International Conference on Multi-Material Micro Manufacture (4M), Cardiff (United Kingdom), 9th-11th September 2008 (in press).
- Heckele M., Worgull M., Mappes T., Tosello G., Metz T., Gavillet J., Koltay P., Hansen H.N. (2008) Hot embossing of high aspect ratio sub-µm structured surfaces for micro fluidic applications, 4th International Conference on Multi-Material Micro Manufacture (4M), Cardiff (United Kingdom), 9th-11th September 2008 (in press).
- Griffith C., Tosello G., Nestler J., Sha B., Hoyle R.T. (2008) Micro Engineering: Experiments conducted on the use of polymeric materials in micro injection moulding, 1st European Conference on Medical Polymers, Belfast (United Kingdom), 2nd-4th September 2008 (in press).
- Griffith C., Tosello G., Nestler J., Sha B., Hoyle R.T. (2008) Micro Engineering: Experiments conducted on the use of polymeric materials in micro injection moulding, Medical Moulding & Extrusion 2008, Cologne (Germany), 16th-18th June 2008 (in press).
- Heckele M., Worgull M., Mappes T., Tosello G., Metz T., Gavillet J., Fugier P., Koltay P., Hansen H.N. (2008) Sub-µm structured surfaces manufacturing using e-beam machining, X-Ray lithography, electroforming and polymer replication for micro fluidics applications, 10th Anniversary International Conference of the European Society for Precision Engineering and Nanotechnology (Euspen), Zurich (Switzerland), 18th-22nd May 2008 (in press).
- Heckele M., Worgull M., Mappes T., Tosello G., Metz T., Gavillet J., Fugier P., Koltay P., Hansen H.N. (2008) Hot embossing of high aspect ratio sub-µm structured surfaces for micro fluidic applications, Society of Plastic Engineers (SPE) – 66th Annual Technical Conference (ANTEC), Milwakee (WI, USA), 4th-8th May 2008 (in press).
- Worgull M., Heckele M., Mappes T., Matthis B., Tosello G., Metz T., Gavillet J., Fugier P., Koltay P., Hansen H.N. (2008) Sub-µ structured Lotus Surfaces

Manufacturing, DTIP (Design, Test, Integration & Packaging) of MEMS/MOEMS Conference, Nice (France), 9th-11th April 2008 (in press).

- Gava A., Tosello G., Lucchetta G., Hansen H.N., Salvador M. (2007) A new approach for the validation of filling simulations in micro injection moulding, 9th International Conference on Numerical Methods in Industrial Forming Processes (NUMIFORM), Porto (Portugal), 17th-27th June 2007, pp.307-312.
- Hansen H.N., Tang P.T., Islam A., Tosello G. (2007) Process chains for manufacturing of miniaturised moulded interconnect devices (MID), 7th International Conference of the European Society for Precision Engineering and Nanotechnology (Euspen), Bremen (Germany), 20th-24th May 2007, pp.176-179.
- Barini E.M., De Maddis M., Ruffa S., Tosello G. (2007) A DOE approach for robustness analysis of a shape recognition statistical method, Joint ENBIS-DEINDE 2007 Conference (European Network for Business and Industrial Statistics & DEsign of INDustrial Experiments) “Computer Experiments versus Physical Experiments”, Torino (Italy), 11th-13th April 2007, pp.40-49.
- Barini E.M., Tosello G., De Chiffre L. (2007) Uncertainty analysis of point by point sampling complex surfaces using touch probe CMMs, 10th CIRP International Seminar on Computer Aided Tolerancing (CAT2007), Erlangen, 21st-23rd March 2007, pp.1-13.
- Barbato G., Barini E.M., De Chiffre L., Levi R., Tosello G. (2007) Optimization of a complex surface measurement with touch probe CMM using the design of experiment, Joint ENBIS-DEINDE 2007 Conference (European Network for Business and Industrial Statistics & DEsign of INDustrial Experiments) “Computer Experiments versus Physical Experiments”, Torino (Italy), 11th-13th April 2007, pp.28-39.
- Azcarate S., Uriarte L., Schoth A., Bigot S., Tosello G., Roth G., Staemmler L. (2006) Hybrid Tooling: A Review of Process Chains for Tooling Microfabrication within 4M, Proceedings of 2nd International Conference on Multi-Material Micro Manufacture (4M), Grenoble (France), 20th-22nd September 2006, pp.305-308.
- Hansen H.N., Tosello G., Gegeckaite A., Arentoft M., Marin L., Classification of assembly techniques for micro products, 1st International Conference on Multi-

Material Micro Manufacture (4M), Karslruhe (Germany), 29th June-1th July 2005, pp.283-286.

10.4 Research and technical reports on micro manufacturing and polymer micro technology

- Tosello G., Gava A., Kanevcev O., Zhang Y., Influence of process parameters on the weld lines of a micro injection moulded component, IPL-DTU report, pp.1-98, June 2006.
- Tosello G., Micro Injection Moulding (μIM): Manufacturing Technology for Mass-Microfabrication, IPL/DTU report, pp.1-128, December 2005.
- Tosello G., Dai J., Kasper J., Friis L., Islam A., Wiwe B.D., Design, Manufacturing, and Testing of Micro Fluidic Device, IPL-DTU report, pp.1-81, June 2005.
- Tosello G., Gegeckaitė A., Life cycle design, recycling, and environmental issues for micro and nano products, IPL-DTU report, pp.1-28, May 2005.

DTU Mechanical Engineering
Section of Manufacturing Engineering
Technical University of Denmark

Produktionstorvet, Bld. 427S
DK- 2800 Kgs. Lyngby
Denmark
Phone (+45) 45 25 47 63
Fax (+45) 45 93 01 90
www.mek.dtu.dk
ISBN: 978-87-89502-77-9